Contrails

WADC TECHNICAL REPORT 55-156
PART 1
AD 97136

INSTALLATION OF AN AUTOMATIC CONTROL SYSTEM IN A T-33 AIRPLANE FOR VARIABLE STABILITY FLIGHT RESEARCH

Part 1 — Preliminary Investigation and Design Studies

EDITED BY J. N. BALL

FLIGHT RESEARCH DEPARTMENT
CORNELL AERONAUTICAL LABORATORY, INC.

SEP 14 1956

JULY 1956

AERONAUTICAL RESEARCH LABORATORY
CONTRACT AF 33(616)-2578
PROJECT 1364
TASK 70525

WRIGHT AIR DEVELOPMENT CENTER
AIR RESEARCH AND DEVELOPMENT COMMAND
UNITED STATES AIR FORCE
WRIGHT-PATTERSON AIR FORCE BASE, OHIO

Carpenter Litho & Prtg. Co., Springfield, O.
100 - September 1956

Approved for Public Release

Contrails

FOREWORD

The work covered by this report has been carried out by the Flight Research Department of the Cornell Aeronautical Laboratory. The report has been prepared by J. N. Ball, C. L. Muzzey, W. J. Thayer, W. Close, C. B. Notess, H. S. Radt, Jr., E. R. Schultz, and J. L. Beilman. The work has been done under Air Force Contract AF33(616)-2578, Project No. 1364, "Flight Control Technical Requirements," Task No. 70525. The project is being administered by Mr. P. P. Cerussi of the Aeronautical Research Laboratory, Wright Air Development Center.

Approved for Public Release

Contrails

ABSTRACT

The Cornell Aeronautical Laboratory has completed the preliminary design phase of a project under which a T-33 will be equipped as a variable stability airplane for a program of flight research on airplane handling characteristics. Irreversible hydraulic servos will be used to operate the control surfaces so as to provide artificial stability about all three axes. Variable stick force characteristics will be provided by an artificial feel system. Simulation of other airplanes will be possible with this highly versatile system. Special equipment is also being included for research on cockpit controls. A satisfactory preliminary design study has been completed for the control system. Methods have been developed for handling the major problems of detailed design. It has been found that the T-33 is a satisfactory airplane for the purposes of the program.

PUBLICATION REVIEW

This report has been reviewed and is approved.

FOR THE COMMANDER:

Nathan L. Krisberg

NATHAN L. KRISBERG, Colonel, USAF
Chief, Aeronautical Research Laboratory
Directorate of Research

Approved for Public Release

Contrails

TABLE OF CONTENTS

Approved for Public Release

Page

Approved for Public Release

Contrails

TABLE OF CONTENTS (CONT'D)

Approved for Public Release

Contrails

LIST OF ILLUSTRATIONS

Approved for Public Release

Controls

LIST OF ILLUSTRATIONS (CONT'D)

Approved for Public Release

Contrails

LIST OF ILLUSTRATIONS (CONT'D)

Approved for Public Release

Contrails

LIST OF TABLES

Approved for Public Release

Contrails

SECTION I

INTRODUCTION

The design requirements for present-day high-performance military aircraft have resulted in a series of airplanes which differ markedly from their predecessors. Performance requirements have dictated configurations involving highly swept-back, low-aspect-ratio wings, high wing loadings, and unconventional mass distributions. Operational altitudes are becoming higher and higher, and operation over an increasingly wide range of Mach numbers is required. All of these developments have made the problems of achieving adequate stability and control characteristics in the military aircraft of the immediate future more complex than they formerly were. In fact, it seems that all of the changes which have permitted performance improvements have also introduced new stability problems. Furthermore, it seems certain that the continuing development of airplanes to reach higher and higher Mach numbers and altitudes will constantly bring up new and different stability and control problems.

In addition to the stability problems introduced by new configurations, operational requirements are introducing more stringent requirements on the handling characteristics of military aircraft. The constantly increasing speeds of fighter airplanes mean that the time available in making a run on a target is becoming shorter and shorter. A high degree of tracking accuracy is required to insure a reasonably high probability of a successful attack. Ease of tracking depends on stability and control characteristics. To improve tracking accuracy, we must learn better than we have before exactly what handling characteristics we want and how to produce them.

The growing importance of good tracking characteristics calls for careful attention to the whole question of matching the airplane's handling characteristics to the pilot. One particular aspect of this question which seems now to merit special attention is the design of the cockpit controls. The prevalent use of power control systems has opened up the possibility of designing cockpit controls with a wide range of characteristics. It seems opportune, then, to

Manuscript released by the authors April 1955 for publication as a WADC Technical Report.

Approved for Public Release

Contrails

re-examine the traditional use of wheel, stick, and pedal controls, and to inquire whether airplanes can be made to fly better by the use of modified or new types of cockpit control configurations. In particular, it is of interest to know whether cockpit controls can be designed so as to make more accurate tracking of targets possible.

The general area of stability and control and handling characteristics of airplanes is thus developing in several ways. New knowledge and methods are needed to cope with the various problems that are arising. The present project is aimed at meeting a part of this need through a program of flight research.

Several of the flight test programs which have been conducted for the Air Force by the Cornell Aeronautical Laboratory have demonstrated that the use of automatic control equipment in test airplanes provides a powerful means for tackling stability and control problems. Such equipment has been used to vary the stability and control characteristics of test airplanes over wide ranges. This development has progressed to the point where a control system can be designed so that it is possible essentially to vary all the important stability and control characteristics of an airplane independently. This means that we now are able to set up a test airplane so that it can be used to simulate other airplanes.

To achieve the flexibility implied by the ability to simulate other airplanes is in itself a worthwhile aim. In general, if research is to be effective, we must be able to vary the important parameters independently and freely. In the case of stability and control flight research, the important parameters include such things as wing span, tail area, and moment of inertia. These are intractable variables, and it is obviously convenient if we can in effect vary them by means other than rebuilding airframes.

More specifically, an effective and expeditious way of attacking current stability and control problems is provided by a test airplane which can simulate other airplanes. When a new generation of airplanes turns out to be afflicted with a new sort of stability and control difficulty, flight research on the problem can be undertaken by setting up the test airplane to simulate the undesirable characteristics. Now this in itself is little help, because we

Approved for Public Release

Contrails

already have airplanes with these characteristics. The important point is that we can systematically and quickly vary the characteristics of the test airplane so as to discover the promising approaches to the problem. In some cases, the problem will become well enough understood to be solved. In other cases, at least a large amount of effort may be saved by eliminating at the outset approaches to the problem which will be fruitless.

A more general and far-reaching application is the simulation of new types of airplane configurations which are still in the design stages. For example, the new supersonic fighter airplanes tend to have low moments of inertia in roll compared to the moments of inertia about the pitch and yaw axes. This situation can readily be simulated, and well in advance of flight test the handling characteristics of such an airplane could be tried out. If the results were not wholly favorable, variations in control system dynamics could be tried, and various sorts of artificial stability devices could be simulated. From such tests, we can expect to derive useful principles of design for the control systems of new types of airplanes. It might also be that a new type of airplane designed to old criteria for handling characteristics would turn out not to be satisfactory in all respects, even where it met the criteria. If this can be found out early, current design can be oriented toward suitably revised criteria. In some cases, design calculations will predict that an airplane will have some stability and control characteristic which is out of the ordinary. The question will be, will this characteristic be satisfactory to a pilot and will it affect his ability to track a target? The answer is found by having pilots fly an airplane which has the characteristic. In general, the possibility is open of obtaining answers to stability and control questions well in advance of flight test and under conditions where the test configuration can be readily varied. It seems quite clear that this possibility presents real advantages.

A test airplane of the sort described is adaptable to research in the specific area of cockpit control design, which was mentioned above. This area includes not only the physical design of the controls in the cockpit which the pilot manipulates, but also the type of response of the airplane to the use of the controls. For example, on a variable stability and control airplane, the effective

Approved for Public Release

Contrails

gearing ratio between stick movement and elevator angle can be varied over wide ranges, or the control system can be set up to provide automatic turn coordination. One special possibility that is of interest is to make the control system operate so that instead of a rolling velocity, a steady bank angle is obtained in response to a steady lateral stick deflection. Various similar configurations could be set up and tried.

In short, stability and control problems are continually at hand, and many of them are such that their solutions are to be found only through flight testing. For work on these problems, we now have a powerful new tool, the variable stability and control airplane. This report covers the first stages of a program, sponsored by the Air Force, under which the Cornell Aeronautical Laboratory will equip a T-33 as a variable stability and control airplane and will undertake with it a program of flight research.

Approved for Public Release

Contrails

SECTION II
CONTRACT AND PROGRAM STATUS

Air Force Contract AF33(616) -2578 has been awarded by the Air Force to the Cornell Aeronautical Laboratory for the purpose of outfitting a T-33 as a variable stability and control airplane for flight research along the lines indicated above. The contemplated program has been divided into six phases:

I. Preliminary Design
II. Detailed Design
III. Fabrication
IV. Installation
V. Ground Check-Out
VI. Flight Tests

The contract initially covered Phase I only, which was scheduled for a nine-month period starting 1 July 1954, and which now has been completed. The work accomplished in this phase is the subject of this report. At the end of March 1955, negotiations were nearly complete for an extension of the contract to cover Phases II and III. The scheduled completion date for these phases is 1 April 1956. It is anticipated that when appropriate, further extensions will be arranged so that the work can be continued without pause into the later phases.

The T-33A airplane to be used for the project. Serial No. 51-4120. was delivered to Cornell on 14 October 1954. It has been bailed to the Laboratory under Bailment Agreement AF33(600)-2214. It is being used for design studies. and will continue to be so used until Phase IV of the program (Installation) is reached.

Phase I has included a study to determine the suitability of the T-33 airplane for simulating the flight characteristics of various USAF fighter aircraft. Further study has been directed toward research in design of cockpit controls. Systems for automatic coordination of turns and for providing bank angle proportional to lateral control displacement have been worked out. Design requirements have been formulated to define the functions of the control system and

Approved for Public Release

Contrails

the performance required of it. On the basis of these requirements, preliminary design work has been undertaken on the mechanical, servo, and electronic installations. Bench test programs have been carried out to obtain servo design data and electronic design data. With Phase I complete, the methods to be used have been worked out, and the necessary design information is available for proceeding to detail design and procurement of components.

The work accomplished so far is described in the later sections of the report. It seems convenient at this point, however, to outline briefly the general status of the program. The methods to be used in simulating other airplanes have been worked out. They have been checked out analytically and also have been checked on the BEAC and EASE analog computers. Particular attention has been paid to the requirements for servo dynamic performance. Methods have been worked out for setting up the control system to compensate for servo lag. It appears that this can be done well enough so that the servo performance requirements can be kept within practical bounds.

The general configuration of the control system has been settled, and essentially final block diagrams are presented in a later section. Preliminary aerodynamic design data have been issued for all the components.

Preliminary servo design has been carried out and a position servo test rig has been designed, fabricated and tested with satisfactory results. A feel servo test rig has also been set up and tested with generally satisfactory results. It is believed, however, that some improvements can be made in the feel servo by doing a moderate amount of additional testing and development.

Satisfactory layouts have been made for the interchangeable wheel and stick, and for the servo installations. A choice has still to be made, though, between locating two aileron servos in the wings, or one at the fuselage centerline. This decision will be made early in Phase II on the basis of evaluating in detail the servo test results as well as the other pertinent studies of Phase I.

The block diagrams as now developed define the electrical and electronic functions of the control system. Design principles have been worked out for all major electronic components. Preliminary bench test results are available for most of them. In several instances, the purchase of computing components from outside firms appears to be advantageous. These possibilities are being actively investigated.

Approved for Public Release

Contrails

SECTION III

DESCRIPTIVE OUTLINE OF THE GENERAL APPROACH AND METHODS

BY J.N. BALL

The purpose of this section is to furnish a broad and somewhat simplified description of the concepts which have governed the design of the control system for the variable stability and control T-33. More technical presentations of the analytical studies and design work accomplished so far are presented in later sections.

The reasons for choosing the T-33 airplane as the test aircraft should perhaps first be noted. The program is concerned with the handling characteristics of fighters, rather than bombers or other such large aircraft. Therefore, a small jet-propelled aircraft of relatively high performance is required. With an experimental control system installation, it is prudent to provide a safety pilot whose controls are independent of the experimental equipment. Thus a two-place airplane with controls in both cockpits is desired. The T-33 is believed to be the best available aircraft meeting these requirements.

The front cockpit is to be the test cockpit. The controls in this cockpit will be permanently disconnected from the regular control system and will be used only to operate the special control system to be described below. The rear cockpit will have its normal, complete set of flight controls. When the experimental control system is disengaged, the airplane is flown in the normal manner from the rear cockpit. When performing tests, the pilot in the front seat flies the airplane. The rear pilot can always resume control at once in the event of any malfunction or unusual occurrence. The front cockpit will be designed with an interchangeable wheel and stick control. This feature will be used in the research to be done on cockpit control configurations.

The control system is to be designed so that it is possible to simulate other airplanes. To accomplish this, the control surfaces must perform two functions. First they must respond to the pilot's use of his controls; second, they must move in response to the airplane's motion so as to alter its stability

Approved for Public Release

Contrails

characteristics. To provide both functions, irreversible hydraulic power controls are used to drive the control surfaces. The power control servo loops are built to receive and respond to electrical inputs. Inputs received from the cockpit controls provide the first function, and inputs from pickups measuring the motion of the airplane provide the second function. With this arrangement, the two functions are kept separate and do not interfere with each other. Furthermore, the use of electrical signals makes it easy to vary the gains on the various input channels and to alter the control system configuration in flight.

To provide artificial stability, the airplane's motion is measured by various standard pickups, such as rate gyros and accelerometers, and signals from these devices are used as inputs to the control surface servos. The T-33 control system will have the following inputs to its control surface servos. (In addition, as explained below, there is an auxiliary surface for control of the phugoid motion, responding to speed and rate of change of speed.)

Elevator servo:

1. Angle of attack, α
2. Rate of change of angle of attack, $\dot{\alpha}$
3. Pitching velocity, $\dot{\theta}$
4. Pitching acceleration, $\ddot{\theta}$

Aileron servo:

1. Rolling velocity, p
2. Rolling acceleration, $\dot{p}$
3. Yawing velocity, r
4. Yawing acceleration, $\dot{r}$
5. Sideslip angle, β
6. Rate of change of sideslip angle, $\dot{\beta}$

Rudder servo:

1. Rolling velocity, p
2. Rolling acceleration, $\dot{p}$
3. Yawing velocity, r
4. Yawing acceleration, $\dot{r}$

Approved for Public Release

Contrails

5. Sideslip angle, β
6. Rate of change of sideslip angle, $\dot{\beta}$

The primary effect of a motion of the elevator, for example, is to produce an incremental pitching moment coefficient, ΔC_m. Thus, when the elevator is made to respond to changes in α, the result is an artificial $dC_m/d\alpha$. Similarly, the response of the ailerons to rolling velocity produces a rolling moment proportional to rolling velocity. This provides damping in roll, or artificial C_{ℓ_p}. In the same way the various other stability derivatives of the T-33 can be altered by the addition of the artificial stability inputs listed above. By adjusting the gains on the various channels, the test airplane may be set up so that its derivatives match those of the airplane to be simulated.

Simulation of inertia distributions as well as aerodynamic characteristics must be considered. In general, the equations of motion may be set up so that the coefficients are aerodynamic derivatives divided by inertia parameters. The gains of the various artificial stability channels are chosen then to match these coefficients, and no separate consideration of inertia is required. Alternately, the T-33 moments of inertia may be varied in effect by having the control surfaces respond to angular accelerations. Practical considerations such as resolution and noise in the control system channels will help to determine the relative advantages of the two approaches. The T-33 control system is being designed so that either approach may be used. In either case, the control system will have the capability of simulating unusual inertia distributions which differ considerably from the normal T-33.

It may be desirable or necessary to fly the test airplane at a flight condition (speed and altitude) other than the flight condition of the airplane being simulated. Also, the test airplane will generally not have the same wing loading as the other airplane. The values of the test airplane's artificial stability derivatives can be systematically chosen to allow for these differences. Proper choice of speed and altitude for the test airplane will make up for the fact that of the test airplane's derivatives, one of the important ones, the lift curve slope, is not easily adjustable by artificial means.

The result will be that the dynamic stability of the test airplane will

Approved for Public Release

Contrails

match the characteristics of the airplane being simulated. If the test airplane is disturbed by a gust or a control motion, and if then the controls are held fixed, the resulting natural modes of motion will be correct. The natural frequencies and damping ratios of the various modes will be duplicated.

This, of course, is only the stability half of the story. It is necessary also to duplicate the control characteristics that the pilot feels. To be specific, let us talk in terms of the longitudinal short-period motion as an example. We consider short-term maneuvers at essentially constant speed. To move the stick back, the pilot has to exert a pull force on it. The result is an upward deflection of the elevator. This trims the airplane to an increased normal acceleration, which produces a nose-up curvature of the flight path. The pilot feels the stick force that he has applied, and to some extent also he may sense the change in stick position. The primary response that he feels as a result of his use of the controls is normal acceleration. To a large extent, this is what he flies by. The other important thing that the pilot senses is the rate at which he sees the horizon move, i. e., pitching velocity. (In the particular case of tracking a target, pitching velocity may be the primary variable rather than normal acceleration.) Angle of attack is in itself not important, as the pilot has no way of directly sensing the relative wind direction. Finally the pilot senses, from what he feels and sees, the dynamic characteristics of the airplane's motion in response to his use of the controls; he senses whether the airplane's response is fast or slow, sluggish or oscillatory. This whole situation is what we have to simulate.

One way to set up a control system to do this will be described, and then some possible variations will be mentioned. First a position transducer is used to generate an electrical signal proportional to stick position. This signal goes to the elevator surface servo. Thus the elevator is made to move in response to the pilot's motion of the stick. The effective gearing between the two is determined by an electrical gain adjustment. The gain is chosen to give the right steady-state response to an incremental motion of the stick. The fact that we have already matched dynamic stability insures that the transient motion in going from one steady-state condition to another will be correct. One question at this point is whether we match steady-state normal accelera-

Approved for Public Release

Contrails

tion or pitching velocity. The two quantities are related as follows:

$$\dot{\gamma} = (g/V)\ \Delta n$$

$\dot{\gamma}$ = rate of change of flight path angle, which equals pitching velocity in the steady-state condition, rad/sec

Δn = increment in normal acceleration over the 1g required for level flight, dimensionless

g = acceleration due to gravity, ft/sec^2

V = true speed, ft/sec

From this relation it can be seen that if we match true speed, we will have the correct relation between Δn and $\dot{\gamma}$. Then if we match one, we simultaneously match the other. If we cannot match V, however, a compromise must be made. If our test V is low, for instance, and we match Δn, the pitching velocity will come out too large. If we match pitching velocity, normal acceleration comes out low. To minimize this effect, we should match V as nearly as is practical. Then if we are interested in general handling characteristics, we should probably give priority to matching normal acceleration. It is possible though, that if we are specifically interested in tracking, pitching velocity should have priority. An in-between compromise is of course also possible.

The remaining thing now to be simulated is stick force. First we need a stick force proportional to stick displacement, and we require that the "spring rate" relating the two be easily and continuously adjustable. The spring rate has to be set to give the proper stick force per g. Also, if we are to simulate natural aerodynamic feel, the spring rate must vary with dynamic pressure. To accomplish this we use a servo arrangement. A hydraulic cylinder is attached to the stick. The differential pressure in the cylinder, and hence the force that it exerts on the stick, is controlled by a pressure control valve. This valve produces a differential pressure proportional to an electrical input signal. By using a stick position signal as the input, a control force is generated proportional to stick deflection. The spring rate is easily varied by a simple electrical gain adjustment.

Approved for Public Release

Contrails

Since the valve works from electrical inputs, it is easy to introduce additional types of stick force. A signal proportional to normal acceleration produces the effect of a bob-weight. A signal proportional to rate of stick motion produces the effect of a viscous damper. A signal proportional to angle of attack represents the effect of angle of attack on hinge moment coefficient. The system is basically flexible, so that almost any desired input can be generated and fed to it. The system can also be supplemented by mechanical devices if desired. For example, it is believed that a satisfactory representation of dry friction can be computed, but there is the alternate possibility of fastening a mechanical friction device to the control system.

Now when the pilot moves the stick, he will feel the right stick forces, the transient motion of the airplane will have the right character, and the airplane will settle down to the correct new steady-state condition.

There are two main variations on the method described above for simulating the control characteristics. The input to the elevator servo can come from a strain gage which picks up stick force, instead of from a stick position transducer. It is possible to use a computer to derive the correct elevator angle variation from the measured stick force. If it is considered that a pilot flies primarily by applying stick forces and that the resulting stick motions are of lesser importance to him, it may be that this method is actually the direct way of making the control surfaces follow the pilot's intentions. This method also makes it practical to operate with very small cockpit control motions or even with the stick and pedals rigidly fixed. Another variation is to use an ordinary position servo with a flow-control valve instead of the pressure-control valve arrangement. This is made to act like a spring as follows. A strain gage picks up the pilot-applied force; this signal is fed to the servo loop; and the servo drives the stick to the proper displacement. The basic plan of simulation remains the same, and the choices among the different variations are based on practical considerations of satisfactory operation. Another consideration is complexity of the system. Block diagrams were drawn for both the pressure-control and flow-control feel servo systems. It was found that the number of components and the number of connections were roughly comparable, so that this is not a determining factor. A particular

Approved for Public Release

Contrails

question is dynamic stability of the feel system. Previous experience with systems using a flow-control valve has shown that closed-loop instability can arise. The probable explanation of the observed instability is that the position servo was required to operate with an excessive inertia load composed of the control stick and wheel and increased by the pilot's hands and arms. It is shown elsewhere in this report, and in Reference 10, that a position servo with a large inertia load will exhibit a large phase shift due to oil compressibility effects. It is now believed that this rapid phase shift within the position servo was responsible for the over-all instability when the strain gages were connected to make the system operate as a feel servo. Preliminary analysis has shown that the pressure-control system is less subject to this trouble. Accordingly, it has been decided that the pressure-control valve will be used, provided satisfactory results are obtained from the servo test program.

Very much the same considerations apply to simulation of the lateral motions of an airplane. As already mentioned, dynamic stability is simulated by generating suitable artificial stability derivatives. The effective control gearings of the rudder and ailerons are chosen so that the right amounts of rolling and yawing result from given displacements of the controls. (This requires feeding lateral stick displacement to both the aileron and rudder servos; rudder position also must go to both servos.) Stick and pedal forces are generated by the method described above.

In simulating lateral motion, it is believed that the important things to simulate are the rolling and yawing motions. These are what the pilot sees as he watches the ground and the horizon, or as he tracks a target. Lateral acceleration is another thing that he can sense, but it is by no means as important a quantity to fly by as is normal acceleration in the longitudinal case. Generally speaking, a pilot is trained to use coordinated maneuvers, and any lateral acceleration that he feels indicates to him only that he has not achieved coordination. He does not try to adjust his rate of turn by increasing or decreasing the lateral acceleration. (Lateral acceleration can comprise an important part of the feel of severe rolling pullout maneuvers. It seems though that at this point it is not worth giving particular attention to simulating this

Approved for Public Release

Contrails

special case.) As with angle of attack, simulation of sideslip angle is of little interest, as the pilot has no direct way of sensing it. The point about the desirability of matching true speed shows up again here. In steady turns, the turning rate comes out high if the speed is low.

The longitudinal phugoid mode receives special treatment for practical reasons. Its period can be varied by producing a pitching moment proportional to change of speed from a reference condition; and its damping can be varied by a pitching moment proportional to rate of change of speed (dV/dt). These effects can be produced by working through the elevator, but the required variations of the elevator angle would be so small that very fine resolution would be required in the elevator servo for satisfactory operation. Instead of working with this problem, it is convenient to use a small auxiliary horizontal surface in the nose of the airplane, driven by a separate servo. This small surface produces the desired results with reasonably large deflections. It would be undesirable to have this surface produce sudden large pitching moments in response to apparent changes in speed caused by gusts. Accordingly, a slow-acting electric servo is used so that an abrupt large deflection cannot be produced. Since the phugoid motion is slow, a slow servo is satisfactory.

It is worth pointing out the need for a considerable degree of versatility in the T-33 feel system. First, it is to be capable of simulating an airplane with plain aerodynamic feel which comes from the control surface hinge moments. Then it must also be capable of simulating artificial feel systems. Some of these are designed, at least in part, to simulate natural aerodynamic feel. Others rely on or emphasize mechanical feel which is not related to hinge moments, by using such devices as bob-weights, springs, and dashpots. A versatile system is needed to cover the simulation of the current wide variety of types of feel. In time, it may be that the design of artificial feel systems will settle down to a relatively small number of standard types, and then the job of simulating them will become easier. Meanwhile, flexibility is necessary. The following types of stick force are to be provided in the T-33:

Elevator

1. Aerodynamic hinge moment due to elevator deflection
2. Aerodynamic hinge moment due to angle of attack

Approved for Public Release

Contrails

3. Trim tab
4. Linear spring, with trimming of position for zero force
5. Non-linear spring
6. Bob-weight
7. Viscous damper
8. Dry friction

Aileron

1. Linear spring
2. Non-linear spring
3. Dry friction

Aerodynamic hinge moments at a particular flight condition can be simulated by choosing a correct linear spring rate. It is believed unnecessary in the aileron case to provide automatic variation of the force gradient with dynamic pressure. This is because current fighter airplanes with irreversible control systems almost universally use simple mechanical springs in the aileron system without speed feel.

Rudder

1. Aerodynamic hinge moment due to rudder deflection
2. Aerodynamic hinge moment due to sideslip angle
3. Linear spring
4. Non-linear spring
5. Dry friction

A further purpose of the T-33 control system is to permit research on cockpit control configurations and various types of response to use of the controls. The system as already described has sufficient flexibility to permit a considerable amount of such work. Unusual combinations of stability derivatives can be set up to give unconventional responses to the controls. Also, as mentioned previously, the test cockpit will be provided with an interchangeable wheel and stick control. Any set of control responses can be evaluated with either the wheel or the stick configuration.

In addition, several special features will be included in the control system

Approved for Public Release

Contrails

to permit evaluation of different types of response to the cockpit controls. One is a computer which will work the rudder to provide automatic coordination of turns. This is aimed simply at reducing the pilot's task by giving him only two controls to work, elevator and ailerons. Another computer will produce an increment of elevator angle as a function of bank angle so that the normal acceleration required to maintain altitude in a turn is automatically provided. These two computers will operate together so that only one control, the ailerons, has to be worked by the pilot in making a turn.

Another idea is to provide a basically different response of the airplane to lateral stick deflection. Normally, a lateral stick deflection produces a steady rolling velocity. An arrangement is to be provided so that instead of this response, a steady bank angle will be produced proportional to lateral stick or wheel deflection.

These specific provisions plus the basic flexibility of the system should be sufficient for conducting a worthwhile initial program of cockpit control research. Further development of the control system can follow from the flight test results of the initial program.

Approved for Public Release

Contrails

SECTION IV

ANALYSIS OF AIRPLANE DYNAMICS AND METHODS OF SIMULATION

BY C.B. NOTESS, H.S. RADT, JR., AND E.R. SCHULTZ

This section includes an analysis of flight simulation, considering the dynamic equations of motion of the airplane. The presentation illustrates how the dynamics of the T-33 can be modified to simulate other aircraft. A discussion of the simulation of control systems is included. The Appendix presents quantitative data for the T-33.

This section is divided into five parts as follows:

A. Simulation of the short period motion within the plane of symmetry
B. Analog computer study of short-period simulation
C. Simulation of the long-period (phugoid) motion within the plane of symmetry
D. Simulation of lateral modes of motion
E. Simulation of control systems

A. SIMULATION OF THE SHORT PERIOD MOTION WITHIN THE PLANE OF SYMMETRY

The following analysis of the short period motion will be based upon the usual approximation of negligible speed changes. The equations of motion taken from Reference 1 can be written as follows:

$$\left[D + 1/2\,(C_{L_\alpha} + C_D)\right]\Delta\alpha - D\Delta\theta = -1/2\,C_{L_{\delta_e}}\,\delta_e \qquad (1)$$

$$\left[C_{m_{D\alpha}}\,D + C_{m_\alpha}\right]\Delta\alpha + \left[-\left(i_y/2\mu_1\right)D^2 + C_{m_{D\theta}}\,D\right]\Delta\theta = -C_{m_{\delta_e}}\,\delta_e \qquad (2)$$

$\Delta\alpha$, $\Delta\theta$ and δ_e are deviations from initial steady values.

Approved for Public Release

Contrails

These equations have been linearized, assuming small disturbances. The coefficient of the $\Delta\theta$ term in equation (1) was simplified by omitting the term $1/2\,(T_c' - C_D)$. T_c' is defined as $\left[\frac{\text{thrust}}{1/2\,\rho V^2 S}\right]$ and therefore, this term is zero if the initial condition of steady level flight is assumed. $C_{m_{D\delta_e}}\, D\delta_e$ was assumed negligible.

In discussing simulation techniques, it is best to work with true time. Therefore, the operator D is replaced by τd which equals $\tau\left(d(\,)/dt\right)$. Rewriting the equations in true time, they become:

$$\left[d + 1/2\,\frac{(C_{L_\alpha} + C_D)}{\tau}\right]\Delta\alpha - d\,\Delta\theta = -1/2\,\frac{C_{L_{\delta_e}}}{\tau}\,\delta_e \qquad (3)$$

$$\left[C_{m_{D\alpha}}\, d + \frac{C_{m_\alpha}}{\tau}\right]\Delta\alpha + \left[-\frac{i_y \tau}{2\mu_1}\, d^2 + C_{m_{D\theta}}\, d\right]\Delta\theta = -\frac{C_{m_{\delta_e}}}{\tau}\,\delta_e \qquad (4)$$

To avoid the need for simulating the coefficient of $d^2\Delta\theta$, multiply equation (4) by $2\mu_1/i_y\tau$

$$\left[\frac{2\mu_1}{i_y\tau}\, C_{m_{D\alpha}}\, d + \frac{2\mu_1}{i_y\tau^2}\, C_{m_\alpha}\right]\Delta\alpha + \left[-d^2 + \frac{2\mu_1}{i_y\tau}\, C_{m_{D\theta}}\, d\right]\Delta\theta = -\frac{2\mu_1}{i_y\tau^2}\, C_{m_{\delta_e}}\,\delta_e \qquad (5)$$

A discussion of the equations (3) and (5) can be simplified by making substitutions of the form $M_\alpha = 2\mu_1 C_{m_\alpha}/i_y\tau^2$, which are defined in Table I. (Note that these definitions are not the same as those sometimes used in writing dimensional equations of motion. For example, L_α in this report does not equal $(1/m)(dL/d\alpha)$.

δ_e can be replaced by $K\delta_s$, where K is the elevator to stick gearing ratio and δ_s is the stick deflection. The equations then become:

$$(d + L_\alpha)\Delta\alpha - d\,\Delta\theta = -L_\delta K\delta_s \qquad (6)$$

$$(M_{\dot\alpha}\, d + M_\alpha)\Delta\alpha + (-d^2 + M_{\dot\theta}\, d)\Delta\theta = -M_\delta K\delta_s \qquad (7)$$

Approved for Public Release

Contrails

The first approach considered for dynamic simulation is that if all the coefficients of the equations of motion can be simulated, the motions in response to a given forcing function will be similar. This implies the simulation of L_α , $M_{\dot{\alpha}}$, M_α , and $M_{\dot{\theta}}$. It will also be necessary to simulate the control effectiveness, that is, the magnitude of the response obtained per unit stick deflection. If these coefficients are all simulated, the variables $\Delta\alpha$, $\Delta\theta$, and δ_s will be simulated. However, it can be shown that unless true speed is simulated, the normal acceleration will not be simulated even though $\Delta\alpha$ and $\Delta\theta$ are simulated. For this reason, the following approach was taken.

The variables present in the short period motion are $\Delta\alpha$, $\Delta\theta$, and δ_s . The normal acceleration or load factor, n_z , can also be considered a variable. Considering the pilot and what he feels in flight, it would appear that the variables to be simulated are $d\theta/dt$ and n_z The correct variation of these quantities is desired in response to a given variation of stick deflection, δ_s . The variable α as such is not of interest to the pilot, as he has no way of sensing it. The question that arises is whether $d\theta/dt$ and n_z can be simulated simultaneously. The change in n_z from the original equilibrium condition is defined as follows:

$$\Delta n_z = \Delta L/W$$

The analog computer program has shown the term $L_\delta K\delta_s$ to be of minor importance. Assuming that it may be neglected, we have

$$\Delta n_z = \frac{C_{L_\alpha} \Delta\alpha \; 1/2 \rho V^2 S}{W}$$

$$= \frac{C_{L_\alpha} V}{2 \frac{m}{\rho V S} g} \Delta\alpha$$

In the definition of $L_\alpha = \frac{C_{L_\alpha} + C_D}{2\tau}$, C_D is usually negligible in comparison to C_{L_α} . Assuming C_D is negligible, we can say

Approved for Public Release

Contrails

$$\frac{\Delta n_z}{\Delta \alpha} = L_\alpha \, V/g \tag{8}$$

Assuming again that the term $L_\delta K \delta_s$ is negligible, equation (6) can be rewritten as:

$$\frac{\Delta \alpha}{\Delta \theta} = \frac{d}{d + L_\alpha} \tag{9}$$

Combining equations (8) and (9):

$$\frac{\Delta n_z}{\dot{\theta}} = \frac{V}{g} L_\alpha \frac{1}{d + L_\alpha} \tag{10}$$

Equation (10) can yield considerable insight into the possibilities of simulating Δn_z and $\dot{\theta}$ at the same time.

It has been shown in Reference 2 that by artificially varying M_α and $M_{\dot{\alpha}}$ it is possible to vary the period and damping of the short period motion over a wide range. Therefore, if this is done, and if $\Delta n_z / \dot{\theta}$ is simulated, the time histories of θ and Δn_z will be simulated.

It remains to be shown whether $\Delta n_z / \dot{\theta}$ can be simulated.

For the steady state case, $d = d( )/dt = 0$ Then

$$\left.\frac{\Delta n_z}{\dot{\theta}}\right|_{ss} = V/g \tag{11}$$

It is clear that unless the true speed is simulated, the steady state value of $\Delta n_z / \dot{\theta}$ will not be simulated. At the higher frequencies used in relatively rapid longitudinal maneuvering (including, in general, the short period natural frequency), the angle of attack and pitch attitude variations become nearly the same:

$$\frac{\Delta \alpha}{\Delta \theta} = \frac{d}{d + L_\alpha} \longrightarrow 1$$

Approved for Public Release

Contrails

This gives

$$\frac{\Delta n_z}{\Delta \theta} \approx L_\alpha \frac{V}{g} = \frac{C_{L_\alpha} \tfrac{1}{2} \rho V^2 S}{W} \qquad (12)$$

By proper choice of a flight altitude and speed, $L_\alpha V/g$ may be simulated. Hence, it is quite possible to simulate very closely the short period transient motion. The short period steady state motion will be simulated only as well as the T-33 can simulate true speed. (Simulation of L_α itself would give the correct phasing between Δn_z and $\dot{\theta}$, but would not give the correct amplitude ratio in transients unless true speed were simulated. We think that it is more important to simulate amplitude ratio than phase.)

We have shown above that for an airplane denoted by the subscript A, it is possible to simulate, as well as the velocity ratio (V_{T-33}/V_A) permits, the time histories of Δn_z and $\dot{\theta}$ with the T-33. The period and damping of the short period motion, as mentioned previously, can be varied over a wide range. By the same methods as used in Reference 2, the amount of artificial stability required can be determined. The results are:

$$\Delta M_\alpha + L_\alpha \Delta M_{\dot{\theta}} = -(k_A - k_{T-33}) \qquad (13)$$

$$\Delta M_{\dot{\alpha}} + \Delta M_{\dot{\theta}} = -(b_A - b_{T-33}) \qquad (14)$$

where

$k_A = \omega_{n_A}^2$

$b_A = 2 \zeta_A \omega_{n_A}$

ω_{n_A} = desired undamped natural frequency (rad/sec)

ζ_A = desired damping ratio

$k_{T-33} = -M_\alpha - L_\alpha M_{\dot{\theta}}$ for the T-33

$b_{T-33} = L_\alpha - M_{\dot{\theta}} - M_{\dot{\alpha}}$ for the T-33

Approved for Public Release

Contrails

L_α on the left side of equation (13) is the value for the T-33

It is seen that there is a choice as to the relative amounts of $\Delta M_{\dot{\alpha}}$ and $\Delta M_{\dot{\theta}}$ to be used in providing artificial damping. It may be desirable in practice to use both, rather than to operate only one channel at a higher gain. The choice makes no basic difference in the short-period motion, but it affects the amount of artificial stability required to simulate the phugoid motion.

The control effectiveness can easily be adjusted to the proper value. The input to the elevator servo from the stick is an electrical signal, and a simple gain adjustment in this channel varies the control effectiveness. Generally, this gain will be set to give the correct Δn_z per unit stick deflection. As described later, the feel system will give the correct stick force per unit stick deflection. Thus, stick force per g will be simulated.

We have been discussing thus far ideal simulation, i. e., simulation without time lags. The lags inherent in the sensing instrumentation, the amplifiers, and the servo actuators affect the results and must be considered.

The method of compensating for the effects of time lags on the artificial derivatives will be discussed in the section on the analog computer investigation, and again in the section on lateral simulation. Therefore, at this time, the fact that compensation for time lag effects on the simulation is possible for the short period motion will be mentioned briefly.

Formulae (13) and (14) can be rewritten as follows for the case of a first order time lag of τ_1 seconds. The additional terms serve to compensate for the time lag effect.

$$\Delta M_\alpha + L_\alpha \Delta M_{\dot{\theta}} = -(k_A - k_{T-33}) - \epsilon k_A \qquad (15)$$

$$\Delta M_{\dot{\alpha}} + \Delta M_{\dot{\theta}} = -(b_A - b_{T-33}) - \tau_1 (k_A - k_{T-33}) - \epsilon b_A \qquad (16)$$

where

$$\epsilon = -\tau_1 (b_A - b_{T-33})$$

Approved for Public Release

Contrails

Experience with equations (15) and (16) indicates that even for values of τ_1 representing reasonably good servo performance, the time lag compensation terms may not be small.

Time lag formulae, equations (15) and (16), are based on two simplifying assumptions; a first order time lag and the same time constant for all input channels. Our experience so far indicates that corrections to the results of the above analysis, due to considering second order time lags and various time constants for the different channels, are relatively small.

One extension of the above analysis is of interest. If an elevator signal proportional to pitching acceleration is provided, the apparent moment of inertia of the airplane can be altered. It has been seen that it is not necessary to do this in order to match the period and damping ratio of the short-period motion. It may, however, be a convenient thing to do, because if some of the required artificial stability is provided this way, there is less to be provided by the other channels. The question of simultaneous matching of n_z and $\dot{\theta}$ is not affected by the addition of this type of artificial stability.

Equations corresponding to (15) and (16) can be derived, including "artificial inertia". The results are as follows:

$$\Delta M_\alpha + L_\alpha \Delta M_{\dot\theta} = -(k_A - k_{T-33}) - \epsilon k_A \tag{17}$$

$$\Delta M_{\dot\alpha} + \Delta M_{\dot\theta} = -(b_A - b_{T-33}) - \tau_1(k_A - k_{T-33}) - \epsilon b_A - k_{\ddot\theta} L_\alpha M_\delta \tag{18}$$

where now

$$\epsilon = -k_{\ddot\theta} M_\delta - \tau_1 (b_A - b_{T-33})$$

$$k_{\ddot\theta} = \partial\delta_e / \partial\ddot\theta \ , \ sec^2$$

L_α , M_δ are T-33 values

It has been assumed that the artificial inertia channel has the same first order time lag as was assumed for the other artificial stability channels. It is seen that $k_{\ddot\theta}$ can be used to allow changes of the required values of the other

Approved for Public Release

Contrails

artificial stability derivatives.

B. ANALOG COMPUTER STUDIES OF SHORT PERIOD SIMULATION

1. GENERAL

The purpose of the first work carried out on the analog computer was to establish typical short-period characteristics for supersonic aircraft, and then to simulate these characteristics with the T-33 aircraft. A particular problem investigated was the effect of servo system lags on the short period stability. Both the BEAC and EASE analog computers owned by the Laboratory were used in these studies.

The initial approach was to try to match the equations of motion term by term. This meant, among other things, choosing speed and altitude to match the derivative L_α. It was during this investigation that it was found better to match $L_\alpha \, V/g$. As will be seen, this was a principal result of the analog computer work.

The basic short-period equations used were developed in part A of this section. Equations (6) and (7) can be rewritten as:

$$(d + L_\alpha)\Delta\alpha - d\Delta\theta = -L_\delta \delta_e \tag{19}$$

$$(-M_{\dot\alpha} d - M_\alpha)\Delta\alpha + (d^2 - M_{\dot\theta} d)\Delta\theta = M_\delta \delta_e \tag{20}$$

(See Table I for the particular definitions used here.)

2. SIMULATION WITH NO SYSTEM TIME LAG

For simulation of the characteristic longitudinal short-period mode by the T-33 aircraft, the following approach was used, assuming an ideal servo (i.e., no system time lag):

(a) Write the short-period equations for the T-33, including the artificial derivatives, and for the aircraft to simulated,

Approved for Public Release

Contrails

T-33

$$\left[d + (L_\alpha)_{T-33}\right]\alpha - d\theta = -(L_\delta)_{T-33}\,\delta_e \tag{21}$$

$$-\left[(M_{\dot\alpha})_{T-33}\,d + \Delta M_{\dot\alpha}\,d + (M_\alpha)_{T-33} + \Delta M_\alpha\right]\alpha + \left[d^2 - (M_{\dot\theta})_{T-33}\,d - \Delta M_{\dot\theta}\,d\right]\theta = (KM_\delta)_{T-33}\,\delta_S \tag{22}$$

Aircraft "A"

$$\left[d + (L_\alpha)_A\right]\alpha - d\theta = -(L_\delta)_A\,\delta_e \tag{19}$$

$$-\left[(M_{\dot\alpha})_A\,d + (M_\alpha)_A\right]\alpha + \left[d^2 - (M_{\dot\theta})_A\,d\right]\theta = (KM_\delta)_A\,\delta_S \tag{20}$$

(b) Equate the coefficients of the two sets of equations as follows:

$$(L_\alpha)_{T-33} = (L_\alpha)_A$$

$$(M_\alpha)_{T-33} + \Delta M_\alpha = (M_\alpha)_A$$

$$(M_{\dot\alpha})_{T-33} + \Delta M_{\dot\alpha} = (M_{\dot\alpha})_A$$

$$(M_{\dot\theta})_{T-33} + \Delta M_{\dot\theta} = (M_{\dot\theta})_A$$

$$(KM_\delta)_{T-33} = (KM_\delta)_A$$

It is not practical to vary the C_{L_α} term in L_α, but the terms may be matched by the proper selection of altitude and Mach number.

(c) Solve for the artificial derivatives:

$$\Delta M_\alpha = (M_\alpha)_A - (M_\alpha)_{T-33} \tag{23}$$

Approved for Public Release

Contrails

$$\Delta M_{\dot{\alpha}} = (M_{\dot{\alpha}})_A - (M_{\dot{\alpha}})_{T-33} \tag{24}$$

$$\Delta M_{\dot{\theta}} = (M_{\dot{\theta}})_A - (M_{\dot{\theta}})_{T-33} \tag{25}$$

(d) The artificial stability is obtained physically by positioning the elevator proportional to α , $\dot{\alpha}$, and $\dot{\theta}$. Therefore, the elevator motion may be rewritten as follows:

$$\delta_e = \delta_0 + \delta_\alpha \alpha + \delta_{\dot{\alpha}} \dot{\alpha} + \delta_{\dot{\theta}} \dot{\theta} \tag{26}$$

where $\delta_0 = K\delta_S =$ Pilot's input

$$\delta_\alpha = \Delta M_\alpha / (M_\delta)_{T-33}$$

$$\delta_{\dot{\alpha}} = \Delta M_{\dot{\alpha}} / (M_\delta)_{T-33}$$

$$\delta_{\dot{\theta}} = \Delta M_{\dot{\theta}} / (M_\delta)_{T-33}$$

(e) The complete equations for the longitudinal short-period mode of the T-33 with an ideal servo can now be written as follows:

$$[d + (L_\alpha)_{T-33}]\alpha - d\theta = -(L_\delta)_{T-33}\,\delta_e \tag{19}$$

$$-[(M_{\dot{\alpha}})_{T-33}\,d + (M_\alpha)_{T-33}]\alpha + [d^2 - (M_{\dot{\theta}})_{T-33}\,d]\theta = (M_\delta)_{T-33}\,\delta_e \tag{20}$$

$$\delta_e = \delta_0 + \delta_\alpha \alpha + \delta_{\dot{\alpha}} \dot{\alpha} + \delta_{\dot{\theta}} \dot{\theta} \tag{26}$$

3. SIMULATION WITH FIRST-ORDER SERVO LAG

The short-period equations of motion for the T-33, considering a first order elevator servo lag, may be written as follows:

Approved for Public Release

Contrails

$$[d + L_\alpha]\alpha - d\theta = -L_\delta \delta_e \tag{27}$$

$$\left[-M_{\dot\alpha} d - \frac{\Delta M_{\dot\alpha} d}{1+\tau_1 d} - M_\alpha - \frac{\Delta M_\alpha}{1+\tau_1 d}\right]\alpha$$

$$+\left[d^2 - M_{\dot\theta} d - \frac{\Delta M_{\dot\theta} d}{1+\tau_1 d}\right]\theta = (K M_\delta)\ \frac{\delta_s}{1+\tau_1 d} \tag{28}$$

where τ_1 = elevator servo time lag.

For fixed-control stability, assume the pilot's input equals zero. Actually the elevator in providing artificial stability will move in response to α , $\dot\alpha$, and $\dot\theta$. The resulting effects on lift due to C_{L_δ} are negligible, and so the lift equation becomes

$$d\theta = [d + L_\alpha]\alpha$$

Substituting this into the moment equation:

$$\left[-M_{\dot\alpha} d - \frac{\Delta M_{\dot\alpha} d}{1+\tau_1 d} - M_\alpha - \frac{\Delta M_\alpha}{1+\tau_1 d}\right.$$

$$\left. + \left(d - M_{\dot\theta} - \frac{\Delta M_{\dot\theta}}{1+\tau_1 d}\right)\ (d + L_\alpha)\right]\alpha = 0 \tag{29}$$

or

$$d^2 + \left[L_\alpha - M_{\dot\alpha} - \frac{\Delta M_{\dot\alpha}}{1+\tau_1 d} - M_{\dot\theta} - \frac{\Delta M_{\dot\theta}}{1+\tau_1 d}\right] d$$

$$+\left[-M_\alpha - \frac{\Delta M_\alpha}{1+\tau_1 d} - L_\alpha M_{\dot\theta} - L_\alpha\left(\frac{\Delta M_{\dot\theta}}{1+\tau_1 d}\right)\right] = 0$$

If the artificial stability is removed, the equation reduces to that of a second-order system.

$$d^2 + (L_\alpha - M_{\dot\theta} - M_{\dot\alpha})d + (-M_\alpha - L_\alpha M_{\dot\theta}) = 0 \tag{30}$$

For the T-33 let

$$b_{T-33} = L_\alpha - M_{\dot\theta} - M_{\dot\alpha} \tag{31}$$

Approved for Public Release

Contrails

$$k_{T-33} = -M_\alpha - L_\alpha M_{\dot\theta} \tag{32}$$

then

$$d^2 + b_{T-33}\, d + k_{T-33} = 0 \tag{33}$$

This equation defines the short-period characteristics of the normal T-33.

Equation (29) for the T-33 with artificial stability may now be rewritten as follows:

$$d^2 + \left[b_{T-33} - \frac{\Delta M_{\dot\theta}}{1+\tau_1 d} - \frac{\Delta M_{\dot\alpha}}{1+\tau_1 d}\right] d$$
$$+ \left[k_{T-33} - \frac{\Delta M_\alpha}{1+\tau_1 d} - L_\alpha \frac{\Delta M_{\dot\theta}}{1+\tau_1 d}\right] = 0$$

Multiplying by $(1+\tau_1 d)$:

$$\tau_1 d^3 + \left[1+\tau_1 b_{T-33}\right] d^2 + \left[b_{T-33} + \tau_1 k_{T-33} - \Delta M_{\dot\theta} - \Delta M_{\dot\alpha}\right] d$$
$$+ \left[k_{T-33} - \Delta M_\alpha - L_\alpha \Delta M_{\dot\theta}\right] = 0 \tag{34}$$

Assume this can be factored as follows:

$$(\tau_1 d + 1 + \epsilon)(d^2 + b_A d + k_A) = 0 \tag{35}$$

Now assume an Aircraft "A" which has the typical short-period characteristics mentioned above. We wish, then, to make the two roots represented by the quadratic factor in equation (35) equal to those of Aircraft "A", which is to be simulated. Hence the subscript A in equation (35) refers to Aircraft "A". (The third root is a mode associated with the servo dynamics.)

Expanding equation (35), the following is obtained:

$$\tau_1 d^3 + (1 + \epsilon + \tau_1 b_A) d^2 + (b_A + \epsilon b_A + \tau_1 k_A) d + (k_A + \epsilon k_A) = 0 \tag{36}$$

This equation has the two roots which define the short-period mode of Aircraft "A". In order to determine the value of the T-33 artificial derivatives,

Approved for Public Release

Contrails

it is now necessary to equate the coefficients of equation (36) with those of equation (34), with the following results:

$$\epsilon = -\tau_1 (b_A - b_{T-33}) \tag{37}$$

$$\Delta M_{\dot{\alpha}} + \Delta M_{\dot{\theta}} = -(b_A - b_{T-33}) - \epsilon b_A - \tau_1 (k_A - k_{T-33}) \tag{38}$$

$$\Delta M_{\alpha} + L_{\alpha} \Delta M_{\dot{\theta}} = -(k_A - k_{T-33}) - \epsilon k_A \tag{39}$$

Knowing the dynamics of the normal T-33 and the aircraft to be simulated, it is possible to solve for the required artificial derivatives. The choice of the artificial damping term $\Delta M_{\dot{\theta}}$ was made assuming no time lag, i.e.,

$$\Delta M_{\dot{\theta}} = (M_{\dot{\theta}})_A - (M_{\dot{\theta}})_{T-33}$$

The elevator deflection equation may be written as follows:

$$\delta_e = \frac{\delta_0 + \delta_\alpha \alpha + \delta_{\dot{\alpha}} \dot{\alpha} + \delta_{\dot{\theta}} \dot{\theta}}{1 + \tau_1 d} \tag{40}$$

4. SIMULATION WITH SECOND-ORDER SERVO SYSTEM LAG

The compensated artificial derivatives were calculated assuming a first order time lag as in the preceding section. The value of time lag used was taken as $\tau_1 = 2\zeta/\omega_n$ seconds, where ζ and ω_n refer to the damping ratio and undamped natural frequency of the second-order servo. ($2\zeta/\omega_n$ is the time lag of a second-order system in response to a ramp input. It also closely represents the lag of a second-order system in response to frequencies much lower than ω_n .) This approximation is sufficiently accurate if the ratio of the airplane short-period frequency to the natural frequency of the servo is small compared to 1.0. In the analog computer tests discussed in the next section, certain runs were made representing a second-order servo lag but with the artificial derivatives selected for compensation with a first-order lag.

Approved for Public Release

Contrails

The equation defining the motion of the elevator powered by a second-order servo is as follows:

$$\delta_e = \frac{\delta_0 + \delta_\alpha \alpha + \delta_{\dot\alpha} \dot\alpha + \delta_{\dot\theta} \dot\theta}{1 + 2\zeta/\omega_n \, d + d^2/\omega_n^2} \qquad (41)$$

5. RESULTS OF ANALOG COMPUTER TESTS

(a) Simulation of Case "A".

In order to simulate the typical characteristics assumed for Case "A", it is first necessary to know the aerodynamic characteristics of the T-33. For the T-33, a Mach number of 0.65 at an altitude of 10,500 feet was chosen to obtain the desired L_α . The aerodynamic coefficients required for the solution of the short-period equations are presented below:

COEFFICIENT	T-33
L_α	2.34
L_δ	0.135
M_α	-8.73
$M_{\dot\alpha}$	-0.531
$M_{\dot\theta}$	-1.173
M_δ	-27.7

(See Table I for the particular definitions used here.)

The artificial derivatives required for simulation of the typical characteristics are presented below:

ARTIFICIAL DERIVATIVE	TIME LAG	
	NONE	0.05 SECONDS FIRST-ORDER LAG
ΔM_α	-97.4	-93.3
$\Delta M_{\dot\alpha}$	-0.250	-4.98
$\Delta M_{\dot\theta}$	-0.527	-0.527

Approved for Public Release

Contrails

Particularly noteworthy is the large increase in damping required to compensate for the time lag. This occurs because ΔM_α is so large. This particular case was chosen to give the largest ΔM_α likely to be required. In more normal cases, considerably less compensation would be required. In this case, with time lag, $\sigma_{\dot{\alpha}}$ has a value of 0.180 deg/(deg/sec), which would indicate the advisability of keeping the noise level on the α pickup as low as possible.

The accuracy with which the T-33 can simulate aircraft "A" is perhaps best shown by comparing the damping and frequency of the normal accelerations, n_z, for the two aircraft as determined from calculations and from the analog computer.

Figure 1 presents BEAC runs of the T-33 simulating the typical characteristics represented by Aircraft "A". The data presented in Table II were obtained from these traces.

The steady-state n_z has been simulated by adjusting the pilots input (σ_0). This can be obtained physically on the T-33 by varying the elevator-stick gear ratio. In comparing the frequency and damping ratio of n_z on Record 6 with Record 1, it will be noted that excellent simulation was obtained.

Record 5 shows the effect of time lag without compensating the artificial derivatives. Record 6 illustrates the effect of compensating the artificial derivatives for time lag. It will be noted that with the proper compensation, the simula-

Approved for Public Release

Contrails

tion of normal acceleration is certainly accurate to the point that a pilot would not be able to distinguish the difference in the n_z of the two aircraft.

It is not possible to simulate both steady-state n_z and $\dot{\theta}$ unless the true speed can be matched. Since the T-33 is limited to 0.8 Mach number, it is not possible to obtain simultaneous simulation of both parameters at transonic and supersonic speeds.

It will be noted in Figure 1 that the simulation of the $\dot{\theta}$ transient motion was poor in that the magnitude of the variation for the T-33 was considerably too large. The T-33 flight condition was selected to match the L_α terms in the short-period equation, i.e., $(L_\alpha)_{T-33} = (L_\alpha)_A$. If, however, the flight condition had been selected such that C_{L_0}/C_{L_α} (which equals $L_\alpha V/g$) was matched, then the $\dot{\theta}$ transient would have been more accurately simulated. Unfortunately, records were obtained at only one flight condition so it was not possible to check this theory on the aircraft "A" runs.

(b) Simulation of Case "B"

A set of less severe typical characteristics was determined in order to investigate the effects of T-33 flight condition on accuracy of simulation. These characteristics will be referred to as those of aircraft "B", and are representative of transonic aircraft. Case "B" was simulated by the T-33, considering two different flight conditions for the T-33. The first flight condition considered was the same as that used in the simulation of case "A", while the second flight condition was such as to match L_α. A summary of the results is presented in Table III.

Approved for Public Release

Contrails

Sample traces from which the above damping ratios and frequencies were measured are presented in Figure 2. It will be noted that in all cases the simulation of normal acceleration (n_z) was satisfactory with the exception of runs 8 and 9 in which simulation was not expected.

In comparing records 3 and 4 with record 1, it can be seen that the simulation of α and $\dot{\theta}$ is superior at 10,500 ft altitude. At 10,500 ft altitude the T-33 was at a C_L more nearly approximating the relationship

$$(C_L)_{T-33} = \frac{(C_{L_\alpha})_{T-33}}{(C_{L_\alpha})_B} (C_L)_B$$, which accounts for the improved simulation of the transient variation of α and $\dot{\theta}$.

Records 10 and 11 show the effect of time lag on the elevator motion. In both records, the upper trace is the signal to the servo with no lag. The lower trace is the actual elevator motion with time lag.

(c) Effect of Time Lag on the Short-Period Stability

Figure 3 presents the effect of time lag on the short-period stability. Records 1 through 5 show the effect of incremental increases in time lag holding the artificial derivatives constant. The most obvious result of increasing time lags is the decrease in damping. With a 0.06 second first-order lag, the aircraft is only slightly damped and is approaching neutral stability.

Records 6 through 10 present the effect of incremental increases in time lag but with the artificial derivatives selected to compensate for the lag. With a lag of 0.10 seconds (Record

Approved for Public Release

Contrails

10), which is much higher than would be obtained with a good servo, there is no indication of instability.

In conclusion, it appears that the physical parameters (n_z and $\dot{\theta}$) which the pilot senses during the longitudinal motion of the typical supersonic fighters considered in this study, can be satisfactorily simulated using the T-33 aircraft. Care must be taken in setting up the initial flight conditions on the T-33 to simulate true speed as closely as possible, and then to adjust the altitude so as to simulate C_{L_o} / C_{L_α}.

The system time lags considered in the analysis could be compensated for by adjusting the values of the artificial derivatives, resulting in satisfactory values of frequency and damping being obtained. In general, however, it is believed that the most satisfactory over-all performance will be obtained if the required amount of compensation for time lag is kept to a reasonable minimum. Considering this and also the question of what servo performance is reasonably attainable, it was decided that the control system should be designed to have no more lag than a second-order system with an undamped natural frequency of 7.5 cps and a damping ratio of 0.7. The results given in this section show that compensation for this amount of time lag should be practical and satisfactory.

C. SIMULATION OF THE LONG PERIOD (PHUGOID) MOTION WITHIN THE PLANE OF SYMMETRY

The three equations of motion necessary for the phugoid analysis were taken from Reference 1.

$$\left[D + C_D - T_V + \frac{MC_{D_M}}{2}\right]\frac{\Delta V}{V_o} + \left[\frac{C_{D_\alpha} - C_L}{2}\right]\Delta\alpha + \left[\frac{C_{L_o} + nT_c'}{2}\right]\Delta\theta = 0 \quad (42)$$

Approved for Public Release

Contrails

$$\left[C_L + \eta T_V + \frac{MC_{L_M}}{2}\right]\frac{\Delta V}{V_0} + \left[D + \frac{C_{L_\alpha} + C_D}{2}\right]\Delta\alpha + \left[-D + \frac{T_c' - C_D}{2}\right]\Delta\theta = -\tfrac{1}{2}C_{L_\delta}\delta_e \qquad (43)$$

$$\left[-DC_{m_{DV}} - C_{m_V} - 2C_{m_o} + 2\left(\tfrac{z_T}{c}\right)T_V - MC_{m_M}\right]\frac{\Delta V}{V_0} + \left[-DC_{m_{D\alpha}} - C_{m_\alpha}\right]\Delta\alpha + \left[\frac{i_y}{2\mu_1}D^2 - DC_{m_{D\theta}}\right]\Delta\theta = (C_{m_\delta})\delta_e \qquad (44)$$

(T_V represents the variation of thrust with speed. It is defined as $T_V = \dfrac{dT/dV}{\rho V_0 S}$)

In the discussion of the short-period motion it was noted that the natural initial approach to the question of simulating an airplane is to try to simulate each coefficient in the equations of motion. However, if equations (42) and (43) are considered, it should be clear that it will be very difficult, if possible at all, to simulate C_{D_α}, T_V, C_D, C_L and C_{L_α} all at the same time. Therefore, the simulation of the phugoid motion must be accomplished in another way. Reference 2 has shown that the phugoid period and damping can be varied over a wide range with the aid of an auxiliary surface which provides artificial C_{m_V} and $C_{m_{DV}}$.

The coefficients C_{m_V} and $C_{m_{DV}}$ are artificial terms which are zero for a normal airplane. They were added here because they are useful in varying the character of the phugoid oscillation as will be seen later.

Simulation of the phugoid will be approached in a manner similar to that of that of Reference 3. A quadratic equation closely representing the phugoid oscillation may be obtained by dividing the quartic characteristic equation by the constant speed short period quadratic characteristic equation. A derivation of the phugoid oscillation quadratic characteristic equation employing the

Approved for Public Release

Contrails

preceding method is given below.

Using the notation defined in Table I, equations (42), (43), and (44) can be simplified to:

$$(d + D_v)\frac{\Delta V}{V_o} + D_\alpha \Delta\alpha + D_\theta \Delta\theta = 0 \tag{45}$$

$$L_v \frac{\Delta V}{V_o} + (d + L_\alpha)\Delta\alpha - d\Delta\theta = -L_\delta K\delta_s \tag{46}$$

$$(M_{\dot{v}} d + M_v)\frac{\Delta V}{V_o} + (M_{\dot{\alpha}} d + M_\alpha)\Delta\alpha - (d^2 - M_{\dot{\theta}} d)\Delta\theta = -M_\delta K\delta_s \tag{47}$$

Assuming initially straight and level flight, $T_c' = C_D$ and therefore, the coefficient of $\Delta\theta$ in equation (46) reduces to $(-d)$. K is the elevator-stick gearing rato.

The determinant representing the characteristic equation of motion can be written from equations (45), (46), and (47).

$$\begin{vmatrix} d + D_v & D_\alpha & D_\theta \\ L_v & d + L_\alpha & -d \\ -M_{\dot{v}} d - M_v & -M_{\dot{\alpha}} d - M_\alpha & d^2 - M_{\dot{\theta}} d \end{vmatrix}$$

This determinant can be expanded into a quartic expression in the operator d.

$$d^4 + a_3 d^3 + a_2 d^2 + a_1 d + a_0 \tag{48}$$

The quartic can be represented by two quadratic factors

$$(d^2 + b_1 d + k_1)(d^2 + b_2 d + k_2) \tag{49}$$

The phugoid motion is represented by the first factor and the short period by the second. From equations (31) and (32) a good approximation to b_2 and

Approved for Public Release

Contrails

k_2 can be obtained.

$$b_2 = L_\alpha - M_{\dot\theta} - M_{\dot\alpha} \tag{31}$$

$$k_2 = -(M_\alpha + L_\alpha M_{\dot\theta}) \tag{32}$$

A good approximation to the coefficients of the phugoid quadratic can be found as follows: The expression (49) is an alternate representation of the quartic, (48), and so the coefficients of corresponding powers of d should be the same. By setting the constant terms equal to each other, and then the terms in the first power of d, we obtain the following expressions:

$$k_1 = a_0 / k_2 \tag{50}$$

$$b_1 = (a_1 - b_2 k_1) / k_2 \tag{51}$$

The phugoid period and damping ratio are expressed as

$$\zeta_p = \frac{b_1}{2\sqrt{k_1}} \tag{52}$$

$$P = \frac{2\pi}{[k_1(1-\zeta_p^2)]^{1/2}} \tag{53}$$

Now by expanding the determinant, a_1 and a_0 are:

$$a_1 = -D_V(M_\alpha + L_\alpha M_{\dot\theta}) + D_\alpha(M_V + L_V M_{\dot\theta}) + D_\theta(M_{\dot V} + L_\alpha M_{\dot V} - L_V M_{\dot\alpha}) \tag{54}$$

$$a_0 = D_\theta(L_\alpha M_V - L_V M_\alpha) \tag{55}$$

From equations (55), (32), (50), and (53) the period becomes

$$P = 2\pi\left[\frac{M_\alpha + L_\alpha M_{\dot\theta}}{D_\theta(L_V M_\alpha - L_\alpha M_V)(1-\zeta_p^2)}\right]^{1/2} \tag{56}$$

Approved for Public Release

Contrails

Likewise combining the above eight equations, the damping ratio can be obtained as

$$\zeta_p = \left[\frac{M_\alpha + L_\alpha M_{\dot\theta}}{4D_\theta(L_v M_\alpha - L_\alpha M_v)}\right]^{1/2}\left\{D_v - \frac{D_\alpha(M_v + L_v M_{\dot\theta}) + D_\theta(M_v + L_\alpha M_{\dot v} - L_v M_\alpha)}{M_\alpha + L_\alpha M_{\dot\theta}} + \frac{D_\theta(L_v M_\alpha - L_\alpha M_v)(L_\alpha - M_{\dot\theta} - M_{\dot\alpha})}{(M_\alpha + L_\alpha M_{\dot\theta})^2}\right\} \quad (57)$$

(See Table I for the particular definitions used here.)

From equation (56) it is evident that one term which can be varied to affect only the phugoid is M_v. When $M_v = 0$, P is that of the normal T-33. When M_v is not zero the period will be equal to $P + \Delta P$. Divide the equation for P by that for $P + \Delta P$ and solve for M_v. The result, assuming no change in ζ_p, is:

$$M_v = \frac{L_v M_\alpha}{L_\alpha}\,\frac{2\frac{\Delta P}{P} + \left(\frac{\Delta P}{P}\right)^2}{\left(1 + \frac{\Delta P}{P}\right)^2} \quad (58)$$

where P is the phugoid period of the T-33A with $M_v = 0$. ΔP is the desired change in period. The phugoid damping ratio is usually much less than unity so that for a good first approximation to the value of artificial M_v, the change in ζ_p^2 can be neglected.

$M_{\dot v}$ is the only term which affects only the phugoid damping ratio. The amount of artificial $M_{\dot v}$ necessary for controlling ζ_p can be obtained from equation (57) by solving for $M_{\dot v}$. The result is

Approved for Public Release

Contrails

$$M_{\dot{v}} = \frac{M_\alpha + L_\alpha M_{\dot{\theta}}}{L_\alpha D_\theta}\left\{-\zeta_p\left[\frac{4D_\theta(L_v M_\alpha - L_\alpha M_v)}{M_\alpha + L_\alpha M_{\dot{\theta}}}\right]^{\frac{1}{2}} + D_v\right.$$

$$\left. + \frac{D_\theta(L_v M_\alpha - L_\alpha M_v)(L_\alpha - M_{\dot{\theta}} - M_{\dot{\alpha}})}{(M_\alpha + L_\alpha M_{\dot{\theta}})^2} - \frac{D_\alpha(M_v + L_v M_{\dot{\theta}}) + D_\theta(M_v - L_v M_\alpha)}{M_\alpha + L_\alpha M_{\dot{\theta}}}\right\} \quad (59)$$

where ζ_p is the desired damping ratio.

Thus it has been shown that the phugoid period and damping can be controlled by artificial M_v and $M_{\dot{v}}$.

D. SIMULATION OF LATERAL MODES OF MOTION

1. DISCUSSION OF THE EQUATIONS OF MOTION

As mentioned in Section III, the significant variables for lateral simulation are the yawing and rolling motions, possibly the lateral acceleration, and the stick and rudder pedal forces and deflections. Hence, these are the variables which should be made as nearly equal as possible for the test airplane and the airplane to be simulated. In order to demonstrate a method of producing the above result, the lateral equations of motion will be investigated. As defined and written in Reference 1, these equations are:

$$\frac{1}{\mu_2}\left[D - \frac{1}{2}C_{Y_\beta}\right]\beta + \left[\left(2 - \frac{C_{Y_r}}{2\mu_2}\right) - \frac{W\sin\gamma_0}{Sq}D^{-1}\right]\left(\frac{rb}{2V_0}\right)$$

$$+ \left[-\frac{C_{Y_p}}{2\mu_2} - \frac{W\cos\gamma_0}{Sq}D^{-1}\right]\left(\frac{pb}{2V_0}\right) = \frac{1}{2\mu_2}C_{Y_{\delta_r}}\delta_r \quad (60)$$

$$-C_{\ell_\beta}\beta + \left[-i_{xz}D - C_{\ell_r}\right]\left(\frac{rb}{2V_0}\right) + \left[i_x D - C_{\ell_p}\right]\left(\frac{pb}{2V_0}\right) = C_{\ell_{\delta_a}}\delta_a + C_{\ell_{\delta_r}}\delta_r \quad (61)$$

Approved for Public Release

Contrails

$$-C_{n_\beta}\beta+\left[i_z D-C_{n_r}\right]\left(\frac{rb}{2V_0}\right)+\left[-i_{xz} D-C_{n_p}\right]\left(\frac{pb}{2V_0}\right)=C_{n_{\delta_a}}\delta_a+C_{n_{\delta_r}}\delta_r \qquad (62)$$

This non-dimensional form is inconvenient for demonstrating a simulation technique and should therefore be changed to a form using real time and having the actual roll and yaw rates as independent variables. In addition, the equations can be rearranged so that the product of inertia effects are absorbed into the coefficients, and so that the coefficients of the highest order terms are made unity. When these changes are made, the equations become:

$$(d-Y_\beta)\beta+\left[(1-Y_r)-V_\psi d^{-1}\right]r+\left[-Y_\phi d^{-1}-Y_p\right]p=Y_{\delta_r}\delta_r \qquad (63)$$

$$-L_\beta\beta-L_r r+(d-L_p)p=L_{\delta_a}\delta_a+L_{\delta_r}\delta_r \qquad (64)$$

$$-N_\beta\beta+(d-N_r)r-N_p p=N_{\delta_a}\delta_a+N_{\delta_r}\delta_r \qquad (65)$$

The coefficients in the above equations are defined in Table IV. (Note that these definitions are not the same as those sometimes used in writing dimensional equations of motion. For example, Y_β does not equal $(1/m)(dY/d\beta)$, and N_β does not simply equal $(1/I_z)(dN/d\beta)$.) Equations (63), (64), and (65) represent the equations of motion of an airplane to be simulated, while a similar set of equations with the subscript "1" on the coefficients will be used to represent the test airplane. The procedure is now to attempt to obtain identical motions of both airplanes by making the corresponding coefficients on the left hand sides of these equations equal. In addition, the gearing ratios between the cockpit controls and the control surfaces are to be adjusted so that the same rolling and yawing accelerations will result from equal, pilot-applied, control deflections.

The differences in corresponding aerodynamic coefficients in equations (64) and (65) for the two airplanes, may be corrected by de-

Approved for Public Release

Contrails

flecting the rudder and ailerons of the test airplane proportional to the various independent variables, through position servos. Thus, the rudder and aileron deflections may be written:

$$\delta_r = \frac{\partial \delta_r}{\partial \beta}\beta + \frac{\partial \delta_r}{\partial r} r + \frac{\partial \delta_r}{\partial p} p + \frac{\partial \delta_r}{\partial \delta_{RP}} \delta_{RP} + \frac{\partial \delta_r}{\partial \delta_{AS}} \delta_{AS} \tag{66}$$

$$\delta_a = \frac{\partial \delta_a}{\partial \beta}\beta + \frac{\partial \delta_a}{\partial r} r + \frac{\partial \delta_a}{\partial p} p + \frac{\partial \delta_a}{\partial \delta_{RP}} \delta_{RP} + \frac{\partial \delta_a}{\partial \delta_{AS}} \delta_{AS} \tag{67}$$

where δ_{RP} is the rudder pedal deflection and δ_{AS} is the transverse stick or "aileron stick" deflection. Provided the effects of position servo dynamics are negligible, the corresponding coefficients of β in equation (64), for example, may be made equal as follows:

$$L_{\beta_1} + L_{\delta_{r_1}} \frac{\partial \delta_r}{\partial \beta} + L_{\delta_{a_1}} \frac{\partial \delta_a}{\partial \beta} = L_\beta \tag{68}$$

The factors $\frac{\partial \delta_r}{\partial \beta}$ and $\frac{\partial \delta_a}{\partial \beta}$ are adjusted, as required, by suitable gain settings in the control system. Similar relationships may be written for the other coefficients and for the gearing between rudder, ailerons, rudder pedals, and aileron stick, making equations (64) and (65) identical for the two airplanes. If it were also possible to make the side force equations identical, simulation would be accomplished. Matching of all the aerodynamic coefficients as described above would guarantee the proper phase and amplitude relationships among the various independent variables in each of the lateral modes, while adjusting the gearing ratios would determine the proper magnitude of each mode excited for a given control input. It now remains to discuss the effects of servo dynamics and differences in the side force equations.

2. EFFECTS OF THE SIDE FORCE EQUATIONS

In determining the effects of the side force equation it is of

Approved for Public Release

Contrails

interest to substitute equation (66) into equation (63) and to transpose terms.

$$\left[d - \left(Y_{\beta_1} + Y_{\delta_{r_1}} \frac{\partial \delta_r}{\partial \beta}\right)\right]\beta + \left[1 - \left(Y_{r_1} + Y_{\delta_{r_1}} \frac{\partial \delta_r}{\partial r}\right) - Y_{\psi_1} d^{-1}\right] r$$

$$+ \left[-Y_\phi d^{-1} - \left(Y_{p_1} + Y_{\delta_{r_1}} \frac{\partial \delta_r}{\partial p}\right)\right] p = Y_{\delta_{r_1}} \left[\frac{\partial \delta_r}{\partial \delta_{RP}} \delta_{RP} + \frac{\partial \delta_r}{\partial \delta_{AS}} \delta_{AS}\right]$$

The $\left(Y_{r_1} + Y_{\delta_{r_1}} \frac{\partial \delta_r}{\partial r}\right)$ term and the $\left(Y_{p_1} + Y_{\delta_{r_1}} \frac{\partial \delta_r}{\partial p}\right)$ term are generally negligible and the Y_ψ term is zero for a level flight reference condition, which is the principal case of interest. On the other hand, the $Y_{\delta_{r_1}} \left(\frac{\partial \delta_r}{\partial \beta}\right)$ constitutes a considerable change in the effective Y_{β_1} term. Hence, it is desirable to choose the T-33 flight condition such that

$$\left(Y_{\beta_1} + Y_{\delta_{r_1}} \frac{\partial \delta_r}{\partial \beta}\right) = Y_\beta \tag{69}$$

For the spiral mode, the characteristic time is nearly proportional to $1/Y_\phi$ or $\left(V_o / g \cos \gamma_o\right)$. This shows for level flight, that it is necessary to fly at the same true airspeed in order to simulate the spiral mode accurately, providing the coefficients of equations (64) and (65) are chosen as mentioned. If the above conditions are satisfied, then the frequency and damping of the Dutch roll oscillation and the characteristic time of the roll mode would be very nearly matched. The terms on the right-hand side of the side force equation have no effect on the fixed cockpit control motion within each of the separate lateral modes. They do affect the relative magnitudes of these modes for a given cockpit control motion, but are generally not of importance compared to the cockpit control effects on the rolling moment and yawing moment equations.

Approved for Public Release

Contrails

The side load factor at the center of gravity, n_y , is related to the airplane motions by the following expression (for the level flight case)

$$n_y + \sin\phi = \left(V_o/g\right)(r + \dot{\beta}) \tag{70}$$

If the three equations of motion are simulated well enough so that correct variations of ϕ , r , and β , are obtained, and if furthermore true airspeed is simulated, then it is seen that the side load factor also will be matched.

Now assume that the altitude and speed are chosen to satisfy equation (69) but the true airspeed of the test airplane is lower than for the airplane to be simulated. In this condition, the rate of change of flight path direction, $(r + \dot{\beta})$, resulting either from aerodynamic side force or bank angle, will be too large in the same ratio that the speed is too small.

It should be mentioned that under certain test conditions, it may be desirable to determine the flight condition other than by equation (69) for the purpose of matching more closely the side load factor at the pilot's location during a transient maneuver. Also, more accurate simulation of the spiral mode may be attainable by relaxing slightly the conditions for simulation of the other modes of fixed cockpit control lateral motion.

3. EFFECTS OF SERVO DYNAMICS

An investigation has shown that practical position servo performance, combined with a method of correcting for servo dynamic characteristics, is sufficient to make phase lag effects negligible. This method is illustrated for the case of artificial dihedral effect. If the servo system, including measurement of sideslip angle and positioning of the ailerons, is assumed to be represented by an equivalent first-order system of characteristic time τ_1 , then the sideslip term of equation (67) may be written:

Approved for Public Release

Contrails

$$\delta_a = \frac{\partial \delta_a}{\partial \beta} \left(\frac{1}{1 + \tau_1 d} \right) \beta \qquad (71)$$

In order to compensate for phase-lag effects, another aileron term is added, which is nominally proportional to $\dot{\beta}$. This additional term is also affected by servo dynamics and, for the sake of simplicity, the same dynamic characteristics are assumed as for the β term. Now,

$$\delta_a = \frac{\frac{\partial \delta_a}{\partial \beta} \beta + \frac{\partial \delta_a}{\partial \dot{\beta}} \dot{\beta}}{(1 + \tau_1 d)}$$

This can be written

$$\delta_a = \frac{\partial \delta_a}{\partial \beta} \frac{1 + \left(\frac{\partial \delta_a}{\partial \dot{\beta}} \Big/ \frac{\partial \delta_a}{\partial \beta} \right) d}{1 + \tau_1 d} \beta \qquad (72)$$

Then if we choose $\partial \delta_a / \partial \dot{\beta}$ equal to $\tau_1 \, \partial \delta_a / \partial \beta$, the time lag effect is cancelled out, and we have exactly

$$\delta_a = \frac{\partial \delta_a}{\partial \beta} \beta$$

Now let us apply this principle to the example of artificial dihedral. L_β is the derivative for the airplane being simulated. We choose $\partial \delta_a / \partial \beta$ for the T-33 as if there were no effects of servo dynamics, in the way indicated by equation (68):

$$L_{\beta_1} + L_{\delta_{a_1}} \frac{\partial \delta_a}{\partial \beta} = L_\beta$$

Now let L'_β be the actual derivative obtained with the T-33, including the effects of servo dynamics. The aileron is made to respond to $\dot{\beta}$ as well as β .

Approved for Public Release

Contrails

$$L'_\beta = L_{\beta_1} + L_{\delta_{a_1}} \left[\frac{(\partial \delta_a / \partial \beta) + (\partial \delta_a / \partial \dot{\beta}) d}{1 + \tau_1 d} \right] \qquad (73)$$

$$L'_\beta = L_{\beta_1} + L_{\delta_{a_1}} \left(\frac{\partial \delta_a}{\partial \beta} \right) \left[\frac{1 + \left(\frac{\partial \delta_a}{\partial \dot{\beta}} \Big/ \frac{\partial \delta_a}{\partial \beta} \right) d}{1 + \tau_1 d} \right] \qquad (74)$$

Let $f(d) = L'_\beta / L_\beta$, which is the ratio of the actual derivative obtained to the desired derivative. It will be seen that if we choose $\partial \delta_a / \partial \dot{\beta}$ equal to $\tau_1 (\partial \delta_a / \partial \beta)$, then time lag is cancelled out and $f(d) = 1$ for all frequencies.

Now that a general method of compensation has been established, more realistic servo dynamics may be investigated. At and below the usual frequencies involved in airplane motions, a practical combination of measuring system and positioning servo may be represented by an equivalent second-order system of undamped natural frequency, ω_n radians per second, and damping ratio, ζ . Hence, equation (74) becomes:

$$L'_\beta = L_{\beta_1} + L_{\delta_{a_1}} \frac{\partial \delta_a}{\partial \beta} \left(\frac{1}{1 + \frac{2\zeta_1}{\omega_{n_1}} d + \frac{d^2}{\omega_{n_1}^2}} \right) + L_{\delta_{a_1}} \frac{\partial \delta_a}{\partial \dot{\beta}} \left(\frac{d}{1 + \frac{2\zeta_2}{\omega_{n_2}} d + \frac{d^2}{\omega_{n_2}^2}} \right) \qquad (75)$$

Two different undamped natural frequencies and damping ratios are assumed to account for variations in measurement and filtering lag between β and $\dot{\beta}$. Neglecting the "d^2" terms in the denominators, and comparing with the method of compensation for the first-order time lag, the following choice of $\partial \delta_a / \partial \dot{\beta}$ is made:

Approved for Public Release

Contrails

$$\partial\delta_a/\partial\dot{\beta} = \left(2\zeta_1/\omega_{n_1}\right)\partial\delta_a/\partial\beta \qquad (76)$$

This type of compensation is again equivalent to adding phase lead by the use of $\dot{\beta}$ as an input to the aileron servo, but only enough lead is introduced to account for the lag caused by the damping term of the second-order servo system. The result is not perfect compensation, as in the case of the first-order lag, but phase lag effects are kept small up to comparatively high airplane frequencies. To demonstrate this result, the magnitude and phase of $f(d)$ are shown in Figure 4 for the following example. (It will be recalled that $f(d)$ is the ratio of the actual L'_β obtained to the desired L_β.)

$$\omega_{n_1}/2\pi = 7.5 \text{ cps} \qquad \zeta_1 = .70$$

$$\omega_{n_2}/2\pi = 5.0 \text{ cps} \qquad \zeta_2 = .60$$

and

$$L_\beta = 2L_{\beta_1}$$

Since the magnitude of $f(d)$ remains within 6% of unity and the phase lag is less than 1° up to about 2 cycles per second, it may be concluded that use of $\dot{\beta}$, $\dot{p}$, and $\dot{r}$ inputs to the aileron and rudder servos will allow adequate compensation for normal servo dynamic characteristics, provided the significant frequencies involved are below 2 cycles per second. On the basis of this result, it appears that satisfactory compensation for time lag can be achieved if we work to the same requirement as that chosen for simulating the short-period longitudinal motion. The lag is not to exceed that of a second-order system with an undamped natural frequency of 7.5 cps and a damping ratio of 0.7.

It should also be noted that the availability of the roll and yaw angular accelerations, $\dot{p}$ and $\dot{r}$, as servo inputs make possible sim-

Approved for Public Release

Contrails

ulation of moments of inertia about two axes as well as products of inertia. The equations have been written so that this is not necessary, but in practice it may be helpful to take advantage of this fact.

Simulation of an airplane which employs a yaw or roll damper may be accomplished by the use of the above methods, provided that the airplane is assumed to have a set of stability derivatives different from its actual aerodynamic derivatives. That is, each assumed stability derivative is considered to be the sum of a natural airplane derivative and an artificial derivative, caused by the yaw or roll damper. This assumption is valid for the yawing moment and rolling moment equations and has little effect on the airplane motion through the side-force equation.

4. SUMMARY

It has been determined that the use of servos, positioning the rudder and ailerons nominally proportional to sideslip angle, rolling velocity, yawing velocity, and their first derivatives, makes possible term-by-term simulation of the two moment equations. Furthermore, the effects of inexact simulation of the side-force equation were found to be principally restricted to the spiral mode of motion and to the relationship between the rate of change of flight path direction, bank angle, and side load factor. Inaccuracies in the spiral mode and rate of change of flight path direction may be reduced to a minimum by matching of the true airspeed and by proper choice of the altitude of the test airplane. A general method of compensation was developed to allow simulation with the effects of servo dynamics included. An investigation of the lateral control forces is covered in the following section on Simulation of Control Systems.

E. SIMULATION OF CONTROL SYSTEMS

To simulate a control system, it is necessary to provide the correct relationships among cockpit control forces, cockpit control deflections and airplane motions. It is convenient first to describe how the desired control

Approved for Public Release

Contrails

forces are generated in response to the pilot's use of the controls and in response to the motion of the airplane. Then we shall proceed to the question of sending proper corresponding signals to the control surface servos.

In order to simulate various airplanes, a considerable degree of versatility must be provided in the control system. In some airplanes, the feel comes directly from the aerodynamic hinge moments. In others, irreversible power controls are used, in which cases there are artificial feel systems to be simulated. Some of these are designed to reproduce the effects of aerodynamic hinge moments, while others rely on or emphasize mechanical devices such as springs and bob-weights. To be able to produce a variety of effects and at the same time to have a system that is flexible and easily adjustable, it is desirable as far as possible to use electrical means to compute a signal representing the desired force, and then to use a servo to convert this into actual force. The other possibility is to include in the control system various mechanical devices, such as bob-weights, springs, and dashpots, which would directly produce the desired effects. Such installations would be inconvenient and certainly not easy to adjust in flight. In general, it appears that the electrical approach can best be used in the T-33 control system. The block diagrams at present, however, show mechanical devices for producing the effects of dry friction. It is expected that some current work on another contract at Cornell Aeronautical Laboratory will show that a representation of such effects can be generated electrically. If the early results of this work are satisfactory, consideration will be given to changing the T-33 control system accordingly.

The feel servos will apply forces to the stick and rudder pedals by means of hydraulic cylinders. The differential pressures in these cylinders will be determined by pressure-control valves which respond to electrical inputs. Thus electrical signals are converted to control forces. Electrical signals are generated as described below for all the different effects that are to be simulated.

As mentioned in Section III above, an alternate method is to measure stick force and the other pertinent quantities, and then to compute electrically a signal proportional to the proper corresponding stick deflection. This

Approved for Public Release

Contrails

signal is fed to an ordinary position servo which then drives the stick to this deflection. Experience at Cornell Aeronautical Laboratory with this type of "artificial spring" has shown that dynamic stability difficulties can be encountered with it. Inertia forces due to the stick's own mass and the effective mass of the pilot's hand and arm will be picked up by the strain gages and will cause the servo to move the stick. Stick motion produces inertia forces, and so the possibility exists of closed-loop unstable oscillations. A similar situation is possible with the pressure control valve. Here inertia forces cause stick motion. This motion is picked up by a transducer and a signal goes to the pressure control valve. The resulting pressure variation acts on the stick, tending to make it move. Again there is a closed loop. Analysis shows in each case that servo lag is the source of stability difficulties. Analysis has further shown, however, that the system using the pressure-control valve is less subject to this dynamic stability trouble. For this reason, the pressure-control system has been chosen for the T-33. This decision will be verified by testing a rig simulating the feel servo installations.

The elevator feel system is shown in the block diagram of Figure 5. The stick force signal which goes to the valve is computed according to the following equation:

$$F_{ES} = a_1 \delta_{ES} + a_2 \delta_{ES} q + a_3 f(\delta_{ES}) + a_4 \dot{\delta}_{ES} + a_5 n_z + a_6 + a_7 q \qquad (77)$$

(The diagram shows also that a stick force measurement is fed back to the computer to provide closed-loop control of the force. This may not be necessary if the valve has a consistent calibration factor and good enough dynamic performance.) The various terms in equation (77) provide the following effects.

$a_1 \delta_{ES}$	Stick force proportional to stick deflection with constant gradient; represents a spring.
$a_2 \delta_{ES} q$	Stick force proportional to stick deflection; gradient varies with q ; represents aerodynamic hinge moments due to C_{h_σ} or represents artificial system with speed feel.

Approved for Public Release

Contrails

$a_3 f(\delta_{ES})$	An additional stick force which is a non-linear function of stick deflection. This can be used to represent non-linear spring characteristics, springs with dead spots, pre-loaded springs, etc.
$a_4 \dot{\delta}_{ES}$	Stick force proportional to rate of stick motion; effect of a viscous damper; effect of a valve centering spring in a power boost system. (This may also serve a purpose of stabilizing the stick servo dynamics.)
$a_5 n_z$	Stick force proportional to normal acceleration; effect of a bob-weight. This term is also used to account for aerodynamic hinge moments due to C_{h_α}. To a reasonably good approximation, n_z is proportional to αq. Therefore, this term could be written $a_5 \alpha q$ representing an effect proportional to both angle of attack and dynamic pressure. This is like the effect of C_{h_a}.
a_6	Adjustable trimming voltage. Can also be used to represent a constant-force bungee.
$a_7 q$	Trim tab.

Two methods of trimming the stick forces are available. The term $a_7 q$ simulates a trim tab and is the natural one to use when speed feel is provided. The term a_6 furnishes an adjustment which does not vary with speed. This is the natural method to use when there is no speed feel, as with a plain spring. One further adjustment is provided. The pilot can send an adjustable signal direct to the elevator servo. With this he can vary the elevator angle corresponding to a given stick position. Thus, he can make the stick ride at the correct fore-and-aft location in the cockpit. This also pro-

Approved for Public Release

Contrails

vides a type of force trimming which is used with some power control systems. The stick position for zero stick force remains unchanged and trimming is accomplished by sending an independent signal direct to the control surface.

The aileron feel system is shown in the block diagram of Figure 6. The equation represented is simply

$$F_{AS} = b_1 \delta_{AS} + b_2 f(\delta_{AS}) \tag{78}$$

This represents a linear spring plus a non-linear additional function of stick deflection. As explained in Section III it is not considered necessary in the case of the ailerons to provide speed feel. A ground adjustment will be provided to insure that there is zero force at zero stick deflection. For lateral trimming in flight, the pilot will have a control which sends an adjustable signal to the aileron summing amplifier. This will permit him to adjust the aileron angle obtained with zero stick force.

The rudder feel system is shown in the block diagram of Figure 7. The equation represented is

$$F_{RP} = \tau_1 \delta_{RP} + \tau_2 \delta_{RP} q + \tau_3 f(\delta_{RP}) + \tau_4 n_y \tag{79}$$

$\tau_1 \delta_{RP}$	Linear spring.
$\tau_2 \delta_{RP} q$	Aerodynamic hinge moments due to C_{h_δ} or artificial system with speed feel.
$\tau_3 f(\delta_{RP})$	Non-linear additional function of pedal deflection.
$\tau_4 n_y$	Aerodynamic hinge moments due to C_{h_β}. n_y is used as a measure of βq.

Trimming is provided in the same way as for the ailerons.

All of the coefficients in the three equations presented above will be adjustable in flight.

We have now established the control system so that the correct stick forces will result from the pilot's movements of the controls, and also from the response of the airplane. We must next arrange to send the correct com-

Approved for Public Release

Contrails

mand signals to the control surface servos. Two alternate methods are provided for doing this.

The first, and apparently most natural, way is to measure the motions of the cockpit controls (stick and pedals) and to send the resulting signals to the control surface servos. On each of the three block diagrams, this type of operation is obtained when switch S_1 is in the down position.

The second method works basically from control force measurements. To be specific, consider elevator stick force, and suppose that the term $a_2 \delta_{ES} q$ is large compared to $a_1 \delta_{ES}$, i.e., the system primarily has speed feel.

Solve equation (77) for δ_{ES} as follows:

$$a_2 \delta_{ES} = \frac{F_{ES} - [a_1 \delta_{ES} + a_3 f(\delta_{ES}) + a_4 \dot{\delta}_{ES} + a_5 n_z + a_6 + a_7 q]}{q} \qquad (80)$$

The elevator angle computer produces the numerator of this expression, and this signal is then divided by q. The resulting signal is sent to the elevator summing amplifier. For this type of operation, switch S_1 is up and switch S_2 is to the left.

If instead the system primarily does not have speed feel, the equation used is

$$a_1 \delta_{ES} = F_{ES} - [a_2 \delta_{ES} q + a_3 f(\delta_{ES}) + a_4 \dot{\delta}_{ES} + a_5 n_z + a_6 + a_7 q] \qquad (81)$$

This is obtained with switch S_1 up and switch S_2 to the right.

Exactly similar arrangements are provided for the aileron and rudder systems.

The first method is good when the cockpit control motions are large enough to measure easily, and also when the stick forces are small. If the control motions are small, however, there may be resolution difficulties and trouble getting consistent, accurate measurements of small motions. The second method, conversely, is good when the motions are small, and when the forces are large enough to measure easily. It also permits working with a

Approved for Public Release

Contrails

rigid stick which does not move at all, which is of interest for control research. Also, it is believed that a pilot flies more by control force than control position. On this basis, even though it appears indirect, the second method may feel more natural to the pilot. This is a subtle sort of thing and probably can be answered only by trying both systems in flight. On the whole, there are enough pros and cons when considering the wide range of characteristics that we want to have available, that it appears best to provide both methods.

The command signals from the cockpit controls go into the summing amplifiers with adjustable gains. These gains are set to provide the correct amplitude of airplane motion in response to the applied forces.

The dynamics of the control system need also to be considered. There are two questions, the dynamics of the feel servo, and the dynamics of the control surface response to pilot force or stick motion. Satisfactory feel servos have been previously developed on other programs by the Flight Research Department. The feel servo tests described later in this report show that even better dynamic performance than before can be obtained. Accordingly, it is believed that the feel servos can be made to feel like "real springs", so that the pilot will be unaware of the feel servo dynamics.

The signals from the cockpit to the control surfaces can come from either stick force or stick position measurements, and whichever source gives the more desirable over-all system response can be selected. These signals are then subject to the lag of the control surface servos. The requirements of artificial stability call for quite high performance servos, with an undamped natural frequency of about 10 cps and a damping ratio of 0.6 to 0.7. Previous experience indicates that the lag of these servos will be imperceptible to the pilot. Their dynamic performance is comparable to the best being currently achieved in airplane power control systems.

Approved for Public Release

Contrails

SECTION V

DESIGN OF SOME SPECIAL CONTROL SYSTEMS

BY H.S. RADT, JR.

A. INTRODUCTION

Several provisions are to be included in the T-33 control system for the purpose of conducting research on the design of cockpit controls, with regard both to their configurations and their functions. One such provision is the interchangeable wheel and stick arrangement, which is described in Section VIII, below. Other provisions are aimed at making the pilot's task as simple as possible by relieving him of all but the very basic control functions. A specific example is automatic coordination of turns, so that he will not have to bother to work the rudder pedals for this purpose. The simpler his other tasks are, the more he can concentrate on the primary task of hitting his target. Another approach is to investigate unconventional responses to the controls to see if some new ideas can be obtained as to how the handling characteristics of fighter airplanes can be improved. These various provisions include automatic coordination by two distinct methods, one "open-loop" and one "closed-loop", automatic positioning of the elevator to maintain altitude in a turn, and conversion of the aileron controls from roll rate to bank angle position controls. Other systems such as combinations of the above, are available as a result of the great versatility of the T-33 artificial stability system.

Coordination may be considered to be maintenance of either zero sideslip or zero side-load factor, either of which might be significant under various circumstances. In the discussions following, however, the definition involving elimination of sideslip will be employed throughout. The difference is not very great, and this is the convenient case to work with. Referring to equations (63) and (65), and assuming

$\beta = 0$, $Y_{\delta_r} = Y_p = Y_\psi = Y_r = 0$, the reader may verify that

Approved for Public Release

Contrails

$$r = Y_\phi \phi \tag{82}$$

and

$$N_{\delta_r} \delta_r = -\left[N_{\delta_a} \delta_a + N_p p - \dot{r} + N_r r\right] \tag{83}$$

If β is to be kept equal to zero, the rudder must be moved so that this equation remains satisfied. The equation thus defines a method of coordination. Now if r or ϕ from equation (82) is substituted into equation (83) a second and a third equation representing methods of coordination may be written.

$$N_{\delta_r} \delta_r = -\left[N_{\delta_a} \delta_a + \left(\frac{N_p}{Y_\phi} - 1\right)\dot{r} + N_r r\right] \tag{84}$$

$$N_{\delta_r} \delta_r = -\left[N_{\delta_a} \delta_a + (Y_\phi)\left(\frac{N_p}{Y_\phi} - 1\right)p + N_r Y_\phi \phi\right] \tag{85}$$

Equation (83) may be eliminated as impractical since rudder positioning would depend on four inputs, while the other two systems require only three. Note that the first terms of equations (83), (84), and (85) correspond to "adverse yaw" effects, while the second terms of (84) and (85) are necessary when the airplane is rolling during turn entry. The first two terms, then, are needed during the transient part of a turning maneuver, the last term providing the required rudder to prevent sideslip during steady turning. The method suggested by equation (85) is the one chosen for investigation here.

Another general approach to minimizing sideslip is by the use of a "closed-loop" control. Sideslip is measured, and the signal obtained is considered as an error signal. This is then fed back to the control system to move the controls in the direction to reduce the error. The feedback signal includes also the derivative of the error and the integral of the error. Deflecting the rudder in proportion to a measurement of sideslip essentially produces an artificial C_{n_β}. In effect, this minimizes sideslip simply by increasing weathercock stability. Steady-state β is wiped out by integral control, while rudder proportional to $\dot{\beta}$ compensates for the decrease of dynamic stability due to proportional and integral control. $\dot{\beta}$, or derivative control,

Approved for Public Release

Contrails

has a further use in reducing the amount of sideslip developed during turn entry.

It should be noted that several variations of these means of turn coordination are inherently possible with the T-33 artificial stability and control system.

An additional provision to be included is automatic application of the elevator angle required to maintain altitude in turns. With this plus automatic turn coordination, the pilot will have to use only one control, the ailerons, to make a turn. The automatic elevator control operates on the following basis. Consider the equilibrium of forces in a steady, level turn.

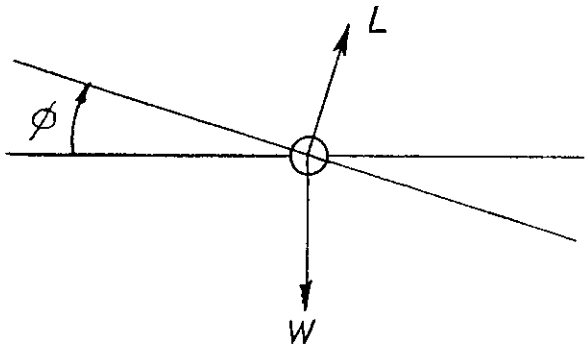

$$\left.\begin{aligned} L\cos\phi &= W \\ L\sin\phi &= \frac{W}{g} V\dot{\psi} \end{aligned}\right\} \qquad (86)$$

L = lift

W = weight

V = true air speed

$\dot{\psi}$ = rate of turn (about a vertical axis)

The load factor required in the turn is

$$n_z = \frac{L}{W} = \frac{1}{\cos\phi}$$

In level flight, the load factor is 1.0. Therefore, the increment required is

Approved for Public Release

Contrails

$$\Delta n_z = n_z - 1 = \frac{1 - \cos\phi}{\cos\phi} \tag{87}$$

This increment of load factor is dependent on the dynamic pressure, incremental elevator deflection, and pitching moment due to pitching velocity.

$$\Delta n_z = -\frac{C_{m\delta_e}}{(W/S)} \frac{1}{\left(\frac{\partial C_m}{\partial C_L}\right)} q \Delta\delta_e - \frac{C_{m_{D\theta}}}{2} \frac{1}{\left(\frac{\partial C_m}{\partial C_L}\right)} \left(\frac{\sin^2\phi}{\cos\phi}\right)$$

Hence, the elevator required is given by the expression

$$\Delta\delta_e = -\left(\frac{W}{S}\right)\left(\frac{\partial C_m}{\partial C_L}\right)\left(\frac{1}{C_{m_{\delta_e}}}\right) \left\{ \frac{1 - \cos\phi + \frac{C_{m_{D\theta}}}{2(\partial C_m/\partial C_L)} \sin^2\phi}{q \cos\phi} \right\} \tag{88}$$

A computer is to be included to provide an elevator deflection of the form

$$\Delta\delta_e = K\left(\frac{1 - \cos\phi}{q \cos\phi}\right) ,$$

which approximates equation (88) in a form more easily computed. When K is chosen properly, there is no significant loss of accuracy.

Finally, an additional arrangement will be furnished to make possible bank angle response proportional to lateral control displacement. The principle of operation is explained by the following simplified analysis. For small sideslip angles, the rolling moment equation (64) may be approximated by:

$$(d - L_p)p = L_{\delta_a} \delta_a , \tag{89}$$

from which it may be seen that steady-state roll rate is proportional to aileron deflection. Aileron deflection is normally proportional to lateral stick displacement, but the proposed system will include aileron response to bank angle, and roll rate in addition. Now aileron deflection may be represented by the expression

$$\delta_a = k_1 \delta_{AS} + k_2 p + k_3 \phi \tag{90}$$

Approved for Public Release

Contrails

Substitution of equation (90) into equation (89) yields

$$\left[d^2 - (L_p + k_2 L_{\delta_a})d - k_3 L_{\delta_a}\right]\phi = k_1 L_{\delta_a} \quad \delta_{AS} \tag{91}$$

with the result that steady-state roll rate is zero and steady-state bank angle is proportional to lateral stick deflection, δ_{AS} .

$$\phi_{ss} = \left(\frac{k_1}{k_3}\right) \quad \delta_{AS} \tag{92}$$

An alternate but less direct approach involves the use of large artificial negative C_{l_r} . Again assuming β very small, equation (64) may be written:

$$-L_r r + (d - L_p)p = L_{\delta_a} \delta_a \tag{93}$$

Now let the ailerons move proportional to yaw rate and to lateral stick displacement,

$$\delta_a = k_4 r + k_5 \delta_{AS} \tag{94}$$

Combining equations (82), (93), and (94) shows that

$$\left[d^2 - L_p d - Y_\phi (L_r + k_4 L_{\delta_a})\right]\phi = (k_5 L_{\delta_a})\delta_{AS} \tag{95}$$

which is a result similar to that of equation (91). Other aileron inputs will include roll acceleration, to vary the new roll oscillation frequency without changing the steady state bank angle response, and roll rate to give added damping.

With automatic turn coordination, only the aileron and elevator controls are used by the pilot in turning. If the elevator to maintain altitude is also included, then he need only operate the aileron control. This results in a "one-control" airplane. A final additional refinement is the transformation of the lateral stick control from a roll rate control to a turning rate control. The result is an airplane with a type of turn control which is similar to the

Approved for Public Release

Controls

"steering" of an automobile. In summing up, there exist several combinations of these special control systems which will be investigated to determine their effect on the pilot's ability to control the airplane.

1. Automatic coordination, or two-control airplane.
2. Automatic elevator to maintain altitude (another "two-control" airplane).
3. Automatic coordination and elevator to maintain altitude, or "one-control" airplane.
4. Proportional bank control.
5. Combination of proportional bank control and automatic coordination.
6. Combination of automatic coordination, elevator to maintain altitude and proportional bank.

B. DEFINITION OF COORDINATION

There are two possible definitions of coordination, one implying zero sideslip and another implying zero side load factor. The two are related as follows:

$$n_y = \frac{Sq}{W}\left\{C_{Y_\beta}\beta + C_{Y_r}\frac{rb}{2V} + C_{Y_p}\frac{pb}{2V} + C_{Y_{\delta_r}}\delta_r\right\}$$

Neglecting the yaw and roll rate terms, this may be shortened to

$$n_y = \frac{Sq}{W}\left\{C_{Y_\beta}\beta + C_{Y_{\delta_r}}\delta_r\right\} \tag{96}$$

Under normal circumstances the amount of rudder required to prevent sideslip is small, and $C_{Y_{\delta_r}}$ is about one-third of C_{Y_β}. Thus, minimization of β and minimization of n_y are nearly equivalent. It may be seen, however, that the method of coordination may differ depending on which of the above variables is minimized. Let us consider, then, the significance of zero load factor and of zero sideslip.

The pilot is able to judge the magnitude of side-load factor by observing his ball-bank indicator, or rather approximately, by feel through "the seat of

Approved for Public Release

Confidential

his pants." Side-load factor, then, has its chief effects on the pilot directly. On the other hand, sideslip has special significance during firing of rockets or projectiles. If a rocket is fired from an airplane flying with a sideslip angle it will "weathervane" toward the direction of the relative wind. As a result it will be deflected from its intended trajectory. For this reason $\beta = 0$ will be taken as our definition of coordination.

C. AUTOMATIC TURN COORDINATION BY THE USE OF RUDDER PROPORTIONAL TO BANK ANGLE, ROLL RATE, AND AILERON DEFLECTION

The procedure here is to analyze the problem of coordination from the equations of motion, following the methods suggested in the introduction. Attention is also paid to the resulting lateral gust response and, in a later section, the possibility of programming the various necessary gains. Analog computer solutions verifying some of the conclusions, are included.

By assuming $Y_r = Y_\psi = Y_p = 0$, solving for r from equation (63) and substituting for r in equations (64) and (65), slightly different rolling moment and yawing moment equations may be written.

$$(L_r d - L'_\beta)\beta + (d - L_p - L_\phi d^{-1})p = L_{\delta_a}\delta_a + L'_{\delta_r}\delta_r \tag{97}$$

$$(-d^2 - N'_{\dot\beta} d - N'_\beta)\beta + (-N'_p - N'_\phi d^{-1})p = N_{\delta_a}\delta_a + N'_{\delta_r}\delta_r - Y_{\delta_r} d\delta_r \tag{98}$$

The primed ($'$) coefficients are derivatives changed or introduced by the substitution employed above, and are defined in Table V. Now, substitute

$\delta_r = k_a \delta_a + k_p p + k_\phi \phi$, as suggested by equation (85) in the introduction to this section. Equations (97) and (98) become

$$(L_r d - L'_\beta)\beta + [d - (L_p + L'_{\delta_r} k_p) - (L'_\phi + L'_{\delta_r} k_\phi) d^{-1}]p = (L_{\delta_a} + L'_{\delta_r} k_a)\delta_a \tag{99}$$

and

Approved for Public Release

Contrails

$$(-d^2 - N'_{\dot\beta} d - N'_\beta)\beta + [Y_{\delta_r} k_p d - (Y_{\delta_r} k_\phi - N'_{\delta_r} k_p - N'_p) - (N'_{\delta_r} k_\phi + N'_\phi) d^{-1}]p$$

$$= [(N_{\delta_a} + N'_{\delta_r} k_a) - Y_{\delta_r} k_a d]\delta_a \qquad (100)$$

Our aim now is to have the rudder produce yawing moments in such a way as to minimize sideslip angle. We examine the yawing moment equation to see what can be done to minimize the coupling between β and the other variables. As a result, we make:

$$N'_{\delta_r} k_p + N'_p = 0$$

$$N'_{\delta_r} k_\phi + N'_\phi = 0$$

and

$$N'_{\delta_r} k_a + N_{\delta_a} = 0$$

Equation (100) now becomes:

$$(-d^2 - N'_{\dot\beta} d - N'_\beta)\beta + Y_{\delta_r}(k_p d - k_\phi)p = -Y_{\delta_r} k_a d\delta_a \qquad (101)$$

If Y_{δ_r} is negligible, this reduces to $\beta = 0$, which is exactly the desired result. In practice, Y_{δ_r} will be a secondary effect producing small departures from perfect coordination. The sideslip angle response to an aileron deflection and to a gust induced sideslip angle, β, are given in Laplace transform notation in equations (102) and (104), respectively.

Equation (103) shows the ratio of sideslip to bank angle in complex form for aileron induced sinusoidal rolling, while in equation (105) is given the roll angle resulting from a gust induced sideslip. Equations (103), (104), and (105) are approximate expressions.

$$\frac{\mathcal{L}\{\beta\}}{\mathcal{L}\{\delta_a\}} = Y_{\delta_r} \frac{\{k_a d^2 + [k_p(L_{\delta_a} + L_{\delta_r} k_a) - k_a(L_p + L'_{\delta_r} k_p)]d + [L_{\delta_a} k_\phi - L'_\phi k_a]\}}{\{[d - (L_p + L'_{\delta_r} k_p) - (L'_\phi + L'_{\delta_r} k_\phi) d^{-1}][d^2 + N'_{\dot\beta} d + N'_\beta] + Y_{\delta_r}[k_p d + k_\phi][L_r d - L'_\beta]\}} \qquad (102)$$

Approved for Public Release

Contrails

$$\frac{\beta}{\phi} \cong Y_{\delta_r} \frac{\{[j\omega_f][L_{\delta_a} k_\phi - L'_\phi k_a - k_a \omega_f^2] - [\omega_f]^2 [k_p (L_{\delta_a} + L'_{\delta_r} k_a) - k_a (L_p + L'_{\delta_r} k_p)]\}}{[L_{\delta_a} + L'_{\delta_r} k_a][(N'_\beta - \omega_f^2) + j(\omega_f N'_{\dot\beta})]} \quad (103)$$

$$\frac{\mathcal{L}\{\beta - \beta_0\}}{\mathcal{L}\{\beta_0\}} \cong -\left\{\frac{N'_\beta}{d^2 + N'_{\dot\beta} d + N'_\beta}\right\} \quad (104)$$

$$\frac{\phi}{\beta_0} \cong -\frac{(L_r N'_\beta + L'_\beta N'_{\dot\beta}) + j(\omega_f L'_\beta)}{[(N'_\beta - \omega_f^2) + j(\omega_f N'_{\dot\beta})]\left[-(L_p + L'_{\delta_r} k_p) + j\left(\omega_f + \frac{(L'_\phi + L'_{\delta_r} k_\phi)}{\omega_f}\right)\right]} \quad (105)$$

A typical flight test condition at $M = 0.70$ and an altitude of 10,000 feet was chosen for the following analysis. For this condition the various aerodynamic, gravity, and inertia coefficients of the T-33 are given in Table VI. The sideslip frequency response to sinusoidal bank angle oscillations, as obtained from equation (103), is plotted in Figure 8 in terms of the ratio of sideslip to bank angle, for the T-33 with automatic coordination. Also included for comparison is a similar plot for the normal T-33. Figure 8 shows that the peak sideslip is reduced to less than 3% of the value for the normal T-33.

A similar demonstration of the decrease in sideslip appears in Figure 9, which shows the results of an analog computer investigation. In order to include steady turning as well as turn entry, an aileron deflection was applied and then neutralized. The method of doing this was to apply a sudden aileron deflection of 4 degrees, and then allow it to decay exponentially with a time constant of 2 seconds. It should be mentioned that at the flight condition chosen, the T-33 remains almost coordinated with the use of ailerons alone. Thus, only a small amount of rudder deflection is required to produce almost perfect coordination. However, the principle of automatic rudder positioning to avoid sideslip is well illustrated. Figures 9A and 9B show that the sideslip angle is decreased from a maximum of 0.33° to practically zero by the addition of automatic rudder. In Figure 9C is shown the response to the same aileron input but with the amount of rudder proportional to roll-rate low by

Approved for Public Release

Contrails

20%. This case was included simply to check the effect of departure from the correct setting. It is seen that considerable improvement compared to the normal airplane is obtained even with the incorrect setting. It can be noticed by comparison of Figures 9A and 9C that the maximum sideslip is 0.125° or about 40% of the value for no artificial coordination. Hence the amount of rudder deflection is not extremely critical in maintaining small sideslip. Comparison of Figures 9A and 9C further shows that the frequency of the sideslip and yaw oscillation is unchanged by the addition of rudder to coordinate.

Equation (104) is an approximate expression for the lateral gust response in sideslip. The roll coupling terms in the yawing moment equation, N'_p and $N'_\phi d^{-1}$, are neglected for the normal airplane and Y_{δ_r} is assumed small for the automatically coordinated airplane in deriving this equation. Omitting the same terms also reduces the expression for the roll response to equation (105). A similar expression representing the normal airplane roll response is

$$\frac{\phi}{\beta_0} = -\frac{(L_r N'_\beta + L'_\beta N'_{\dot\beta}) + j\omega_f L'_\beta}{[(N'_\beta - \omega_f^2) + j\omega_f N'_{\dot\beta}][-L_p + j(\omega_f + L'_\phi/\omega_f)] + [L'_\beta - j\omega_f L_r][N'_p - j N'_\phi/\omega_f]}$$

Thus, for N'_p and N'_ϕ neglected, and $L'_{\delta_r} k_p$ and $L'_{\delta_r} k_\phi$ small, the roll response appears to be about the same for the T-33 with and without automatic coordination when a lateral gust input is considered.

D. AUTOMATIC TURN COORDINATION BY THE USE OF RUDDER PROPORTIONAL TO SIDESLIP, ITS DERIVATIVE, AND ITS INTEGRAL

Now, let us investigate a method of coordination which uses only sideslip as the basic variable. The object is to provide a control of the rudder which acts to reduce sideslip to zero regardless of its origin. Three separate rudder inputs are used: β, $\dot\beta$, and the integral of β. The rudder deflection may then be written:

Approved for Public Release

Contrails

$$\delta_r = k_\beta \beta + k_{\dot\beta} \dot\beta + k_{\int\beta} \left(\int_0^t \beta dt \right) \tag{106}$$

Integral control, $k_{\int\beta}$, moves the rudder so as to wipe out steady sideslip; proportional control, k_β, tends to increase the stiffness to sideslip so as to return the sideslip quickly toward zero; and derivative control, $k_{\dot\beta}$, compensates for the decrease of damping due to integral control.

Here, there exists the possibility of changing the dynamic characteristics of the Dutch roll oscillation, but the approach will be to adjust the above three gains so as to maintain the same frequency and damping as for the normal airplane. Substitution of equation (106) into equations (97) and (98) yields

$$\left\{ (L_r - L'_{\delta_r} k_{\dot\beta}) d - (L'_\beta + L'_{\delta_r} k_\beta) - L'_{\delta_r} k_{\int\beta} d^{-1} \right\} \beta + \left\{ d - L_p - L'_\phi d^{-1} \right\} p = L_{\delta_a} \delta_a \tag{107}$$

$$\left\{ -(1 + Y_{\delta_r} k_{\dot\beta}) d^2 - (N'_{\dot\beta} + N'_{\delta_r} k_{\dot\beta} - Y_{\delta_r} k_\beta) d - (N'_\beta + N'_{\delta_r} k_\beta - Y_{\delta_r} k_{\int\beta}) \right.$$
$$\left. - N'_{\delta_r} k_{\int\beta} d^{-1} \right\} \beta + \left\{ -N'_p - N'_\phi d^{-1} \right\} p = N_{\delta_a} \delta_a \tag{108}$$

Note that the cubic coefficient of β in equation (108) now replaces the quadratic of equation (98). If the effects of rolling velocity are neglected, an equation which determines the Dutch roll natural frequency and damping ratio is obtained by setting this coefficient of β equal to zero. For the T-33, this has been checked and found to be a very good approximation. Thus, in order to maintain the same Dutch roll frequency and damping, it is necessary to choose k_β, $k_{\dot\beta}$, and $k_{\int\beta}$ such that the cubic is the product of a factor representing a real and stable root, $\left(1 + \frac{1}{\tau} d^{-1} \right)$, and the original quadratic. Hence, make

$$-(1 + Y_{\delta_r} k_{\dot\beta}) d^2 - (N'_{\dot\beta} + N'_{\delta_r} k_{\dot\beta} - Y_{\delta_r} k_\beta) d - (N'_\beta + N'_{\delta_r} k_\beta - Y_{\delta_r} k_{\int\beta})$$
$$- N'_{\delta_r} k_{\int\beta} d^{-1} = -(d^2 + N'_{\dot\beta} d + N'_\beta)\left(1 + \frac{1}{\tau} d^{-1}\right)(1 + Y_{\delta_r} k_{\dot\beta}) \tag{109}$$

Approved for Public Release

Contrails

The right-hand side of equation (109) may now be expanded, and coefficients of equal powers of d may be equated, with the result that k_β, $k_{\dot\beta}$, and $k_{\int\beta}$ may be determined for any given flight condition and desired time constant, τ, of the extra root. For the flight condition already investigated in part C of this section, and for $\tau = .05$ seconds, the following rudder gains have been determined:

$$k_\beta = -.959$$

$$k_{\dot\beta} = -1.330 \text{ sec.}$$

$$k_{\int\beta} = -18.20 \text{ sec}^{-1}$$

Now, using the above condition, let us investigate the lateral gust response as well as the turn coordination of the T-33 with and without automatic rudder positioning. Equation (104) gives the normal T-33 response, while equation (110) shows that, with the addition of this type of rudder positioning, the normal response is multiplied by the factor on the right.

$$\frac{\mathcal{L}\{\beta-\beta_o\}}{\mathcal{L}\{\beta_o\}} = -\frac{N'_\beta}{(d^2 + N'_{\dot\beta}d + N'_\beta)} \cdot \frac{\{(1 + N'_{\delta r}/N'_{\dot\beta}\, k_\beta - Y_{\delta r}/N'_\beta\, k_{\int\beta})d + N'_{\delta r}/N'_{\dot\beta}\, k_{\int\beta}\}}{\{1 + Y_{\delta_r}\, k_{\dot\beta}\}\{1/\tau + d\}} \qquad (110)$$

This factor is $\{1+0.11d\}/\{1+0.05\,d\}$ for the condition investigated, showing that the lateral gust response is changed.

Figure 10 shows analog computer solutions for the response of the T-33 to the same aileron deflection as employed in part C of this section. Again the A part gives the normal airplane response while the B part shows the results of moving the rudder according to:

$$\delta_r = -.959\beta - 1.330\dot\beta - 18.20\int_o^t \beta\, dt$$

Approved for Public Release

Contrails

The peak sideslip is decreased to about one-sixth of the normal value with the frequency of the oscillation in sideslip unchanged. It is significant that the rudder deflections shown in Figures 9B and 10B are very similar. This is to be expected since there is only one possible rudder motion to produce identically zero sideslip.

In conclusion, sideslip during a pilot induced turn may be considerably reduced by the use of either the "direct" approach (equation (85)) or the "feedback" approach (equation (106)). The lateral gust response is not necessarily improved by either method.

E. PROPORTIONAL BANK CONTROL

It is felt that the method suggested in the introduction, using bank angle feedback to the ailerons for proportional bank control, is more direct than the use of large values of C_{ℓ_r}. Hence, only the bank angle system is considered here.

The aileron deflection represented by equation (90), when substituted into equations (97) and (98) yields:

$$\left(L_r d - L'_\beta\right)\beta + \left\{d - \left(L_p + L_{\delta_a} k_2\right) - \left(L'_\phi + L_{\delta_a} k_3\right) d^{-1}\right\} p = L_{\delta_a} k_1 \delta_{AS} \quad (111)$$

$$-\left(d^2 + N'_\beta d + N'_\beta\right)\beta + \left\{-\left(N'_p + N_{\delta_a} k_2\right) - \left(N'_\phi + N_{\delta_a} k_3\right) d^{-1}\right\} p = N_{\delta_a} k_1 \delta_{AS} \quad (112)$$

Using equations (111) and (112), we may now solve for the bank angle ϕ, in Laplace transform notation,

$$\frac{\mathcal{L}\{\phi\}}{\mathcal{L}\{\delta_a\}} = \frac{L_{\delta_a}\left(d^2 + N'_\beta d + N'_\beta\right) + N_{\delta_a}\left(L_r d - L'_\beta\right)}{\left(d^2 - L_{p_T} d - L_{\phi_T}\right)\left(d^2 + N'_\beta d + N'_\beta\right) - \left(N_{p_T} d + N_{\phi_T}\right)\left(L_r d - L'_\beta\right)}$$

where

$$L_{p_T} = L_p + L_{\delta_a} k_2$$

$$L_{\phi_T} = L'_\phi + L_{\delta_a} k_3$$

Approved for Public Release

Contrails

$$N_{p_T} = N_p + N_{\delta_a} k_2$$

$$N_{\phi_T} = N'_\phi + N_{\delta_a} k_3$$

Since the right-hand terms of both numerator and denominator are negligible,

$$\frac{\mathcal{L}\{\phi\}}{\mathcal{L}\{\delta_a\}} \cong \frac{L_{\delta_a}}{(d^2 - L_{p_T} d - L_{\phi_T})} \tag{113}$$

Hence, it is shown that the bank angle response to aileron deflection now very closely approximates a second-order system of undamped natural frequency ω_n and damping ratio, ζ where:

$$\omega_n = (-L_{\phi_T})^{1/2} = (-L'_\phi - L_{\delta_a} k_3)^{1/2} \tag{114}$$

$$\zeta = \left\{\frac{-L_{p_T}}{2(-L_{\phi_T})^{1/2}}\right\} = 1/2 \left\{\frac{-L_p - k_2 L_{\delta_a}}{(-L'_\phi - k_3 L_{\delta_a})^{1/2}}\right\} \tag{115}$$

Furthermore, the steady-state bank angle resulting from a lateral stick deflection, δ_{AS}, is

$$\phi_{SS} = -\left(\frac{L_{\delta_a}}{L_{\phi_T}}\right)\left(\frac{\partial \delta_a}{\partial \delta_{AS}}\right)(\delta_{AS}) \tag{116}$$

Hence, for a steady coordinated turn the turning rate is proportional to lateral stick deflection.

Figure 11 shows a comparison of the normal T-33 and the T-33 with the proportional bank control system included. For the flight condition of $M = 0.70$ at an altitude of 10,000 feet, the lateral stick displacement in both cases, neglecting cable stretch in the aileron linkages, is 1.53 inches. A steady roll rate of 35 deg/sec results for the normal airplane shown in Figure 11A. The T-33 with proportional bank control reaches a maximum roll rate of 20 deg/sec and a maximum bank angle of 12 degrees. The aileron is de-

Approved for Public Release

Contrails

flected according to:

$$\delta_a = 0.333\,\phi - 2.59\,\delta_{AS} \qquad (117)$$

with the result that the undamped roll natural frequency is 4.65 rad/sec. The roll oscillation has a period of 1.87 seconds and a damping ratio of 0.69. For this condition no additional damping (k_z) was required to produce the optimum damping of about 70% critical. The aileron deflection required and bank and sideslip resulting are shown in Figure 11B.

Approved for Public Release

Contrails

SECTION VI

DETERMINATION OF DESIGN INFORMATION FOR THE AUTOMATIC CONTROL SYSTEM

BY C.B. NOTESS AND H.S. RADT, JR.

This section includes a determination of control system design data, specifically the maximum positive values of gain (e.g. $\partial\delta_e/\partial\alpha$ or $\partial F_s/\partial\delta_{ES}$), the maximum negative values of gain, and the maximum anticipated values of the inputs (e.g., α, θ, p, etc.). These various gains appear in the functional block diagrams, Figures 5, 6, and 7, as the values of K, G, H, a, b, and c.

In determining the design requirements, four jet fighter aircraft designed for operation in the supersonic regime were chosen as airplanes which the T-33 should be able to simulate as well as is practicable. Stability and response data on these four aircraft were used to determine the design requirements for the T-33 automatic control system.

This section is divided into five parts as follows:

A. Design Information for Control of the Phugoid Motion by an Auxiliary Surface

B. Design Requirements for Control of the Longitudinal Short Period Motion

C. Design Requirements for Control of the Lateral Motion

D. Design Requirements for the Artificial Feel System

E. Design Requirements for the Special Control Systems

A. DESIGN INFORMATION FOR CONTROL OF THE PHUGOID MOTION BY AN AUXILIARY SURFACE

The sections on phugoid control in References 2 and 3 show that an effective and practical method of varying the period and damping of the phugoid oscillation is by the use of an auxiliary surface. The theory of this method is also discussed in Section IV above. The angle of incidence of the auxiliary surface is varied

Approved for Public Release

Contrails

proportional to the change of forward velocity from a reference condition, and also to the rate of change of forward velocity, or to two analogous quantities. Positioning the surface proportional to change of airspeed is equivalent to adding an artificial component to the aerodynamic derivative M_V, as appearing in equations (56) through (59) of Section IV. A variation of this parameter has its principal effect in changing the period of the phugoid oscillation, while positioning the surface proportional to rate of change of airspeed adds an artificial parameter, $M_{\dot{V}}$, which essentially allows variation of the phugoid damping.

1. DESIGN OF THE AUXILIARY SURFACE

The minimum area of the auxiliary surface is determined on the basis of providing sufficiently large pitching moments for maneuvers in which the phugoid period and damping are considerably different from the normal T-33 values. At the same time it is necessary to make the surface small enough so that the positioning resolution has a negligible effect on the phugoid motion. In addition, since the surface acts as a canard surface, it must be small enough to avoid a large decrease of static margin. According to these criteria, a surface has been chosen which has the same aspect ratio but twice the area of a similar control surface used on an F-94 airplane currently being employed for variable stability research at Cornell Aeronautical Laboratory. Reference 2 describes the geometric information and considerations involved in the design of the auxiliary surface used on the F-94 airplane. The F-94 surface was designed primarily to vary the period and damping of the normal subsonic phugoid motion over fairly wide ranges. In simulating other airplanes, the T-33 will, in some cases, be called upon to reproduce variations due to Mach number which alter the character of the phugoid motion considerably. To allow for such cases, it was thought that the T-33 surface should be larger than that on the F-94. It was found that it could be made twice as large without raising practical difficulties. As shown below, this surface is effective enough to alter the phugoid motion very consider-

Approved for Public Release

Contrails

ably. If any still more severe aerodynamic effects should have to be simulated, they would probably best be handled by working the elevator directly. Table VII contains a list of proposed design data for the auxiliary surface to be used on the T-33.

2. QUANTITIES TO BE USED AS INPUTS TO THE AUXILIARY SURFACE SERVO

Let us now consider the artificial part of the aerodynamic derivative, M_V. There are several quantities, such as Δq, $\Delta q/q$, $\Delta V/V$, or $\Delta(1/q)$, any one of which might be chosen as the input to the auxiliary surface servo in providing artificial M_V. Note here that the " Δ " symbol represents the difference between the actual quantity and some reference condition at the start of a maneuver. It has been found that the use of $\Delta q/q$ is the most logical choice for the following reasons:

(a) Measurement of dynamic pressure is more direct than velocity measurement.

(b) The maximum ratio of the change in dynamic pressure, Δq, to the total dynamic pressure, q, is not expected to vary greatly with reference condition. In other words, large speed changes are expected at high speed; small changes at low speed, in response to control motions of normal magnitude. For example, if a pilot pulls 1.1g and then holds the stick fixed while the airplane slows down to a new trim speed, q will decrease by 10% regardless of its initial value (apart from Mach number effects). As a result of this, the quantity of $\Delta q/q$ will provide reasonable signal levels over the range of expected flight conditions.

(c) The range of gain variation required to allow large changes of phugoid period are not excessive, regardless of flight test condition.

(d) Considering variations of speed about some reference condi-

Approved for Public Release

Contrails

tion, the use of the input $\Delta q/q$ will make the artificial, non-dimensional derivative, C_{m_v}, vary inversely as the dynamic pressure.

Equation (56) may be written as follows:

$$P = 2\pi \left[\frac{1}{D_\theta} \frac{1}{1-\zeta_p^2} \frac{1 + \left(L_\alpha / M_\alpha\right) M_{\dot{\theta}}}{L_v - \left(L_\alpha / M_\alpha\right) M_v} \right]^{1/2}$$

An approximate expression is obtained by using the definitions given in Table I, neglecting thrust, drag, and Mach number effects:

$$P = 2\pi \left[\frac{2\tau}{C_{L_0}} \frac{1}{1-\zeta_p^2} \frac{1 + 1/2 \left(C_{L_\alpha} / C_{m_\alpha}\right) C_{m_{D\theta}}}{1/\tau\, C_{L_0} - 1/2\, \tau \left(C_{L_\alpha} / C_{m_\alpha}\right) C_{m_v}} \right]^{1/2}$$

Rearranging

$$P = \pi \sqrt{2}\, \frac{V_0}{g} \left[\frac{1 + \frac{1}{2} \left(C_{L_\alpha} / C_{m_\alpha}\right) C_{m_{D\theta}}}{1-\zeta_p^2} \right]^{\frac{1}{2}} \left[\frac{1}{1 - \frac{1}{2} \left(C_{L_\alpha} / C_{m_\alpha}\right) \left(C_{m_v} / C_{L_0}\right)} \right]^{\frac{1}{2}} \tag{118}$$

Now C_{m_v} appears only in the second bracket, so this bracket is the factor by which the phugoid period is modified. Since $C_{L_\alpha}/C_{m_\alpha}$ will be relatively constant for subsonic flight, C_{m_v} should be proportional to C_{L_0} to keep the factor constant as flight conditions change. On this basis, it appears desirable to have C_{m_v} vary inversely as the dynamic pressure.

For the case of the artificial derivative $M_{\dot{v}}$, it is possible to

Approved for Public Release

Contrails

use dV/dt , $d/dt(\Delta V/V)$, $d/dt(\Delta q/q)$, dq/dt , or $\frac{1}{q}\, dq/dt$.

Here, however, the choice is not as clear as for the case of artificial M_V . There does not seem to be any simple, "natural" way for $M_{\dot{V}}$ to vary with speed. Equation (59) shows that the required $M_{\dot{V}}$ depends on many parameters, including ones which are affected by the artificial stability used to adjust the short-period motion. Even if attention is confined to D_V (which is the basic damping term without artificial stability), the situation is not simple, because the variations of both parasite drag and induced drag with speed are involved. Variation of drag coefficient with Mach number is a further complication.

The decision has been made to use dq/dt as an input because of the relative simplicity of generating this signal.

3. SPECIFICATIONS FOR SERVO GAINS

Using the above design conditions and $\Delta q/q$ and dq/dt as servo inputs, values of the auxiliary surface servo gains have been determined. Values of $\partial \delta_p / \partial (\Delta q/q)$ will be variable from -300 degrees to +300 degrees, with a minimum gain change of 1 degree. A summary of phugoid periods obtainable at different T-33 flight test conditions appears in Table VIII. Several conditions are shown to demonstrate:

(a) a condition in which the surface is quite effective,

(b) a condition in which the surface is relatively ineffective, and

(c) a typical test condition.

In the first two cases the amount of artificial stability required for short-period simulation has been chosen to be representative of extreme values that are likely to be used at the flight conditions chosen. Case (c), on the other hand, demonstrates the extreme flexibility in phugoid period when no additional static stability is employed ($\Delta C_{m_\alpha} = 0$). Conditions using the large positive gain of 300

Approved for Public Release

Contrails

degrees show the ability of the servo to produce static instability of the phugoid motion.

$\partial \delta_p / \partial (dq/dt)$ will be variable from -10 deg/$\frac{psf}{sec}$ to +10 deg/$\frac{psf}{sec}$ with a minimum gain change of ±.05 deg/$\frac{psf}{sec}$. Table IX shows the resulting available changes in phugoid damping ratio at similar test conditions to those in Table VIII.

In most cases, these phugoid periods and damping ratios are more extreme than are required for simulation of the four airplanes under consideration. However, there are certain flight regimes of transonic and supersonic airplanes for which Mach number effects cause the phugoid oscillation to be transformed into two exponential solutions, one of which is unstable. This condition is commonly known as "tuck-under". Preliminary investigations indicate that simulation of the more severe cases of this condition would require positioning of the elevator with Mach number. It is felt that arrangement for the addition of this input to the elevator servo is best delayed until a definite need has been established for adding this complication.

The maximum positive and negative values of the servo gains for the auxiliary surface are listed in Table X along with the other gains calculated in this section.

4. RESPONSE TO A FORWARD VELOCITY GUST

With the use of an auxiliary surface deflection proportional to $\dot{q}$, as obtained by a dynamic pressure measuring system, it becomes necessary to investigate the effects of a forward velocity gust on the normal acceleration response of the T-33. If a rapid change of airspeed occurs due to a forward velocity gust, then the signal proportional to rate of change of dynamic pressure will have a large magnitude for a short duration. This is then the command signal to the surface servo, calling for a large deflection for a short time, which in turn would produce a sudden pitching moment and a resulting

Approved for Public Release

Contrails

normal acceleration of considerable magnitude. Since this result is not similar to the response of a normal airplane to either a horizontal or vertical gust, it is necessary to limit the maximum surface rate of motion to avoid abrupt large deflections. Assuming a minimum phugoid period of about 45 seconds with the surface traveling through its full range of 30 degrees, the required maximum control rate is about 2 degrees per second. This 2 deg/sec rate will be used as an upper limit and has been checked, as follows, for the normal acceleration response. Assume that the product of servo gain $\partial\delta_p / \partial\dot{q}$ and rate of change of dynamic pressure, $\dot{q}$ due to the gust, is sufficiently large to call for greater than 6 degrees of surface deflection. Further assume that $\dot{q}$ due to the gust maintains its magnitude for 3 seconds and that the ground speed of the airplane does not change during this time. A typical flight condition of the T-33 is at a Mach number of 0.65, and an altitude of 10,500 feet, with a center of gravity location at 28.3% of the mean aerodynamic chord. At this condition the normal acceleration response, in g's, for the above gust may be represented by the expression:

$$n_z = 1 + .0554\left[e^{-2.02t}(\cos 2.72t - .303 \sin 2.72t) + 2.72t - 1\right] \quad (119)$$

which is the airplane response to a deflection of the auxiliary surface starting from zero and increasing at a rate of 2 deg/sec. After 3 seconds the net change of normal acceleration will be close to .4 g. This disturbance is considered to be safe since it builds up at a slow enough rate to remain controllable by the pilot through the elevator. The result of such an "artificial" forward velocity gust response would probably appear to the pilot as the response to a vertical gust and would, therefore, not feel unusual. It is further considered that the above condition is severe because the buildup of horizontal gust velocity usually occurs within 200 to 300 feet so that, at a Mach number of 0.65, the time during which $\dot{q}$ is large is less than .5 seconds, rather than the suggested value of 3 seconds.

Approved for Public Release

Contrails

5. RANGES OF VARIABLES USED AS INPUTS TO THE AUXILIARY SURFACE SERVO

The dynamic pressure will assume values between 80 psf, or approximately 150 knots indicated airspeed, and 800 psf. Allowance will be made for a maximum speed change of 10% of the speed at any reference flight condition. This accounts for dynamic pressure changes of 20% of the reference, during a maneuver in which the phugoid oscillation is excited. Hence the allowed maximum value of the auxiliary surface input, $\Delta q / q$, will be ±. 20. This is to apply to both high and low speed reference conditions so that a maximum dynamic pressure change, Δq , of 144 psf results for q_o = 720 psf. A maximum value of the rate of change of dynamic pressure, $\dot{q}$, at ±10 psf/sec is determined assuming a phugoid period of 60 seconds, a reference dynamic pressure of 500 psf, and a relative speed change of 10%. The above maxima are summarized as part of Table XIII.

B. DESIGN REQUIREMENTS FOR CONTROL OF THE LONGITUDINAL SHORT PERIOD MOTION

This section includes the gains and maximum inputs needed in designing the elevator control system. Artificial stability provided by the elevator control system can be used to vary the character of the short-period longitudinal motion as discussed in Section IV. The stability derivatives considered in this section are C_{m_α} , $C_{m_{\dot{\alpha}}}$, $C_{m_{\dot{\theta}}}$, and $C_{m_{\ddot{\theta}}}$. Final values of maximum and minimum gains appear in Table X. Maximum values of input are tabulated in Table XIII.

$\partial \delta_e / \partial \alpha$

1. Maximum Positive Gain

This derivative was obtained from the following formula for simulating the coefficient M_α in equation (7).

Approved for Public Release

Contrails

$$\frac{\partial \delta_e}{\partial \alpha} = \left[\frac{i_y}{4}\,\frac{\bar{c}}{g}\,\frac{C_{L_\alpha}}{(-C_{m_\delta})}\right]_{T-33}\,\frac{C_{L_0}}{C_{L_\alpha}}\,(-\Delta M_\alpha)$$

$$\frac{\partial \delta_e}{\partial \alpha} = 1.7\,\frac{C_{L_0}}{C_{L_\alpha}}\,(-\Delta M_\alpha) \qquad (120)$$

The coefficient 1.7 will be closely representative of all T-33 flight conditions. C_{L_0} / C_{L_α} will be the same for the T-33 and the airplane simulated in order to simulate the short period transient motion. ΔM_α was obtained from equation (15), neglecting the term $L_\alpha \Delta M_{\dot{\theta}}$ and the term involving τ_1 both of which are relatively small compared to the maximum ΔM_α .

A critical case of simulation occurs for one of the airplanes at a supersonic Mach number at 35,000 feet. At this condition ΔM_α will be large. The short period frequency is 1.54 cps and $C_{L_0}/C_{L_\alpha} = .021$ rad. The T-33 flight condition is $M = 0.75$ at 20,000 feet, which is chosen to give the same C_{L_0} / C_{L_α} . From equation (15), $\Delta M_\alpha = 85.8 \text{ sec}^{-2}$. Therefore,

$$\left(\frac{\partial \delta_e}{\partial \alpha}\right)_{max} = 1.7\,(.021)(85.8) = 3.06 \text{ deg/deg}$$

A large margin is desirable for this gain because of extreme conditions arising when simulating certain cg locations, and to cover other perhaps more extreme conditions that might arise in considering still other airplanes. A final value of 5 deg/deg was chosen.

2. Maximum Negative Gain

A maximum negative value for $\partial \delta_e / \partial \alpha$ was taken as that necessary to make the static margin of the T-33 zero at an extreme flight condition (most forward cg and gear up with tip tanks on). The value was $\partial \delta_e / \partial \alpha = -.90$ and was conservatively taken as

$$\frac{\partial \delta_e}{\partial \alpha} = -1.0 \text{ deg/deg}$$

Approved for Public Release

Contrails

3. Range of Input

The maximum input is taken as α = 10° which yields 90% of $C_{L_{max}}$ (with flaps up). The maximum negative input is taken as α = -8° to allow a margin for negative g maneuvers.

4. Cockpit Control Research

The range chosen above permits the static margin ($-dC_m/dC_L$) to be varied by +.733 or -.146. This is considered to provide an ample range for the purposes of the cockpit control research program.

5. Additional Notes

The system uses a measurement of n_z/q instead of α directly. For actual design, the values above have to be converted on the following basis:

$$\frac{\Delta n_z}{q} = \frac{C_{L_\alpha}}{W/S} \Delta\alpha$$

In design it is conservative to use a maximum value of $C_{L_\alpha} / \frac{W}{S}$ rather than the average value of .00188 ft^2/lb-deg. The value chosen was .00217 ft^2/lb-deg.

$$\therefore \frac{\Delta n_z}{q} = .00217\,\Delta\alpha \quad (\Delta\alpha \text{ in degrees})$$

The maximum range of n_z will be the airplane limits of -3g to +7.33g. The range of q is from 80 psf to 800 psf.

$\partial\delta_e / \partial\dot{\alpha}$

1. Maximum Positive Gain

This derivative was obtained from the following formula:

Approved for Public Release

Contrails

$$\frac{\partial \delta_e}{\partial \dot{\alpha}} = \left[\frac{i_y}{4}\,\frac{\bar{c}}{g}\,\frac{C_{L_\alpha}}{(-C_{m_\delta})}\right]_{T-33}\,\frac{C_{L_0}}{C_{L_\alpha}}\,(-\Delta M_{\dot{\alpha}})$$

$$\frac{\partial \delta_e}{\partial \dot{\alpha}} = 1.7\,\frac{C_{L_0}}{C_{L_\alpha}}\,(-\Delta M_{\dot{\alpha}}) \qquad (121)$$

$\Delta M_{\dot{\alpha}}$ can be obtained from equation (16) with the $\Delta M_{\dot{\theta}}$ term neglected. Neglecting $\Delta M_{\dot{\theta}}$ will be conservative.

A critical case of simulation occurs at a supersonic Mach number for one of the airplanes at 35,000 feet. C_{L_0}/C_{L_α} for both airplanes equals .021 rad. The T-33 flies at M = .75 and 15,000 feet. ζ = .12 and ω_n = 9.7 rad/sec for the simulated airplane, and ζ = .5 and ω_n =4.0 rad/sec for the T-33. A servo loop time lag of τ_1 = .05 sec was chosen. This value is conservative. From equation (16)

$\Delta M_{\dot{\alpha}}$ = -3.6 per sec, and from equation (121)

$\partial \delta_e/\partial \dot{\alpha}$ = .128 sec

The first two terms in equation (16) are $-(b_A - b_{T-33})$. Now, from equation (30), $b = L_\alpha - M_{\dot{\theta}} - M_{\dot{\alpha}}$. Considering relative orders of magnitude, L_α is the major term. Now, when an attempt is made to simulate C_{L_0}/C_{L_α} since $L_\alpha \frac{V}{g} = C_{L_\alpha}/C_{L_0}$, L_α will also be simulated to the extent that V is simulated. For this reason $\Delta M_{\dot{\alpha}}$ and subsequently, $\partial \delta_e/\partial \dot{\alpha}$ tend to be small. To cover possible cases where L_α is poorly simulated (perhaps due to simulating a very high speed condition) a large margin was chosen. As a final value:

$$\partial \delta_e/\delta \dot{\alpha} = .50 \text{ sec.}$$

Approved for Public Release

Contrails

2. Maximum Negative Gain

A maximum negative gain can be obtained by choosing a condition with negligible servo time lag. This is conservative. An extreme condition is simulating zero damping ratio with the T-33 flying at $M = .3$ at 15,000 feet.

The equation for $\partial\delta_e / \partial\dot{\alpha}$ is

$$\frac{\partial\delta_e}{\partial\dot{\alpha}} = \frac{i_y}{4}\,\frac{\bar{c}}{g}\,\frac{1}{\tau}\,\frac{C_{L_0}}{C_{m_\delta}}\left(\frac{C_{L_\alpha}}{2} - \frac{2\mu_1}{i_y}C_{m_{D\theta}} - \frac{2\mu_1}{i_y}C_{m_{D\alpha}}\right) \quad (122)$$

Substitution of the T-33 values yields

$$\frac{\partial\delta_e}{\partial\dot{\alpha}} = \frac{4.81}{4}\left(\frac{6.72}{32.2}\right)\frac{1}{3.49}\left(\frac{.711}{-.82}\right)\left[\frac{5.4}{2} - \frac{2(164.2)}{4.81}(-.0207)\right.$$

$$\left. - \frac{2(164.2)}{4.81}(-.00923)\right]$$

$$\frac{\partial\delta_e}{\partial\dot{\alpha}} = -.30\,\text{sec.}$$

To allow for a margin, a final value of $\partial\delta_e/\partial\dot{\alpha} = -.4$ sec was chosen.

3. Range of Input

The maximum input was chosen on the basis of information presented in Reference 4. The value of $\dot{\alpha}_{max}$ was taken to be ±35 deg/sec.

4. Cockpit Control Research

The range chosen above exceeds that given for the F-94 in Reference 2. Hence, it should be ample for the purposes of cockpit control research.

Approved for Public Release

Contrails

5. Additional Notes

The system uses a measurement of $\frac{d}{dt}\left(\frac{n_z}{q}\right)$ instead of $\dot{\alpha}$ directly. For actual design, the values above have to be converted on the following basis:

$$\frac{d}{dt}\left(\frac{n_z}{q}\right) = \frac{C_{L\alpha}}{W/S}\,\dot{\alpha}$$

As for item 5 under $\partial\delta_e/\partial\alpha$ a conservative value was chosen. Hence,

$$\frac{d}{dt}\left(\frac{n_z}{q}\right) = .00217\,\dot{\alpha} \quad (\dot{\alpha} \text{ in deg/sec})$$

$\partial\delta_e/\partial\dot{\theta}$

Equation (16) indicates that $\Delta M_{\dot{\theta}}$ can be used to decrease the values of $\Delta M_{\dot{\alpha}}$ required for simulation.

Considering equation (16) the requirements for $\partial\delta_e/\partial\dot{\theta}$ will be equivalent to those of $\partial\delta_e/\partial\dot{\alpha}$. For such values of $\partial\delta_e/\partial\dot{\theta}$ its effect upon ΔM_α in equation (15) will be small.

In addition to the above purpose $\partial\delta_e/\partial\dot{\theta}$ will also be used to simulate pitch dampers installed in the airplanes. The pitch dampers installed in the aircraft considered, have average gains of under 0.5 deg/(deg/sec). To simulate the effect of a pitch damper, $M_{\dot{\theta}}$ due to the pitch damper must be simulated. By equating the formulae for $M_{\dot{\theta}}$, namely $M_{\dot{\theta}} = \Delta C_{m_{0\theta}} \frac{2\mu_1}{i_y \tau}$ the following equation results.

$$\frac{\partial\delta_e}{\partial\dot{\theta}} = \left(\frac{\partial\delta_e}{\partial\dot{\theta}}\right)_1 \frac{(\bar{c}\,i_y)C_L}{(\bar{c}\,i_y)_1 C_{L_1}} \frac{C_{m_{\delta_{e_1}}}}{C_{m_{\delta_e}}} \qquad (123)$$

where $(\ )_1$ indicates the simulated airplane. A maximum value for

Approved for Public Release

Contrails

$\partial\delta_e / \partial\dot{\theta}$ occurs when simulating one of the supersonic airplanes at a condition where $C_L / C_{L_1} = 2.60$. The values of the coefficients are

$$\frac{\bar{\tau} i_y}{(\bar{\tau} i_y)_1} = 1.05 \qquad \frac{C_L}{C_{L_1}} = 2.60$$

$$\frac{C_{m_{\delta_{e_1}}}}{C_{m_{\delta_e}}} = 1.05 \qquad Max.\left(\frac{\partial\delta_e}{\partial\dot{\theta}}\right)_1 = .26 \ deg/\frac{deg}{sec}$$

Hence,

$$\frac{\partial\delta_e}{\partial\dot{\theta}} = .26(1.05)(2.60)(1.05)$$

$$\left(\frac{\partial\delta_e}{\partial\dot{\theta}}\right)_{max} = .742 \ deg/\frac{deg}{sec}$$

To allow a margin for covering future configurations choose 1 deg/(deg/sec) as the maximum gain necessary for the pitch damper. Thus, the maximum positive gain for $\partial\delta_e / \partial\dot{\theta}$ is 1 sec and the maximum negative gain is -.30 sec.

$\partial\delta_e / \partial\ddot{\theta}$

1. Maximum Positive and Negative Gains

This derivative can be used to vary the effective inertia in pitch. In so doing it will relieve the requirements on $\partial\delta_e / \partial\alpha$ and $\partial\delta_e / \partial\dot{\alpha}$. It appears that it would not be prudent to decrease the moment of inertia by more than 50%. It can be shown that decreasing the effective moment of inertia has a destabilizing effect on the real root represented by the factor $(\tau_1 d + 1 + \epsilon)$ in equation (35). Decreasing the moment of inertia by 50% makes ϵ more negative by

Approved for Public Release

Contrails

0.5, which is quite an appreciable change. The case of artificially increasing the moment of inertia appears to be of less interest. An increase of 50% seems ample. The corresponding $\partial \delta_e / \partial \ddot{\theta}$ is derived as follows. In equation (2), the moment of inertia appears only in the term $-\frac{i_y}{2\mu_1} D^2 \Delta\theta$. If we make the elevator respond to $\ddot{\theta}$, we shall in effect be adding a term $C_{m_{D^2\theta}} D^2 \Delta\theta$. Thus, the coefficient of $D^2 \Delta\theta$ becomes $\left(-\frac{i_y}{2\mu_1} + C_{m_{D^2\theta}}\right)$, and so adding $C_{m_{D^2\theta}}$ is equivalent to changing $\left(\frac{-i_y}{2\mu_1}\right)$. If Δi_y represents the desired change of inertia, we need

$$C_{m_{D^2\theta}} = -\frac{\Delta i_y}{2\mu_1}$$

Now

$$C_{m_{D^2\theta}} = \frac{1}{\tau^2} \frac{\partial C_m}{\partial \delta_e} \frac{\partial \delta_e}{\partial \ddot{\theta}}$$

Therefore, we require

$$\frac{\partial \delta_e}{\partial \ddot{\theta}} = -\frac{\Delta i_y}{2\mu_1} \tau^2 \frac{1}{C_{m_{\delta_e}}}$$

$$= -\frac{C_L}{4} \frac{\bar{c}}{g} \frac{\Delta i_y}{C_{m_{\delta_e}}}$$

Setting $\Delta i_y = \pm 0.5 i_y$

$$\frac{\partial \delta_e}{\partial \ddot{\theta}} = \pm \frac{C_L}{8} \frac{\bar{c}}{g} \frac{i_y}{C_{m_{\delta_e}}}$$

To have a good margin for the gain $\partial \delta_e / \partial \ddot{\theta}$, i_y was taken at its maximum value of 4.81. C_L was taken as .613. An average

Approved for Public Release

Contrails

value of -.85/rad was used for $C_{m_{\delta_e}}$. $\bar{c}$ = 6.72 feet.

Substituting

$$\frac{\partial \delta_e}{\partial \ddot{\theta}} = \pm .0905 \text{ sec}^2$$

This is rounded off to a design value of

$$\left(\frac{\partial \delta_e}{\partial \ddot{\theta}}\right)_{max} = \pm 0.1 \text{ sec}^2$$

2. Maximum Value of $\ddot{\theta}$

The maximum value of $\ddot{\theta}$ was obtained from Reference 4. A maximum operational value of 2 rad/sec^2 is indicated. To be conservative the value chosen was

$$\ddot{\theta}_{max} = 2.5 \text{ rad/sec}^2$$

C. DESIGN REQUIREMENTS FOR CONTROL OF THE LATERAL MOTION

The determination of maximum and minimum values for the artificial stability derivatives to be provided by the rudder and aileron servos can be handled by dividing them into two groups. The first group consists of the ordinary static and damping derivatives. The second group consists of derivatives due to angular accelerations and rate of change of sideslip angle. Table X summarizes the design ranges of gain chosen for the various artificial stability channels, and Table XIII shows maximum anticipated values of the input variables.

1. $\frac{\partial \delta_r}{\partial r}$, $\frac{\partial \delta_a}{\partial r}$, $\frac{\partial \delta_r}{\partial p}$, $\frac{\partial \delta_a}{\partial p}$, $\frac{\partial \delta_r}{\partial \beta}$ and $\frac{\partial \delta_a}{\partial \beta}$

A conservative solution was undertaken in order to avoid the necessity of choosing many specific flight conditions for several airplanes to locate exactly the critical conditions. Some arbitrary mar-

Approved for Public Release

Contrails

gins are required in any case to allow for the possible characteristics of future airplane designs.

Simulation of the lateral motion is to be obtained by simulating the coefficients of equations (64) and (65). These coefficients are defined in Table IV. The values of the T-33 stability derivatives required for simulation can be obtained by equating the coefficients defined in Table IV for the T-33 to the coefficients of the simulated airplane, and solving for the T-33 derivatives.

The formulae for calculating the values of the T-33 stability derivatives are given below.

$$C_{n_r} = K_1 \frac{\tau}{\tau_1} \left[AC_{n_{r_1}} + BC_{\ell_{r_1}} \right]$$

$$C_{\ell_r} = K_1 \frac{\tau}{\tau_1} \left[CC_{\ell_{r_1}} + DC_{n_{r_1}} \right]$$

$$C_{n_p} = K_1 \frac{\tau}{\tau_1} \left[AC_{n_{p_1}} + BC_{\ell_{p_1}} \right]$$

$$C_{\ell_p} = K_1 \frac{\tau}{\tau_1} \left[CC_{\ell_{p_1}} + DC_{n_{p_1}} \right]$$

$$C_{n_\beta} = K_1 \frac{C_L b}{C_{L_1} b_1} \left[AC_{n_{\beta_1}} + BC_{\ell_{\beta_1}} \right]$$

$$C_{\ell_\beta} = K_1 \frac{C_L b}{C_{L_1} b_1} \left[CC_{\ell_{\beta_1}} + DC_{n_{\beta_1}} \right] \qquad (124)$$

$( )_1$ Simulated airplane values

$( )$ T-33 values (normal plus artificial)

Approved for Public Release

Contrails

$$K_1 = \frac{1}{1 - \frac{i_{xz_1}^2}{i_{x_1} i_{z_1}}}$$

$$A = \frac{i_z}{i_{z_1}} - \frac{i_{xz} i_{xz_1}}{i_{z_1} i_{x_1}} \qquad C = \frac{i_x}{i_{x_1}} - \frac{i_{zx} i_{xz_1}}{i_{x_1} i_{z_1}}$$

$$B = \frac{i_{xz_1} i_z}{i_{x_1} i_{z_1}} - \frac{i_{xz}}{i_{x_1}} \qquad D = \frac{i_{xz_1} i_x}{i_{x_1} i_{z_1}} - \frac{i_{zx}}{i_{z_1}}$$

K_1 varies so little from unity that its effect is negligible

b/b_1 reaches a maximum of 1.72 for one of the airplanes under consideration

$\frac{\tau}{\tau_1}$ and $\frac{C_L}{C_{L_1}}$: upon examining tabulated airplane data for the four airplanes, it appears that the τ ratio and C_L ratio are extreme at similar flight conditions. By trying to simulate τ and C_L ratios as closely as possible by choosing the optimum flight condition, the maximum τ ratio can be kept under 1.8 and the C_L ratio, under 2.75.

Considering the four airplanes, Table XI, giving maximum positive and negative values of the stability derivatives and inertia coefficients, was compiled. Since these values are not all for one airplane at one flight condition they contribute to conservatism.

A solution was made for the case of full tip tanks. However, this solution was found to be too conservative. For this reason a solution was made for a less conservative, more practical condition of empty tip tanks with full internal fuel. In order to simulate some flight conditions, the tip tanks must be empty. For the simulation of other flight conditions, some tip tank fuel may be allowable.

Approved for Public Release

Contrails

The maximum values of the artificial derivatives were obtained from equation (124). These were converted to gain ratios by equations of the form

$$\frac{\partial \delta_r}{\partial r} = \Delta C_{n_r} \frac{1}{C_{n_{\delta_r}}} \frac{b}{2V} \tag{125}$$

$$\frac{\partial \delta_r}{\partial \beta} = \Delta C_{n_\beta} \frac{1}{C_{n_{\delta_r}}} \tag{126}$$

The minimum values of control effectiveness are:

$$C_{n_{\delta_r}} = -.072/rad$$

$$C_{\ell_{\delta_a}} = -.14/rad \text{ (tip tanks on)}$$

The maximum value of $b/2V$ was taken to be .0356, which implies that V will be greater than 310 knots true speed. This is expected to be the case for most of the contemplated flight testing. Tests can be made, of course, at lower values of V, with somewhat reduced ranges of artificial stability available.

With the above information, maximum and minimum values of gain were computed. Average typical values of the T-33 normal stability derivatives were used in obtaining the incremental values of each artificially varied stability derivative. The results are tabulated on the following page.

Approved for Public Release

Contrails

	RANGE OF VALUES
$\partial\delta_r/\partial r$	1.30 to -.46 sec
$\partial\delta_a/\partial r$	-.80 to .19 sec
$\partial\delta_r/\partial p$	.65 to -.80 sec
$\partial\delta_a/\partial p$	.55 to -.22 sec
$\partial\delta_r/\partial\beta$	-39.0 to 9.1 deg/deg
$\partial\delta_a/\partial\beta$	-20.4 to -5.6 deg/deg

The yaw rate and roll rate derivatives tabulated above are reasonable but the sideslip derivatives seem too large to be practical. This is a result of the conservatism imposed by not using consistent data from one airplane at one flight condition. Accordingly the sideslip derivatives were re-examined on the basis of considering various consistent conditions for individual airplanes. On this basis, it was possible to reduce the required gains so that the maximums are no greater than 10 deg/deg. It is thought that it would be difficult in practice to use gains higher than this, because of the possibility of excessive response to gusts in rough air and the possibility of undue amplification of noise. The reduced ranges for the sideslip derivatives are

$\partial\delta_r/\partial\beta$	-10 to +9 deg/deg
$\partial\delta_a/\partial\beta$	+10 to -6 deg/deg

A check on the practicality of the above results was obtained by a comparison with minimum values necessary to change the T-33 response by about 10%. In Reference 5 the changes in Dutch roll period and damping were calculated for corresponding changes in the stability derivatives for the F-80 airplane at M = .3, h = 15,000 feet. The results appear on the following page.

Approved for Public Release

Contrails

EFFECT ON DUTCH ROLL OF CHANGES IN F-80 STABILITY DERIVATIVES

(FROM REFERENCE 5)

STABILITY DERIVATIVE	VARIATION %	NORMAL F-80 VALUE NO TIP TANKS	RESULTING VARIATION OF THE DUTCH ROLL, %	
			P	$T_{1/2}$
C_{n_r}	15	-.0989	0	11.4
C_{ℓ_r}	25	.1308	0	5.0
C_{n_p}	25	-.0337	1.0	6.0
C_{ℓ_p}	15	-.464	0.5	9.5
C_{n_β}	15	.0960	7.5	2.3
C_{ℓ_β}	15	-.0572	0.8	3.5

For the purposes of this approximate check, it was assumed that for the T-33 airplane at the same flight condition, the same percent variations in aerodynamic derivatives would produce the same percent variation of the Dutch roll period and damping. Next the percent variations were derived which would change either P or $T_{\frac{1}{2}}$ by 10%. From these percent variations of aerodynamic derivatives, corresponding gains were calculated, using the following data:

V = 316 ft/sec, $C_{n_{\delta_r}}$ = -0.072 per radian, $C_{\ell_{\delta_a}}$ = -0.14 per radian.

The results are shown in the following table.

Approved for Public Release

Contrails

APPROXIMATE GAINS REQUIRED TO CHANGE THE T-33 DUTCH ROLL RESPONSE BY 10% AT $M = 0.3$ AND $h = 15{,}000$ FT.

DERIVATIVE	T-33 VALUES TIP TANKS ON	% VARIATION CAUSING 10% RESPONSE CHANGE	GAIN VALUES
C_{n_r}	-.15	15	$\partial\delta_r/\partial r = \pm 0.0185$ SEC
C_{ℓ_r}	.18	50	$\partial\delta_a/\partial r = \pm 0.038$ SEC
C_{n_p}	-.03	40	$\partial\delta_r/\partial p = \pm 0.0099$ SEC
C_{ℓ_p}	-.56	15	$\partial\delta_a/\partial p = \pm 0.0355$ SEC
C_{n_β}	.075	20	$\partial\delta_r/\partial\beta = \pm 0.208$ DEG/DEG
C_{ℓ_β}	-.145	40	$\partial\delta_a/\partial\beta = \pm 0.415$ DEG/DEG

The gain values thus derived are considered to be the minimum values which will produce an appreciable change in the Dutch roll mode. We now compare these minimums with the total ranges of gain that were previously determined. Taking $\partial\delta_r/\partial r$ as an example, the range is from 1.30 to -0.46 sec for a total variation of 1.76. Dividing by the minimum of 0.0185, we find a ratio of 95. The minimum ratio is 26 for $\partial\delta_a/\partial r$ and the maximum ratio is 144 for $\partial\delta_r/\partial p$.

These ratios are large enough to make it clear that the available ranges of gain will produce very substantial alterations in the stability of the T-33. On the other hand, the maximum is not so large that difficulty with resolution would be expected in making small changes in the settings. While this analysis has been made for only one flight condition, it is felt that it gives a useful general check as to reasonable orders of magnitude for the ranges of the various gains.

One more consideration must be made before the final ranges of

Approved for Public Release

gain for $\partial\delta_r/\partial r$ and $\partial\delta_a/\partial p$ are decided. The yaw and roll dampers in the aircraft considered must be simulated.

The yaw and roll dampers installed in the aircraft considered have average gains of 1 deg/(deg/sec) with 1.5 deg/(deg/sec) the maximum. The action of the damper is limited to a few degrees of control surface deflection. Using a similar approach to that used in deriving formulae (124) and (125), the formulae for δ_r/r and δ_a/p can be derived.

Starting with the equality $N_{\delta_r}\,\delta_r = N_{\delta_{r_1}}\,\delta_{r_1}$ and $r = r_1$ the following formula is obtained. Terms with subscript 1 refer to the simulated airplane.

$$\frac{\partial\delta_r}{\partial r} = \frac{K_1}{K}\,\frac{i_z}{i_{z_1}}\,\frac{C_L b}{C_{L_1} b_1}\left[\frac{C_{n_{\delta_{r_1}}} + \dfrac{i_{xz_1}}{i_{x_1}}\,C_{\ell_{\delta_{r_1}}}}{C_{n_{\delta_r}} + \dfrac{i_{xz}}{i_x}\,C_{\ell_{\delta_r}}}\right]\frac{\partial\delta_{r_1}}{\partial r_1} \tag{127}$$

The product of i_{xz}/i_x and the cross control effectiveness, $C_{\ell_{\delta_r}}$, is small compared to the control effectiveness term and can be neglected. (In the corresponding equation for δ_a/p, the product of i_{xz}/i_z and $C_{n_{\delta_a}}$ is similarly neglected.)

Also, K_1/K is nearly unity.

The result is

$$\frac{\partial\delta_r}{\partial r} = \frac{i_z}{i_{z_1}}\,\frac{C_L b}{C_{L_1} b_1}\left(\frac{C_{n_{\delta_{r_1}}}}{C_{n_{\delta_r}}}\right)\frac{\partial\delta_{r_1}}{\partial r_1} \tag{128}$$

$$\frac{\partial\delta_a}{\partial p} = \frac{i_x}{i_{x_1}}\,\frac{C_L b}{C_{L_1} b_1}\left(\frac{C_{\ell_{\delta_{a_1}}}}{C_{\ell_{\delta_a}}}\right)\frac{\partial\delta_{a_1}}{\partial p_1} \tag{129}$$

Conservative values of the coefficients based on information from one

Approved for Public Release

Contrails

of the four airplanes are as follows:

$i_z / i_{z_1} = 0.31$ (T-33 with empty tip tanks)

$i_x / i_{x_1} = 1.68$

$b / b_1 = 1.72$

$C_L / C_{L_1} = 2.75$

$C_{n_{\delta_{r_1}}} / C_{n_{\delta_r}} = 2.39$

$C_{\ell_{\delta_{a_1}}} / C_{\ell_{\delta_a}} = 0.32$

Using an average value of damper gain of 1 deg/(deg/sec) for an airplane to be simulated, we obtain

$$\left(\frac{\partial \delta_r}{\partial r}\right)_{max} = 3.5 \ deg/\frac{deg}{sec}$$

$$\left(\frac{\partial \delta_a}{\partial p}\right)_{max} = 2.5 \ deg/\frac{deg}{sec}$$

These values of gain are larger than those required for simulation of the basic airplanes without dampers. This is reasonable, however, because the Dutch roll motions of the airplanes without dampers are in general lightly damped. It is felt that the T-33 control system should be capable of making the lateral motions well-damped.

The final values of the six gains discussed in this section appear in Table X.

2. $\frac{\partial \delta_r}{\partial \dot{r}}$, $\frac{\partial \delta_a}{\partial \dot{r}}$, $\frac{\partial \delta_r}{\partial \dot{p}}$, $\frac{\partial \delta_a}{\partial \dot{p}}$, $\frac{\partial \delta_r}{\partial \dot{\beta}}$ and $\frac{\partial \delta_a}{\partial \dot{\beta}}$

There are six lateral derivatives based upon angular accelerations and rate of change of sideslip which can be handled together,

Approved for Public Release

Contrails

namely $C_{\ell_{\delta r}}$, $C_{\ell_{\delta p}}$, $C_{n_{\delta r}}$, $C_{n_{\delta p}}$, $C_{\ell_{\delta \beta}}$, and $C_{n_{\delta \beta}}$. These derivatives can be used to vary the effective inertias and to compensate for time lags.

Equation (76) is representative of the method used for time lag compensation. It gives the amount of artificial control, $\partial \delta_a / \partial \dot{\beta}$, necessary to overcome the effect of time lag upon the response of the aileron, δ_a, to sideslip angle, β. It is assumed that the control system dynamics can be represented by a second-order system of damping ratio ζ, and undamped natural frequency ω_n. As explained in Section IV, $\partial \delta_a / \partial \dot{\beta}$ is chosen to compensate for a time lag of $2\zeta/\omega_n$ seconds. A damping ratio of $\zeta = 0.7$ and a natural frequency of $\omega_n = 10\pi$ rad/sec are assumed. The various channels of the actual control system are expected to have less lag than these values represent. Hence, $2\zeta/\omega_n = .045$ sec and equation (76) becomes:

$$\frac{\partial \delta_a}{\partial \dot{\beta}} = .045 \frac{\partial \delta_a}{\partial \beta}$$

Thus the required range of $\partial \delta_a / \partial \dot{\beta}$ is determined from the design range of $\partial \delta_a / \partial \beta$. This method is applicable, of course, to the other five derivatives being considered here.

This method was used to derive the values of $\partial \delta_a / \partial \dot{\beta}$ given in Table X. It was used also to determine the positive design value of +0.41 for $\partial \delta_r / \partial \dot{\beta}$. The other value for $\partial \delta_r / \partial \dot{\beta}$ was determined on the basis that this derivative provides Dutch roll damping in somewhat the same way as the derivative $\partial \delta_r / \partial r$. The possibility of using it as an alternate source of damping led to the choice of the same maximum value as determined for $\partial \delta_r / \partial r$. For the other four derivatives, the requirements for time lag compensation are less critical than the requirements for "artificial inertia," which are explained next.

It is desirable also to allow for the possibility of varying the

Approved for Public Release

effective inertia. This can be done to decrease the gains necessary to simulate the static and damping derivatives. The case of full internal fuel and empty tip tanks is used. The inertia coefficients are $i_x = .101$ and $i_z = .244$. The artificial inertia in roll is represented by

$$C_{\ell_{Dp}} = C_{\ell_{\delta_a}} \frac{\partial \delta_a}{\partial D\left(\frac{pb}{2V}\right)}$$

$$= C_{\ell_{\delta_a}} \frac{1}{\tau} \frac{\partial \delta_a}{\partial\left(\frac{\dot{p}b}{2V}\right)}$$

$$\frac{\partial \delta_a}{\partial \dot{p}} = C_{\ell_{Dp}} \frac{1}{C_{\ell_{\delta_a}}} \frac{\tau b}{2V}$$

$$= C_{\ell_{Dp}} \frac{1}{C_{\ell_{\delta_a}}} \frac{bC_L}{4g}$$

Thus for the T-33

$$\frac{\partial \delta_a}{\partial \dot{p}} = C_{\ell_{Dp}} \frac{1}{C_{\ell_{\delta_a}}} .291 C_L \qquad (130)$$

Likewise

$$\frac{\partial \delta_r}{\partial \dot{r}} = C_{n_{Dr}} \frac{1}{C_{n_{\delta_r}}} .291 C_L \qquad (131)$$

The coefficient $C_{\ell_{Dp}}$ is directly equivalent to an increment in i_x. That is, in order to vary the inertia by 50%, $C_{\ell_{Dp}}$ should equal $i_x/2$. The maximum variation in the moment of inertia was taken as ±50%. As in the pitch case, this is considered a maximum

Approved for Public Release

Contrails

practical amount. The maximum value of C_L was taken to be .613 which corresponds to about 160 knots EAS. At lower speeds, the available variation of effective moment of inertia will be reduced from ±50%. The final results are given below.

$$\left(\frac{\partial \delta_a}{\partial \dot{p}}\right)_{max} = .0644 \text{ sec}^2$$

$$\left(\frac{\partial \delta_r}{\partial \dot{r}}\right)_{max} = .302 \text{ sec}^2$$

These values are larger than those based on time lag compensation and so they appear in Table X.

To alter the effective product of inertia, we provide artificial $C_{\ell_{Dr}}$ and $C_{n_{Dp}}$. We have the following relations, derived as before.

$$\frac{\partial \delta_a}{\partial \dot{r}} = C_{L_{Dr}} \frac{1}{C_{\ell_{\delta_a}}} .291 C_L$$

$$\frac{\partial \delta_r}{\partial \dot{p}} = C_{n_{Dp}} \frac{1}{C_{n_{\delta_r}}} .291 C_L$$

It is believed that an adequate range of products of inertia will be available if the direction of the principal axes can in effect be tipped ±20°. This requires $\Delta i_{xz} = \pm 0.060$. To achieve this result, we require $C_{\ell_{Dr}} = C_{n_{Dr}} = \pm 0.060$. Again using $C_L = 0.613$, we find

$$\frac{\partial \delta_a}{\partial \dot{r}} = \pm 0.076 \text{ sec}^2$$

$$\frac{\partial \delta_r}{\partial \dot{p}} = \pm 0.149 \text{ sec}^2$$

Approved for Public Release

Contrails

3. CONVERSION OF n_y/q MEASUREMENT TO SIDESLIP

The sideslip measurement will be obtained by dividing the lateral accelerometer reading (n_y) by q . If $C_{y_{\delta_r}}$ is neglected, we have

$$\beta = \frac{W}{C_{y_\beta} S} \frac{\Delta n_y}{q}$$

An average value for the derivative C_{y_β} is -.63/rad. For a weight of 12,500 lb with S = 234.8 sq ft,

$$\beta = -4850 \frac{\Delta n_y}{q}$$

The above equation is based on β in degrees. Δn_y is a non-dimensional load factor, and q is in psf. An investigation will be made in the detailed design phase of the program to determine whether special measures should be taken to correct for the effect of $C_{y_{\delta_r}}$.

The gains listed in Table X can be converted to represent $\Delta n_y/q$ inputs by use of the above formula. The gains in Table X should be multiplied by -4850 and the input changed to n_y/q or $\frac{d}{dt}\left(\frac{n_y}{q}\right)$.

D. DESIGN REQUIREMENTS FOR THE ARTIFICIAL FEEL SYSTEM

The design of the artificial feel installation is to be such that simulation of the feel systems of the four typical airplanes considered in this program will be possible and such that existing and future ideas on desirable feel characteristics may be investigated.

In order to design the artificial feel control system outlined in Figures 5 to 7, the maximum and minimum values of gain for the various computer inputs must be determined along with maximum values of the variables. These data

Approved for Public Release

Contrails

will be derived below. Table XIV gives maximum values of the variables. The gains are tabulated in Table XII.

1. ELEVATOR FEEL SYSTEM

$$a_1 = \frac{\partial F_{ES}}{\partial \delta_{ES}}$$

The first feel coefficient or gain to be considered is the spring constant $\frac{\partial F_{ES}}{\partial \delta_{ES}}$ in lbs per inch. It is desirable to be able to vary the spring constant over a wide range, extending up to gradients which would make the stick seem essentially fixed. Calculations on the rigidity of the T-33 stick show that a force of 100 lbs at the hand grip with the bottom held rigidly fixed will bend the stick . 2 in. at the hand grip. A deflection of less than one inch for a 100 lb stick force would make the stick appear quite rigid to a pilot; hence a value of 250 lbs/inch spring constant was chosen as the maximum value. This will give a total deflection of .6 inches for a 100 lb force. In addition the system is designed so that the stick can be rigidly locked, with a stick force measurement used as the signal to the elevator.

The minimum gain was derived by choosing a value of spring constant below the lowest constant of the four airplanes. A reasonable value was found to be 0. 8 lb/in. This amounts to about 7 lb at full aft stick deflection.

Current design specifications for elevator stick force specify $F_{ES_{max.}} = 200$ lb. This is taken as the design maximum value for the T-33 control system. Considering the four airplanes investigated, an inclusive range for δ_{ES} is 5 in. stick forward and 9 in. stick back.

$$a_2 = \frac{\partial F_{ES}}{\partial (q\delta_{ES})}$$

Another spring constant to be simulated is the aerodynamic spring constant

Approved for Public Release

Contrails

$$\frac{\partial F_{ES}}{\partial (q\delta_{ES})} = \frac{\partial F_{ES}}{\partial \delta_{ES}} \left(\frac{1}{q}\right)$$

The design range of dynamic pressure is taken to be 80-800 psf. A minimum stick force gradient of 0.8 lb/inch is assumed at q = 200 psf. This gives $\frac{\partial F_{ES}}{\partial (q\delta_{ES})}$ = 0.004 ft^2/in. This setting would give still lower gradients at q less than 200 psf. At the maximum q, it would give 3.2 lb/inch, which is very light for such a high speed condition. A maximum stick force gradient of 250 lbs/inch is assumed at q = 500 psf. This gives $\frac{\partial F_{ES}}{\partial (q\delta_{ES})}$ = 0.5 ft^2/in. Thus, an essentially rigid stick is available at this q and higher. At q = 80 psf, a maximum of 40 lb/inch is available, which is very heavy for low speed flight. The ratio of maximum to minimum gains is $\frac{0.5}{0.004}$ = 125, which is considered a practical value.

The sketch below illustrates the extreme gains

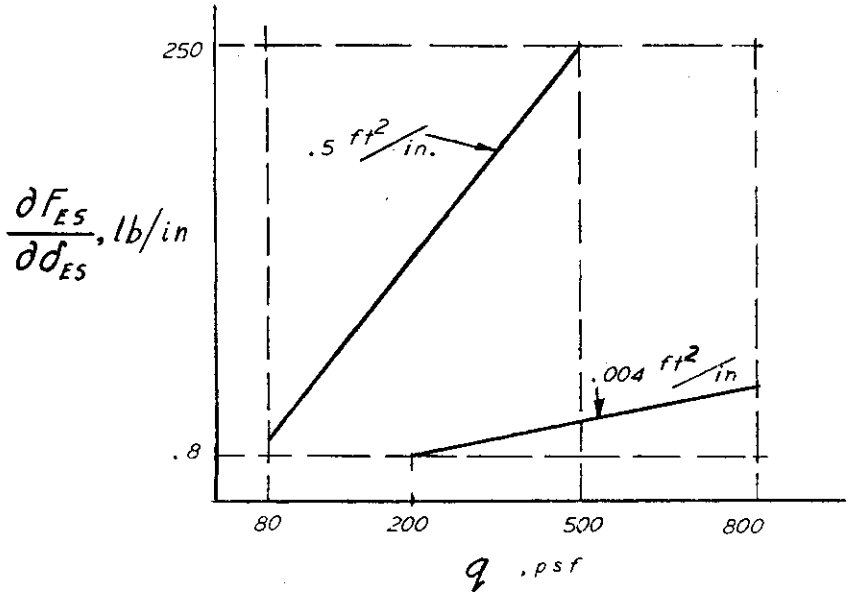

Approved for Public Release

Contrails

$$a_4 = \frac{\partial F_{ES}}{\partial \dot{\delta}_{ES}}$$

This gain represents viscous damping. The largest value of viscous damping for the four airplanes considered is 3 $\frac{\text{lb-sec}}{\text{in.}}$. This value was doubled to yield a maximum design value of 6 $\frac{\text{lb-sec}}{\text{in.}}$. The minimum gain was defined as an imperceptible force at a large stick rate. A force of 0.5 lb at 10 in/sec was chosen giving a minimum gain of .05 $\frac{\text{lb-sec}}{\text{in.}}$.

$$a_5 = \frac{\partial F_{ES}}{\partial n_z}$$

According to Air Force specifications, 3 to 8 $\frac{\text{lbs}}{\text{g}}$ is the permissible range of stick force per g for fighters. A maximum design value of 25 lbs/g is chosen to provide an adequate margin to cover the requirements of various investigations of control systems. A value of 0.5 lbs/g is chosen as the minimum value that would be significant. There is no requirement for negative gradients.

a_6 , Trimming Force (No Speed Feel)

This force is needed to balance out forces such as those due to spring constants, in order to vary the neutral (zero stick force) stick position. The neutral stick position is to be variable over half of the total range of +5 in. to -9 in. This leaves the remaining half for maneuvering. The largest spring constant used among the four airplanes is 10 lb/in. This value was doubled to give a maximum design value of 20 lb/in. This spring constant coupled with +2.5 in. to -4.5 in. of stick deflection yields forces to be trimmed of 50 lb push and 90 lb pull.

It is true that spring constants larger than 20 lb/in will be available. Such cases generally imply working with a reduced range of stick travel, and so a reduced range of trim in inches of stick travel is acceptable

Approved for Public Release

Contrails

with high spring constants. The range in terms of stick force is considered ample. With high spring constants, the position of the stick in the cockpit can also be adjusted by altering the linkage between the stick and the stick position transducer.

A total range of 140 lb of trim force is believed reasonable and is not expected to give any difficulty with resolution in trimming small forces.

a_7 , Trimming Force (With Speed Feel)

This force is similar to the trimming force with no speed feel, except that its effect varies with q . It represents the effect of a trim tab. A minimum value of a_7 times trimming voltage would be a barely perceptible force to be balanced out at a high q ; say 1 lb. at 800 psf. This gives a minimum value of .00125 ft^2.

A maximum value of a_7 times trimming voltage would occur at low q equal to 80 psf. At a low q , the stick force gradients will not be maximum. Allowance is to be made at q = 80 psf for trimming out forces ranging from a 35 lb pull to a 15 lb push, for a total range of 50 lb. This gives a range of a_7 times trimming voltage of 0.625 ft^2.

The variation from the minimum increment of 0.00125 ft^2 to the maximum range of 0.625 ft^2 is thought to be about as broad as is practical without running a risk of difficulties with resolution.

K_β , Elevator to Trim

This is the elevator deflection commanded by a pilot's trim voltage setting. For this quantity all that need be specified is the range of δ_e desired. The design values are taken as up 15° and down 5°.

$\frac{\partial \delta_e}{\partial \delta_{ES}}$

This gain is the stick to elevator gearing. For a very high spring constant $\left(\frac{\partial F_{ES}}{\partial \delta_{ES}} = 250 \text{ lb/in} \right)$ it is desirable to have some elevator deflection available for maneuvers. On this basis a maximum value

Approved for Public Release

Contrails

of 20 deg/in was chosen. The minimum gain should provide some maneuverability, say at least two degrees of elevator for a full stick deflection of 9 inches. Hence a minimum value of .2 deg/in was chosen. This range varies from about one-tenth normal to about ten times normal.

$$\frac{\partial \delta_e}{\partial (a_1, \delta_{ES})}$$

This gain is actually a ratio $\dfrac{\partial \delta_e}{\partial \delta_{ES}} \quad \dfrac{1}{\partial F_{ES} / \partial \delta_{ES}}$

The design range for this gain is found by assuming a normal value of 2 deg/ in. for the elevator-stick gearing. $\partial \delta_e / \partial \delta_{ES}$, and combining it with the range of design values for $a_1 \left(= \partial F_{ES} / \partial \delta_{ES} \right)$.

This procedure is justified on the basis that it is unrealistic to combine extremes of both the gearing ratio and the stick-force gradient. Minimum gearing with maximum force gradient would make the elevator essentially immovable, while maximum gearing with minimum force gradient would give an extremely sensitive control. The results obtained from the procedure adopted are considered reasonable. They are as follows.

$$\left(\frac{\partial \delta_e}{\partial (a_1, \delta_{ES})} \right)_{max} = -2.5 \ \frac{deg}{lb.\ Pull}$$

$$\left(\frac{\partial \delta_e}{\partial (a_1, \delta_{ES})} \right)_{min} = -.008 \ \frac{deg}{lb.\ Pull}$$

$$\frac{\partial \delta_e}{\partial (a_2, \delta_{ES})}$$

This gain is actually a ratio $\dfrac{\partial \delta_e}{\partial \delta_{ES}} \quad \dfrac{1}{\partial F_{ES} / \partial (q \delta_{ES})}$

Approved for Public Release

Contrails

By similar reasoning as for the preceding gain calculations, extremes of $\frac{1}{\partial F_{ES}/\partial(q\sigma_{ES})}$ are used to obtain:

$$\left(\frac{\partial \sigma_e}{\partial(a_2 \sigma_{ES})}\right)_{max} = -500 \ \ deg/ft^2$$

$$\left(\frac{\partial \sigma_e}{\partial(a_2 \sigma_{ES})}\right)_{min} = -4.0 \ \ deg/ft^2$$

2. AILERON AND RUDDER FEEL SYSTEMS

Aileron Trimming

An aileron deflection is commanded by a pilot's trim voltage setting. For this ratio all that need be specified is the maximum σ_a desired. The value chosen for design is half the maximum deflection;

$$(\sigma_a)_{TRIM} = (\sigma_{a_L} + \sigma_{a_R}) = \pm 20°.$$

$\partial F_{AS}/\partial \sigma_{AS}$

This spring constant should be similar to that for the elevator. According to Air Force specifications, 100 lb is a maximum stick force for aileron deflection. A total deflection of .6 in for 100 lb provides an essentially rigid stick, so that assuming the stick itself deflects .2 in. for 100 lb of load, .4 in./100 lb remains for a maximum spring constant of 250 lb/in.

A minimum value of .5 lb/in.was chosen. This is somewhat below the elevator value because light gradients are thought to be more useable in the case of the ailerons.

$\partial \sigma_a/\partial \sigma_{AS}$

This is the stick to aileron gearing. For the case of a large spring

Approved for Public Release

Contrails

constant of 100 lb/in., there is to be available 40° deflection for 1 in. of stick deflection, with this nearly rigid stick condition. Hence $(\partial\delta_a/\partial\delta_{AS})_{max}$ = 40 deg/in. The minimum gain should provide some maneuverability, say at least two degrees of each aileron, for a full stick deflection of seven inches. Hence $(\delta_a/\delta_{AS})_{max.}$ = 4/7 = .57 deg/in.

$\partial\delta_a/\partial(b_1\delta_{AS})$

This ratio is actually a ratio $(\partial\delta_a/\partial\delta_{AS})\left(\frac{1}{\partial F_{AS}/\partial\delta_{AS}}\right)$.

A good average value to use for $\partial\delta_a/\partial\delta_{AS}$ is $40/7 = 5.7\ \frac{\text{deg}}{\text{in}}$. Extremes of $\partial\delta_a/\partial(b_1\delta_{AS})$ can be obtained from 5.7 divided by extremes of $\partial F_{AS}/\partial\delta_{AS}$.

The results are 11.4 deg/lb to .023 deg/lb.
It is reasonable to use an average value of $\partial\delta_a/\partial\delta_{AS}$ in the above evaluation for the same reason that such a value could be used in the longitudinal case. (See $\partial\delta_e/\partial(a,\delta_{ES})$).

$\partial\delta_a/\partial\delta_{r_c}$

This ratio may be approximately determined in terms of i_x/i_z, $C_{n_{\delta_r}}$, $C_{\ell_{\delta_a}}$, and $C_{\ell_{\delta_r}}$ for the T-33 and the airplane to be simulated. δ_{r_c} represents a rudder command signal, or $(\partial\delta_r/\partial\delta_{RP})\,\delta_{RP}$.

$$\frac{\partial\delta_a}{\partial\delta_{r_c}} = \frac{\left[\left(\frac{i_z}{i_x}\right)\left(\frac{C_{\ell_{\delta_r}}}{C_{n_{\delta_r}}}\right)+\frac{i_{xz}}{i_x}\right]_{\text{airplane to be simulated}} \left[\left(\frac{i_z}{i_x}\right)\left(\frac{C_{\ell_{\delta_r}}}{C_{n_{\delta_r}}}\right)+\frac{i_{xz}}{i_x}\right]_{T-33}}{\left[\left(\frac{i_z}{i_x}\right)\left(\frac{C_{\ell_{\delta_a}}}{C_{n_{\delta_r}}}\right)\right]_{T-33}}$$

Approved for Public Release

Contrails

By choosing maximum and minimum values of the preceding ratios for four of the airplanes to be simulated and for the T-33, one may estimate that the range of $\partial\delta_a/\partial\delta_{r_c}$ falls between -1.2 deg/deg and +.4 deg/deg.

Rudder Trim

This is a rudder deflection commanded by a pilot's trim voltage setting. For this ratio all that need be specified is the maximum δ_r desired. The value chosen for design is half the maximum deflection; $\delta_{r_{TRIM}} = \pm 15^\circ$.

$C_1 = \partial F_{RP}/\partial\delta_{RP}$

The maximum spring constant is one which would make the rudder pedals seem essentially rigid. 300 lb/in.is estimated to be sufficient for this purpose. A minimum spring constant is taken to be 5 lb pedal force for a full deflection of 3.75 in. or about 1.5 lb/in. This is light enough to represent almost no feel.

$C_2 = \partial F_{RP}/\partial(q\delta_{RP})$

The reasoning behind this gain factor is the same as that for the factor $\partial F_S/\partial(q\delta_{ES})$. The maximum gain was taken as 300 lb/in. pedal spring constant at a q = 500 psf or 0.6 ft^2/in. The minimum gain was obtained from 1.5 lb/in.spring constant at a q = 200 psf or .0075 ft^2/in.

$\partial F_{RP}/\partial n_y$

This gain factor represents a C_{h_β} effect, with n_y used as a measure of βq. It will be of interest only where the pilot feels the aerodynamic hinge moment. For the T-33 using the values

Approved for Public Release

Contrails

$C_{h_\beta} = 1/2\ C_{h_{\delta_r}}$ = -.287/rad, C_{y_β} = -.65/rad, W/S = 54, a gearing ratio of 1.5 and using the relationship

$$\frac{\partial F_{RP}}{\partial n_y} = \frac{W/S}{C_{y_\beta}} \frac{1}{q} \frac{\partial F_{RP}}{\partial \beta}$$

$$= \frac{W/S}{C_{y_\beta}} (1.5) S_R C_R C_{h_\beta}$$

The result is

$$\frac{\partial F_{RP}}{\partial n_y} = 200 \text{ lb.}$$

This value is considered representative of that for other airplanes with aerodynamic hinge moment feel. To allow an appreciable margin over this representative value, a design value of 400 lb is chosen. A value of 10 lb is chosen as a minimum significant value.

$\partial \delta_r / \partial \delta_{RP}$

This is the pedal to rudder gearing. When using a large spring constant a maximum δ_r of 30° should be available with a minimum practical δ_{RP} of $\frac{1}{2}$ inch. Hence $(\partial \delta_r / \partial \delta_{RP})_{max}$ = 60 deg/in. The minimum gain should provide at least four degrees of rudder for full pedal deflection. Hence $(\partial \delta_r / \partial \delta_{RP})_{min} = \frac{4}{4}$ = 1.0 deg/in.

$\partial \delta_r / \partial (C, \delta_{RP})$

The gain $\partial \delta_r / \partial (C, \delta_{RP})$ is actually $\partial \delta_r / \partial \delta_{RP} \dfrac{1}{\partial F_{RP} / \partial \delta_{RP}}$. A good average value to use for $\partial \delta_r / \partial \delta_{RP}$ is 7 deg/in. Extremes of $\dfrac{1}{\partial F_{RP} / \partial \delta_{RP}}$ are $\frac{1}{300}$ in./lb to $\frac{1}{1.5}$ in./lb Hence

Approved for Public Release

Contrails

$$\left(\partial\delta_r/\partial(C_1\delta_{RP})\right)_{max} = 4.67 \ deg/lb$$

$$\left(\partial\delta_r/\partial(C_1\delta_{RP})\right)_{min} = .023 \ deg/lb$$

By similar reasoning as for the elevator, use of an average $\partial\delta_r/\partial\delta_{RP}$ = 7 deg/in is reasonable.

$$\partial\delta_r/\partial(C_2\delta_{RP})$$

This gain is actually $\partial\delta_r/\partial\delta_{RP} \cdot \dfrac{1}{\partial F_{RP}/\partial(q\delta_{RP})}$. An average value of 7 deg/in was used for $\partial\delta_r/\partial\delta_{RP}$. Extremes of $\dfrac{1}{\partial F_{RP}/\partial(q\delta_{RP})}$ are $\frac{1}{.0075}$ in/ft^2 to $\frac{1}{.60}$ in/ft^2.

Therefore

$$\left(\partial\delta_r/\partial(C_2\delta_{RP})\right)_{max} = 933 \ deg/ft^2$$

$$\left(\partial\delta_r/\partial(C_2\delta_{RP})\right)_{min} = 11.7 \ deg/ft^2$$

By similar reasoning as for the elevator, use of an average $\partial\delta_r/\partial\delta_{RP}$ = 7 deg/in is reasonable.

$$\partial\delta_r/\partial\delta_{a_c}$$

The ratio of rudder deflection to aileron command signal δ_{a_c} or $\left(\partial\delta_a/\partial\delta_{AS}\right)$ δ_{AS} is found from the approximate expression

Approved for Public Release

Contrails

$$\frac{\partial \delta_r}{\partial \delta_{a_c}} \cong \frac{\left[\left(\frac{i_x}{i_z}\right)\left(\frac{C_{n_{\delta_a}}}{C_{\ell_{\delta_a}}}\right)+\left(\frac{i_{xz}}{i_z}\right)\right]_{\substack{\text{airplane to be}\\ \text{simulated}}} - \left[\left(\frac{i_x}{i_z}\right)\left(\frac{C_{n_{\delta_a}}}{C_{\ell_{\delta_a}}}\right)+\left(\frac{i_{xz}}{i_z}\right)\right]_{T\text{-}33}}{\left[\left(\frac{i_x}{i_z}\right)\left(\frac{C_{n_{\delta_r}}}{C_{\ell_{\delta_a}}}\right)\right]_{T\text{-}33}}$$

Choice of maximum and minimum value of the ratios involved for four of the airplanes to be simulated and for the T-33 yields a range for $\partial\delta_r/\partial\delta_{a_c}$ from -1.50 deg/deg to +1.50 deg/deg.

E. DESIGN REQUIREMENTS FOR SPECIAL CONTROL SYSTEMS

(The following requirements are summarized as part of Table XII.)

1. ELEVATOR ANGLE REQUIRED TO MAINTAIN ALTITUDE IN A TURN

As explained in Section V, the elevator angle to be used in a turn at bank angle, ϕ, is

$$\delta_e = K\left\{\frac{1-\cos\phi}{q\cos\phi}\right\} \quad \text{where} \quad K = \frac{W}{S}\,\frac{\partial C_m}{\partial C_L}\,\frac{1}{C_{m_{\delta_e}}}\,A$$

The term in the brackets will be generated by a special computer and is discussed in Part 3 of the computing functions division of Section VII. The constant, K, will be variable as a separate gain control. Allowance is made for variations of gross weight from 9900 to 15,300 lb, static margin from 2.5 to 8.0% and variation of the elevator effectiveness from -.8 to -.9 rad.$^{-1}$ A is an additional factor to make δ_e approximate, closely, equation (88). It varies between 1.0 and 1.5. Hence K must be available from -60 to -400 deg-psf.

Allowance will be made for bank angles up to a magnitude of 75°, and elevator deflections from this source to -20°. The design range of q is 80 to 800 psf.

Approved for Public Release

Contrails

2. PROPORTIONAL BANK CONTROL

It has been decided to allow variations of k_1 , k_2 and k_3 of equation (90) by manual setting but not by automatic programming. The range of k_2 (artificial C_{l_p}) has already been covered in part C of this section and is sufficient to allow large damping ratio variations at all necessary flight conditions. The range of k_1 (aileron-stick gearing) is also considered in part C of this section.

k_3 , or $\frac{\partial \delta_a}{\partial \phi}$, must be available up to a value of 2 degrees per degree in order to allow an undamped natural frequency, $\omega_n / 2\pi$, as high as 1.0 cps at an indicated airspeed of 230 knots. Maximum bank angles of ±75° are considered to be sufficient for flight investigation of this system.

3. COORDINATION USING SIDESLIP DERIVATIVES

The gains k_β and $k_{\dot\beta}$ will not be programmed with flight condition but will be adjustable by manual setting. The maximum values required for these two gains are determined according to the needs of simulation as covered in part C of this section. These gains are checked here for their application to turn coordination. At an indicated airspeed of 250 knots and for the maximum gains k_β = -10, $k_{\dot\beta}$ = -3.5 sec, and for $k_{\int\beta}$ = 0, the bracketed coefficient of β in equation (108) is equivalent to a second-order system with an undamped natural frequency of 1.5 cps and a damping ratio of 1.60. This is sufficient to considerably reduce the sideslip occurring during transient turning.

The amount of sideslip in a steady turn for the normal T-33 may be determined from equation (98) and is given here for $\delta_r = d^2\beta = d\beta = dp = p = 0$ and $N_{\delta_a} = 0$.

$$\beta_{ss} \cong -\frac{N'_\phi}{N'_\beta} \phi_{ss}$$

Approved for Public Release

Contrails

Now, to determine the order of magnitude of β_{ss}, neglect the minor terms which contribute to N'_β, N_β, and N_r. Then,

$$\beta_{ss} \cong -\frac{1}{2}\left(\frac{bg}{V_o^2}\right)\left(\frac{C_{n_r}}{C_{n_\beta}}\right)\phi_{ss}$$

For the T-33 flying at a true airspeed as low as 316 fps, a steady sideslip angle of 1° results from a bank angle of 75°. This is obviously so small that sideslip in a steady turn may be neglected at all flight conditions of the T-33. Thus, the use of integral control, $k_{J\beta}$, to wipe out steady sideslip is unnecessary for automatic coordination of the T-33.

4. COORDINATION USING BANK ANGLE, ROLL RATE AND AILERON DEFLECTION

Rudder proportional to bank angle is also unnecessary because of the negligible magnitude of sideslip during a steady turn. k_a and k_p will be programmed with n_z/q to account for the effects of lift coefficient. The manner of programming k_a is determined from the equation

$$N'_{\delta_r} k_a + N_{\delta_a} = 0 \qquad \text{or} \qquad k_a = -\frac{N_{\delta_a}}{N'_{\delta_r}}$$

Substitution for N'_{δ_r} and N_{δ_a} yields approximately

$$k_a \cong -\frac{C_{n_{\delta_a}} + \frac{i_{xz}}{i_x}\left(C_{\ell_{\delta_a}}\right)}{C_{n_{\delta_r}}}$$

$C_{n_{\delta_a}}$ and (i_{xz}/i_x) vary with both lift coefficient and Mach number while $C_{\ell_{\delta_a}}$ and $C_{n_{\delta_r}}$ vary principally with Mach number. The Mach number variations, however, amount to only a small scatter

Approved for Public Release

Contrails

of k_a at any one lift coefficient, over the range of flight conditions of the T-33. It is felt that programming of k_a with Mach number is not worth the added complications involved. An average Mach number of 0.65 is chosen to determine the effects of lift coefficient. The following approximate linear expressions, for the T-33 with empty tip tanks, may be obtained from the data in the appendix of this report.

$$C_{n_{\delta_a}} \cong -.0015 + .0145\, C_L$$

$$\frac{i_{xz}}{i_x} = \frac{I_{xz}}{I_x} = \frac{1}{2}\left(1 - \frac{I_z}{I_x}\right)\tan 2(\alpha - \epsilon) \cong .0354 - .0815\, C_L$$

$$C_{\ell_{\delta_a}} \cong -.166$$

$$C_{n_{\delta_r}} \cong -.082$$

Hence: $k_a \cong .09 - .342\, C_L$

Now by substituting

$$C_L = \left(\frac{W}{S}\right)\left(\frac{1}{144}\right)\left(\frac{n_z}{q_{psi}}\right) = 0.37\left(\frac{n_z}{q_{psi}}\right)$$

one obtains

$$k_a = .09 - .127\left(\frac{n_z}{q_{psi}}\right)$$

Hence programming of the rudder deflection with aileron deflection and lift coefficient will take the form

$$\delta_r = C_1\left\{\delta_a - C_2\left[\frac{n_z}{q_{psi}}\right]\delta_a\right\}$$

Approved for Public Release

Contrails

Provision will be made for C_1 as high as .5 and C_2 as large as 4.0, to allow a margin for the effects of Mach number and inaccuracy in estimated aerodynamic data.

By a similar analysis the rudder servo input from roll rate, p, may be determined. k_p may be obtained from the equation

$$N'_p + N'_{\delta_r} k_p = 0$$

Solving for k_p, substituting for N'_p and N'_{δ_r}, and neglecting terms of small magnitude, we obtain approximately

$$k_p \cong \frac{i_z C_L - C_{n_p} \left(\frac{i_{xz}}{i_x}\right) C_{l_p}}{C_{n_{\delta_r}}} \frac{b}{2V_o}$$

Again a reference condition of M =0.65 is chosen for which

$$C_{n_p} = .015 - .087\, C_L$$

$$C_{l_p} = -.671$$

$$i_{xz}/i_x = .0354 - .0815\, C_L$$

$$C_{n_{\delta_r}} = -.082$$

$$i_z = .258$$

$$C_L = 0.37 \frac{n_z}{q_{psi}}$$

Thus

$$k_p \cong -\frac{1}{V_o}\left(2.1 + 24.5 \frac{n_z}{q_{psi}}\right)$$

Approved for Public Release

Contrails

The first term is neglected and a variable coefficient, C_3 , is used to allow for speed changes. As a result the rudder deflection due to roll rate, for coordination, may be written

$$\delta_r = - C_3 \left(\frac{n_z}{q_{psi}} \right) p$$

where C_3 has a maximum value of 0.2.

Approved for Public Release

Contrails

SECTION VII

INSTRUMENTATION AND ELECTRONIC DESIGN

BY J.L. BEILMAN

A. OBJECTIVES

The proposal for Phase I of the T-33 program established as one of the goals of that phase the creation of a block diagram of the automatic control system. It was required that this diagram indicate a workable system based on specific components and circuits. Bench tests were to be conducted as necessary for the procurement of data in order to achieve this result. The final purpose was to become sufficiently familiar with the required system that its detailed design could be launched immediately at the beginning of the next phase of the program.

A desired result of Phase I was, then, a state of knowledge such that for each block on the system block diagram, a component instrument, a circuit, or a combination of these could be specified. It was anticipated that some functions might be required which would demand new techniques. In such cases, if insufficient time was available for complete development of the technique, the most promising approach to the problem was to be indicated. For each block in the system, it would at least be known that there were available practical and workable methods that could be used to meet the design requirements.

B. CHRONOLOGICAL DEVELOPMENT OF INSTRUMENTATION ACTIVITY

Quite obviously, a considerable amount of aerodynamic study had to be completed before the system requirements could be defined in detail sufficient for preparation of complete block diagrams. However, because of the value of a functional block diagram in presenting a single picture of a complex, multi-channeled system, one was prepared in the early stages of Phase I work. This block diagram showed a kind of skeletal system, with most of the inputs and outputs, but it was quite incomplete as to the internal cross-coupling and programming.

With the block diagram as a guide, the system was studied in order to

Approved for Public Release

Contrails

select the features which might be investigated before specific data became available as a result of the aerodynamic studies. These features were necessarily of a general nature, relating to such things as reliability, miniaturization, the choice between AC and DC signals, the means of mixing and amplifying signals, schemes for differentiating, integrating and generation of non-linear functions, and a review of our own experience with various types of primary sensing instruments. Several specific activities resulted immediately from the initial consideration of the functional block diagram of the system.

Detailed information was requested of the aerodynamics group to determine whether there were any unusual requirements for the primary signal transducers. As the aerodynamic studies progressed, the desired information relative to the transducers was made available. Catalogs of the various manufacturers were then consulted in order to find satisfactory instruments, meeting the requirements of range and static and dynamic response. The instrument meeting these requirements were then compared on the basis of design, size, and type of pickoff employed, signal level, quality of construction and cost.

In connection with reliability and miniaturization of the system, it was decided to consider the use of transistors. These appear to offer tremendous advantages over vacuum tubes in size, power consumption and heat dissipation. It is also claimed that they are more reliable than vacuum tubes. In order to gain first-hand experience in working with these devices, a number were purchased and a transistorized servoamplifier was developed. This amplifier is capable of driving one of the hydraulic flow control valves being considered for the control surface position servos. Satisfactory bench tests of this unit were conducted but it has not been tried in an actual servo test setup. A detailed account of this unit, along with our conclusions regarding the use of transistors, will be found later in this section.

As a result of this investigation, the following instruments have been found satisfactory and have been selected.

Approved for Public Release

Contrails

PARAMETER TO BE MEASURED	TYPE OF INSTRUMENT	PROPOSED INSTRUMENT
ϕ	VERTICAL GYRO	KEARFOTT 520160-1
r	RATE GYRO	U. S. TIME MODEL 40
$\dot{\theta}$	RATE GYRO	U. S. TIME MODEL 40
p	RATE GYRO	U. S. TIME MODEL 400
n_z	ACCELEROMETER	SCHAEVITZ ENGINEERING MODEL VC
n_y	ACCELEROMETER	SCHAEVITZ ENGINEERING MODEL HC

By the time that the instrument specification studies were complete, much new information regarding system requirements was available from the continuing aerodynamic studies. It was desirable to incorporate this information into the system block diagram and the second functional block diagram resulted. The system so represented was felt to be fairly close to the final configuration as far as the artificial aerodynamic stability section was concerned. The section relating to the artificial feel for the pilot's controls was still quite primitive but, soon after the second block diagram had been prepared, a great deal of study was given to the requirements of this part of the system. As part of this study, various configurations of the system were considered from the standpoint of obtaining the required functions with a minimum of complexity. Minor modifications of the system requirements were made where this permitted a significant reduction in the electronic circuitry and the number of components such as amplifiers, function generators, controls and switches.

A third functional block diagram was then prepared which incorporated the desired features of the pilot's artificial feel system. Due to the complexity of the over-all system,this "diagram" actually consisted of three separate diagrams; one each for the pitch axis, yaw axis, and roll axis control systems. (See Figures 5, 6, and 7).

A study of these functional diagrams then began for the purpose of developing the electrical block diagrams of the system (Figure 12). Such electrical diagrams are a prerequisite for a well organized approach to the problem of detail design. A system must be defined in terms of blocks which represent physically separate units or electrically independent circuits before it is practical to undertake the detail design.

Approved for Public Release

Contrails

The study of the functional block diagrams of the three-axis control system consisted of looking for the optimum scheme for integrating all of the required functions into a single system. Figures 5, 6, and 7 show a duplication of input devices, but in general, a single instrument will be used for each flight parameter to be measured. Where a particular signal must modify several other signals it is a good scheme to utilize instrument-type servomechanisms. In special cases, it may be satisfactory to make the excitation voltage of one instrument a function of the output voltage of another instrument and this is the simplest way of combining signals. This is not usually satisfactory when an unmodified output of the first instrument is required elsewhere in the system, for then the inverse operation must also be performed.

Inspection of Figures 5, 6, and 7 reveals numerous multiplications and divisions by q In one instance the "incremental q " signal must be divided by q and nowhere is an unmodified "incremental q " signal required. In most instances particular signals are required both modified by q and unmodified by q In some cases, the stick position signals, for example, both q proportional and inverse q proportional outputs are required in addition to an unmodified output. To arrive at a scheme which seemed to be most efficient for performing all of these functions required consideration of many of the possible combinations and sequences of operating on the various signals. Such consideration was based on the specific electrical and mechanical details of instruments or systems already designed and available. By observing this limitation the scheme which evolved was one which can be implemented more easily than any which would have resulted if new and very specialized instruments were required.

The process of "tailoring" the system to fit instruments and sub-systems of proven design has been followed wherever possible. For this reason a certain manufacturer may literally be a "sole source" supplier of a particular piece of equipment required for the system if he is the only one who can supply the equipment without first undertaking a development program. This is true, for example, of the Pressure Monitor System which we contemplate purchasing from the Kollsman Instrument Corporation of Elmhurst, Long Island, New York. They have designed a servo type instrument capable of supplying three of the

Approved for Public Release

Contrails

four required dynamic pressure functions. Our specific requirements can be met, without changes in the basic design, by merely changing details such as gear ratios and the number and type of output devices. A more detailed account of this system appears in this section under Computing Functions and Major Sub-systems.

Several other activities related to the instrumentation phase of this program were carried on parallel to the system development. These were, however, of a more detailed nature and, consequently, they will be discussed below.

It should be pointed out that the finished functional block diagrams still present only a simplified picture of the control system. Many elements such as amplifiers, power supplies, filters, and phase-shifters are not shown. The detail design problem is further complicated by the undesirable effects of stray couplings of a magnetic, capacitive or conductive type. The system contains such a large number of components that packaging it to suit the space available in the T-33 will consume a major share of the detail design effort. Solution of these very practical problems will be undertaken in the detail design phase of the program.

C. ACTIVITY ON ELECTRONIC DETAILS

In an attempt to maintain continuity in the account of the chronological development of a preliminary design for the system, no account was given of a number of other activities, concerned with specific details, which were carried out during this same period. These will now be discussed briefly. It should be noted that a 400 cps carrier system is contemplated. This will permit the use of stable, feedback-type AC amplifiers in the many circuits where various signals must be amplified and/or combined.

1. POSITION TRANSDUCER

Due to reliability considerations, it was desired to use an inductive type pickoff, rather than a potentiometer, as the position feedback element on the hydraulic servopistons. Inductive type

Approved for Public Release

Contrails

devices are also capable of providing better resolution than potentiometers. Since there was no linear-motion inductive type pickoff of suitably small dimensions available commercially, the design and fabrication of such a unit was undertaken. A photograph of the prototype unit is shown in Figure 13. This unit has a linear motion range of ±2.5 inches with a body length of 6 inches, overall lengths of 7 inches when fully retracted and 12 inches when fully extended. The essential parts of the device are a linear cam, a spring loaded cam follower and a linear-variable differential transformer. The maximum output voltage is about 300 millivolts with a phase reversal occurring at the central position. This unit was used as part of the equipment for the hydraulic servo performance studies which are discussed in Section IX of this report. It was not a purpose of these tests to evaluate specifically the performance of position pickoffs but the performance of this particular unit was satisfactory throughout the tests.

2. AUXILIARY SURFACE SERVO

The auxiliary surface of the T-33 airplane will be operated by a separate servo system comprised of an electric actuator with internal gearing, a position feedback element, an amplifier and input signal circuitry.

The system planned is similar, but with some improvements, to that which is now employed in the F-94 variable stability airplane at Cornell Aeronautical Laboratory in conjunction with USAF Contract No. AF33(038)-20659. A description of the variable stability installation in this F-94 can be found in Reference 6. The actuator and amplifier are of the latest designs being produced by Minneapolis-Honeywell. These parts have been received and their bench tests will soon begin.

3. PHASE SHIFTER

Due to the variety of output or signal devices used in the various

Approved for Public Release

Contrails

instruments (synchros, microsyns, strain gauge bridges, etc.) consideration must be given to the carrier-phase compensation required to permit combining these signals properly. A phase-shifting circuit for this purpose has been designed, constructed and tested (Figure 14). This device employs only one vacuum tube plus associated components and provides a wide range of phase adjustment (0 to ±120 degrees) at a constant voltage and impedance level.

4. TRANSISTORS

Developments in silicon junction-type transistors prompted the Instrument section to investigate the possibilities of using them in place of vacuum tubes. With this in mind, some were purchased from Texas Instruments, Inc. and an experimental study was initiated. The first step was determining their characteristics as amplifiers of 400 cps sine waves. Many different configurations of two stage circuits were tried in an attempt to get as high a voltage gain as possible while keeping the input impedance at a reasonably high value of a least 1000 ohms. Another desired feature was interchangeability of transistors. Manufacturing problems have been such that, at this writing, the closest obtainable power gain matching between transistors is two to one.

During these experiments it was found that interchangeability in a non-feedback amplifier was impossible without a readjustment of the transistor bias. With this an accepted feature, the next step was the development of a phase detector. Again different configurations were tried with the final result being the push-pull grounded base connection. With the phase detector and a two-stage amplifier driving it, both forming the basis of a servoamplifier, a subminiature unit was constructed (Figures 15 and 16). Tests showed that when the unit was driving resistive loads of 1000 ohms in each collector, which is equivalent to the resistance of each winding in the hydraulic flow control valve used on the servo test rig, the DC output current is linear for 20ma over an input voltage range of 70mv rms, 0 and π phase. This is a load

Approved for Public Release

current to input voltage ratio of approximately 0.6 ma/mv as determined by the slope.

The satisfactory results of the servoamplifier led to experiments to determine the feasibility of using transistors in a summing amplifier. For this service it would be desirable to have a high overall voltage gain amplifier, before feedback, of about 60 db with a high input impedance. This would then be reduced by some 40 to 45 db of feedback bringing the overall gain down to 20 or 14 db which is a gain of 10 or 5 times. It was further felt that the interstage coupling should consist of RC networks, with a minimum of by-pass capacities that could introduce phase shifts.

These experiments resulted in a four-stage amplifier preceded by a 100,000 ohm isolation resistor. The overall voltage gain from input resistor to output was 52 db or 400 times. Inserting 36 db of negative feedback resulted in an overall gain of 16 db or 6 times. Transistor interchangeability was tried and found to be quite successful in all but the second stage. In the hopes that this offered a workable arrangement, the servoamplifier was connected to the summing amplifier and experiments conducted. During this period the summing amplifier failed. It was found that the summing amplifier was very sensitive to bias changes and this could result from a slight change in either bias resistor or transistor characteristics.

Since this particular circuit seemed unreliable, a further investigation into stable, high voltage gain, RC coupled amplifiers was undertaken. In the limited time available for this further study, no other configurations of RC coupling were found which yielded the gains desired.

In an effort to ascertain what performance and reliability were being obtained by others in the field, a visit was made to several organizations in the New York City area. Transistors have been successfully used in airborne electronic equipment for at least a year now. Servo and summing amplifiers of the types we need, using silicon junction transistors, have been developed and give excellent results. The

Approved for Public Release

Contrails

organizations which are now using transistors with such success, however, have developed their ability and experience in this field over a number of years. Discussion with these organizations confirmed our growing judgment that we lack sufficient experience with transistors to start using them in this particular system.

5. SERVO TEST RIG

In order to conduct the desired studies of hydraulic servo systems employing both flow control and pressure control hydraulic valves, it was necessary for the Instrument Group to supply the Mechanical Design Group, who were primarily responsible for these studies, with certain electronic equipment. After the general requirements of the tests were defined, an electronic unit which would facilitate the conduct of these tests was designed and constructed (Figures 17 and 18). The unit was designed to perform the following major functions:

a. Sum 400 cps command, position feedback, force feedback and velocity feedback signals and feed the resultant signal to a servoamplifier capable of driving either a flow control or pressure control hydraulic valve.

b. Provide for the introduction of command signals of either a sinusoidal or transient (step function) nature.

c. Provide a means of recording the various system parameters of interest.

A number of special features were incorporated in this unit. It was possible to vary the servoloop gain by known amounts with a calibrated gain control. A mechanical chopper converter was used to convert the linear-velocity generator output to a modulated 400 cps carrier signal. This signal was then used to provide servo rate damping through a calibrated attenuator. Another chopper converter was used to derive a modulated carrier signal from the output of an electronic low frequency oscillator. This facilitated the sinusoidal frequency response measurements of the servo performance. There were four high-gain AC carrier amplifiers with chopper demodulators and

Approved for Public Release

Contrails

two DC recording channels. All six recording channels had calibrated attenuators and the output circuits were designed to drive C. E. C. Type 7-315 galvanometers. All six channels were adjusted to have nearly identical phase lags so that the phase difference of any two recorded parameters could be read directly from the records without applying correction factors.

6. CHOPPER DIFFERENTIATOR

The concept of differentiating is mathematical, and no electrical or mechanical system exists whose transfer function is truly a derivative in the mathematical sense. However, a number of physical arrangements presently in use do provide an output which approximates the time derivative of the input quantity, with an acceptably small error over a limited range of frequencies.

The physical arrangements involved are usually described by a first-order, linear differential equation with constant coefficients. A capacitor in series with a resistor is an example of one of these arrangements and the transfer function (ratio of the voltage across the resistor to the voltage across the combination) has the general form

$$j\omega\tau / 1 + j\omega\tau$$

Inspection of this transfer function reveals one of the basic difficulties with all analog differentiators. The ideal transfer function is simply $j\omega$, i. e., the output should lead the input 90° in phase and be linearly proportional to the frequency. In order to make the above expression approximate $j\omega$, it is necessary to make the product $\omega\tau$ so small compared with unity that the denominator is approximately unity. This in turn means that the amplitude ratio of output to input is also very small. For example, if it is decided to tolerate a maximum phase error of 10° (output leading input by 80°) in an RC differentiator, it means that at the highest frequency which can be differentiated with this error the amplitude ratio will be about 0.18, while at lower frequencies the amplitude ratio will be even smaller.

Approved for Public Release

On the other hand, if 5° is decided upon as the maximum tolerable phase error, the amplitude ratio will be only about 0.09, at the highest frequency which can be differentiated with the specified error. Thus, it can be seen that in practice the limit on the obtainable accuracy is a function of the noise in the system, because theoretically, no matter how small the amplitude ratio becomes it can be compensated for by an amplifier with sufficiently high gain.

An additional point worth adding to this brief introduction to the problem of analog differentiation is that, of all the physical systems it is possible to use, few permit so simple an adjustment of parameters as is possible with the RC network.

In signal systems employing a modulated AC carrier voltage, it is frequently necessary to obtain the first time derivative of the modulating or intelligence frequency. A number of schemes for doing this are known, but they are generally more complex than the RC network which can be used to differentiate a signal having no carrier component. Therefore, one solution, and a technique which has been used frequently, is to remove the carrier component by rectification. The rectification process must be phase sensitive in order to preserve the sense or directional information of the signal. Thus, one phase of carrier voltage will produce a rectified voltage which is positive while another phase, opposite by 180°, will produce a rectified voltage which is negative. This is quite simple. The situation becomes more complicated when it is necessary to have a carrier voltage for the differentiated intelligence.

At this point it is necessary to examine briefly some of the basic characteristics of available rectifying elements. These fall into three general classes: vacuum tubes, semi-conductor diodes, and mechanical or contact rectifiers. Henceforth, our consideration of contact rectifiers will be limited to a particular type with which we have had considerable experience--the chopper. The chopper has been defined as "an electro-mechanical switch for the production of modified square waves of the same frequency as, and bearing a definite phase relation-

Approved for Public Release

Contrails

ship to, a driving sine wave."

A chopper is basically a phase sensitive device while vacuum tubes and semi-conductors require special circuit techniques to make them so. Vacuum tubes and semi-conductors are capable of handling far more current than choppers. Vacuum tubes and choppers require power for their operation while semi-conductors do not. In size there is little to choose between vacuum tubes and choppers but, for signal level currents, semi-conductor diodes can be made extremely small--on the order of 0.05 in.^{3}, volume. Both vacuum tubes and semi-conductor diodes suffer in comparison to choppers in a characteristic which is important in signal circuits, i.e., noise discrimination. Rectifiers in the first two classes show practically no noise discrimination while choppers (a) completely eliminate even harmonic components, regardless of phase with respect to the driving voltage, (b) reduce and may even eliminate odd harmonic components, depending upon the phase with respect to the driving voltage, and (c) provide normal rectifying action only at the driving frequency so that "white" noise produces no net DC voltage in the output as it would with vacuum tubes or semi-conductor diodes.

Now, returning to the differentiator problem, a scheme was described in which the modulated carrier is rectified so that the intelligence may pass through an RC differentiator network. Reconversion of the differentiated intelligence to a modulated carrier signal poses a problem. In past instances this has been solved quite simply by using a chopper to inject a carrier with the desired phase relationship. Since, for reasons stated above, a chopper has also been used as the rectifying element, this has resulted in two choppers being used each time it was necessary to differentiate the envelope of a carrier voltage.

In a previous study (Reference 7) an analysis was made of a "Synchronous Notch Filter" employing a chopper. Observation of the theoretical amplitude and phase characteristics of this device suggested the possibility of using a single chopper, in conjunction with suitable

Approved for Public Release

Contrails

resistances and capacitances, to accept a modulated carrier voltage input and produce a modulated carrier voltage output, such that the output modulation is the time derivative of the input modulation. Furthermore, it was suspected that this circuit would possess a characteristic basically more important than the elimination of the second chopper. Due to the synchronous nature of the chopper action, it appeared that such a circuit would be insensitive to variations of the carrier frequency. This would be an important advantage over the frequency selective networks frequently used for rate signal derivation in AC servomechanisms. The transfer functions of these networks are such that a change in carrier frequency will produce an output as well as a change of modulation.

The schematic arrangement of the chopper differentiator is as follows:

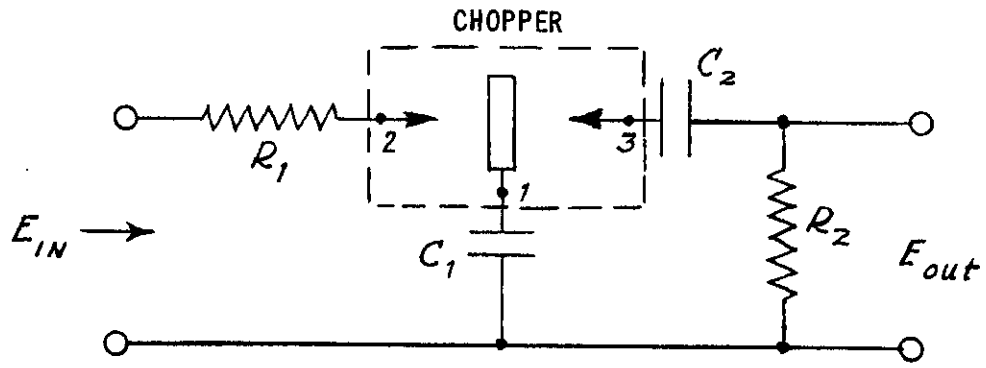

It is possible to gain some physical insight into the operation of this circuit by considering the sequence of events when a 400 cps sinusoidal carrier voltage, of fixed amplitude, is suddenly introduced. This will amount to an input of a step function on the carrier voltage envelope. A description will then be given of the time variation of the envelope of the output carrier voltage. Figure 19 shows the corresponding waveforms.

A particular set of conditions is chosen for the sake of illustration. They are:

Approved for Public Release

Contract

a. The input time constant R_1 C_1 is so short compared to the period of one cycle at the carrier frequency (ω_c) that C_1 can always charge to the peak amplitude of the carrier voltage (E_{max}).

b. The phase of the input carrier voltage ($\phi_{c'}$) lags the phase of the reed driving voltage or reference carrier voltage (ϕ_c) by 90°. This is a necessary feature in order that the reed (1) and therefore C_1 will always break away from chopper contact (2) when the amplitude of the carrier voltage is $+ E_{max}$.

c. The transit time of the reed is negligibly small and the duty cycle at each chopper contact is about 50%, i.e., during one cycle reed (1) is connected with contact (2) for one-half the period and with contact (3) for the other half of the period.

d. The output time constant R_2 C_2 is long compared to the period of one cycle at the carrier frequency.

e. C_1 is much greater than C_2 so that its voltage remains nearly constant while transferring charge to C_2 through R_2, thus approximating a battery.

f. There is no initial charge on C_2 and neither C_1 nor C_2 have any internal leakage.

g. At $t = 0$ the reed (1) is connected to the input contact (2) which has a voltage $- E_{max}$.

Now consider the following sequence of events. At the end of the first one-half cycle, the reed moves so that C_1 is connected to C_2 and R_2 with a voltage $+ E_{max}$ corresponding to a charge $C_1 E_{max} = Q$. Because C_2 cannot change its charge instantaneously, E_{max} appears across R_2 but immediately begins to decay exponentially as C_2 accumulates the charge surrendered by C_1. (For the conditions chosen, this decay is $e^{-t/R_2 C_2}$). However, before the amplitude has decayed very much the first cycle ends and C_1 is disconnected from C_2, leaving a certain net charge on C_2. During the first half of the second cycle the charge on C_1 is replenished. At the start of the second half of the second

Approved for Public Release

Contrails

cycle C_1, with a voltage E_{max}, is again connected to C_2 and R_2. Now, because of the charge retained from the previous cycle, C_2 has a voltage already appearing on it. Consequently, a voltage less than E_{max} by this amount appears initially across R_2. Again, this voltage immediately starts to decay and the decay is interrupted when C_1 is disconnected from C_2 at the end of the cycle.

Each subsequent cycle will be a repetition of the above processes until C_2 has acquired a voltage E_{max}, when there will no longer be an output. Thus, it can be seen that, for a step function of carrier voltage amplitude as an input, the output will be a series of somewhat rectangular pulses with each pulse having a lower amplitude than the previous one. In fact, the amplitudes decrease in a geometric ratio and the envelope of the pulses decays exponentially with time. This response is the same as the response of an RC network to a step input of DC voltage. We then infer that, for the proper choice of parameters, we have the same transfer function. Consequently, we have a differentiator.

Bench tests of the chopper differentiator have been conducted and the results show it to be a practical and workable device. An important electrical requirement is that the chopper differentiator circuit be power driven, i. e., the signal should be supplied from a low impedance source capable of providing a level of one or two volts. The low impedance is required in order that the input capacitor can charge to the peak voltage of the input carrier. Also, by having a signal level of several volts, the effects of internally generated chopper noise (on the order of one millivolt) are minimized.

Tests conducted to date have been in the region of 0.2 to 2.0 cps, where a phase error of 10 degrees is tolerated at 2 cps. For the various parameter configurations which have been tested, good and consistent results have been obtained. Both the phase and the amplitude responses obtained show good linearity, as a function of frequency, within the operating range (Figure 20).

Approved for Public Release

Contrails

Experimental evidence has also been obtained that the chopper differentiator is indeed insensitive to variations of the carrier frequency, as originally anticipated. Variations up to 10% in the carrier frequency produced no detectable change in the output. Analysis of the circuit shows the effect of a change in carrier frequency to be a proportional change in the effective time constant, but so long as there is no change in amplitude modulation, a change in carrier frequency should produce no output.

Tests on this circuit are continuing in order to develop circuit techniques, to establish practical upper and lower frequency limits for satisfactory operation and to verify and supplement our present design criteria.

7. COMPUTING FUNCTIONS - MAJOR SUB-SYSTEMS

Earlier in this section, several references were made to computing schemes and instrument servomechanisms. Some of the proposed schemes will now be described in detail. The descriptions will be on a unit basis, i.e., where it is most efficient to combine a number of functions in a single instrument or sub-system, the functional description of this single device will be given rather than treating the different functions separately.

a. q Computer

The basic system proposed for supplying several of the q or dynamic pressure functions is the Kollsman Pressure Monitor system. This system is connected to the pitot and static lines of the T-33 airspeed system, and accordingly it works from impact pressure, q_c . Impact pressure and dynamic pressure, q , remain nearly enough equal over the T-33 flight range that the use of q_c instead of q does not affect the principles of operation of the system. The difference between q_c and q will be accounted for in actually selecting gain settings. The following is based on the results of a conference with Kollsman engineers regarding the specific application. This servo

Approved for Public Release

Contrails

instrument system would be modified to provide the following specific functions:

1. Three synchros with shaft or armature rotation proportional to q would be available. One of these would have a constant excitation on the primary, and the amount of q proportional output would be controlled directly by the pilot. This signal would then go to the stick force computer, providing the pilot with a trimming stick force that varies with q. The other two synchros would be used to multiply the the elevator stick position and rudder pedal position signals by q, which is required by the artificial feel system.
2. One synchro would be available with armature position proportional to the change in q from any selected reference value. This is accomplished by means of an electrically operated clutch between a servo-controlled shaft and a spring-centered synchro. With the clutch disengaged the synchro rests at a null or electrical zero position. After the clutch is engaged, any changes in dynamic pressure produce changes in the synchro position and proportional changes in the output voltage. The phase of the output voltage is 0° or 180° according to the direction of the change in q. The excitation voltage to this synchro would be inversely proportional to q so that the net output signal would vary as $\Delta q/q$. This signal is needed for control of the auxiliary surface.
3. One signal proportional to the first time derivative of q would be available. Depending upon range and resolution requirements, this may be the same induction generator signal used for rate damping of the instrument servo system or it may be derived from a second induction generator coupled to the servo through an appropriate gearing.

More detailed information on the basic Pressure Monitor System may be found in the Kollsman Instrument literature. The diaphragm actuated mechanism which is the heart of the system, is

Approved for Public Release

Contrails

described specifically in Reference 8. Some of the important features of the system are: small internal volume for rapid response time, temperature compensation of the basic mechanism plus thermal isolation from the motor-generator (and amplifier if internally located), and a usable resolution as high as 1 part in 50, 000.

b. Inverse q Computer

Voltages inversely proportional to q are required for excitation of the "incremental q " synchro in the Kollsman Pressure Monitor and as inputs to both the bank angle function computer and the turn coordination computer ($\partial\delta_R / \partial\delta_{AS}$ programmed with q). In addition, there are four signals whose amplitude must be inversely proportional to q , namely the normal and lateral accelerometer signals and, when simulating aerodynamic feel, the rudder pedal and elevator stick force signals. If only the voltages were required, it might be satisfactory to use a potentiometer type pressure pickup, as has been done in the past, and to generate the inverse function by resistance loading of the output. This is felt to be generally undesirable from both a reliability and an accuracy standpoint. In addition, when there are good reasons for not operating on the excitation of particular pickups, such as the accelerometers and strain gauges in this case, it then becomes necessary to use an instrument servo anyway, in order to drive the attenuating elements. As long as an instrument servo is required, it is just as easy and more desirable to use the servo to generate the inverse or hyperbolic function, eliminating the potentiometer instrument.

Figure 21 shows the proposed scheme for handling the inverse q functions. The principal of operation is as follows. The feedback synchro produces a voltage proportional to the product of the impact pressure, q_c , and the shaft angle, θ . The servoloop shown operates to keep this voltage constant. Ac-

Approved for Public Release

Contrails

cordingly, θ will vary inversely as q_c . There would be five output synchros, one having a constant voltage excitation and the other four serving as variable attenuators for the accelerometer and pilot control force signals. The 8 to 1 variation of the feedback synchro excitation would cause an 8 to 1 variation of servo stiffness if it were not for the servoloop gain compensator. This refinement may not be necessary because of the low dynamic requirements for this system (equivalent to a 1 cps second order system with a damping ratio of .6 of critical). It may well be possible to design the servo system to be stable over a $\sqrt{8}$, or about 3 ,to 1 range of natural frequencies without special compensation because the highest frequency would be only about 3 cps.

c. Bank Angle Function Computer

The required bank angle function is $1 - \cos\phi / q \cos\phi$ which simplifies to $1/q\ (\sec\phi - 1)$. Figure 22 shows a scheme for generating this function which has been discussed with Servomechanisms, Inc., Westbury, Long Island, New York. It was found that this computer sub-system could be made up of a standard servoamplifier and a standard "positioner" unit with minor modifications. These devices have been built in production quantities for the Air Force A-1CM Computing Gun-Bomb-Rocket Sight.

The scheme shown in Figure 22 employs a non-linear potentiometer. This potentiometer is made to approximate the secant minus unity function in the range from minus 75 degrees to plus 75 degrees by means of 6 linear slopes of resistance versus rotation. The secant function has a value of unity at zero degrees and therefore, the secant minus unity function is zero at zero degrees. The subtraction of unity is conveniently accomplished by the grounded fixed center-tap on the potentiometer.

A feature of this scheme is that it in no way restricts rolling

Approved for Public Release

Contrails

maneuvers. The attitude gyro has unlimited freedom about the roll axis and employs a synchro position transmitter. Since the computing servo also employs a synchro for position feedback and since there are no mechanical stops on the non-linear potentiometer, the servo will always maintain a one to one correspondence to the attitude gyro, even through 360 degree roll maneuvers.

D. DETAILED DESIGN

A brief discussion of the plans for proceeding with the detail electronic design of the three-axis artificial stability system follows, pointing out some problems not previously mentioned.

The first step will be to write the detailed specifications for all of the subsystems which are to be purchased from other companies. Purchase orders will then be placed for these items as well as all of the primary sensing instruments (gyros, accelerometers, etc.) which we require. Work will then begin on the items which are to be designed and constructed by Cornell Aeronautical Laboratory, particularly power supplies, junction boxes, control panels and amplifiers. Close coordination will be required because all of the blocks must be electrically and mechanically compatible. Decisions must be made as to the physical placement of the system in the airplane so that the units may be packaged accordingly.

The next stage will be one of testing both Cornell Aeronautical Laboratory built and sub-contractor items, which should be supplied by that time. After this, the entire computer system will be assembled and interconnected on the bench for an extensive period of functional testing. One of the primary efforts during this phase will be, as previously mentioned, the elimination or reduction of noise and unwanted couplings between circuits. This will be accomplished chiefly by physical rearrangement of system components, magnetic and electrostatic shielding and by modifications of cabling and wiring.

The final success of this effort will be indicated when it is possible to connect the computer system into the various servo systems and obtain the desired overall gains (servo position output to flight parameter input) without objection-

Approved for Public Release

Contrails

able noise apparent in the servo output. At the same time the system must exhibit the required resolution, or ability to respond to very small signals.

Another problem of considerable magnitude, which must be solved in the detail design phase and which has not yet been mentioned, is the matter of operational safety. All aspects of the system which could conceivably affect the safety of flight must be considered and appropriate steps taken to insure safe operation. This holds not only for considerations of the system during periods when the artificial stability system is engaged and operating, but also for the transient operations involved in turning on, engaging and disengaging the system. In addition, these operations have to be carried on in a manner compatible with all of the electrical, mechanical and hydraulic elements of the system. Attention will be given to making the required operational sequences and interlocks as simple as possible so as to meet all the requirements of safety with maximum reliability.

When all of the above problems have been considered, solved and the necessary equipment constructed, the artificial stability system will be ready for installation in the airplane.

Approved for Public Release

Contrails

SECTION VIII

PRELIMINARY LAYOUT OF SERVO AND MECHANICAL INSTALLATIONS

BY W. CLOSE

A. INTRODUCTION

At the commencement of the preliminary design investigation in July 1954, the only information available was contained in the T-33 Erection and Maintenance and Structural Repair Handbooks. This was supplemented later by twenty-three relevant blueprints from Lockheed Aircraft. Still later, T-33A aircraft, Serial No. 51-4120, was delivered to Cornell Aeronautical Laboratory and complete structural information could be obtained.

Early in the design investigation, it was decided that a 1000 psi hydraulic system should be used, this also being the normal T-33 system. Servo sizes were arranged to utilize half system pressure at maximum working load in order to allow the servo valve to work at a reasonably low load. However, the size penalty was considered excessive for the aileron position servo and 700 psi was used as top working pressure. The elevator and rudder position servos were subsequently redesigned to agree.

Objectives in the design investigation were, first, to determine where feel servos and position servos could be installed and to prepare layouts to confirm this, and, secondly, to evaluate the most suitable installations. To begin with, position servos were to be mounted as close to their control surfaces as possible to reduce undesirable spring effects in the connections. It will be seen in the detailed account which follows that this criterion was subsequently relaxed. An additional objective was to design interchangeable wheel and stick installations for the test cockpit which could be readily changed from one configuration to the other.

B. PRELIMINARY LAYOUT OF ELEVATOR SERVO

Figure 23-a. The first survey showed that since the stabilizer is only about 2-1/2 inches thick at the 70% line 30 inches outboard from the centerline of the aircraft, it was not practical to mount an actuator inside the

Approved for Public Release

Contrails

stabilizer to give direct connection to the elevator.

Figure 23-b. An external mounting on the underside of the stabilizer was considered very briefly but discarded since it was not thought desirable to add excrescences to the aircraft.

Figure 23-c. Working back along the elevator control run, it was thought that space inside the dorsal fairing might be used. At this point elevator motion is transmitted via an idler lever working through a slot in the outer skin. By fitting a new lever at this point the actuator may be connected into the system. This layout gives some protection from jet pipe heat, good accessibility if the dorsal fairing is modified, and direct action through push-pull rods to the elevator. It would be necessary to widen the dorsal fairing slightly to provide sufficient room for the actuator inside, depending on the final actuator design.

Figures 24 and 25. At a much later date in the design investigation, it was decided that it would be feasible to mount the position servo at some distance from the elevator. There is ample space in the forward end of the engine compartment, and the existing upper bell crank assembly in the elevator control system behind station 228 may be replaced by a new triple lever and servo assembly, motion being transmitted back to the elevator through the existing system of push-pull rods, which are considered to be of ample rigidity. This arrangement appears the best since there is adequate space for the installation and good accessibility with short hydraulic and electric lines which are not broken when the aft section of the fuselage is removed for engine changes.

Figures 26 and 27. Provision of a pilot controlled lockout on the elevator spring tab mechanism is difficult and it is proposed to lock this mechanism permanently as was done on the F-94 aircraft modified by the Flight Research Department, Cornell Aeronautical Laboratory, under Contract AF33(038)-20659. Figure 26 shows the T-33 mechanism before locking and Figure 27 shows the F-94 mechanism after locking.

C. PRELIMINARY LAYOUT OF RUDDER SERVO

The provision of a position servo close to the rudder is complicated by two factors--proximity to the jet pipe heat, and the impenetrable bulk of the stabil-

Approved for Public Release

Contrails

izer center section.

Figures 28-a and 28-b. The addition of a push-pull rod to the rudder lever is impractical because of the frame modifications involved.

Figure 28-c. A position aft of the rudder hinge line was given some thought but discarded because the mounting in the tail jet pipe fairing presented great difficulties.

Figures 29, 30, and 31. It was decided to investigate the use of part of the existing rudder control cable system to connect the actuator to the rudder. If the small, half-moon-shaped bulkhead just forward of Sta. 376 is removed and the shroud over the jet pipe continued forward to bulkhead ring Sta. 364, space is made available forward of the stabilizer front spar. In this box, a servo may be fitted which would be connected to a short vertical shaft at whose bottom end is a triple lever assembly. The control cables would be divided on both sides and connected up as shown in Figure 31. This arrangement would provide a short, closed-circuit cable system between the servo and the rudder, while still maintaining a closed circuit between the rear cockpit rudder pedals and the rudder.

The structural modification to the fuselage between stations 364 and 376 would require advice from Lockheed Aircraft.

Figure 32. Although considered practical, the previous arrangement does involve some aircraft structural modification. An investigation was made, therefore, of a position servo mounted in the engine compartment and operating the rudder through the existing cable run. These cables are, of course, of ample strength but their elasticity is questionable. However, improvement may be obtained by fitting larger diameter cables or swaging tubes over the cables in the runs between the guide pulleys. In order to complete a closed circuit from the servo to the rudder, a rocking beam across the top of the engine compartment is proposed, with the position servo operating the beam. Although the beam is about 32 in. long, its polar moment of inertia could be kept to a reasonable minimum by careful design. The gear ratio between the beam and the rudder would further reduce the effective moment of inertia of the beam by a factor of about 12 when referred to the rudder axis. Provided that the question of cable stiffness can be satisfactorily settled, this arrange-

Approved for Public Release

Contrails

ment is the best. It avoids major structural modification at the rear of the fuselage, and has advantages similar to those of the elevator position servo installation shown in Figures 24 and 25.

D. PRELIMINARY LAYOUT OF AILERON SERVO

First design efforts were spent in investigating actuator positions adjacent to the ailerons. Space between the front and rear wing spars is completely occupied by fuel tanks. Aft of the rear spars, the wing ribs and auxiliary beam form a series of cells in which the aileron mass balances are located. The cables operating the ailerons run from a drum near wing station 171 inboard via a guide pulley. Since turnbuckles are necessary here, there is no length available to add a servoactuator.

Outboard of the drum, it is possible to install a small servo concealed in the wing and connected directly to the aileron (Figure 33), but when control forces were checked, assuming a working pressure of 700 psi, the resultant actuator size overruled this possibility.

Consideration was next given to an external mounting for the servo under the wing, and some layouts were drawn up for various possibilities. The best arrangement, Figure 34, using an idler lever to increase leverage, involves a large blister under the wing (9 inches wide, 7 inches deep, length = wing chord at this point). The actuator has a stroke of 4-3/8 inches, and an area of 2.66 square inches. This arrangement permits a unit assembly of position servo and idler lever to be attached directly to the front and rear spars and gives excellent accessibility.

The required blister turned out to be fairly sizeable and it was doubtful if an external installation was the best design compromise. Accordingly, it was decided that further consideration should be given to an internal mounting, even if some loss of fuel capacity was involved. Layouts were prepared for a servo installation in the cell occupied by the outer outboard wing tanks (between Sta. 171 and 216). See Figure 35. This installation involves a total loss of 16 gallons fuel capacity equal to 4.5% of capacity without drop tanks, or 1.97% of capacity with drop tanks. The actuator piston rod would work through a reinforced slot in the rear spar and be connected to a lever added to the existing

Approved for Public Release

Contrails

control drum (Figure 36) giving a direct connection to the aileron. The actuator has a stroke of 5-5/16 inches and an area of 2.55 square inches. Access to the servo would be through a stress carrying door in the under wing skin.

At this stage, calculations had been made of the effect of long cable connections between the servo and the aileron. The results were sufficiently promising for design consideration to be given to a single servo mounted in the fuselage and operating both ailerons through the existing cables. A layout was prepared for mounting in the forward end of the engine compartment below the left-hand duct entry and a connection to the cable drum on which the aileron booster unit works (Figure 37). Actuator stroke for this installation is 3-1/2 inches, and piston area is 4.37 in^2.

This installation requires a new position for the ship's hydraulic accumulator and rearrangement of the hydraulic piping in this vicinity. A check was made of the relationship between the aileron movement and the aileron drum movement, which proved to be linear.

At present, this arrangement is preferred, provided the question of cable stiffness can be handled. This question has two aspects. One is the effect of cable stiffness on the servo's dynamic performance. The other is the fact that cable stretch reduces the available rolling performance compared to that available with servos in the wings. (The rolling performance would be the same as a normal T-33 however.) The wing installation would be quite tight and would involve structural modification and loss of fuel capacity. The center-line installation avoids these difficulties and also has the advantages mentioned previously for the elevator and rudder position servo locations in the engine compartment.

E. PRELIMINARY LAYOUT OF AUXILIARY SERVO

No design investigation and layout work has been done on this installation, since it is considered that the similar arrangement used on the F-94 aircraft modified by the Flight Research Department under Contract AF33(038)-20659 is readily adaptable to the T-33 project. This is shown in Figure 38.

Approved for Public Release

F. PRELIMINARY LAYOUT OF COCKPIT CONTROLS AND FEEL SERVOS

The control system is to be designed so that the front pilot will fly on the servo controls and the rear pilot will retain manual control.

Designwise, this means that the rudder, aileron, and elevator controls in the front cockpit are disconnected from the existing system and operate feel servos, while the rear cockpit controls are not changed except as necessary to maintain their functions without benefit of the front cockpit system.

More detailed changes are as follows:

1. The front elevator push rod connecting the two sticks is removed.
2. The aileron torque tube bearing at fuselage station 138.5 is moved aft about eighteen inches and the forward part of the tube deleted. This leaves the rear cockpit aileron control undisturbed.
3. Cables forward from the quadrant at fuselage station 158 are changed so that they connect cross-ship to complete the system (Figure 39-a). No layout has been made for this modification as it does not seem to present any great problems and may be solved more easily by actual "mock-up" on the aircraft.

The installation of the rudder feel servo is straightforward, as space is available at the fuselage side forward of the shelves, which allows a servo to be connected directly to the lever which formerly operated the cable. One servo only is necessary for movement in either direction since a rocking bar linkage already cross connects the two rudder pedals (Figure 39-b). This feel servo has a 4-3/4 inch stroke. Although Figure 39-b shows it attached to the LH pedal, it may be installed on either LH or RH side of aircraft depending on which gives an easier run for hydraulic pipe lines, etc.

Strain gauge pedals of the type developed at Wright Field and shown in photo 48-1-37 of the Instrumentation Section MCRFTI Flight Test Division, Wright Field, are readily adaptable to the existing ship's pedals.

The aileron and elevator feel servo installations have to be considered together since they both operate on the one control unit. Three design requirements influence the final arrangement. They are:

1. that easily interchangeable "stick" and "wheel" control units be pro-

Approved for Public Release

Contrails

vided for the aileron,

2. that the wheel control unit uses a strain gauge wheel for force readings and the stick unit is similarly instrumented,
3. that existing cockpit pressure sealing is preserved. This is important since lack of space around the pilot requires that the feel servos be installed outside the pressurized cockpit area.

Volume II of the USAF Handbook of Instructions for Aircraft Designers gives data on basic cockpit dimensions. Drawing AD1 Sheet 1 shows dimensions for "stick" control and Drawing AD3 Sheet 2 shows dimensions for "wheel control." These are not, of course, intended to be interchangeable and the addition of a wheel control to an aircraft not designed for a wheel will require that some compromise be made on dimensions established in AD3 Sheet 2 as being desirable. A tabular comparison of the two requirements follows:

	STICK CONTROL IN.	WHEEL CONTROL IN.	DIFFERENCE IN.
HEIGHT OF NEUTRAL SEAT REFERENCE POINT ABOVE HEEL REST	8.50	10.50	2.00
* HEIGHT OF STICK OR WHEEL REFERENCE POINT ABOVE NEUTRAL SEAT REFERENCE POINT	13.50	20.25	6.75
HEIGHT OF STICK OR WHEEL REFERENCE POINT ABOVE HEEL REST	22.00	30.75	8.75
FORWARD TRAVEL OF STICK OR WHEEL REFERENCE POINT FROM NEUTRAL POSITION	5 MAX	5 MAX	----
BACKWARD TRAVEL OF STICK OR WHEEL REFERENCE POINT FROM NEUTRAL POSITION	9 MAX	9 MAX	----

* *Stick or wheel reference point is defined as the point at which pilot's second finger is in contact with the forward face of the stick or wheel.*

Approved for Public Release

Contrails

It may be necessary to restrict aileron wheel control movement to about ±60° dependent on the size of the wheel. It is probable that a strain gauge wheel of the type developed at Wright Field will be used. This is shown on USAF official photograph 48-11-63 of the Instrumentation Section MCRFTI, Flight Test Division, Wright Field.

Simple interchangeability of stick and wheel control units can be attained by using the arrangement shown schematically in Figures 40, 41 and 42.

Figure 40 (a and b) illustrates the operations of the aileron feel servo when the "stick" unit is used, while Figure 41 (a and b) shows the action of the "wheel" unit on the feel servo.

Figure 42 (a and b) indicates the connections to the elevator feel servo. The fitting of either "wheel" or "stick" units to the control assembly has no effect on the function of the elevator feel servo.

Design pilot forces being used for strength and rigidity of the controls are:

	LIMIT	ULTIMATE
LATERAL WHEEL *	100 LB	150 LB
LATERAL STICK **	100 LB	150 LB
FORE AND AFT **	200 LB	300 LB
RUDDER	300 LB	450 LB

* *Applied tangent to wheel rim*
** *Applied at stick grip reference point*

Actual working forces will be lower.

Since the radius of the wheel reference point above the pivot centerline is greater than that of the stick reference point, and stops are fitted at the feel servo end of the linkages, the greater moments are to be used for design loads. The same servo is used for both "stick" and "wheel" installations. Consequently, the pilot's forces are reduced for the wheel installation with stops disengaged.

Figure 43 shows a wooden mock-up of the front cockpit wheel control. This mock-up provides vertical adjustment for the wheel unit so that clearances from the pilot's knees can be checked. It can be seen from the photo that both the

Approved for Public Release

Contrails

Student Lockout/Indicator Light box and the AN/ARN-6 control panel require either elimination or repositioning to clear the wheel pillar in its most forward position. Clearance between the wheel and the canopy locking handle is considered insufficient and a folding handle would be an improvement here.

The clearance problems just mentioned are of a minor character, however. The most important problem concerns clearance for the pilot's feet and knees, should it be necessary to abandon the aircraft in flight by using the seat ejector mechanism. To provide indisputable clearance, the control column should be fully forward at the moment of ejection. It is not practical to expect that the pilot can always do this during emergency and this indicates that special mechanism must be incorporated to make clearance automatic during ejection. Two arrangements are possible. Either the spokes of the control wheel should "break" and allow the hand grips to fold forward or the whole control column may "break" at the bottom and fold forward. Some thought has been given to possible mechanisms but no layouts have been made as yet. However, the "breaking" column arrangement seems most promising.

Approved for Public Release

Contrails

SECTION IX

SERVO THEORY AND TESTING

BY C.L. MUZZEY AND W.J. THAYER

A. SUMMARY

This section presents the results of a series of studies and tests conducted to provide design information for the position and feel servos to be used in the T-33 variable stability airplane.

It is shown theoretically and verified by tests that position servo performance can be made relatively independent of loading effects by suitable choice of piston area and gearing to the load. The test servo, set up to represent the aileron control servo, proved satisfactory in practice as well as in theory. Dynamic responses are presented in Figures 64, 66, and 67. Design values for piston area and gear ratio for all position servos are tabulated in Table XV.

A satisfactory feel servo has been constructed and operated on a test rig. Additional tests are required to verify the theory for the feel servo. Results of dynamic tests are shown in Figure 73. Table XVI gives the design values selected for the feel servos.

In general, the servos do not require electrical compensating networks; the only objective in design of amplifiers and other electrical components is minimum time lag (time constant,on the order of three milliseconds). Additional understanding of the feel servo theory may call for compensating electronic networks.

It is concluded that servos designed according to the information in this section of the report will successfully meet the requirements of the flight test program.

B. INTRODUCTION

STATEMENT OF THE PROBLEM

The Flight Research Department of Cornell Aeronautical Laboratory, Inc.

Approved for Public Release

Contrails

has conducted a series of research projects over the past six years in which the dynamics of a research airplane, as they appear to a human pilot, can be altered in flight by the use of automatic controls. The earlier projects were not concerned with all axes of control simultaneously. The pilot had, for the most part, ordinary aerodynamic loads on his controls. Later, artificial feel was introduced and as the science of predicting the response of the controlled airplane to specific artificial inputs became more accurate, it was realized that very high performance servo systems were needed to drive the flight control surfaces. No less important is the quality of the feel servos used to provide artificial loads on the cockpit controls, especially when it is desired to simulate some particular attribute of a proposed control system. To meet the needs of these research projects it has been necessary to adopt hydraulic control systems and to study them intensively to get the most performance from them.

The T-33 Variable Stability and Control project under Air Force Contract AF33(616)-2578 will equip a T-33 jet trainer airplane with hydraulic servos on its flight control surfaces, and with hydraulic feel servos on the cockpit control-stick, wheel, and pedals. Motions of the airplane will be appropriately sensed and fed into the control surface servos to alter the airplane stability, while various signals will be supplied to the feel servos to simulate aerodynamic and artificial stick and pedal forces.

SERVO PERFORMANCE

In the operation of an artificial stability airplane, a typical problem is to alter the characteristics of the test airplane so that it behaves like some other aircraft. Frequently, the two airplanes will be governed by the same equations of motion, but the system constants or stability derivatives will be of different magnitudes. If the two sets of derivatives are known, and the servo control system of the research airplane acts without appreciable time lag, the stability derivatives of the test airplane can be effectively made equal to those of the vehicle being studied. If the control-surface servos introduce time lags, they no longer act simply to change the system constants, but they change the equations governing the airplane. It is still possible to simulate the new airplane,

Approved for Public Release

Contrails

but the job of selecting the proper set of artificial stability system inputs and gains becomes much more complicated, and the difficulty is greater for greater servo lags. Thus, it becomes desirable to build the best servos possible for a program such as the T-33, and with this end in mind it was decided to conduct a preliminary theoretical analysis and supporting test program to obtain design data for the servo systems required. At the same time, it was believed desirable to simulate the feel servos to be used, since several new ideas and components were available for this type of control. Also, it was considered that the technique of feel servo design was not yet backed by adequate theory, so that test work was needed to be sure of obtaining a satisfactory design.

PURPOSE OF PHASE I

Phase I of the T-33 program was to include, therefore, an analysis and a test program for the purpose of establishing a sound theory, verified by experiment, by which to design the high performance servo systems required for installation in the airplane. This section presents the results of the servo work conducted under Phase I.

C. SERVO REQUIREMENTS

At the outset of the program, it was realized in a general way that the control surface servos (as well as the information channels feeding the servos proper) should have high dynamic performance and should, in addition, meet certain requirements for resolution, accuracy, etc. It was also realized that servos which would perform under load and still contribute negligible dynamic lags were not practically attainable. Hence, realistic values of lag were assumed in an analog computer study, and minimum acceptable performance specifications established.

It was assumed for the analog study that an entire stability channel, including the sensing instrument, amplifiers or mixers, and the power servo, could be represented as a second-order system. With such a control system it was found that, with an undamped natural frequency of 7.5 cps and a damping ratio of 0.70, the job of pre-calculating the proper corrections for servo lag

Approved for Public Release

Contrails

was fairly simple. It was also believed that response of this rapidity would give the pilot the impression that his stick motions were being faithfully followed by the servo-operated control surfaces. The lags attending this specified performance were to be apportioned among the sensing instrument, the signal channel, and the power servo. so the initial goal for servos was taken to be a ten-cycle natural frequency or better.

Performance requirements of the feel servos were based on experience which said that a system with five-cycle natural frequency and 100% critical damping would "feel right" to a human operator.

Static requirements were also considered. For the control-surface servos, probably resolution is of prime importance followed by short-term drift, static stiffness, maximum velocity, and limitation of maximum force output. The latter requirement is tied in with detail design features and is only mentioned here since it must eventually be incorporated.

D. INSTALLATION PROBLEMS

NATURE OF THE T-33 INSTALLATION

The ideal installation of a flight control servo system has the servoactuator as close as possible to the surface which it is controlling. This permits motion of the servo to be transmitted directly to the flight control surface with no lost motion in transmission. At the same time, control surface inertia and aerodynamic loads would be transmitted directly to the servo without modification by any intervening springs. So, provided the servoloop itself has the required performance, the system will yield the best possible performance from the servo to the flight control surface. An installation of this type is generally possible,and is usually accomplished on a new airplane design. However, where an airplane is being modified, as in the case of the T-33, it is often necessary to locate a servo at some distance from the flight control surface. The connection between the surface and the servo is usually accomplished by push-pull rods, or in some cases, by relatively compliant control cables, with the result that high performance is difficult to obtain.

A layout design study has been undertaken to see where servos could be readily located in the T-33 airplane. The results of this study indicate that

Approved for Public Release

Contrails

there are two possible locations for the aileron servos. The ship's aileron control layout consists of a hydraulic booster unit, located in the fuselage, driving the ailerons through control cables. The cockpit control stick connects to the booster through push rods and torque tubes. In one design layout the aileron flight control servo was located very close to the ship's boost unit, but this makes it necessary to transmit motion to the ailerons through the existing cables in the wing. The compliance of the cables and the inertia of the aileron control surfaces has been found to produce an undamped natural frequency of 22 cps when the aileron is vibrated with the center point of the cables fixed to the fuselage. With this information it is possible to predict the nature of the transmission of motion from the servo at the center of the wing to the aileron. It was realized that this compliance would have an effect on both the static performance and on the dynamic performance of the installation, and accordingly another design study was undertaken to see if a servo could be located directly at the aileron in each wing. Several designs were considered with the servo located both within and outside the cross section of the wing. The external installation, with a rather large fairing, was undesirable from an aerodynamic standpoint, so an internal arrangement was worked out with no bulges in the wing contour. For this installation, however, one cell of each wing fuel tank had to be removed to make room for the servoactuator and its valves, with a resultant total loss of about 16 gallons of fuel. The choice between the two installations will have to be made on the basis of lost fuel in one case, which results in lost endurance for test flights, and in lost static and dynamic performance for the servo located in the center of the fuselage. The latter installation is probably easier to make physically.

The elevator control system is a push-pull rod installation from the elevator to the cockpit. The load path of the push rod is fairly straight from the elevator horn to the front end of the engine plenum chamber, at which point a right angle bell-crank transfers fore and aft push rod motion from the top of the fuselage down to a level below the floor of the cockpit. It was found possible to locate a servo at this right angle bell-crank and it is believed that the push rod will introduce relatively little compliance between the servo and the elevator. Stiffening of the bulkhead used as a mount for the servo and bell-crank may be

Approved for Public Release

Contrails

required. There is ample room in the engine plenum chamber and the installation should be simple mechanically.

The T-33 rudder is controlled by cables running from the cockpit to the rudder horns. The afterpart of the T-33 fuselage is very slim and there is little room around the tail fairing in the area where the rudder cables run forward. Without modification of the fuselage structure, it appears that the only volume of any size available for mounting a rudder control surface servo is in the engine plenum chamber near the location chosen for the elevator servo. In spite of the resulting cable flexibility and the consequent loss in static and dynamic performance, it is believed that this is the most practical location for the rudder servo and that performance can be made satisfactory, possibly by use of larger cables. Calculations of the natural frequency of the rudder restrained by two cables of the required length and a diameter now in use show a 24 cps natural frequency.

SERVO LOADS

To analyze the performance of a flight control servo, it is necessary to know the aerodynamic load acting on the control surface, the moment of inertia of the control surface, and the nature of the connection between the control surface and the servo itself. In addition to this, of course, the dynamic performance of each element in the servoloop must be know. Moments of inertia of the surfaces and gear which will move with them have been estimated from structural data and are tabulated on the following page.

Approved for Public Release

Contrails

FLIGHT CONTROL ITEM	MOMENT OF INERTIA* LB-IN.^{2}
AILERON SURFACE AND COUNTERWEIGHTS (ONE AILERON)	832
PILOT'S CONTROL STICK ($\frac{1}{2}$ OF ONE STICK)	690
TOTAL	1522
ELEVATOR SURFACE AND COUNTERWEIGHTS (BOTH SIDES)	616
PILOT'S CONTROL STICK (ONE STICK)	210
TOTAL	826
RUDDER SURFACE AND COUNTERWEIGHTS	378
PILOT'S PEDALS (ONE SET)	216
TOTAL	594

* *Moments of Inertia referred to respective surface hinge axes*

Moments of Inertia of T-33 Flight Controls

The ailerons are believed to be most critical to cable stretch and the aileron cable compliance has been estimated from the aileron natural frequency and the moment of inertia of the control surfaces.

For the purpose of analyzing servo performance, it has been assumed that the aerodynamic flight loads on a control surface behave like a spring and a small amount of damping. The spring constant is the basic aerodynamic load and is obtained easily from flight test data or from static wind tunnel data. The ratio of the damping component of the load to the spring component is taken from flutter data. A method for estimating the aerodynamic damping is given in the following section.

AERODYNAMIC LOADS

As a basis for estimating the maximum loads which the T-33 control surface servos should handle, it was decided to use the hinge moments which correspond to certain cockpit loads which are within the strength capabilities of the human pilot. For the power boosted aileron system, the hinge moment included the normal increment supplied by the hydraulic boost servo. For the

Approved for Public Release

Contrails

elevator, no boost action was assumed from the tab. The following tabulation lists the limit hinge moments and pilot applied loads.

CONTROL SURFACE	LIMIT HINGE MOMENT (IN.-LB)	STICK OR PEDAL FORCE (LB)
AILERONS	7200 (EACH)	100 LB SIDE LOAD TOTAL (1000 PSI IN BOOST CYLINDER)
ELEVATOR	2625	200 LB PULL (OR PUSH)
RUDDER	2480	300 LB PUSH

Limit Hinge Moments for T-33 Control Surface Servos

Surface deflections resulting from the limit hinge moments were calculated for the flight condition M = 0.80, h = 5000 ft. and q = 790 lb/ft^2. From these deflections and moments the aerodynamic spring rates were taken and tabulated below.

CONTROL SURFACE	MAX. HINGE MOMENT (IN.-LB)	MAX. DEFLECTION (DEG)	MAX. RATE (IN.-LB/DEG)
AILERON (ONE)	7200	4.8	1500
ELEVATOR	2625	4.66	563
RUDDER	2480	3.84	645

Maximum Aerodynamic Spring Rates

From these figures, it is evident that the aileron system is by far the most heavily loaded control in the airplane.

SERVO PROBLEMS CAUSED BY INSTALLATION

The installation design study has shown that the aileron servo installation

Approved for Public Release

Contrails

will probably be critical from the performance point of view. The ailerons must handle large aerodynamic loads and it may also be necessary to drive them through flexible cables. In addition, the rolling performance of an airplane is important to the pilot. The Phase I Analysis and Test Program was therefore set up to investigate the particular problem of the aileron servo. In the case of the fuselage-mounted aileron servo, the principal problem is likely to be the resonant effect of the aileron inertia and the flexibility of the control cables. For the wing-mounted servos, two problems may possibly arise. First, the aerodynamic and inertia loads of the control surface are felt directly by the servo without the softening effect of a spring connection between them. Thus, more characteristics of the load will be reflected into the internal loop of the servo. On the other hand, if servoloop performance is satisfactory, motion of the actual ailerons will also be satisfactory. The second problem with the wing-mounted servos is that two servo systems must be operated in parallel, with no means for load equalization except stretch of interconnecting cables. One complete servoloop will be required for each control surface and since the ailerons are physically connected through their cable systems, it will sometimes be necessary for the servos to work against each other if they are not in exact synchronism. This opposing component of servo motion will act as an additional load on each of the servos and this effect must be considered in the servoanalysis. The theoretical method for handling these loads will be described under Analysis of Servo Performance and the description of the servo test rig will show how the loads are simulated physically.

E. ANALYSIS OF POSITION SERVO PERFORMANCE UNDER LOAD

The block diagram of a position servo is given in Figure 44 wherein the important system variables are defined. The output of the servo is the control-surface position, σ_c whether it be the rudder, the aileron, or the elevator. The servo itself supplies the power amplification required to position the output in response to the stability input commands. These commands are in the form of electrical signals which provide very little power. Within the servoloop, the electrical signals control a servovalve which regulates hydraulic fluid flow to a servopiston. The servopiston drives the control surface through an intermedi-

Approved for Public Release

Contrails

ate mechanical linkage and the position of the servopiston is sensed for feedback purposes by a transducer which furnishes electrical signals to the servoloop.

To predict the servo performance relating servo input signals to the control surface position, it is first necessary to solve for the closed-loop response from the input to the servopiston position, and then to multiply by the transfer function of the mechanical transmission system in series with the loop. Actually, the hydromechanical system, the mechanical transmission system, and the external air loads must be treated simultaneously since the loading impedance of the following block has a distinct effect on the preceding block. However, by recognizing that these loading effects of one component on another are present, it is possible to write component performance equations including the load impedances. It is then possible to evaluate the impedances for different parts of the system and see how various loads, inertias, and springs contribute to block performance and finally to system performance. Dynamics of the air loading are taken first.

CONTROL SURFACE LOADING

Fairly accurate information is available on all parameters of the servo system except the aerodynamic loading of the control surface. Considerable effort has been expended on the theory and the measurement of aerodynamic hinge moments in conjunction with flutter investigations, and data presented by Smilg and Wasserman (Reference 9) were used to estimate the dynamic air-loading of the servo-controlled surfaces. Smilg and Wasserman develop an expression for the aerodynamic torque about a control-surface hinge line based on the two-dimensional flutter theory of Theodorsen. This flutter theory neglects compressibility effects but has been found substantially unchanged to $M = 0.5$. The following expression for the aerodynamic torque per unit span about the leading edge of a control surface due to control surface deflection has been taken from Reference 10 for the case of no tab motion and zero overhang of the control surface ahead of the hinge line.

$$T_{LE} = \pi \rho \left(\frac{c_w}{2}\right)^4 \omega^2 \delta_s T_\delta \qquad (132)$$

Approved for Public Release

Contrails

where

T_{LE} = torque about control-surface leading edge per length of span (ft-lb/ft)

ρ = air density (slug/ft^3)

c_w = chord of wing section including control surface and tab (ft)

$\omega = 2\pi f$ = oscillation frequency of control surface ω in rad/sec; f in cps

δ_s = control-surface angular deflection (radians)

T_δ = aerodynamic moment coefficient due to control-surface oscillations (non-dimensional)

The moment coefficient T_δ has been tabulated as a function of reduced frequency by Smilg and Wasserman for wings of constant chord but of various control-surface chord to total chord ratios. The term reduced-frequency is one familiar to flutter theorists and can be expressed in serveral ways:

$$\omega_{RED} = \frac{\omega c_w}{2V} = \pi \frac{f}{\gamma} = \pi \frac{c_w}{\lambda} \qquad (133)$$

where

ω_{RED} = reduced frequency (non-dimensional)

$\gamma = \frac{V}{c_w}$ frequency with which the wing traverses its chord length (sec^{-1})

$\lambda = \frac{2\pi V}{\omega}$ wavelength of the oscillation in space (ft)

An estimation of the control-surface, aerodynamic loading for use in the servo analysis was obtained from these data by a series of manipulations. The conventional non-dimensional, hinge moment coefficient, C_h, is expressed

Approved for Public Release

Contrails

as:

$$C_h = \frac{T}{S_q c_s} \tag{134}$$

where

T = total hinge moment (ft. lb)

S = control-surface area aft of hinge line (ft^2)

$q = \frac{1}{2}\rho V^2$ = dynamic pressure (lb/ft^2)

V = true velocity (ft/sec)

c_s = control-surface chord aft of hinge line (ft)

Substituting equation (132) in equation (134) and using b_s as the control-surface span-length in feet, we have

$$C_h = \frac{\pi\rho\left(\frac{c_w}{2}\right)^4 \omega^2 \delta_s T_\delta b_s}{S q c_s} \tag{135}$$

or

$$\frac{\partial C_h}{\partial \delta_s} = T_\delta 2\pi\left(\frac{\omega c_w}{2V}\right)^2\left(\frac{c_w}{2c_s}\right)^2 \tag{136}$$

which expresses the hinge-moment coefficient per unit angular deflection as a function of the torque coefficient T_δ, the reduced frequency $\left(\frac{\omega c_w}{2V}\right)$ and the ratio of chords $\left(\frac{c_w}{2c_s}\right)$. The amplitude ratio and phase angle of the dynamic response $\left(\frac{\partial C_h}{\partial \delta_s}\right)$ as a function of reduced frequency was computed from equation (136) for various ratios of $\left(\frac{c_s}{c_w}\right)$ from the

Approved for Public Release

tabulated values of T_σ given in Reference 9. The results of these calculations, when normalized to a 1:1 amplitude ratio at the lowest oscillation frequency appear as plotted in Figure 45.

The resemblance of these curves to those of a first-order system in the region below $\omega_{RED} = 1$ prompted a comparison of the two. Consider the first-order system composed of a rotational spring and damper as sketched below

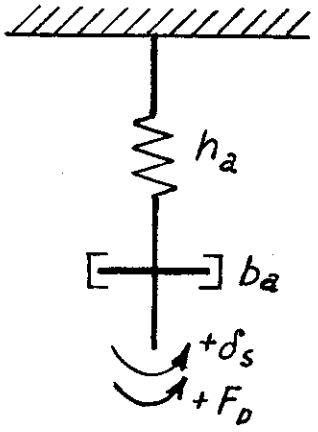

F_D = deflection torque (in. lb)

$F_s = -F_D$ restoring torque (in. lb)

δ_s = angular deflection (radians)

h_a = torsional spring (in. lb/rad)

b_a = angular viscous damping ($\frac{\text{in. lb}}{\text{rad/sec}}$)

Simple First-Order Rotational System

From this sketch, the restoring torque as a function of position can be written as:

$$\left(\frac{F_s}{\delta_s}\right)(\omega) = -(h_a + j\omega b_a) = -h_a(1 + j\omega\tau_1) \qquad (137)$$

where the time constant τ_1 equals $\frac{b_a}{h_a}$ in seconds. The non-dimensional plot presented in Figure 46 may be drawn to represent the dynamics of equation (137). Figures 45 and 46 have been drawn to the same scales so that direct superposition of the plots is possible. When this is done it is apparent that the first-order curves can be shifted in order to give close agreement to any specific loading curve. The amplitude ratio of the two curves can generally be matched within 5%, but the corresponding phase angle of the first-order system does not correlate as closely, indicating that the surface loading is higher than

Approved for Public Release

Contrails

first order. It was felt, however, that, considering the limited information available on the dynamics of the surface loads and the number of assumptions necessary for the derivation of the loading curves, the degree of correlation more than justified the representation. Therefore, the aerodynamic surface loads used for the servodynamics studies were assumed to be represented by a simple spring-damper arrangement with a time constant selected for each specified airspeed. The procedure for determining the first-order time constant of the loading parameters for a specified flight condition is as follows. From the geometry of the wing and control surface, the ratio c_s / c_w may be determined (for a mid-span location). This ratio specifies one of the family of loading curves and the non-dimensional axes of the first-order system can be shifted to the position of optimum correlation. Then, at the point on the two matched frequency scales where $\omega \tau_1 = 1$ and $\left(\frac{\omega c_w}{2V}\right) = \varkappa$, we can solve simultaneously for τ_1, giving:

$$\tau_1 = \left(\frac{c_w}{2V\varkappa}\right) \tag{138}$$

The zero frequency aerodynamic load, $\left|\frac{\partial C_h}{\partial \delta_s}\right|_{ss} = h_\alpha$ can be obtained from steady state wind tunnel or flight test data, then the frequency dependent damping load can be evaluated from the appropriate first-order time constant as, $b_\alpha = \tau_1 h_\alpha$. For maximum servo loading, the flight condition of maximum hinge-moment should be used.

SERVO LOAD IMPEDANCE AND TRANSMISSION RATIO

Having determined a representation for the dynamic air loads, it is then necessary to translate this effect to the servo. Two aspects of this problem are significant: (1) the effective servo load impedance or the load the servo actually sees (F_p / δ_p of Figure 44) and (2) the servo-to-surface position transfer function; i.e., the transmission ratio (δ_t / δ_p of

Approved for Public Release

Contrails

Figure 44. A mechanical representation of the surface drive system ($K_6\ G_6\ (s)$ of Figure 44) can be drawn as sketched below, from which the desired relationships are readily derived.

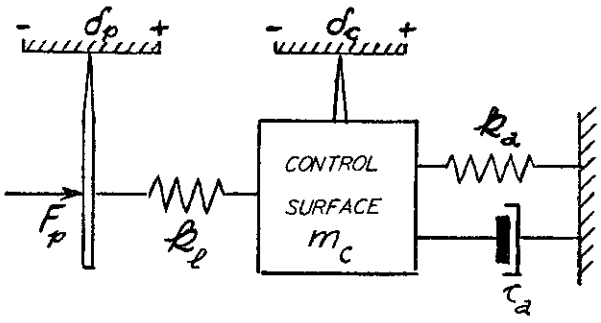

F_p = servopiston force (lb)

δ_p = servopiston position (in.)

δ_c = control surface position (in.)

k_ℓ = linkage stiffness (lb/in.)

k_a = translational equivalent of air-load hinge moment (lb/in)

c_a = equivalent air damping, in the air ($\frac{lb}{in/sec}$)

c_g = equivalent air damping, on the ground ($\frac{lb}{in/sec}$)

m_c = control surface mass ($\frac{lb}{in/sec^2}$)

Translational Representation of Surface Drive System

From the equations of motion for the system of this sketch, the position transmission ratio, T , is found to be:

$$T(s) = \left(\frac{\delta_c}{\delta_p}\right)(s) = \frac{1}{1 + \left(\frac{s}{\omega_n}\right)^2 + \left(\frac{Z_a}{k_\ell}\right)} \qquad (139)$$

where $Z_a = (k_a + s c_a)$ = impedance of the aerodynamic load as seen by the control surface (lb/in.)

$\omega_n = \sqrt{\frac{k_\ell}{m_c}}$ = natural frequency of transmission system (rad/sec)

and the load impedance seen by the servopiston Z_p is:

Approved for Public Release

Contrails

$$Z_p(s) = \left(\frac{F_p}{\delta_p}\right)(s) = T(s)\left[Z_a(s) + s^2 m_c\right] \qquad (140)$$

The transmission ratio may be determined from equation (139) from the estimated air-load impedance $Z_a(s)$ (as discussed in the preceding section), the linkage stiffness, k_ℓ, and the natural frequency of the drive system, ω_n. Both k_ℓ and ω_n can be measured from ground tests. When the servo is operated on the ground, the air-load impedance very nearly disappears (except for a slight damping load, c_g) and the transmission ratio is that of a lightly damped, second-order system. With or without air loads, however, the transmission ratio is attenuated rapidly at high frequencies, approaching the asymptote $\frac{1}{(s/\omega_n)^2}$. The servo load impedance (from equation (140)) is the sum of the air load impedance and the control surface mass as seen through the transmission ratio. At high frequencies, the impedance as seen by the servopiston approaches that of the linkage stiffness, k_ℓ, because the mass of the control surface tends to remain stationary.

Representative plots of the transmission ratio and the impedance function are given in Figures 47 and 48, respectively. Included in these plots are responses for both ground and air operation. The data from which these plots were taken was compiled for a fuselage located aileron servo for the T-33.

SERVOLOOP DYNAMICS

The components of the position servoloop are specified in the block diagram of Figure 44. By knowing the transfer function of each block of this servoloop we may analyze the stability of the servo and estimate an equivalent servo natural frequency and damping ratio for a specified loop gain.

The servoamplifier transfer function, $K_2 G_2(s)$ can be approximated by a first-order time constant, or

$$\left(\frac{i_\epsilon}{e_\epsilon}\right)(s) = K_2 G_2(s) = K_2\left(\frac{1}{1 + s\tau_2}\right) \qquad (141)$$

Approved for Public Release

Controls

For the general complexity of the position servoamplifier, experience indicates that a representative time constant is $\tau_2 = 0.003$ seconds.

The flow-control servovalve has been represented as a single block in Figure 44, relating fluid flow into the hydromechanical system as a function of the current output of the servoamplifier. Actually the valve flow response is not solely dependent on control current, but is a function of other variables, primarily load pressure. To include valve dependence on load pressure, a truer block diagram representation for the valve would be as sketched below, where $K_3 G_3(s)$ is the valve flow response to control current and $K_7 G_7(s)$ is the change in flow due to differential pressure at the valve output (ΔP in psi, F_o in lb). Written mathematically:

$$\delta_o(s) = K_3 G_3(s)\, i_\epsilon(s) - K_7 G_7(s)\, F_o(s) \qquad (142)$$

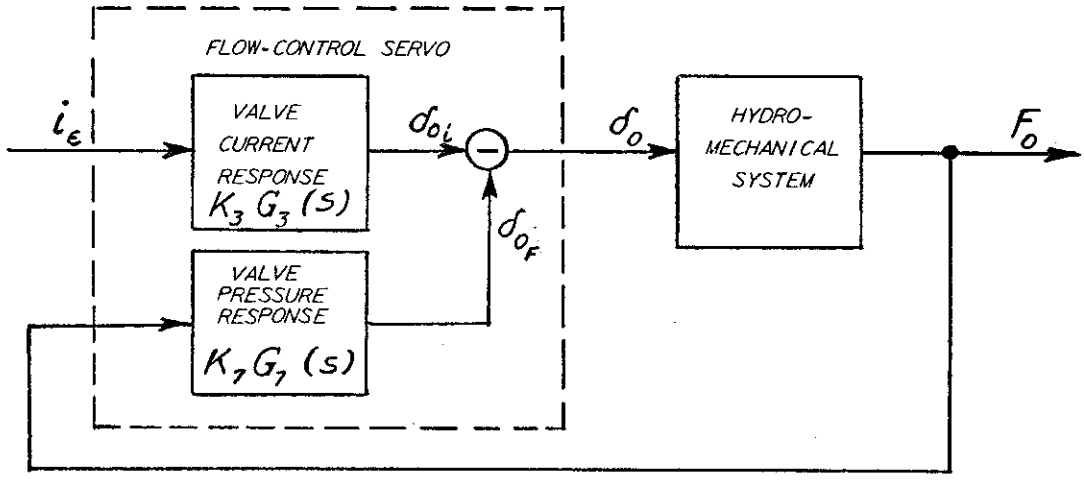

Flow-Control Servovalve Block Diagram

Actually, the response of a four-way, flow-control valve with zero overlap tends to be insensitive to load pressure in the region where the differential pressure (ΔP) is appreciably smaller than the supply pressure (P_s). This is clearly seen from the valve response curves of Figure 49. If the maximum differential pressure is never greater than one-half the supply pressure, the flow-valve pressure response can usually be neglected.

Approved for Public Release

Contrails

Assuming, then, that the flow-valve response is given by $K_3 G_3 (s)$ we can assign equivalent dynamics to the response $G_3 (s)$ on the basis of manufacturer's test data. A second-order approximation for a typical valve would have a natural frequency of 570 rad/sec (90 cps) and damping ratio 0.7. Actually, in the servo frequency range (through 50 cps), a first-order approximation is sufficient and a typical time constant would be $\tau_3 = 0.004$ seconds. In our analysis, the valve transfer function relates an equivalent fluid displacement and force to the valve input, rather than the actual flow and pressure variables. The valve transfer function $K_3 G_3 (s)$, includes the integrating action of the valve and the area of the servopiston, so has the form:

$$\left(\frac{\delta_0}{i_\epsilon}\right)(s) = K_3 G_3 (s) = \frac{K_{VAL}}{As}\left(\frac{1}{1 + \tau_3 s}\right) \qquad (143)$$

where K_{VAL} is the valve static sensitivity in $\left(\frac{in.^3/sec}{ma}\right)$ and A is the servopiston area ($in.^2$).

The remaining servoloop block with appreciable dynamics and, in fact, the only element which allows the load influence to enter the servo loop, is the hydromechanical system between the servovalve and the feedback point which, in Figure 44, is the servopiston. If the hydraulic system (the oil and its containers) is infinitely stiff and no leakage occurs across the servopiston, the valve will deliver a quantity of oil in response to an electrical signal (valve pressure dependence assumed negligible) and the feedback signal would be directly proportional to the oil delivery. Stated more concisely, the performance of the servo would not be influenced by the load. However, because of hydraulic system compliance (and leakage, if present), the servopiston motion is not in exact correspondence with oil delivery from the valve, and the deficiency is a function of the load at the servopiston. Therefore, in order to analyze the servoloop performance, it is necessary to know the response of the servopiston position to oil delivered by the valve. A schematic representation of this system is given on the following page.

Approved for Public Release

Contrails

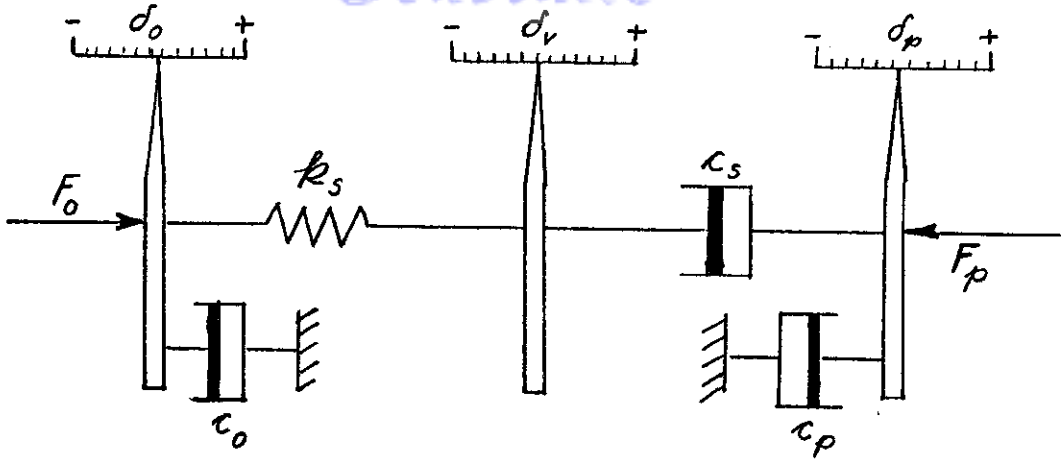

δ_o = equivalent fluid displacement from servovalve (in.)

δ_v = equivalent fluid displacement into servopiston (in.)

δ_p = servopiston position (in.)

F_o = hydraulic pressure at servovalve (lb)

F_p = servopiston force (lb)

k_s = effect of hydraulic compressibility (lb/in.)

c_s = effect of servomotor leakage ($\frac{\text{lb}}{\text{in./sec}}$)

c_o = equivalent damping at servovalve, ($\frac{\text{lb}}{\text{in./sec}}$)

c_p = equivalent damping at servopiston, ($\frac{\text{lb}}{\text{in./sec}}$)

Representation of Servoloop Hydromechanical System

The elements of this sketch represent corresponding hydraulic effects: i. e., hydraulic compressibility (in^3/psi) is represented by a stiffness, k_s (lb/in.); oil damping ($\frac{\text{psi}}{\text{in.}^3/\text{sec}}$) by dampers, c_o and c_p ($\frac{\text{lb}}{\text{in./sec}}$); and servomotor

Approved for Public Release

Contrails

leakage ($\frac{in^3/sec}{psi}$) by a series damper, c_s ($\frac{lb}{in/sec}$).

In this system the transfer function of interest is:

$$\left(\frac{\delta_p}{\delta_0}\right)(s) = \left[\frac{1}{1 + (Z_p + sc_p)(1/k_s + 1/sc_s)}\right] = K_4 G_4(s) \quad (144)$$

where Z_p is the servo load impedance as defined by equation (140). If the servomotor leakage is negligible, $c_s \longrightarrow \infty$ and equation (144) becomes:

$$\left(\frac{\delta_p}{\delta_0}\right)(s) = \left[\frac{1}{1 + Z_p/k_s + s\tau_4}\right] \quad (145)$$

where τ_4 is a hydraulic time constant, $\tau_4 = c_p/k_s$. Now, if the load impedance is small with respect to the fluid compressibility, the response of equation (145) reduces to the first-order effect of the hydraulic time constant. Evidently, then, the equivalent compliance of the fluid compressibility reflects the dynamics of the external servoload.

An expression for the hydraulic compliance has been developed for a double-acting servopiston (see Reference 10) and is:

$$k_s = \frac{4BA}{\delta_{p_{max}}}\,\eta \qquad (lb/in) \qquad (146)$$

where
- B = bulk modulus of fluid ($lb/in.^2$)
- A = servopiston area (in^2)
- $\delta_{p_{max}}$ = servopiston stroke (in)
- η = volumetric design efficiency (ratio of stroked volume to total fluid volume)

Other compressibility effects such as " O " ring compliance and mechanical stiffness between the servopiston and the feedback transducer should also be included in the compressibility factor k_s.

Approved for Public Release

Contrails

The oil damping factors c_0 and c_p are lumped equivalents of oil turbulence and distributed viscous drag. With the flow-control servovalve (when the valve pressure response is neglected) only the damping which has been assumed to act at the servomotor enters the expression for the loop dynamics. This effect has been evaluated in the past by curve-fitting techniques. In general, the physical design of the hydraulic circuit and the servomotor is made to reduce hydraulic damping (and the hydraulic time constant) by minimizing the complexity of the physical layout.

Servoloop feedback is obtained by sensing the servopiston position in the block diagram of Figure 44. The loss in the position transmission from the servopiston to the control surface could be reduced by sensing control-surface position for feedback. However, the disadvantage of this method is that more compliance is included in the servoloop and the servoloop transfer function $K_4 G_4 (s)$ would reflect more of the external load and servo stability would be greatly impaired. For ground operation and with sufficient compliance within the servoloop, the reflected load may introduce upwards of 180 degrees phase lag within the servoloop near the frequency ω_n .

The servoloop gain required to achieve a finite servo resolution can be determined from an expression given in Reference 10:

$$K_v = \frac{\epsilon \dot{\delta}_{p_{max}}}{\delta_{p_\epsilon}} \quad (sec^{-1}) \tag{147}$$

$$K_v = K_2 K_3 K_4 K_5 = \text{Servoloop Gain } (sec^{-1})$$

where: ϵ = servovalve fractional resolution (non-dimensional ratio of threshold response to maximum response)

$\dot{\delta}_{p_{max}}$ = maximum servopiston rate (in/sec)

δ_{p_ϵ} = minimum servopiston displacement which servo will resolve (in.)

So the required servoloop gain may be determined by the specifications for the system rate of response. The other requirements for servoloop gain are

Approved for Public Release

Contrails

dictated by specifications for over-all servo performance. These performance specifications include an equivalent natural frequency and damping ratio for the entire servoloop. It is recognized that the servoloop is much higher order than second, so these requirements are usually interpreted as: (1) the equivalent natural frequency is that frequency for which the over-all phase shift is 90° lagging and (2) the maximum amplitude ratio of the over-all servoloop response is:

$$AR_{max} = \frac{1}{2\zeta\sqrt{1-\zeta^2}} \tag{148}$$

where ζ is the equivalent damping ratio. (This formula applies to the case $\zeta < 0.7$).

SERVOLOOP STABILITY

The position servoloop response can be written directly from the block diagram of Figure 44 as:

$$\left(\frac{\delta_p}{e_1}\right)(s) = \left\{\frac{K_2 G_2(s) K_3 G_3(s) K_4 G_4(s)}{1 + K_2 G_2(s) K_3 G_3(s) K_4 G_4(s) K_5 G_5(s)}\right\}$$

$$= \frac{1}{K_5}\left\{\frac{1}{\frac{1}{K_V G_2(s) G_3(s) G_4(s)} + G_5(s)}\right\} \tag{149}$$

where K_V is the loop gain

$$K_V = K_2 K_3 K_4 K_5 \ (sec^{-1}) \tag{150}$$

For the servo with only proportional feedback, $G_5(s) = 1$ and equation (149) is of convenient form for solution by the inverse Nyquist plot. Reference 10 explains the technique of preparing an inverse plot from an accumulation of openloop dynamics data and tells how the servoloop stability may be predicted for any specific loop gain. The product of the servoloop dynamics,

Approved for Public Release

Contrails

$G_2(s)$ $G_3(s)$ $G_4(s)$, will be a high-order expression in s and can be evaluated from equations (141), (143), and (144). So equation (149) will have the form:

$$\left(\frac{\delta_p}{e_1}\right)(s) = \frac{1}{K_5}\left\{\frac{1}{1+\frac{a_1 s + a_2 s^2 + a_3 s^3 + \cdots}{K_v}}\right\} \qquad (151)$$

Once the loop gain is established, an equivalent second-order natural frequency and damping ratio may be established for the entire servo directly from the inverse plot.

To improve servo performance, it may be necessary to increase the loop gain; but this increases the natural frequency of the servo (which is determined by the reciprocals of the coefficients of the even-powered s terms) and decreases its damping (determined by the coefficients of the odd-powered s terms). The equivalent loop damping may be increased by the addition of rate feedback which changes the nature of the feedback dynamics as:

$$G_5(s) = (1 + \tau_5 s) \qquad (152)$$

where τ_5 is the rate-feedback time constant.
Then equation (151) will become

$$\left(\frac{\delta_p}{e_1}\right)(s) = \frac{1}{K_5}\left\{\frac{1}{1+\left(\frac{a_1 + K_v \tau_5}{K_v}\right)s + \frac{a_2}{K_v} s^2 \cdots}\right\} \qquad (153)$$

and the damping introduced by the s term is increased by the addition of rate feedback. This method of servocompensation can be analyzed graphically with the inverse plot as is described in Reference 10.

SUMMARY OF THE EFFECTS OF SYSTEM CONSTANTS ON SERVO PERFORMANCE

Figure 47 shows a plot of the position transmission ratio for the T-33

Approved for Public Release

Contrails

aileron system. This function relates the motion of the aileron to the motion of the servopistion for the case of the fuselage-mounted servo which must drive the ailerons through control cables. It can be seen that the amplitude of the response peaks sharply at a resonant frequency determined by the inertia of the control surface and the combined spring effect of the aerodynamic loads and the cable stiffness. Two curves are shown: One for operation on the ground with no aerodynamic loading and another for operating in flight with a very high aerodynamic load. The effects of the aerodynamic load are to reduce the over-all transmission ratio throughout the frequency range and to change the frequency at which the response peaks. In both cases the amplitude of the response falls off very rapidly after resonance and it can be seen that regardless of the performance of the servoloop itself, it will be very difficult to move the aileron to any extent at frequencies above the peak values indicated in Figure 47. Surface inertia and the compliance in the transmission place an upper limit on the frequency response of the complete servo installation, while cable compliance, in relation to the airload spring constant, reduces the transmission ratio throughout the frequency range.

Figure 48 is of interest since it shows the load seen by the servopiston. The plot shows the effect of aerodynamic loads and inertia loads to the extent which they are transmitted through the cable compliance. Again,curves are shown for operation on the ground with no aerodynamic loads and for operation in high speed flight. For operation on the ground, the magnitude of the load rises rapidly to a peak value at load resonance. At this frequency the phase angle of the loading drops rapidly through a range of 150 degrees or more, and above resonance the magnitude of the load approaches a constant value. The phase angle of the load at high frequencies is substantially zero. For operation with high air loads, it is seen that the impedance magnitude rises from one constant level at low frequencies to a higher constant level at frequencies above resonance. In the transition zone the magnitude first drops, then rises to a resonant peak and settles back to the new level at the high frequency. The corresponding phase angle curve starts at zero phase for low frequencies, rises to a peak in the middle of the transition range and falls to zero again at high frequencies. In general, both curves show a sharp peak in amplitude at

Approved for Public Release

Contrails

or near the mechanical resonant frequency, while the corresponding phase curves go through changes of roughly 180 degrees and 90 degrees.

It is somewhat more difficult to see the significance of the load impedance curve than it was for the transmission ratio. However, equation (145), which relates servopiston motion (δ_p) to the theoretical oil-delivery volume of the servovalve, (δ_0), shows that as the magnitude of Z_p rises, the response of δ_p to δ_0 will fall off. Phase angle changes in Z_p will also cause phase angle changes in the right-hand side of equation (145), especially if the term (Z_p / k_s) is appreciable compared to unity. Thus, the effects of mechanical resonance in the load tends to limit servoloop performance just as the same resonance limited the transmission ratio from the servopiston to the control surface. Equation (145) shows, however, that it is possible to minimize servo loading effects by the proper choice of the value k_s in relation to Z_p, and k_s is one factor more or less at the disposal of the servo designer.

If the effects of servo loadings can be successfully minimized, servoloop performance is then determined by the dynamic response of the control valve, the amplifier and other components in the servoloop.

F. ANALYSIS OF FEEL SERVO SYSTEM PERFORMANCE

The problem of creating artificial feel in the pilot's controls can be approached from two distinct standpoints, the most obvious being the use of a force servo to introduce artificial stick forces computed from stick position and aircraft response measurements. The alternate scheme consists of computing a control input for a stick position servo from measurements of airplane dynamics and the force in the pilot's stick. A block diagram for the latter case, which would use a flow-control servovalve in a position servo, is given in Figure 50. The pressure response of the flow valve has been neglected in this figure. Similarly, Figure 51 is a feel servo utilizing a pressure-control servovalve in a force servo. Since the physical system is identical for the two servos, we may draw an equivalent representation, as in the sketch on the following page. Many lesser dynamic effects have been omitted in this sketch; e. g., linkage and servopiston inertia, oil turbulence, and static friction in the piston. Also, angular motions have been replaced by translations.

Approved for Public Release

Contrails

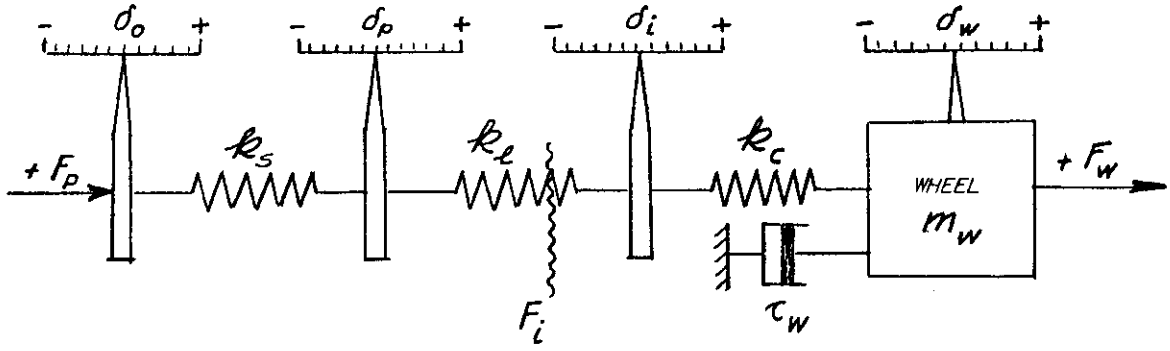

(+ Compression)

δ_o = equivalent fluid displacement at servovalve (in.)

δ_p = servopiston position (in.)

δ_i = servo input position (in.)

δ_w = wheel position (in.)

F_p = servopiston force (lb)

F_i = servo input force (lb)

F_w = wheel force (lb)

k_s = hydraulic stiffness (lb/in.)

k_ℓ = linkage stiffness (lb/in.)

k_c = column stiffness (lb/in.)

τ_w = damping due to air and friction $(\frac{\text{lb}}{\text{in./sec}})$

m_w = mass of wheel $(\frac{\text{lb}}{\text{in./sec}^2})$

Representation of Feel Servo Physical System

The input to the position servo system is the force, F_i , which exists in the physical system between the servopistion, δ_p , and the control force applied by the pilot at δ_w . Since we are assuming all system mass concentrated at the wheel, the physical location of the pickup for F_i along the column and linkage is unimportant. In the analysis of this system, then, the position of the base of the control column (δ_i) is irrelevant and we can assume that the servopiston is connected to the wheel by a single spring, equal in stiffness to

Approved for Public Release

Contrails

the combined series stiffness of the control column and linkage.

In the block diagram for the feel servo with the pressure-control valve (Figure 51) the valve response to fluid flow has been included, indicating a valve response as follows:

$$\Delta P = \Delta P_i - \Delta P_Q = K_3 G_3(s) i_\epsilon - K_6 G_6(s) \delta_0 \qquad (154)$$

Equation (154) indicates a flow dependence of the pressure valve similar to the pressure dependence of the flow-control valve, which was discussed previously (equation (142)). However, it has been demonstrated in previous servo development work performed by Flight Research, that the pressure-control servovalve is much more sensitive to flow than the flow valve is to pressure. Bench tests are being set up to obtain quantitative information on the effect. It has been assumed in the physical diagram of this system that the position input to the servo is sensed at the base of the column, with column flexibility present between the position pickup and the wheel and linkage flexibility between the pick-up and the servopiston.

Both block diagrams of Figures 50 and 51 include an inertia feedback from the servo output to the input due to control wheel inertia. For convenience, the terminology of this section applies to an elevator-control feel servo but all work is equally applicable to the aileron and rudder feel servos. The feel servo test rig will simulate the pilot's elevator controls and will have provisions for either a force or a position servo.

FEEL SERVO SYSTEM RESPONSE EQUATIONS

With the various output-input relationships defined in Figures 50 and 51 and the physical parameters of the sketch above, the system response equations may be written. In general, this entails writing the simultaneous equations of motion of the mechanical system, then solving for the desired transfer functions.

The stick feel can be expressed by the dynamic force-position relationship at the point of control application. These expressions are found to be:

Approved for Public Release

Contrails

(a) for the flow-valve feel servo

$$\left(\frac{F_w}{\delta_w}\right)(s) = m_w s^2 + c_w s + \left\{ \frac{\frac{K_5}{K_1}\left(1+\frac{1}{OL_Q}\right)}{1+\frac{K_5}{K_1}\frac{1}{k_{cl}}\left(1+\frac{1}{OL_Q}\right)} \right\} \qquad (155)$$

where OL_Q = servo open-loop transfer function (non-dimensional)

$$OL_Q = K_2 G_2(s) K_3 G_3(s) K_4 G_4(s) K_5 = K_v (G_2 \; G_3 \; G_4)(s) \qquad (156)$$

K_v = Open loop gain $= K_2 K_3 K_4 K_5 \; (sec^{-1})$ (157)

$$k_{cl} = \frac{k_l k_c}{k_l + k_c} \quad \left(\frac{lb}{in.}\right) \qquad (158)$$

(b) for the pressure-valve feel servo

$$\left(\frac{F_w}{\delta_w}\right)(s) = m_w s^2 + c_w s + \left\{ \frac{\left(\frac{K_5}{K_1}\right) + \frac{K_4 K_6 G_6(s)}{OL_p}}{1+\left(\frac{K_5}{K_1}\right)\frac{1}{k_c} + \frac{1}{OL_p} + \frac{K_4 K_6 G_6(s)}{OL_p}\left(\frac{1}{k_s}+\frac{1}{k_{cl}}\right)} \right\} \qquad (159)$$

where OL_p = servo open-loop transfer function (non-dimensional)

$$OL_p = K_2 G_2(s) K_3 G_3(s) K_4 K_1 = K_0 (G_2 G_3)(s) \qquad (160)$$

K_0 = Open loop gain $= K_2 K_3 K_4 K_1$ (non-dimensional) (161)

In both equations (155) and (159) the first two terms express the normal inertia and damping forces required at the stick, while the large expression is the apparent spring effect of the servo. If the loop gain is high so that $1/OL \ll 1$, and if the column and linkage stiffness is considerably stiffer than the servo, the servo contributed term reduces to K_5/K_1 (lb/in.), the equivalent servo spring rate.

Approved for Public Release

Contrails

The force-position relationships just presented show no obvious tendency towards instability. The physical feedback path due to the inertia reaction of the wheel can cause instability, however, when operating with high servo stiffness. Consider this problem with the flow-valve servo. Referring to the sketch below, it is seen that the force input to the servo is due to external forces applied at the wheel (F_{iw}) and to servopiston forces applied to the bottom of the stick (F_{ip}). In other words, physical feedback exists as servopiston acceleration, $\ddot{\delta}_p$, causes a force, F_{ip} which appears at the servo input.

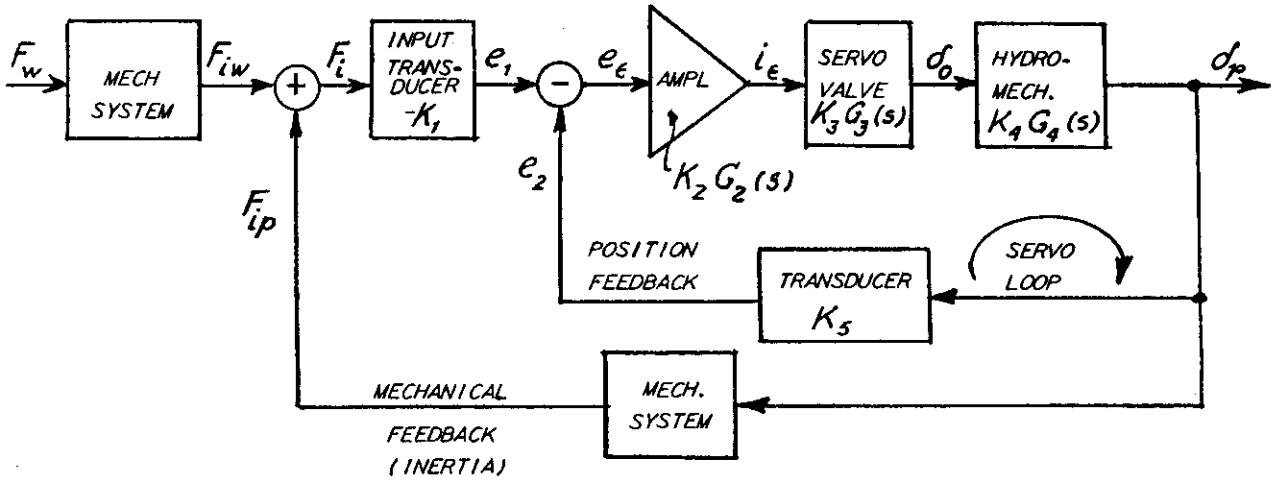

Mechanical Feedback With Flow-Valve Feel Servo

The system of this sketch will be unstable if the denominator of the expression for the response (δ_p / F_{iw}) is zero. Solving for this response and then equating the denominator to zero gives the following equation as the stability criterion for the flow-valve system.

$$1+\left(\frac{K_5}{K_1}\right)\left\{\left[\frac{1}{k_{ce}}\right]\left[1+\frac{1}{OL_Q}\right]\left[\frac{1+2\zeta_1\left(\frac{s}{\omega_{n1}}\right)+\left(\frac{s}{\omega_{n1}}\right)^2}{2\zeta_1\left(\frac{s}{\omega_{n1}}\right)+\left(\frac{s}{\omega_{n1}}\right)^2}\right]\right\}=0 \qquad (162)$$

Approved for Public Release

Contrails

where $\omega_{n_1} = \sqrt{\frac{k_{cl}}{m_w}}$ $\zeta_1 = \frac{1}{2}\frac{\tau_w}{\sqrt{m_w k_{cl}}}$ (163)

Similarly, a stability analysis of the feel servo with a pressure-control servovalve yields a stability equation as follows (where the pressure-valve flow dynamics have been neglected for simplicity):

$$1+\left(\frac{K_5}{K_1}\right)\left(\frac{1}{k_c}\right)\left[\frac{1}{1+\frac{1}{OL_p}}\right]\left[\frac{1+2\zeta_2\left(\frac{s}{\omega_{n_2}}\right)+\left(\frac{s}{\omega_{n_2}}\right)^2}{2\zeta_2\left(\frac{s}{\omega_{n_2}}\right)+\left(\frac{s}{\omega_{n_2}}\right)^2}\right] = 0 \quad (164)$$

where $\omega_{n_2} = \sqrt{\frac{k_c}{m_w}}$ $\zeta_2 = \frac{1}{2}\frac{\tau_w}{\sqrt{m_w k_c}}$ (165)

The dynamic portion of these stability equations may be solved and the result presented as a frequency locus on a polar plot in which the scale represents a steady-state stiffness ratio. With the flow-valve system it is the ratio of the column and linkage in series to the equivalent servo stiffness, or $\left(k_{cl}/\frac{K_5}{K_1}\right)$. For the pressure-valve system, the stiffness ratio would be $\left(k_c/\frac{K_5}{K_1}\right)$. On either plot, the scale value at which the locus crosses the negative real axis is, then, the stiffness ratio which would result in absolute instability, and as this value of stiffness ratio is approached, the system would be highly resonant.

An important difference in the two stability equations is the steady-state stiffness ratio. For the position servo the total stiffness between the control wheel and the servopiston is apparently important while with the force servo, the stiffness between the servopiston and the position pickup does not enter the stability equation. Consequently, if the position pickup is attached to the bottom of the control column, the detrimental effect of the linkage flexibility coupling the column to the servopiston is excluded from the system.

Approved for Public Release

Controlled

Another difference between the stability criterions appears in the terms associated with electrical servoloop dynamics. For the flow-valve servo this term is $\left(1 + 1/OL_Q\right)$ which is phase lead in nature, while with the pressure-valve servo, the term is $\left(\frac{1}{1 + 1/OL_p}\right)$ which would introduce phase lag. The pressure-control feel servo could be made to work open loop; that is without force feedback, K_1 . Open-loop operation is satisfactory with the pressure valve as this valve utilizes internal feedback, so operates as a self stabilizing device. For open-loop operation, the servoloop expression becomes (with $K_1 = 0$):

$$\left(\frac{K_5}{K_1}\right)\left(\frac{1}{1 + 1/OL_p}\right) = K_5\left(K_2 G_2(s) K_3 G_3(s) K_4\right) \qquad \left(^{lb}/_{in}\right) \quad (166)$$

G. SERVO DESIGN PROBLEMS

The preceding sections have presented the theoretical analysis of a position servo and a feel servo and the analyses have shown the relative importance of many of the parameters involved in the performance relations. This section will show the relationships between the system constants appearing in the analyses and the physical elements with which the designer must actually work.

RELATION BETWEEN PHYSICAL DESIGN AND PERFORMANCE PARAMETERS

The servo designer has control of some of the constants which appear in the servo performance equations but obviously does not have control of all of them. The magnitude of the airloads, for example, is entirely fixed by the airplane, its size and the speed at which it is going to fly. Similarly, the moment of inertia of the control surface and the flexibility of the mechanical system between the surface and the servo are fixed quantities once the location of the servo has been selected. The hydraulic servovalve is generally purchased and there is an upper limit on the dynamic performance available in such valves. Electrical components, such as feedback transducers and signal ampli-

Approved for Public Release

Contrails

fiers, are usually not critical from a dynamic performance standpoint and conventional designs are usually satisfactory. The designer does, however, have some freedom in his selection of gear ratios between the servo and the control surface, the hydraulic pressure which he will use and the size of the piston area he will employ. It will be the purpose of this section to show how the choice of these parameters affects the constants of the hydromechanical system.

Equation (145) shows that the ratio of Z_p to k_s is a good measure of the extent to which the external load affects the servo performance. Let us examine this ratio and see how it relates to the actual design of a flight control servo.

The sketch below shows a servo with internal compliance connected by a rigid linkage to a bell-crank which operates an aerodynamic control surface. Forces, motions, dimensions, and other quantities are identified and defined in the sketch.

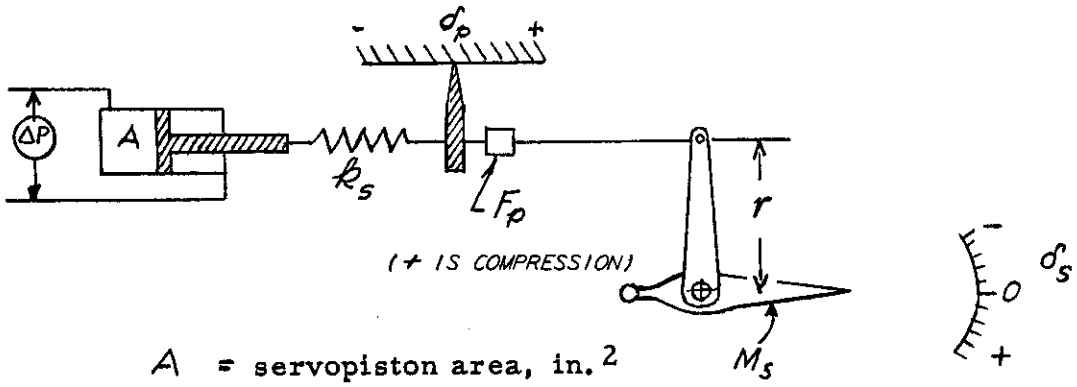

A = servopiston area, in.^{2}

ΔP = differential pressure, lb/in.^{2}

δ_p = servopiston position, in.

δ_s = control surface position, radians

r = bell-crank radius, in.

M_s = sum of air torque and inertia torque acting about hinge, in. lb

F_p = load acting on servopiston, lb

k_s = hydraulic stiffness, lb/in.

Servo Driven Flight Control Surface

Approved for Public Release

Contrails

We will define the impedance as seen by the servo as:

$$Z_p \equiv \frac{F_p}{\delta_p} \tag{167}$$

but,

$$F_p = \frac{M_s}{r} \tag{168}$$

and

$$\delta_p = r\delta_s \tag{169}$$

so

$$Z_p = \left(\frac{M_s}{\delta_s}\right)\left(\frac{1}{r^2}\right) \tag{170}$$

where (M_s/δ_s) is the actual impedance at the control surface hinge caused by air loads and inertia loads. Equation (146) shows that fluid compressibility can be expressed in terms of the bulk modulus of the oil, piston area, piston stroke and an efficiency coefficient. Now, it is customary to make the servo-piston stroke long enough to obtain full control surface deflection.

$$\delta_{p_{max}} = r\delta_{s_{max}} \tag{171}$$

and substituting into equation (146)

$$k_s = \frac{4BA}{r\delta_{s_{max}}}\eta \tag{172}$$

and finally

$$\frac{Z_p}{k_s} = \left(\frac{M_s}{\delta_s}\right)\left(\frac{\delta_{s_{max}}}{4B\eta}\right)\left(\frac{1}{Ar}\right) \tag{173}$$

Thus, if the product of the piston area and the bell-crank radius is made large, the loading effect for any set of air and inertia loads and surface deflection range may be made small. Physically, this means using a large servo operating with low hydraulic pressures to balance out the control surface loads.

Under the discussion of servovalve performance it was shown that the

Approved for Public Release

Contrails

maximum working differential pressure in the servocylinder should be no greater than about 70% of system pressure, P_s, to avoid valve loading effects. It is easily shown that:

$$M_{s_{max}} = \Delta P_{max} (Ar) \tag{174}$$

and if,

$$\Delta P_{max} = (P.R.) P_s \tag{175}$$

where $(P.R.)$ is the working pressure ratio for the valve

then,

$$(P.R.) = \frac{\Delta P_{max}}{P_s} = \left(\frac{M_{s_{max}}}{P_s}\right)\left(\frac{1}{Ar}\right) \tag{176}$$

Thus, not only must the (Ar) product be chosen large enough to minimize system loading effects (equation (173)), but also sufficiently large to minimize valve loading effects (equation (176)).

The upper limit on (Ar) is determined by physical size of units and by the maximum flow rate which can be handled by the valve and its supply, since

$$Q_{max} = (Ar) \dot{\delta}_{s_{max}} \tag{177}$$

The limit of servo resolution due to the threshold sensitivity of the valve depends on the following: threshold level of the valve expressed as a fraction of the maximum rated input, servoloop gain, and the maximum surface angular velocity, expressed as

$$\delta_{s_\epsilon} = \epsilon \frac{\dot{\delta}_{s_{max}}}{K_v} \tag{178}$$

where δ_{s_ϵ} = limit of resolution at control surface, deg.

ϵ = fractional valve resolution, non-dimensional

Approved for Public Release

Contrails

$\dot{\delta}_{s_{max}}$ = max. rate of surface travel, deg/sec

K_v = servoloop gain, sec^{-1}

Equation (178) is derived from equation (147) on the preceding page, but is included to show that the resolution due to valve threshold response cannot be altered by adjusting (A_r) as long as other quantities in equation (178) are kept unchanged.

DESIGN VALUES FOR POSITION SERVOS

The T-33 hydraulic system normally operates at 1000 psi. It was decided to use the same system pressure for the servo installations, and probably connect with the ship's system even though additional pumping and accumulator capacity would be required. It also appears desirable to limit all servos to the same maximum working pressure and use a single controlled reference pressure for this purpose as will be described in a later section. Seven hundred psi was chosen for the maximum working pressure in the surface control servos. Using this working pressure, the loads and inertias presented above, and the relations of equations (173), (176), and (177), some of the significant system characteristics have been computed and are presented in tabular form in Table XV. For comparison, the values for the F-86 non-linear rudder control servo are also listed.

Columns 13 and 14 of this table were computed to show the relative loading effects for the proposed T-33 control systems and for the F-86 servo which was known to be limited by loading. Columns 13 and 14 represent components of the (Z_p/k_s) ratio, not including the relieving effect of spring compliance between load and servo. The values are, nevertheless, indicative of the extent to which loads will influence servo performance. Column 13 is the ratio of air-load spring rate to oil-compressibility spring rate (each referred to a common point in the system; for example, linear motion at the servopiston) and shows quantitatively how much steady air loads would reduce servopiston motion if not

Approved for Public Release

Contrails

corrected by feedback. Viewed in another way it represents the feedback signal required to make up the deficiency in servo motion caused by the air load. Column 14 shows the effect of load inertia in relation to oil compressibility and is expressed as the period in seconds of the undamped oscillation of the control surface inertia and the restraining spring of oil compressibility. The absolute values are not too significant but they are useful in showing the extent to which the servos have been unloaded, compared with the F-86 servo. Columns 16 and 17 show actual servo sizes.

DESIGN VALUES FOR FEEL SERVOS

The theory relating design parameters to performance for the pressure-control type feel servos is not so well developed as for the control surface servos. It is believed, however, that the pressure type servovalves behave best when flow loading is a minimum. Following this principle, the servopiston areas and connecting linkages are adjusted so that full system hydraulic pressure will produce the maximum load specified at the control stick grip, rudder pedal, or control. The sketch below defines the geometry of the feel servo installations.

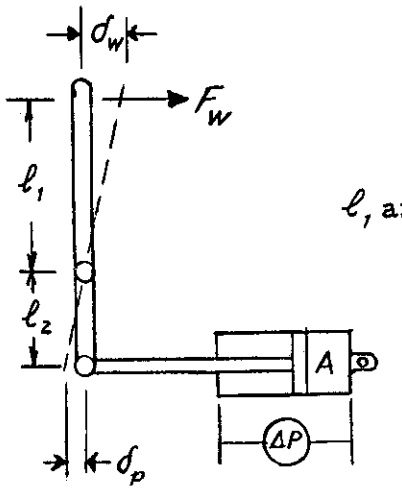

δ_w = pilot's control deflection, in.

F_w = force applied by pilot, lb

ℓ_1 and ℓ_2 = lever arms, in.

δ_p = servopistion deflection, in.

A = piston area, in.^{2}

ΔP = differential pressure across piston, lb/in.^{2}

Simplified Layout of Feel Servo

Elementary considerations of forces and moments show that

Approved for Public Release

Contrails

$$F_w = A \Delta P R \tag{179}$$

where

$$R \equiv \frac{\delta_p}{\delta_w} = \frac{\ell_2}{\ell_1} \tag{180}$$

or

$$(AR) = \frac{F_w}{\Delta P} \tag{181}$$

Maximum flow rate into the servoactuator will be

$$Q_{max} = (AR)\dot{\delta}_{w_{max}} \tag{182}$$

So, (AR) should be as small as possible to minimize flow. On the other hand, the maximum forces corresponding to system pressure must be high enough so that the pilot will not inadvertently exceed the maximum force and produce a large stick deflection which would call for a structurally dangerous airplane maneuver. For this reason, the maximum forces specified in Table XVI (which summarizes design values for the feel servos) are the same as the usual limit loads used for control system design. One servoactuator is to be used for the elevator feel servo for either a stick or a wheel type control. Since the column supporting the wheel must be longer than the plain stick, the maximum force due to maximum differential pressure is less for the wheel type control. The same situation is present to a lesser extent for the aileron control.

H. CONTROL SURFACE POSITION SERVO TESTS

A test rig was designed and built for the test program on the flight control position servos. The theoretical analysis in Phase I of this program, and the practical and theoretical experience of other programs demonstrated that two extremely important aspects of installed servo system performance are servo loading and flexibility in the transmission between servoactuator and flight control surface. The test rig was designed to provide both of these features in a form that could easily be adjusted. The values of constants were selected to simulate the aileron control system of the T-33.

Approved for Public Release

Contrails

TEST RIG

Figure 52 shows the position-servo test rig set up to simulate a fuselage-mounted servo, while Figure 53 shows the test rig for a wing-mounted servo. The test rig provides a mounting for the servoactuator, the piston of which is connected to a lever arm at one end of a torsion bar. This bar represents the flexibility of a cable control circuit. The other end of the torsion bar connects to a rocking beam which carries lead weights at its extremities to represent the inertia of a control surface and its balance weights. The inertia bar is then restrained by an additional torsion bar, clamped at its far end, representing the aerodynamic restoring moments on the control surface. A hydraulic damper is incorporated to simulate aerodynamic damping at the control surface. The damper consists of a piston-cylinder arrangement which pumps oil in a closed circuit through a restricted passage. This damping piston connects directly to the inertia bar. System constants are varied by changing lever arms, substituting different torsion bars, changing weights, and by moving the fixed end of the air load torsion bar. Ground operation is easily simulated by disconnecting the air load spring and damper.

The hydraulic servoactuator was designed for flexibility in testing. A photograph of the actuator and servovalve assembly with the position and rate feedback transducers in place,is given in Figure 54.

The fixed servopiston area was selected for use with the aileron servo system contemplated, and the maximum stroke was similarly determined. Volume of oil under compression is important to servo performance, so shorter stroke lengths are simulated by collars clamped to the piston on either side of the head to limit axial motion, and at the same time to eliminate unstroked oil volume. Chambers were also provided in the actuator that could be opened up to include additional oil volume. The servovalve was mounted directly on the actuator body to eliminate flexible hydraulic lines, but to include these effects, connections were provided for adding flexible hose lines to either side of the servopiston. The "O" ring groove in the piston head is formed by rings and spacers of different dimensions, which permit variations of "O"-ring diametral squeeze, and axial play.

Approved for Public Release

Contrails

The servovalve used in the test program was a Moog flow-control valve, conventional in every way except the design of the magnetic pole pieces and flapper, which were isolated from oil. The purpose of the special design was to prevent the accumulation of magnetic sludge from the oil in the air gap between the magnets and the flapper. Other valve installations had proved very sensitive to magnetic sludging, believed to be caused by the presence of the products of normal wear of ferrous parts in the hydraulic pumps and other moving parts. The new valve design has given no trouble.

The electronic components of the servo and the recording provisions were designed and built especially for the test setup. The servoamplifier was designed to accept an AC carrier signal from the position feedback transmitter, and DC signals from the input command and the velocity feedback generator. Separate attenuators controlled the levels of amplifier gain, and velocity feedback gain. Additional descriptions of this equipment are included in another section of this report.

Hydraulic power was supplied from a motor-driven variable volume pump. The pump was operated at 1000 psi (as in the T-33 airplane system) and the accumulator preload was adjusted to 500 psi to provide some smoothing of pump pulses and to supply sudden heavy oil demands. In addition to the pump accumulator on the hydraulic supply, two smaller accumulators were located near the servovalve, one in the pressure line and one in the return line.

SYSTEMS SIMULATED

A study of the aerodynamic and inertia loads completed early in the analysis phase showed that the aileron system was the most highly loaded control system in the T-33 airplane. Later refinements revised these loads downward so that the aileron loads are comparable with those on the rudder and elevator. The magnitudes of the various loads are listed in an earlier part of this report. Because of the high loads contemplated and the prospect of driving through cables, it was anticipated that most servo troubles would be encountered in the aileron system and it was decided to set up the test rig to represent the aileron servo and its loads.

At the time when the test rig and the test servo were being designed, the

Approved for Public Release

Contrails

most promising installation for the aileron servo appeared to be in the wing. The test servo was designed accordingly, and the test rig was set up to represent the loads imposed by a single aileron on its servo. When these designs were well under way it was decided that a single servo mounted in the center of the fuselage might be acceptable notwithstanding the cable compliance between the servo and the aileron. It was desired to test this configuration on the rig since the airplane installation offered many advantages. The rig was modified to include the effects of cable stretch between the servo and aileron and an arrangement worked out whereby the loads and the required piston area could be represented to proper scale. With the test servo and the rig, therefore, it was possible to simulate a single servo driving a single aileron directly and to simulate a fuselage-mounted servo driving one aileron (half-scale loads) or a fuselage-mounted servo driving both ailerons.

The wing mounted servo system requires two separate, independent servos driving the ailerons with a mechanical connection between them. When the two input signals, or the loads, are the same, the ailerons will move in unison and no loads will be required in the cable system. However, if the command signals or the external loads are different, then one servo must work in part against the other servo. No experience with this problem was available at Flight Research and it was decided that this problem should be checked on the test rig. The sketch on the following page shows two servos connected to the ailerons directly, and the two ailerons connected by the cables, k_c . The motion of the center point of the cables at the point where the booster operates is designated σ_b . Z_w is the impedance of the cockpit control stick. Consider, for example, the input signals, e_L and e_R . Any set of commands to the two servos can be broken down into two parts; one, a symmetrical component which is identical to each servo and, two, an anti-symmetrical part which is exactly opposite for each servo. Thus:

$$e_L = e_s + e_u \tag{183}$$

$$e_R = e_s - e_u \tag{184}$$

Approved for Public Release

Contrails

where

e_s = symmetrical component

e_u = unsymmetrical component

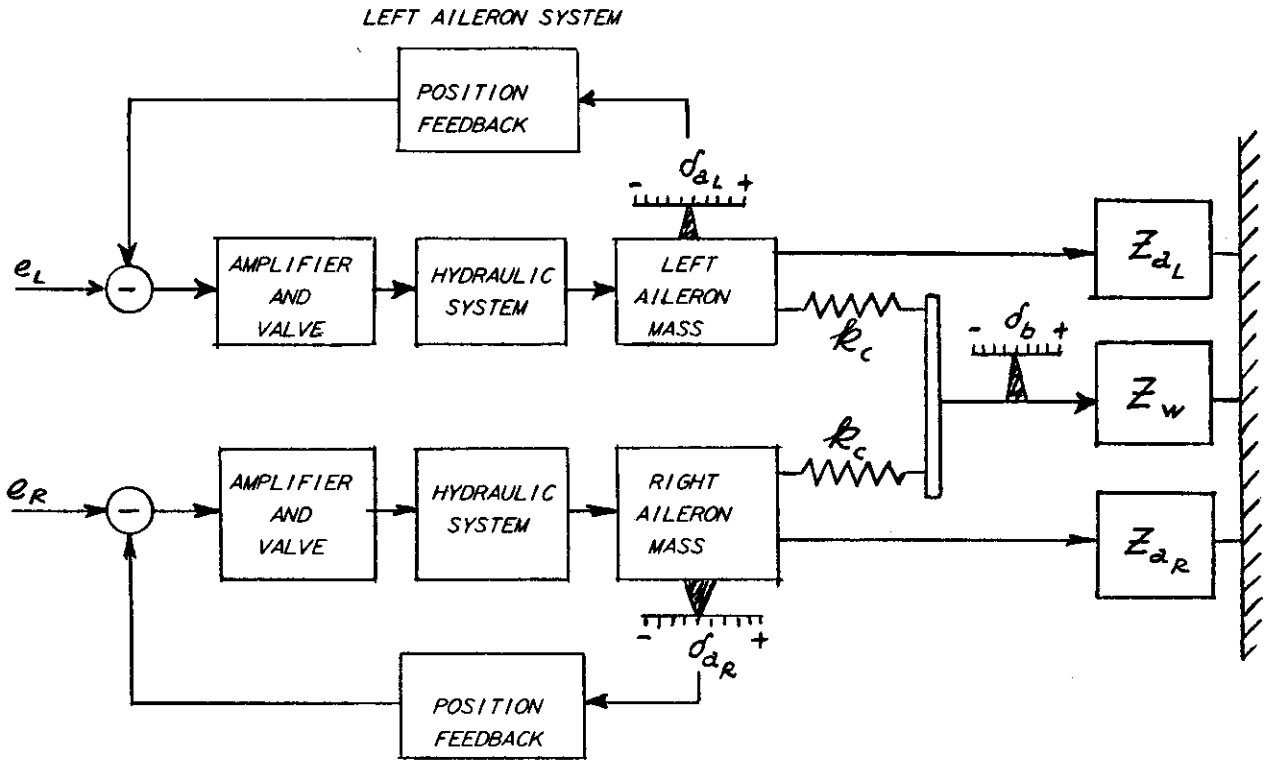

where: $\delta_{a_L}, \delta_{a_R}$ aileron position, left and right

δ_b position of center point of connecting cables

k_c stiffness of one-half cable system

Z_{a_L}, Z_{a_R} impedance of aileron and air loads, left and right

Z_w impedance of cockpit control stick

Schematic Diagram of Individual, Wing-Mounted Aileron Servos

Approved for Public Release

Contrails

Since linearity and superposition are assumed to prevail, it can be reasoned that if servo response to the symmetrical signals is adequate, and, of course, stable, and if the response to anti-symmetrical signals is at least stable, the resulting parallel operation of the servos should be satisfactory. The magnitude of the response to the unsymmetrical component of input signals is not particularly important. Further consideration of the anti-symmetrical case shows that there should be a motion node at δ_b , the center point on the interconnecting aileron cables; therefore, the servos respond individually as if each were trying to move its aileron with the center point of the cables locked. The cables then form a very stiff restraining spring and it was possible to simulate this spring on the test rig. The pilot's control does not move in response to anti-symmetrical signals, and hence, its inertia was deducted from the aileron system during these tests. For symmetrical signals there is no coupling between left and right systems, and each aileron carries half the stick impedance, Z_w , as seen through the cable spring, k_c . Values of numerical constants used in the test rig are tabulated in a later section.

TESTING PROCEDURE (POSITION SERVO)

A consolidated 16-channel oscillograph was used to record the test rig variables associated with servo performance. Referring to the block diagram of Figure 44, these were: (1) the position command signal, e_i ; (2) current in the servovalve coils, i_ϵ ; (3) servopiston position, δ_p ; and (4) control-surface position, δ_c . The servopiston position signal was obtained from the output of the linear-motion differential-transformer used for servo feedback, while control-surface position was measured by fixing a synchro to the aileron rocker arm as indicated in the photograph of Figure 55 which shows the test area. Signal attenuators were incorporated in each recording channel to provide an accurate means of adjusting the galvanometer trace deflections, and all the recording channels were adjusted so that the channels and the galvanometers had equal time lags, thus permitting a direct comparison of the recorded time histories. In general, system response to step inputs was utilized for rapid, qualitative testing while steady-state sinusoidal responses over the range from 2 to 30 cps were used for more complete analysis. Representative sinusoidal

Approved for Public Release

Contrails

oscillograms taken with the test rig appear in Figure 56 and recordings of step inputs are given in Figure 65. With the four variables itemized above, it was possible to obtain the servo response (δ_p/e_1), the over-all system response (δ_c/e_1), the position transmission (δ_c/δ_p) and the response of the combined valve and hydromechanical system (δ_p/i_e). From the latter response, the exact hydromechanical transfer function, $K_4\, G_4(\omega)$, could be obtained by dividing out the valve dynamics which were known from manufacturer's information.

The physical parameters of the test rig were calibrated prior to actual testing so that accurate calculations could be made to predict the test rig response from the servo theory. The torsional spring constants of the rods representing cable stiffness and air loads were determined by a series of static loads imposed by applying various differential pressures to the servopiston. The resonant frequencies of the masses on various combinations of the torsional springs were measured by recording the highly underdamped oscillations of the aileron mass following shock excitation. Three natural frequencies were measured for each configuration of the test rig, these being the frequencies associated with:

(1) the aileron mass on the combined linkage and air springs, or

$$\omega_{n_1} = \sqrt{\frac{k_\ell + k_a}{m_c}} \tag{185}$$

(2) the aileron mass on the air spring

$$\omega_{n_2} = \sqrt{\frac{k_a}{m_c}} \tag{186}$$

and (3) the aileron mass on the linkage spring

$$\omega_{n_3} = \sqrt{\frac{k_\ell}{m_c}} \tag{187}$$

Due to the inertia effect of the crank arms and connecting links of the test rig,

Approved for Public Release

Contrails

the effective aileron mass varies somewhat in each of the above expressions.

Next, the damping in the test rig was calculated from the recordings by measuring the logarithmic decrement of succeeding peak amplitudes. This inherent damping was, then, the test rig equivalent of the actual control-surface damping during ground operation and would be written

$$\zeta_3 = \frac{1}{2} \frac{c_g}{\sqrt{k_\ell m_c}} \tag{188}$$

It was realized that ζ_3 for the test rig would be somewhat less than the actual damping ratio encountered with the airplane servo system, since in the airplane there would be appreciable aerodynamic damping due to motion of the control surface. To represent the damping effect of heavy air loads, a by-passed hydraulic piston was connected to the aileron load arm. The damping force of this piston could be controlled by varying the viscosity of the oil which filled the piston and by-pass line, but the damping force was non-linear with piston rate of travel. The damping action of the piston was calibrated in a separate series of tests in which the force and position of the piston rod were recorded for various sinusoidal displacement frequencies and amplitudes. Then, to represent the damping force analytically, empirical equations were derived by curve fitting which express the damping force in terms of aileron displacement and frequency. The radius arm of the damping piston was selected so that with an aileron frequency-amplitude product of 50 inch-cycles/second the required damping force would be obtained. With the by-passed piston connected to the aileron load arm, the damping ratios associated with ω_{n_1} and ω_{n_2} were calculated from the expressions that follow:

$$\zeta_1 = \frac{1}{2} \frac{c_a}{\sqrt{(k_\ell + k_a) m_c}} \tag{189}$$

$$\zeta_2 = \frac{1}{2} \frac{c_a}{\sqrt{k_a m_c}} \tag{190}$$

Approved for Public Release

A summary of the values of spring rates, natural frequencies, and damping ratios measured for the test rig in each configuration is given in Table XVII.

To complete the calibration of the test rig, it was necessary to measure the static gains of the servo components and compute the maximum servoloop gain, K_V. The maximum servoamplifier gain was measured directly in terms of current in the valve coils per unit RMS signal voltage applied to the mixer, $K_2 = \left|\frac{i_\epsilon}{e_\epsilon}\right|_{ss} = 0.72 \ \frac{ma}{mv}$. A plot of the servovalve static sensitivity was obtained from the valve manufacturer and, knowing the servo-piston area ($A = 2.76$ in.^{2}), the constant K_3 could be computed

$$K_3 = \left|\frac{\dot{\delta}_o}{i_\epsilon}\right|_{ss} = \frac{K_{VAL}}{A} = \frac{6.25}{2.76} = 2.26 \ \frac{in/sec}{ma}$$

For simulation of ground operation, the hydromechanical position transfer is $K_4 = \left|\frac{\delta_p}{\delta_o}\right|_{ss} = 1$. Next, the position feedback constant was measured by actual displacement of the servopiston, giving $K_5 = \left|\frac{e_2}{\delta_p}\right|_{ss} = 73.5 \ \frac{mv}{in}$. The product of these static gains is the maximum servoloop gain, so

$$K_V = K_2 K_3 K_4 K_5 = 119.5 \ sec^{-1},$$

and lower loop gains were obtained by adjusting the calibrated attenuator at the servoamplifier input.

COMPARISON OF THEORY AND TEST RESULTS (POSITION SERVO)

A primary purpose of the test rig program was to verify the servo theory which had been formulated to aid servo design and to predict servo performance. A direct method of verifying the theory was to calculate the system response for a specific configuration of the test rig, then measure the actual response on the

Approved for Public Release

test rig and compare the calculated and measured responses. These calculations were performed for the test rig configuration representing a fuselage servo operating with half-scale loads and a summary of this servoanalysis will now be presented.

The method of solving for the over-all response of the aileron to a command signal is first to account for the servoloop dynamics, then solve for the closed-loop servo response for a specific loop gain and, finally, compute the aileron response from the servo response and the known physical parameters of the aileron, the aileron loads, and the connecting linkages.

The dynamic response of the servoamplifier was measured by sinusoidal tests, then these dynamics were approximated by a first-order time constant. A plot of the measured and assumed amplifier dynamics ($\tau_2 = 0.0032$ seconds) is given in Figure 57. Next, the servovalve dynamics were obtained from the valve manufacturer for valve operation at 1000 psi. The only information available was the amplitude response and the frequency for which the phase lag in flow output with respect to current input was 90 degrees. The valve response is very similar to a typical overdamped, second-order response with a natural frequency of about 75 cps. In the lower frequency region (to 30 cps) these dynamics can be approximated by a first-order lag with a turnover frequency of 29 cps ($\tau_3 = 0.0055$ seconds). A plot of actual and assumed dynamics for the servovalve appear in Figure 58. The remaining servoloop component with appreciable dynamics is the hydromechanical system relating the servopiston position to the equivalent displacement of fluid from the valve ($G_4(\omega)$). Equations have been derived which express $G_4(\omega)$ in terms of various hydraulic effects and the servo load impedance (equations (144) and (145)). But to evaluate $G_4(\omega)$ from these equations it is first necessary to compute the load impedance function Z_p. Expressions have been presented in a previous section for the impedance function; however, these expressions can be expanded in terms of the natural frequencies and damping ratios defined by equations (185) through (190), and in this form are more easily evaluated from the physical constants measured on the test rig. These expressions for the servo load impedance are:

Approved for Public Release

Contrails

$$Z_{p_a}(j\omega) = \left(\frac{F_p}{\delta_p}\right)_a (j\omega) = k_{al}\left[\frac{1-\left(\frac{\omega}{\omega_{n_2}}\right)^2 + 2j\zeta_2\left(\frac{\omega}{\omega_{n_2}}\right)}{1-\left(\frac{\omega}{\omega_{n_1}}\right)^2 + 2j\zeta_1\left(\frac{\omega}{\omega_{n_1}}\right)}\right] \text{ (lb/in)} \quad (191)$$

and

$$Z_{p_g}(j\omega) = \left(\frac{F_p}{\delta_p}\right)_g (j\omega) = k_\ell\left\{1-\left[\frac{1}{1-\left(\frac{\omega}{\omega_{n_3}}\right)^2 + 2j\zeta_3\left(\frac{\omega}{\omega_{n_3}}\right)}\right]\right\} \text{ (lb/in)} \quad (192)$$

where

$$k_{al} = \frac{k_a k_\ell}{k_a + k_\ell} \quad (193)$$

Equations (181) and (192) were evaluated for the half-scale loads on the fuselage servo and the results have been plotted in Figure 59.

The loads imposed on the servo are reflected inside the servoloop through the characteristics of the hydraulic system and by the pressure response of the servovalve. If the valve response is assumed independent of load pressure, then equation (144) relating δ_p to δ_0 in terms of the servo load impedance accounts for the change in servo dynamics with load. The servopiston used in the test rig has a preloaded "O"-ring seal which reduces leakage across the piston to negligible amounts, so we may use the simplified expression for (δ_p / δ_0) given in equation (145). Rewriting equation (145)

$$\left(\frac{\delta_p}{\delta_0}\right)(j\omega) = \left[\frac{1}{1 + j\omega\tau_4 + \frac{Z_p}{k_s}}\right] \quad (194)$$

it is seen that the servo loads are reflected by the ratio (Z_p/k_s). We can compute k_s for the test rig servo from equation (146) as

Approved for Public Release

$$k_s = \frac{4BA}{\delta_{p_{max}}}\eta = \frac{4 \times 0.27 \times 10^6 \times 2.76}{4.4} \times 0.95 = 643 \times 10^3 \quad lb/in$$

The maximum reflected load will occur at the high resonant peak of Z_{pg} and the ratio (Z_p/k_s) at this peak will be

$$\left|\frac{Z_{pg}}{k_s}\right|_{22\,cps} = \frac{16.7 \times 5270}{643 \times 10^3} = 0.137$$

which will be nearly 90 degrees leading. For other frequencies the servo load impedance falls rapidly to values much below this peak, so throughout most of the frequency range the reflected load is negligible. From the sinusoidal data taken with the test rig, the response (δ_p/δ_0) was obtained, and from this data it appeared the hydraulic time constant, τ_4, was about 0.003 seconds. Using this value for τ_4, the response (δ_p/δ_0) was calculated, taking into effect the reflected load. Plots of measured and assumed dynamics for the response (δ_p/δ_0) appear in Figure 60. Scatter of the measured phase angle data is the result of inaccuracies in the recording techniques, largely because it was not practical to measure flow from the valve directly.

Now, summarizing the calculated servoloop dynamics, we have

$$K_2 G_2(j\omega) = 0.72\left(\frac{1}{1+0.0032j\omega}\right) \frac{ma}{mv} \qquad (195)$$

$$K_3 G_3(j\omega) = \frac{2.26}{j\omega}\left(\frac{1}{1+0.0055j\omega}\right) \frac{in/sec}{ma} \qquad (196)$$

$$K_4 G_4(j\omega) = \left(\frac{1}{1+0.003j\omega+\frac{Z_p}{643\times10^3}}\right) \text{ in./in.} \qquad (197)$$

$$K_5 = 73.5 \text{ mv/in.} \qquad (198)$$

Approved for Public Release

Contrails

The product of these terms can be evaluated and the result presented as an inverse polar plot as given in Figure 61. It is seen from Figure 61 that the difference in servo loads between ground and air operation causes little change in the servoloop dynamics, due to the small reflected loads. The scale of the inverse plot has the dimensions of loop gain, K_V , and an operating point is established on the inverse plot by setting the servoloop gain. A simple graphical manipulation then transforms the open-loop dynamics to the closed-loop servo response. The closed-loop dynamics for a servoloop gain of 50 sec^{-1} were computed from Figure 61 and the result is plotted in Figure 62. Actual servo response obtained from sinusoidal data has also been plotted in Figure 62. The next step in evaluating the over-all system response is the calculation of the position transmission ratio between the aileron and the servo-piston for both ground and air operation. This transmission ratio may be re-written in terms of the natural frequencies and damping ratios measured on the test rig as:

$$T_g(j\omega) = \left(\frac{\delta_c}{\delta_p}\right)(j\omega) = \left[\frac{1}{1-\left(\frac{\omega}{\omega_{n_3}}\right)^2 + 2j\zeta_3\left(\frac{\omega}{\omega_{n_3}}\right)}\right] \qquad (199)$$

$$T_a(j\omega) = \left(\frac{\delta_c}{\delta_p}\right)_a(j\omega) = \left(\frac{k_{a1}}{k_a}\right)\left[\frac{1}{1-\left(\frac{\omega}{\omega_{n_1}}\right)^2 + 2j\zeta_1\left(\frac{\omega}{\omega_{n_1}}\right)}\right] \qquad (200)$$

and when the constants for the fuselage servo operating at half-scale loads have been substituted into equations (199) and (200), the responses plotted in Figure 63 result. Measured test data have been plotted in Figure 63 for comparison.

The over-all response of the aileron to an electrical command signal can be calculated by combining the data of the servoloop response and transmission ratio. The calculated and measured aileron responses during both ground and air operation are presented in Figure 64.

The over-all response of the test rig simulating ground operation shows a

Approved for Public Release

Contrails

high resonant peak near the natural frequency of the aileron inertia and the linkage stiffness. This peak is the result of very low damping present in the test rig ($\zeta_3^e = 0.03$) and with the actual airplane system operating on the ground, the damping would be somewhat heavier (est. $\zeta_3^e = 0.1$) due to friction and aerodynamic damping due to motion of the control surfaces. With this increased damping the resonant peak would be reduced to below 1.5.

The dynamic response of the aileron system in the frequency range to 15 cps can be controlled quite readily by adjusting the servoloop gain, as the dynamics of the transmission ratio are not appreciable in this lower frequency range. So, the frequency at which the over-all response has a phase lag of 90 degrees is determined largely by the servoloop gain. The effect of changes in K_v can be visualized from the open-loop plot of Figure 61. It can be seen that as the loop gain is increased, the frequency for which there is 90 degrees phase shift is also increased, but with loop gains much above 75 sec^{-1}, a resonance will develop in the servo response near 15 cps. This effect is noticeable in the step response oscillograms taken with K_v equal to 25, 50, and 100 sec^{-1} shown in Figure 65.

Another consequence of changes in loop gain is the change in system resolution. The loop gain necessary to give the required servoloop resolution can be computed from equation (147), which is

$$K_v = \frac{\epsilon \dot{\delta}_{p_{max}}}{\delta_{p_\epsilon}} \qquad (201)$$

The maximum servopiston rate of travel ($\dot{\delta}_{p_{max}}$) is determined by the capacity of the servovalve, and for the test rig is

$$\dot{\delta}_{p_{max}} = \frac{\dot{\delta}_{o_{max}}}{A} = \frac{26}{2.76} = 9.43 \text{ in/sec}$$

With $K_v = 50$ sec^{-1} and assuming the servovalve has a threshold response of 1%, the servopiston resolution would be

Approved for Public Release

$$\delta_{p_\epsilon} = \frac{\epsilon \delta_{p_{max}}}{K_v} = \frac{0.01 \times 9.43}{50} = 0.0019 \text{ in.}$$

The actual resolution of the test rig servo with $K_v = 50 \text{ sec}^{-1}$ was measured at 0.0038 inch which indicates the valve threshold response is closer to 2%.

POSITION SERVO TEST RESULTS WITH VARIOUS TEST RIG CONFIGURATIONS

From studying the detailed comparison of the servo theory and the measured system performance just presented, it can be seen that actual system behavior can be predicted quite satisfactorily from analytical expressions. Having justified the validity of the servo theory it is then possible to synthesize servo systems with the assurance that the desired response characteristics will be achieved. However, the process of synthesizing complete servo systems is quite laborious and for this reason the test rig was made sufficiently flexible so that a number of servo configurations could be investigated. For each test configuration both step and sinusoidal responses were obtained along with stability and resolution information.

The over-all response measured on the test rig for simulation of a fuselage servo operating under full-scale loads is presented in Figure 66 for both ground and air operation. The high resonant peak measured near 15 cps during ground operation is the highly undamped inertia-spring combination representing the ailerons and drive cables ($\omega_{n_3} = 15.6$ cps; $\zeta_3 = 0.04$). Also, the steady-state amplitude ratio for air operation shows the cable stretch when the ailerons are restrained by heavy air loads. The servo response did not deteriorate with the increased loading of these tests, as the servo has been designed to be relatively insensitive to external loads.

Another phase of the aileron servo test-rig studies was the investigation of the characteristics of a wing-mounted servo driving one aileron. A complete program of testing was conducted for simulation of this servo and the measured over-all response of the aileron in each test configuration is shown in Figure 67. By eliminating the cable drive, the response of the aileron approaches that of the servopiston and is more easily controlled. The response of the

Approved for Public Release

Contrails

servo to symmetrical loads (no interaction between the two aileron servos) is free from resonances and the over-all phase shift is just that of the servoloop. To investigate the possibility of instability due to interaction between the two aileron servos, the coupling between the servos was duplicated on the test rig. The servo response while operating with maximum coupling (unsymmetrical command signals) has been plotted in Figure 67 and it is seen that no stability problems are present.

ADDITIONAL TESTS

Several additional tests, applicable to all position servos, were completed with the test rig. One such test was the addition of rate feedback from the servopiston to stabilize the servo for operation with high loop gains. Physically, rate feedback was obtained by fixing a translational rate generator to the servopiston. The rate signal was used to modulate a suppressed carrier which was added to the position feedback signal at the mixer amplifier. An attenuator was included in the rate feedback path so the feedback time constant, τ_s could be varied. Addition of the rate feedback from the servopiston provides a direct method of increasing the damping of the servopiston. A series of step oscillograms are given in Figure 68 which demonstrates the effectiveness of this damping. The steps of Figure 68 were all taken with a servoloop gain of $K_v = 100\ \text{sec}^{-1}$, but with increasing values of rate feedback.

Another electrical change which was tried was the use of a complex position feedback signal from both the servopiston and the aileron. The two position signals were mixed in a crossover network which passed low frequency information from the aileron and higher frequency information from the servopiston. By adjusting the crossover frequency to about 10 cps, the aileron position feedback was only effective in the low frequency range where the effect of cable compliance within the servoloop would not reflect the resonant frequency of the load. A breadboard setup of the crossover circuitry was made and preliminary testing was completed; however, there was insufficient time available to investigate all aspects of the modification. If it is desirable to reduce the effect of cable stretch in the position servos during flight operation, complex position feedback appears to be a possible solution.

Approved for Public Release

Contrails

A short test which was completed was a study of the effect of increased hydraulic compliance between the valve and servopiston. Three feet of 3/8 inch flexible lines were teed to each passage between the valve and piston in the valve manifold, then a series of stability tests were conducted on the servo under various load configurations. All tests were successful which indicates that the servovalve and actuating piston may be separated distances up to three feet without introducing enough additional hydraulic compliance to be objectionable.

HYDRAULIC PRESSURE LIMITING CIRCUITS

Some thought has been given to the problem of limiting the force output of the hydraulic servos used for operating the flight control surfaces. It has been shown,by theoretical considerations and supported by tests reported above, that good dynamic servo performance can be obtained by unloading the servo, which means that normal operation requires only a fraction of the maximum force available from the hydraulic actuators. For reasons of safety, it then becomes necessary to limit the maximum differential hydraulic pressure which can occur across any of the servopistons to a fraction of the supply pressure. Another function which must be considered is the provision for by-passing the servo-actuator completely when the servo system is not in action, so that manual control of the airplane is possible. This requirement is actually a limit approached when the allowable differential pressure in the servoactuator is reduced to zero.

Several methods of providing these auxiliary hydraulic functions have been used in the past and will be summarized here for possible use in the T-33. The C-45 and the F-86 systems both use specially modified check valves to limit differential servo pressures. The C-45 system used a specially modified, solenoid by-pass valve while the F-86 system used a different, special by-pass valve. A new hydraulic circuit, using standard components, has been devised for performing the by-pass functions outlined above. Schematic diagrams of the three pressure-limiting systems appear in Figure 69. Where the servo system is critical to excess oil volume or flexible hose compliance, this new system can probably be installed with the least added oil volume and hose within the servoloop. Tests have been run to check the pressure-limiting action of the

Approved for Public Release

Contrails

new hydraulic circuit and it was found that, within the flow capacity of the check and relief valves, the setup will limit the differential pressure across the servopiston to the pressure setting of the relief valve plus the preload pressure of two check valves.

A sample oscillogram is given in Figure 70 to illustrate the action of the circuit. For this test, the relief valve pressure was zero (valve removed) to represent by-passed operation as required to move the control surface manually. In this case, a sinusoidal signal was fed into the servoloop, and since the feedback did not cancel the input, the valve was sending full rated flow through the servo and check valves, during much of the input cycle. With no signal to the servovalve, manual motion of the aileron was possible, but the back-pressure caused by the check valve springs was undesirable. Operation will also be tried with check-valve springs removed.

I. FEEL SERVO TESTS

Two approaches to the feel servo design are discussed under the section on theory. Both systems were considered at the outset of the program, but one had to be selected for the tests included in Phase I. The choice was made for the force type servo for the following reasons:

1. The analogy between the servo and the physical spring which it is simulating is more clearly seen for the force type than for the position type servo.
2. Theories of operation indicated better stability at higher gains for the force type servo.
3. Theories for the position type servo were known to be incomplete since they did not predict the instability observed in previous systems when the simulated spring rate was made very low.
4. Auxiliary computing equipment for producing the desired feel and the proper control-surface deflection signal was about the same for the two types.
5. Open-loop operation of the force type servo seemed a good possibility.

It was decided to set up and test the force-type feel servo, but also to keep the test rig and auxiliary equipment as flexible as possible so that a position-

Approved for Public Release

Contrails

type servo could also be rigged up and tested should results prove unfavorable for the force servo.

FEEL SERVO TEST RIG

A feel servo test-rig simulating elevator control-motion was designed for testing either a force or a position type servo. The servo stability problems with the elevator controls are most stringent as the full inertia effect of the control wheel forms a load on the servo. The salient features of the feel servo test-rig can be seen from the photo of Figure 71. In the photo, the normal wheel-type control is in place; however, a stick-type control can be duplicated by removing the wheel assembly. Also, a socket is provided at the base of the control column in the test rig so that columns of various stiffnesses may be used. The column is driven by the piston crank-arm through a short torsion bar which duplicates flexibility between the servopiston and the control column. Provisions have been made at the crank arm for mounting servopistons suitable for either a force or a position type servo. Stick position is measured by a synchro which is located at the base of the control column. Stick force is sensed by strain gages which are oriented to measure torsion in the drive bar between the base of the column and the piston crank. A Cadillac Gage Co., Model PC-2 pressure-control servovalve is used in the force servo, and the hydraulic supply pressure to the servo is 1000 psi. To protect the servo valve, both a micronic and a magnetic filter have been plumbed into the supply line. A stationary member is located at the front of the test rig to provide a foot rest and a pulley support for dead-weight calibration of stick force.

The design parameters of the feel servo test-rig set up for a force servo system are on the following page:

Approved for Public Release

Contrails

NOMINAL STICK RADIUS TO WHEEL	21.2 IN.
WHEEL WEIGHT	5 LB
EFFECTIVE INERTIA OF WHEEL AND COLUMN	3380 LB-IN.^{2}
COLUMN STIFFNESS	250 LB/IN. AT WHEEL
TORSIONAL DRIVE STIFFNESS	38.5 x 10^4 IN.LB/RAD
RESONANT FREQUENCY OF INERTIA ON COLUMN STIFFNESS	113 RAD/SEC = 18 CPS
RESONANT FREQUENCY OF INERTIA ON STIFFNESS OF COLUMN AND DRIVE IN SERIES	100 RAD/SEC = 15.9 CPS

For the force servo, two single-acting pistons were used to drive the stick. The rod-sides of the pistons were plumbed together and the opposite ends of the pistons were connected to the servovalve (see Figure 71). The piston area is 0.786 in.^{2} and the radius of application of piston force was chosen so that a force of 200 pounds could be developed at the wheel for full 1000 psi differential pressure (maximum valve current). This radius is 5.4 inches. The maximum anticipated control rate of travel is 100 deg/sec (37 in/sec at wheel) and to furnish this stick velocity the valve flow capacity must be 7.4 in.^{3}/sec.

A functional diagram of the force servo is given in the sketch on the following page.

Approved for Public Release

Contrails

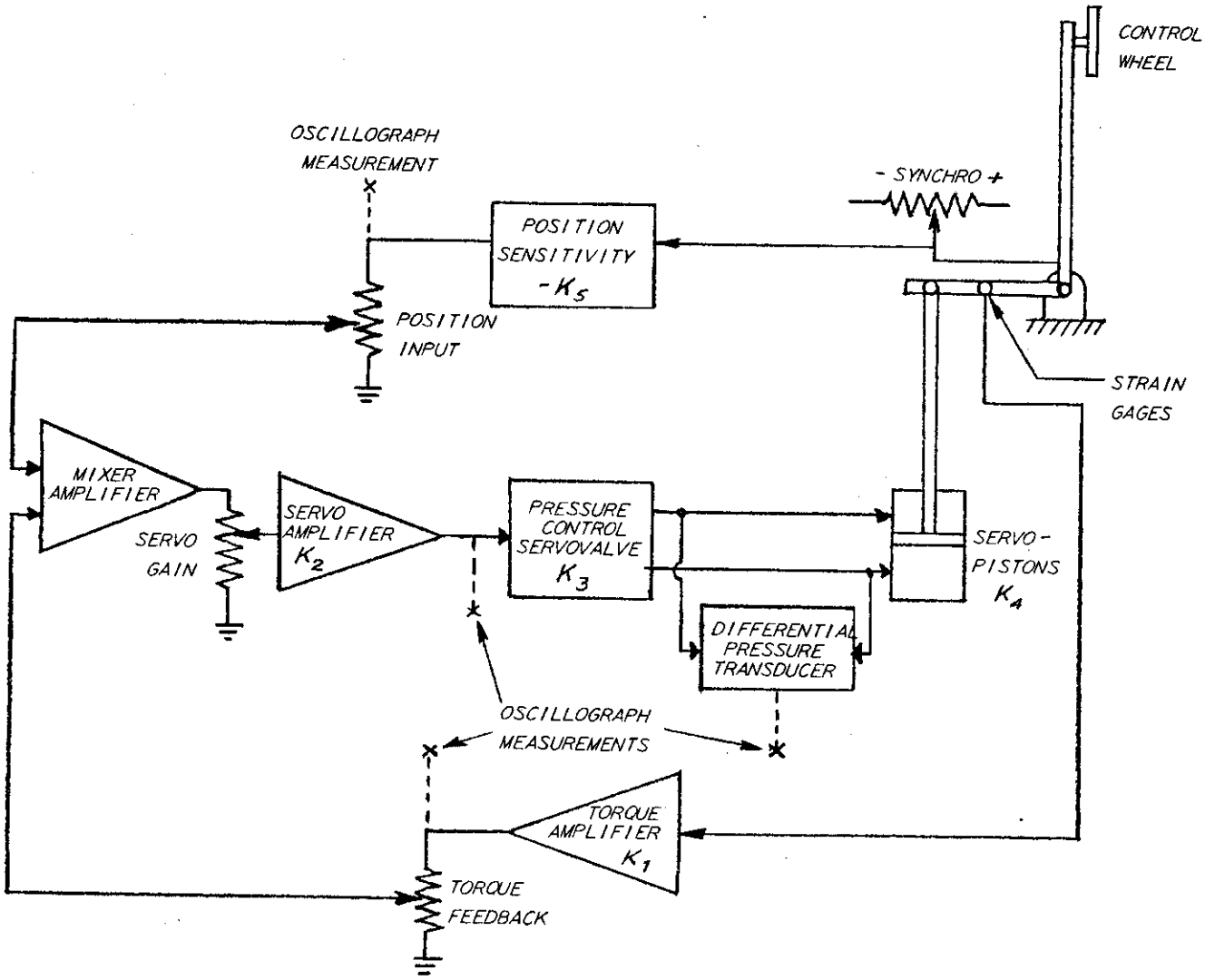

Feel Servo with Pressure Control Servovalve

The apparent steady-state stiffness of the servo can be estimated from equation (159) if we assume the open-loop gain is large with respect to one. From equation (159) we find

$$\left| \frac{F_w}{d_w} \right|_{ss} = \frac{K_5/K_1}{1 + \frac{K_5/K_1}{k_c}} \quad (lb/in.) \qquad (202)$$

Approved for Public Release

Contrails

which is the equivalent series stiffness of the column and the servo. The static gains of the amplifiers shown in the sketch were designed to furnish a maximum loop gain of about 50 and a maximum servo stiffness of approximately 100 lb/in at the wheel. The calibrated gains measured on the test rig are as follows:

K_1 = torque feedback sensitivity 0.054 mv/in. lb maximum or 0.29 mv/lb at servo or 1.15 mv/lb at wheel

K_2 = servoamplifier gain 0.70 ma/mv maximum

K_3 = servovalve sensitivity 250 psi/ma

K_4 = servopiston area 0.786 in^2

K_5 = position sensitivity 42.0 mv/deg maximum or 113 mv/in at wheel

So, with the test rig, the maximum servoloop gain is

$$K_0 = K_1 K_2 K_3 K_4 = 40.0 \text{ (non-dimensional)}$$

and the maximum stick stiffness is (from equation (202))

$$\left|\frac{F_w}{\delta_w}\right|_{ss} = \frac{113/1.15}{1 + \frac{113/1.15}{250}} = 70 \text{ lb/in}$$

with full torque feedback. Higher stiffnesses were obtained by increasing the excitation voltage of the synchro position pickoff or by reducing the torque feedback (which reduces the maximum loop gain).

TEST PROCEDURE

A consolidated oscillograph was used to measure the dynamics of the feel servo, and the variables which were recorded are (1) stick position input to the servo, from the synchro output, (2) stick force feedback, obtained at the output of the strain gage amplifier, (3) servovalve current, and (4) differential pressure across the servopistons, from a Statham differential pressure transducer. Calibrated attenuators were inserted in each oscillograph channel so that the trace deflections could be adjusted conveniently.

Approved for Public Release

Contrails

Two quantitative testing techniques were employed to obtain information on the performance of the feel servo with the pressure-control servovalve. These are (1) open-loop sinusoidal testing to obtain the transfer functions of the servo components, and, (2) step force inputs to the stick to obtain the closed-loop response of the feel servo. The step inputs were obtained by wedging a wooden block between the seat and the stick or between the stationary column and the stick, so that the control wheel was displaced from its neutral position against the restoring torque of the servo. The wedge was suddenly removed by a hammer blow, furnishing a step release of stick force.

FEEL SERVO TEST RESULTS

The test servo was started and run for several hours to familiarize people with its behavior. A number of qualitative observations were first made.

1. It was seen immediately that servoloop gain around the torque feedback loop could not be made even moderately high without instability, regardless of the stiffness adjustment. The stability equations for the pressure control servo (equations (164) and (165)) predicted the approach of instability only as the servo stiffness adjustment was made high with respect to the mechanical stiffness of the stick. Thus, the observed instability came from some source not included in the theoretical analysis.
2. When the servo stiffness setting was increased, with the torque feedback set at a low, stable value, it was noted that the servo stability decreased until at a servo stiffness of 110 lb/in (column stiffness 250 lb/in), oscillations were sustained. Theory in equations (164) and (165) predicted instability at a stiffness ratio of about unity.
3. One of the recordings of system operation with both torque feedback and the position input signals disconnected showed that the pressure output contained small oscillations at a high frequency not found in the input electrical signal.
4. The very moderate useable torque feedback loop gain was effective in eliminating the friction between the valve pressure output and the control stick. This friction was objectionable for open-loop operation.

Approved for Public Release

Contrails

5. With loop gain set to a stable value, a useful range of simulated stick stiffness could be covered, and as far as manual operation was concerned, the dynamic and static characteristics of the feel servo were adequate.

Additional tests are planned for the feel test-rig and only preliminary information obtained from the initial tests is available for inclusion in this report. The torque servoloop as initially set up was found to be unstable with loop gains over $K_0 = 2$ (non-dimensional). Several methods of servo stabilization were attempted, including the use of corrective networks in the torque feedback path. A certain amount of success was obtained with low-pass filters in the torque circuit and several tests were completed on the servo in this configuration. With the filter network, loop gains of 10 were possible; however, at this value of loop gain there was considerable trouble with noise pickup which made the stick twitch erratically. A series of tests was completed with the torque loop-gain reduced to 2. It was found that the servo stiffness could be varied from near zero lb/in to 100 lb/in, but at 120 lb/in the servo was unstable following large step inputs. Oscillograph recordings of step inputs at various stiffnesses are reproduced in Figure 72. The force-position relationship at the wheel (expressed by equation (159) will have a natural frequency determined by the stiffness introduced by the servo, being zero at zero stiffness and approaching the natural frequency of the wheel and column inertia and the column stiffness (calculated 18 cps) at high servo stiffness. The frequency response of the stick position to force relationship (position measured at the base of the column) was determined from the step responses of Figure 72 and these are given in Figure 73. The servo natural frequency, which is concerned with the torque to signal input relationship at the servo, is independent of the position sensitivity and determined only by the dynamics of the servoloop and load and the servoloop gain.

The existence of a system instability not associated with the servo stiffness setting indicates that something was neglected in the analysis, and it is planned to include next the flow response of the pressure control valve. The effect will be introduced into the theory as in equation (154), and a test program will be set up to evaluate K_6 and G_6 of equation (154).

Approved for Public Release

Contrails

SECTION X

SUMMARY OF RESULTS AND CONCLUSIONS

A method by which the T-33 can simulate the longitudinal short-period motion of another airplane has been worked out. The transient response of both normal acceleration and pitching velocity can be simulated, but to the extent that true speed is not matched, there will be some compromise between simulating steady-state normal acceleration and steady-state pitching velocity. The method allows for control system dynamics. Analytic studies and studies made on an EASE analog computer were used to determine the maximum allowable lag in the control system. The control system is being designed to have no more lag than a second order system with an undamped natural frequency of 7.5 cps and a damping ratio of 0.7.

A method has likewise been worked out for simulating the lateral modes of motion. Term by term simulation of the rolling and yawing moment equations can be achieved. Simulation of the side-force equation will generally not be exact, but the effects of this are expected to be small except for the spiral mode. The spiral mode tends to come out too fast if the test airplane true speed is low, and vice versa. The method again allows for control system dynamics. The same requirements on control system lag as mentioned above for the longitudinal case have been chosen for design of the aileron and rudder control systems.

The phugoid period and damping will be controlled by use of an auxiliary surface driven by an electric servo.

Methods have been worked out and functional block diagrams drawn for the simulation of control systems. Feel servos will provide variable stick and pedal force characteristics. Suitable channels with variable gains are provided for sending control signals of the right magnitude from the cockpit controls to the control surface servos. The principles used follow from previous related work done by this laboratory.

Two methods of automatic turn coordination have been worked out and

Approved for Public Release

Controls

checked on the EASE analog computer. The control system is designed so that either method can be tested.

A computing circuit has been laid out for providing the incremental elevator angle required to maintain altitude in turns.

A proportional bank system, providing a steady bank angle proportional to lateral stick displacement, has been designed and checked on the EASE analog computer.

Design information for the control system has been compiled and is presented in Section VI.

Functional block diagrams have been developed for the control system. Consistent with these, an electrical block diagram has been drawn. This diagram shows the major components in the computing and gain control section of the control system, and shows their interconnections.

Bench tests have been run on a position transducer, the auxiliary surface servo, a phase shifter, and a chopper differentiator. These tests have been generally satisfactory and have provided needed design information. Some work was done on transistor amplifiers with some promising results, but it was decided that it would be unwise to undertake any large-scale application of transistors to this control system.

Selections of end instruments have been made and specifications worked out for several computing sub-systems which may be subcontracted.

A layout has been made for installing the elevator servo in the plenum chamber ahead of the engine.

A layout has also been made for installing the rudder servo in the engine compartment. Some checking is still needed to be sure that the cable connection from this point aft will be sufficiently stiff.

An installation of a single aileron servo located at the airplane centerline has been laid out. An alternate installation has been laid out using two servos located in the wings just ahead of the ailerons. The former layout has several practical advantages, but the choice will depend also on analysis of the servo test rig results and further consideration of the effect of cable stretch on the rolling performance of the test airplane. The possible effect on flutter characteristics is also to be considered.

Approved for Public Release

Layouts have been made for the test cockpit control installations, including the feel servos. The interchangeable wheel and stick arrangement has been laid out.

Analysis and design methods have been worked out for designing the control surface servos to give the desired performance with relatively little dependence on load effects. Using these methods, a test servo was designed, built, and set up in a test rig. Very good results were obtained from the test program. The experimental results checked very well with predictions, thus verifying the theory and design methods used. The performance of the test servo was excellent and met the design requirements of the T-33 control system.

Analysis and design methods have similarly been developed for the feel servos. A feel servo test rig, based on use of a pressure-control servo valve, was set up and tested. Good results were obtained, although it became clear that the system as set up could be improved in several respects. More test work is needed to verify the theory of this type of servo. It was demonstrated, however, that the basic principle is sound and workable. An alternate type of feel servo, used in earlier programs, employs an ordinary flow-control servo valve. This type has been analyzed and considered for the T-33 system. The pressure-control system appears advantageous, however, particularly from the point of view of feel system dynamic stability. The present decision is to use the pressure-control valve.

In general, the T-33 appears to be a suitable airplane for the purposes of this program. Methods have been developed by which the T-33 can be made to simulate the handling characteristics of various fighter aircraft. The principles of operation of a special control system which will accomplish this task have been established. It has been found practical to extend the capabilities of this system to permit flight research in the design and function of cockpit controls. The control system has been laid out in general, and preliminary design work has been carried out to develop the methods and data required for detailed design. Layouts of the mechanical installation have been made. Block diagrams have been drawn and workable approaches found to the various

Approved for Public Release

Contrails

instrumentation and electronic problems. The servo analysis and test program has established a sound basis for designing and building the control system servos. It is believed that the purposes of Phase I have been accomplished and that the design, fabrication, and installation of the required control system can proceed with confidence.

Approved for Public Release

Contrails

REFERENCES

1. Newell, F. D. A STANDARIZED SET OF SYMBOLS, NOTATION AND EQUATIONS OF MOTION TO BE USED IN C. A. L. FLIGHT RESEARCH REPORTS. Cornell Aeronautical Laboratory Flight Research Memorandum 161 29 August 1952
2. Heilenday, F. W. and Campbell, G. ARTIFICIAL STABILITY AND CONTROL OF LONGITUDINAL MOTION OF THE F-94 AIRCRAFT - THEORETICAL INVESTIGATION. Wright Air Development Center Technical Report 52-248, Cornell Aeronautical Laboratory Report TB-757-F-7 October 1952
3. Heilenday, F. W. and Campbell, G. ARTIFICIAL STABILITY AND CONTROL OF LONGITUDINAL MOTION OF THE B-26 AIRCRAFT - THEORETICAL INVESTIGATION. United States Air Force Technical Report 6703, Cornell Aeronautical Laboratory Report TB-757-F-2 November 1951
4. Mayer, J. P., Hamer, H. A., and Huss, C. R. A STUDY OF THE USE OF CONTROLS AND THE RESULTING AIRPLANE RESPONSE DURING SERVICE TRAINING OPERATIONS OF FOUR JET FIGHTER AIRPLANES. National Advisory Committee for Aeronautics Research Memorandum RM L53L28 22 June 1954 (Confidential)
5. Notess, C. B. AN ANALYSIS OF ACCURACY REQUIREMENTS FOR INERTIA CHARACTERISTICS USED IN AIRCRAFT RESPONSE CALCULATIONS. Cornell Aeronautical Laboratory Flight Research Memorandum 171 23 March 1953
6. Kidd, E. A. ARTIFICIAL STABILITY INSTALLATIONS IN B-26 AND F-94 AIRCRAFT. Wright Air Development Center Technical Report 54-441, Cornell Aeronautical Laboratory Report TB-757-F-9 September 1954
7. Deazley, W. and Kidder, R. HELICOPTER HANDLING QUALITIES INVESTIGATION, PHASE III - INSTRUMENTATION AND DATA ANALYSIS. Cornell Aeronautical Laboratory Report TB-707-S-3 10 February 1954 (Confidential)

Approved for Public Release

Contrails

8. Kollsman Instrument Division. 1954 EDITION OF KOLLSMAN INSTRUMENT MANUAL. (1954)

9. Smilg, B. and Wasserman, L. APPLICATION OF THREE-DIMENSIONAL FLUTTER THEORY TO AIRCRAFT STRUCTURES. Armed Forces Technical Report 4798 8 July 1942

10. Thayer, W. J. and Muzzey, C. L. FLIGHT CONTROL SERVO DEVELOPMENT. Cornell Aeronautical Laboratory Report CAL-63 28 July 1954

Approved for Public Release

Contrails

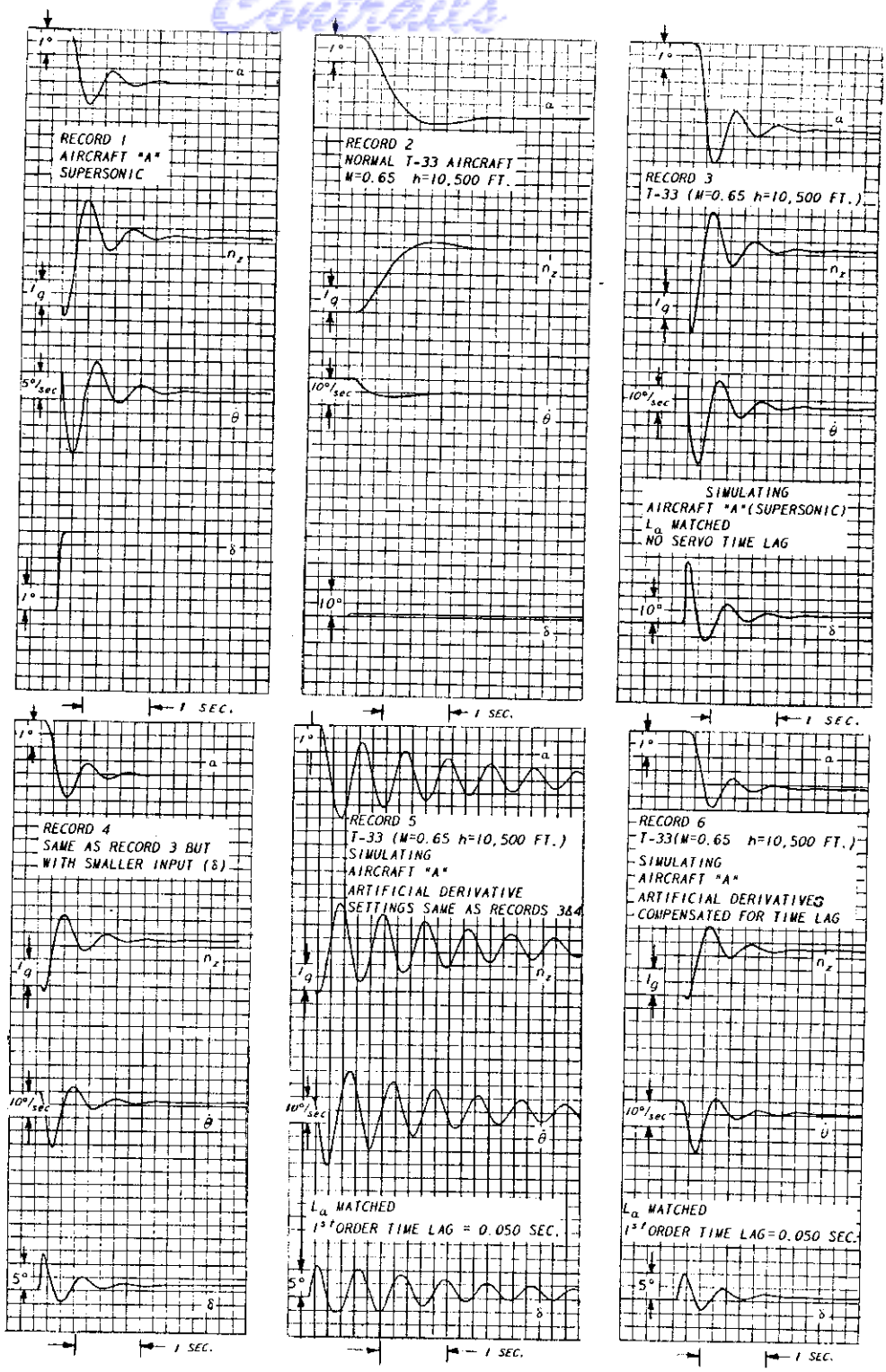

Figure 1 T-33 SIMULATING TYPICAL CHARACTERISTICS REPRESENTED BY CASE "A"

Approved for Public Release

Contrails

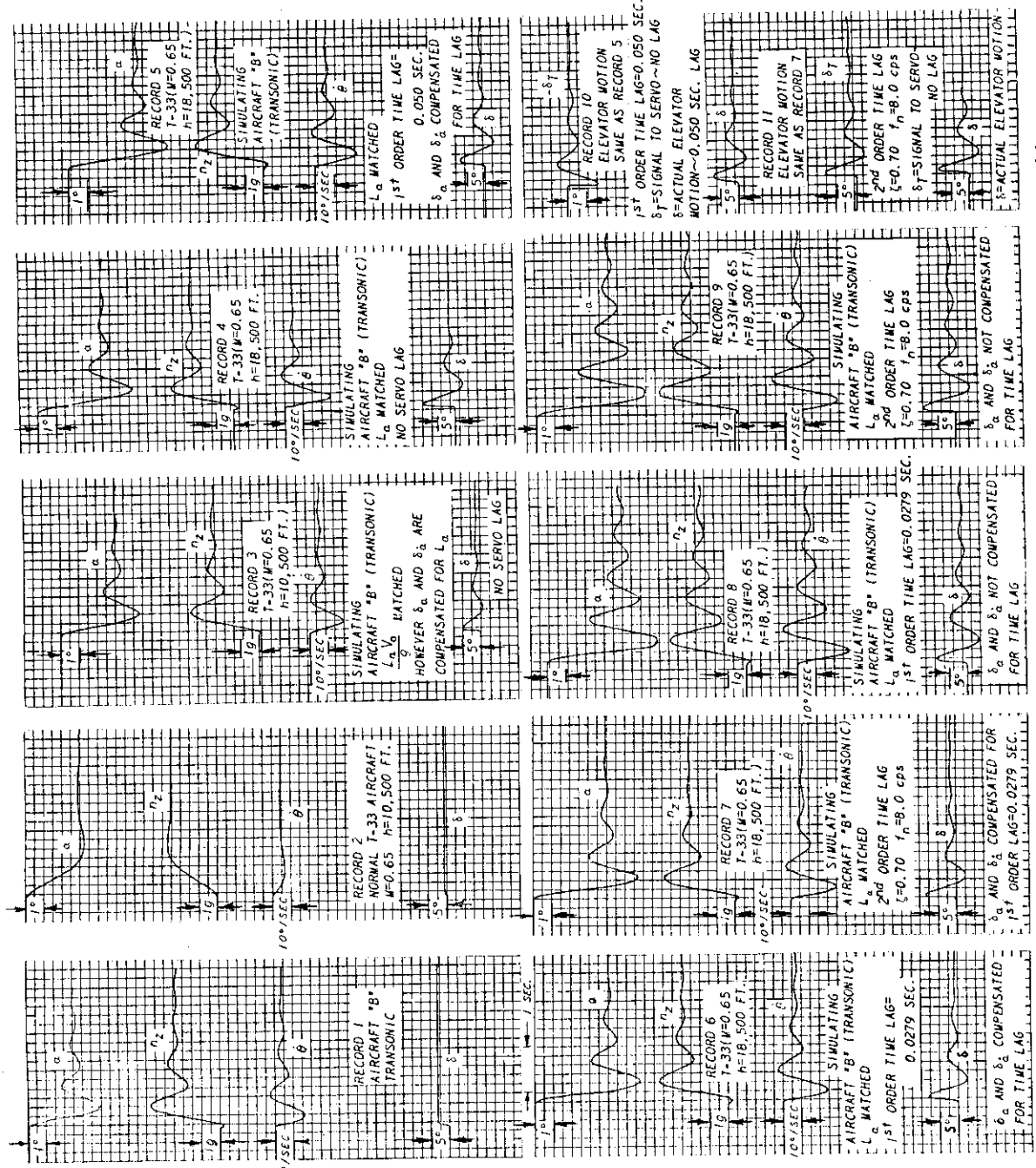

Figure 2 T-33 SIMULATING TYPICAL CHARACTERISTICS REPRESENTED BY CASE "B"

Approved for Public Release

Contrails

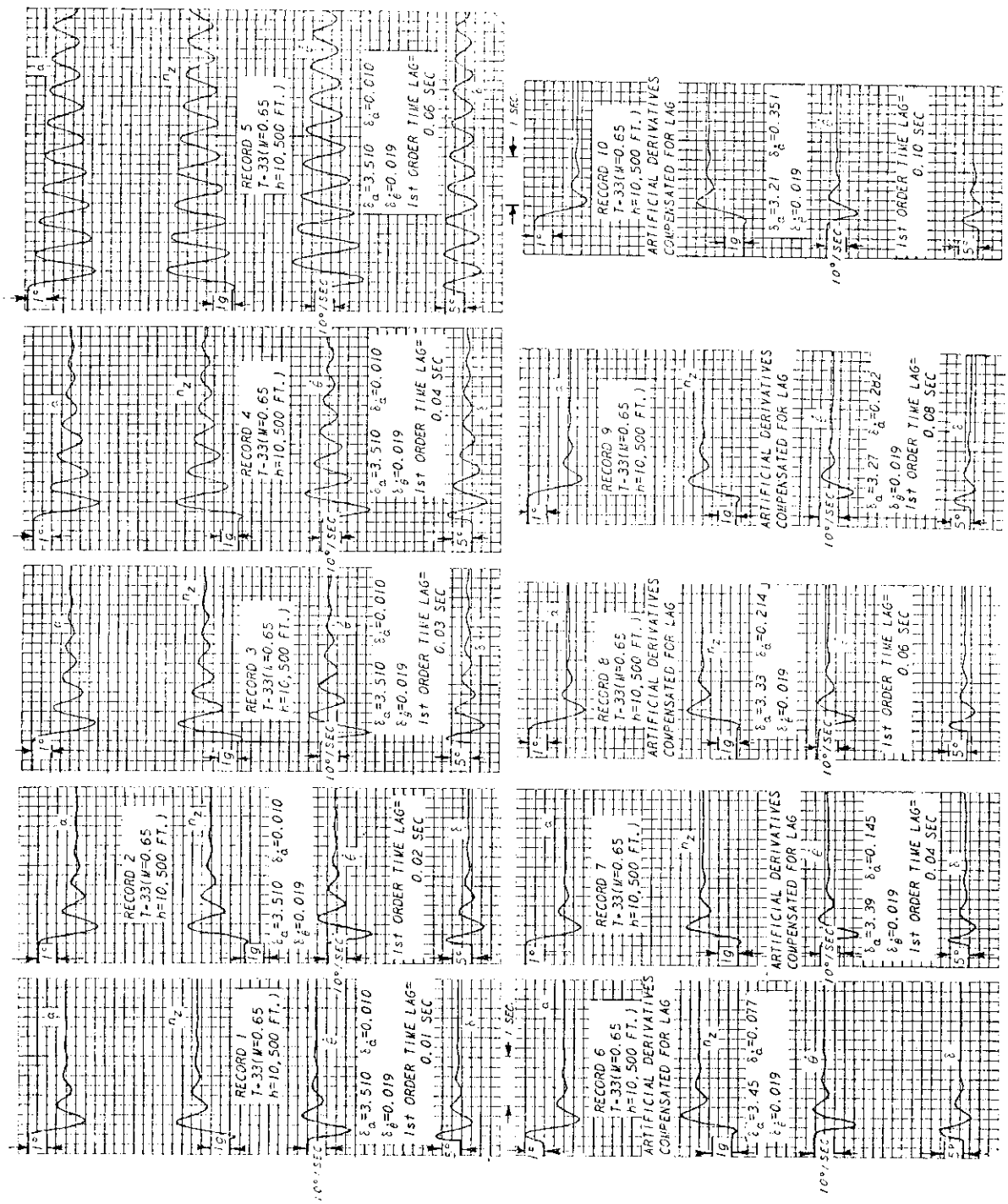

Figure 3 EFFECT OF TIME LAG ON LONGITUDINAL SHORT PERIOD STABILITY

Approved for Public Release

Contrails

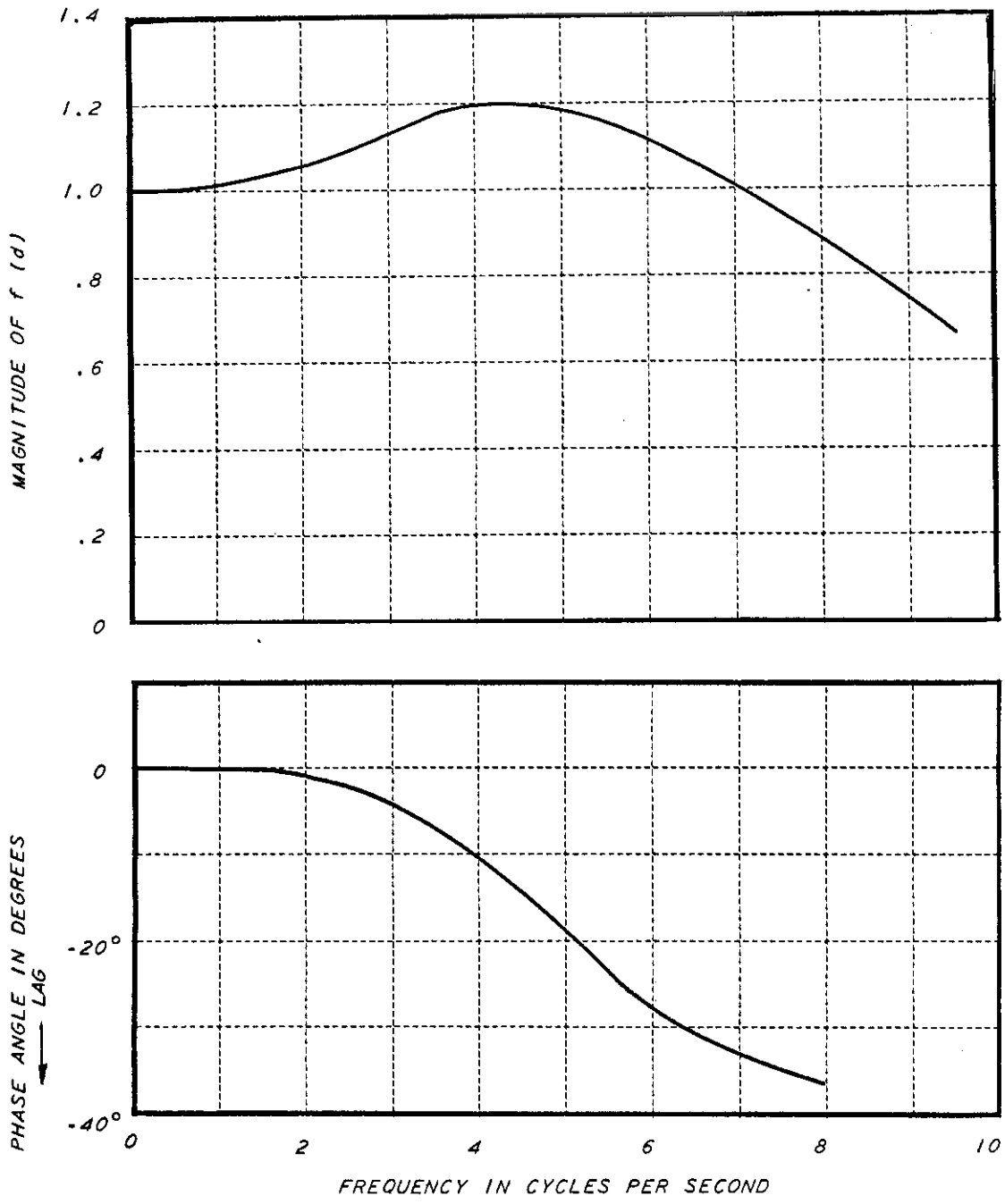

Figure 4 EFFECT OF SERVO DYNAMICS ON ROLLING MOMENT DUE TO SIDESLIP

(RATIO OF ACTUAL L_β' TO THE DESIRED L_β WITH COMPENSATION FOR SERVO DYNAMICS ACCORDING TO EQUATION 75.)

Approved for Public Release

Contrails

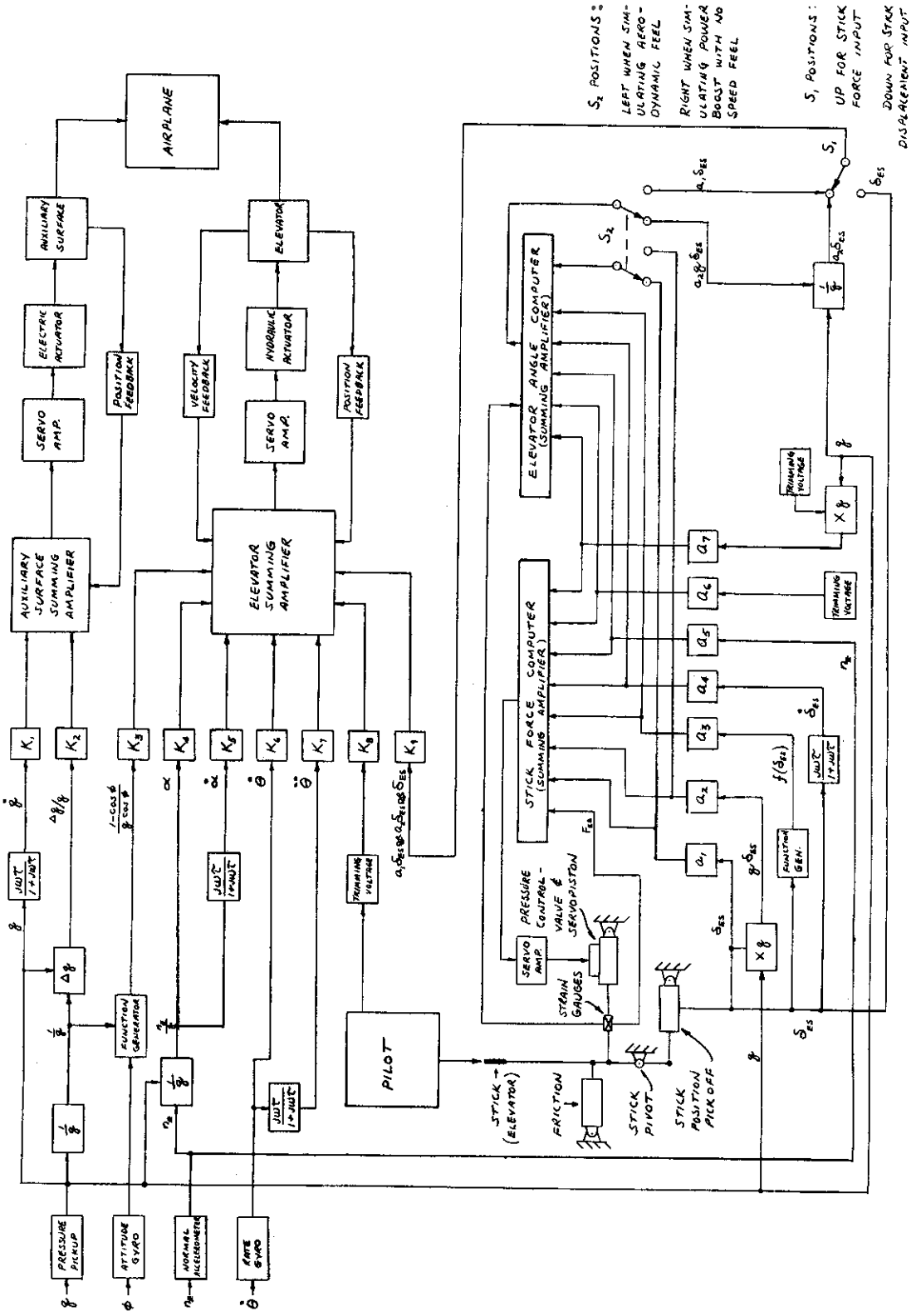

Figure 5 FUNCTIONAL BLOCK DIAGRAM OF LONGITUDINAL CONTROL SYSTEM

Approved for Public Release

Contrails

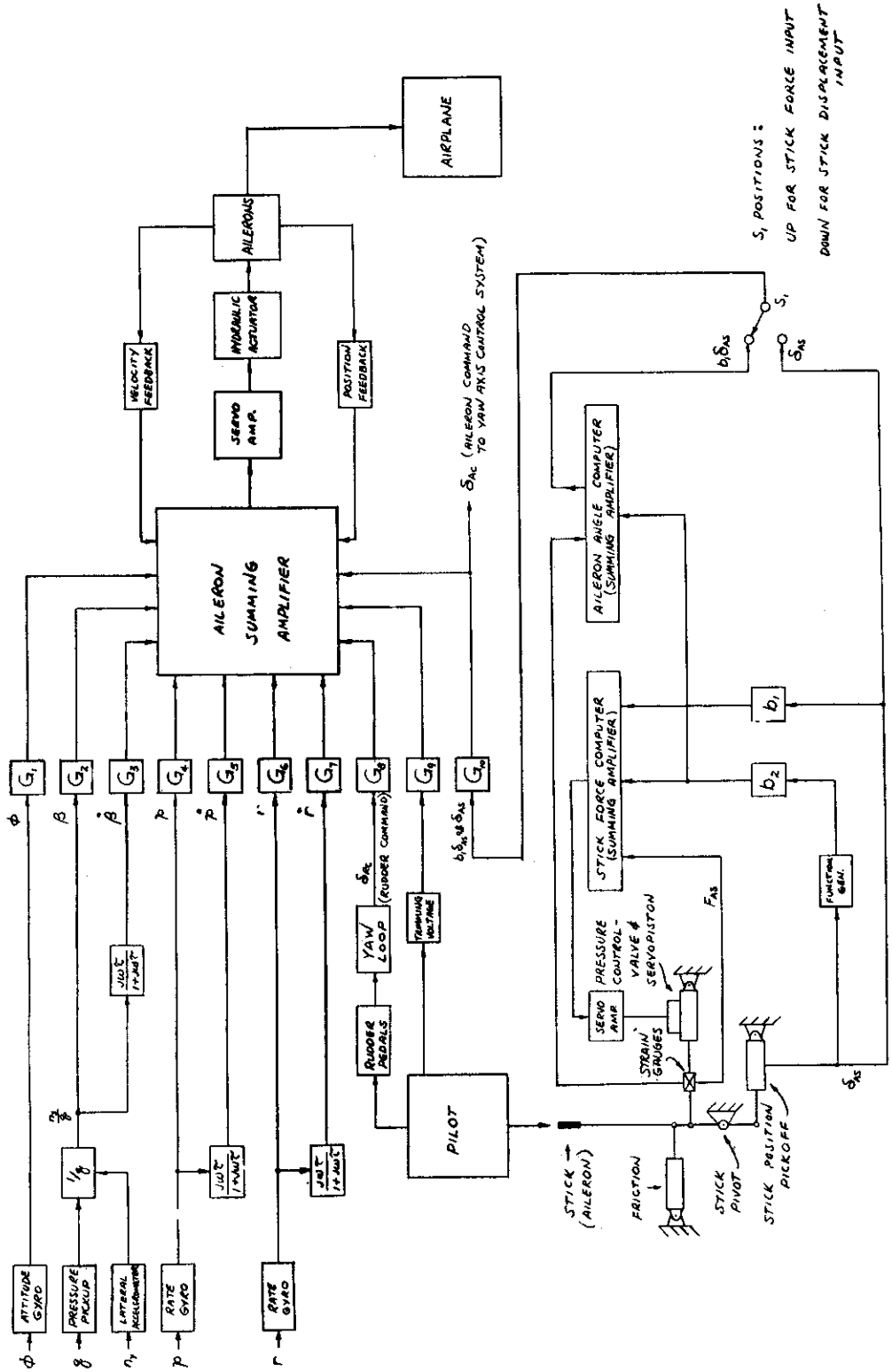

Figure 6 FUNCTIONAL BLOCK DIAGRAM OF ROLL AXIS CONTROL SYSTEM

Approved for Public Release

Contrails

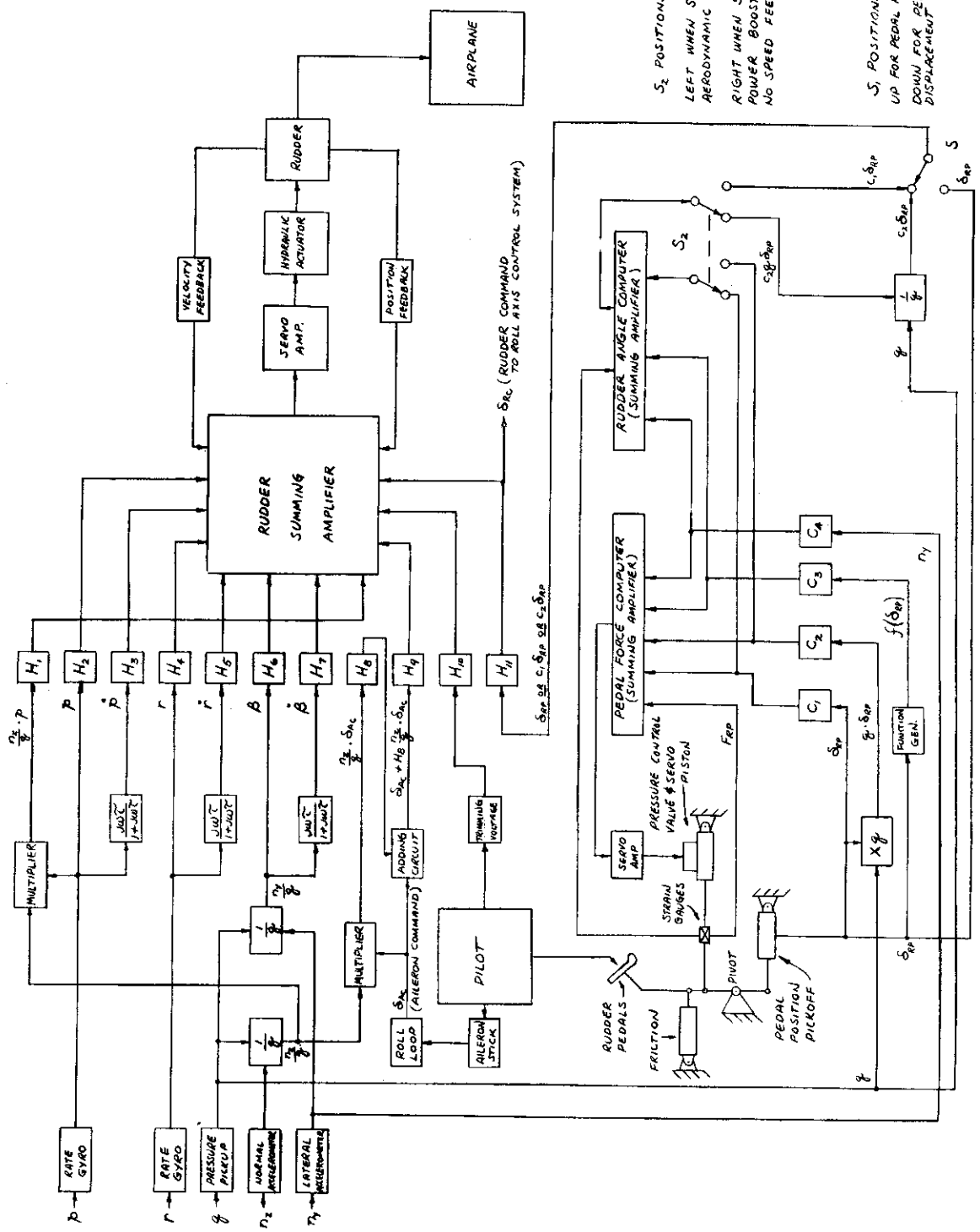

Figure 7 FUNCTIONAL BLOCK DIAGRAM OF YAW AXIS CONTROL SYSTEM

Approved for Public Release

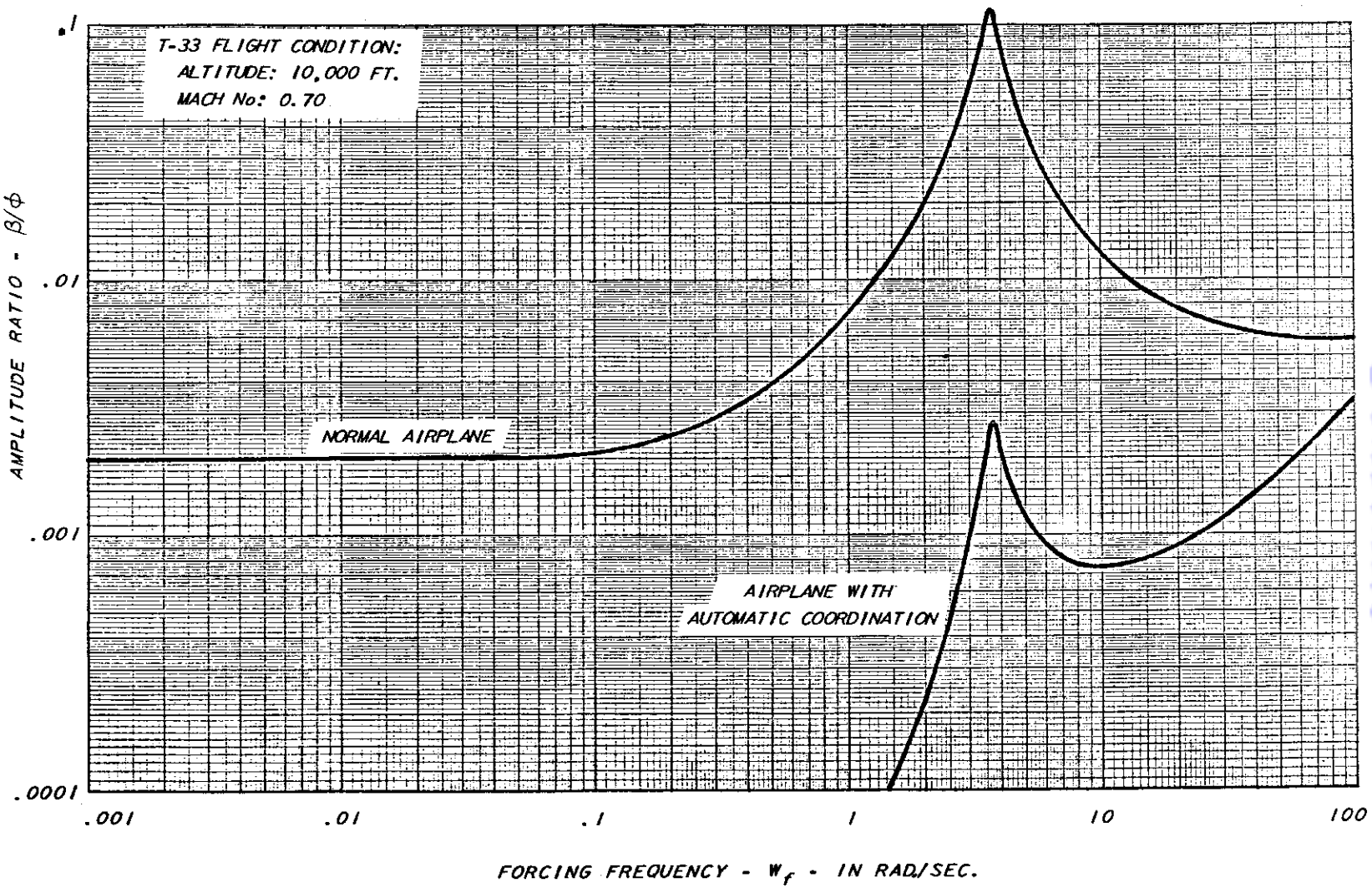

Figure 8 RATIO OF SIDESLIP ANGLE AMPLITUDE TO ROLL ANGLE AMPLITUDE FOR SINUSOIDAL FORCING OF THE AILERONS

Approved for Public Release

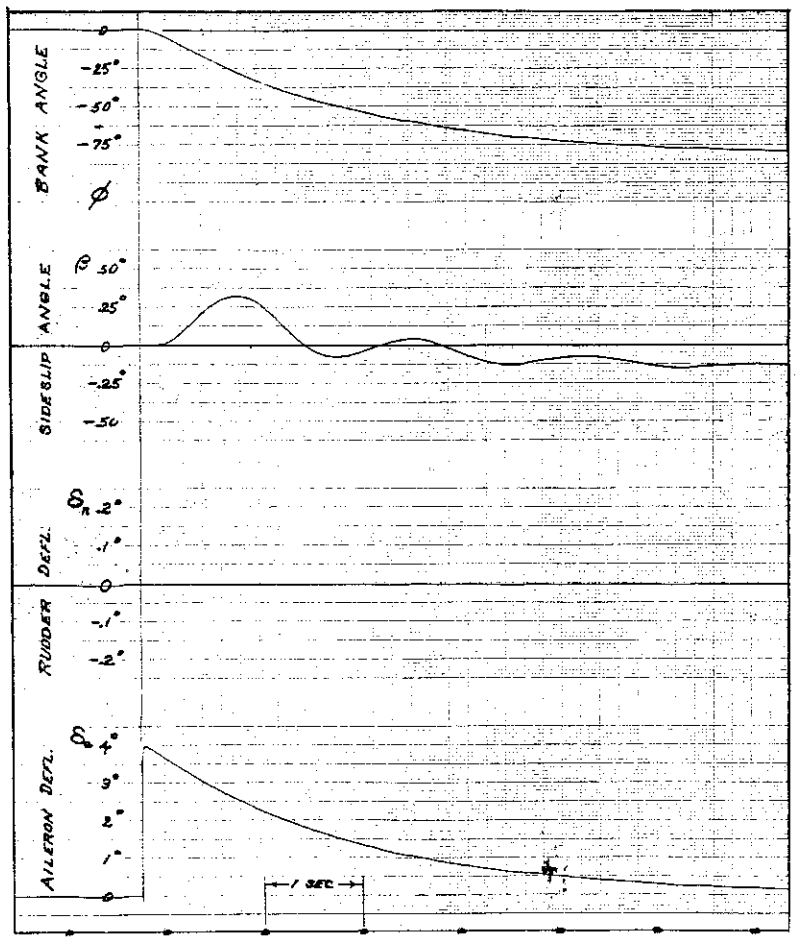

Fig. 9-A

NORMAL T-33
M = 0.70, ALTITUDE = 10,000 FT.
$k_a = 0$; $k_p = 0$; $k_\phi = 0$

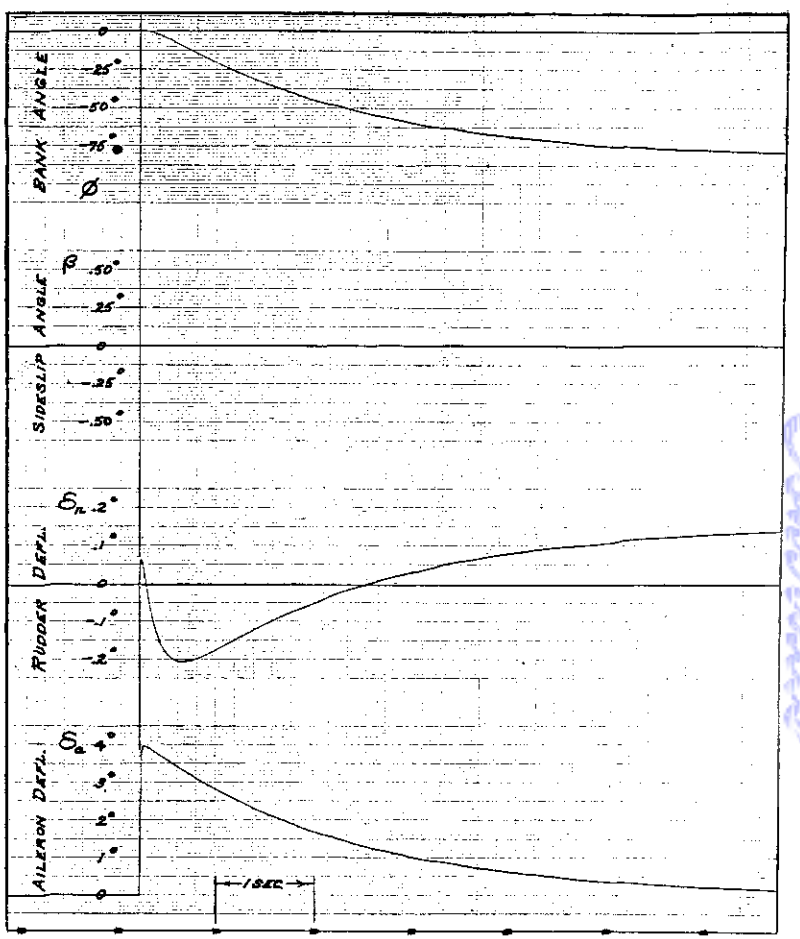

Fig. 9-B

T-33 WITH AUTOMATIC TURN COORDINATION
$k_a = .0272$; $k_p = .00973$ SEC.; $k_\phi = -.00201$

FIGURE 9 RESULTS OF ANALOG COMPUTER INVESTIGATION OF AUTOMATIC TURN COORDINATION

Using: $\delta_r = k_a \delta_a + k_p p + k_\phi \phi$

Approved for Public Release

Contrails

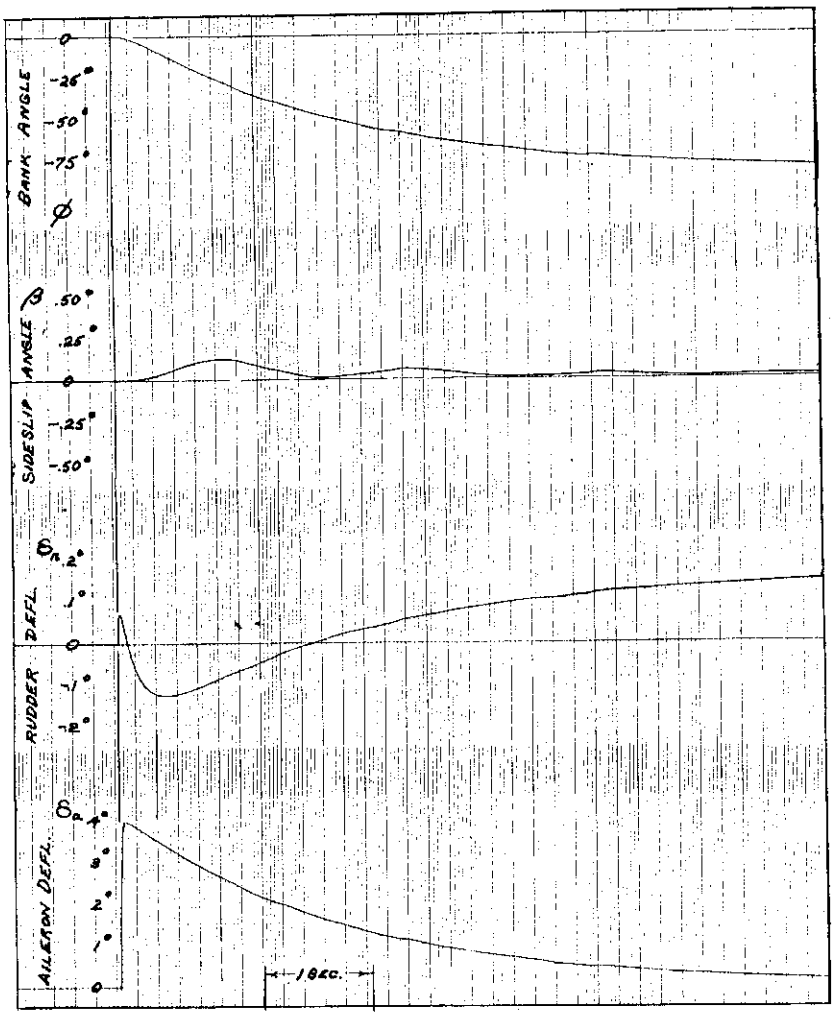

Fig. 9-C

T-33 WITH AUTOMATIC TURN COORDINATION,
BUT WITH k_p 20% LOW
k_a=.0272; k_p=.0078 SEC.; k_ϕ=-.00201

FIGURE 9 (cont.) RESULTS OF ANALOG COMPUTER INVESTIGATION OF AUTOMATIC TURN COORDINATION
Using: $\delta_r = k_a \delta_a + k_p p + k_\phi \phi$

Approved for Public Release

Approved for Public Release

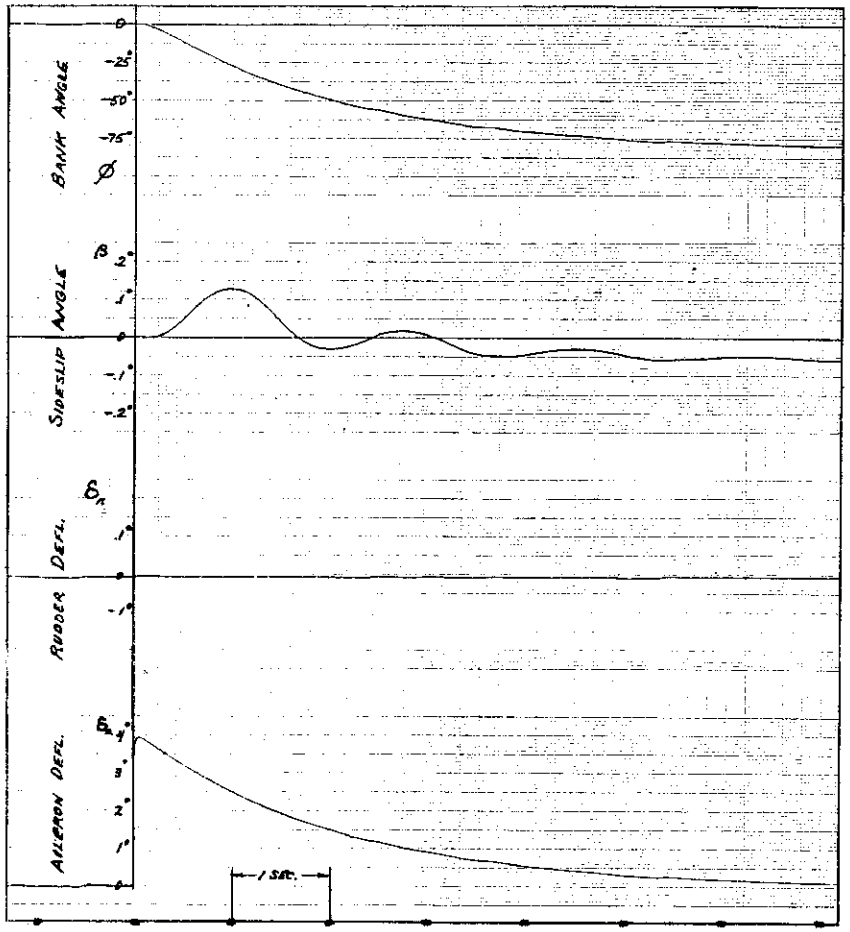

Fig. 10A

NORMAL T-33
M = 0.70; ALTITUDE = 10,000 FT.
$k_\beta = 0$; $k_{\dot\beta} = 0$; $k_{\int\beta} = 0$

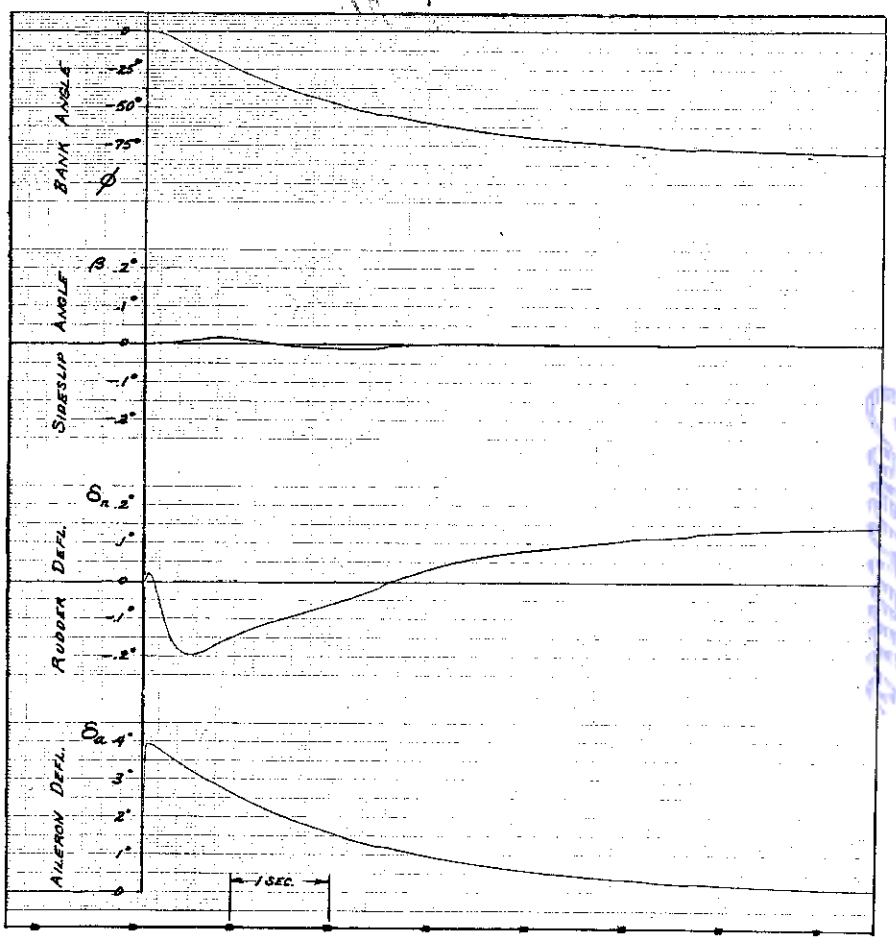

Fig. 10-B

T-33 WITH AUTOMATIC TURN COORDINATION
$k_\beta = -.959$; $k_{\dot\beta} = -1.330$ SEC.; $k_{\int\beta} = -18.2$ SEC

Figure 10 RESULTS OF ANALOG COMPUTER INVESTIGATION OF AUTOMATIC TURN COORDINATION
Using: $\delta_r = k_\beta \beta + k_{\dot\beta} \dot\beta + k_{\int\beta} \left(\int_0^t \beta dt\right)$

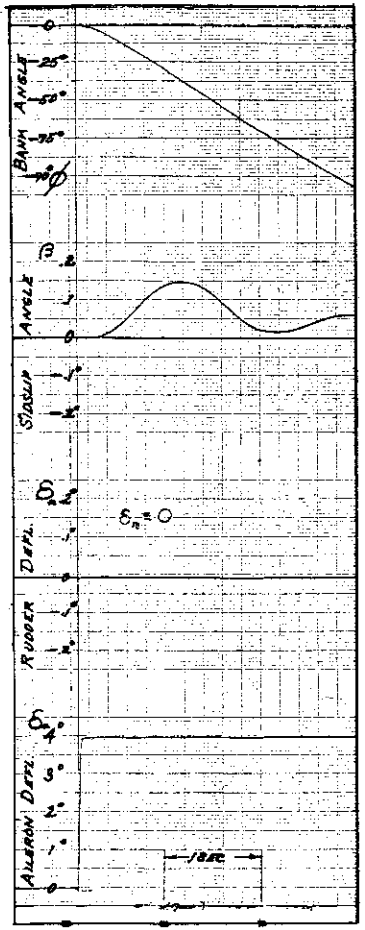

Fig. 11-A

NORMAL T-33, M = 0.70
ALTITUDE = 10,000 FT.
δ_{AS} = 1.53 IN.

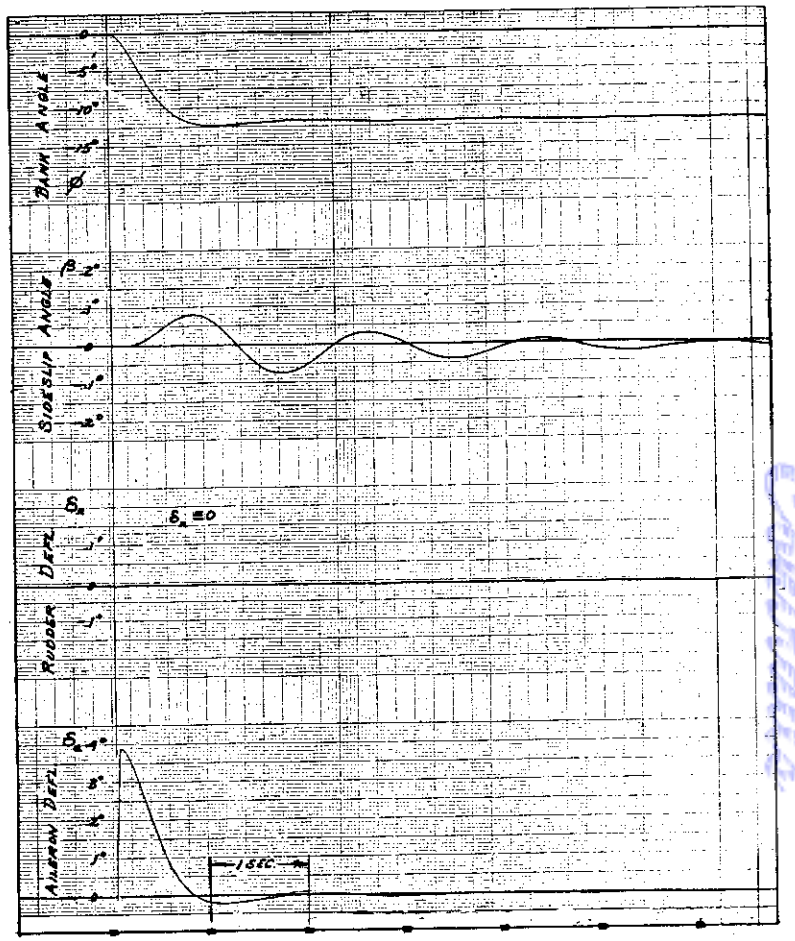

Fig. 11-B

T-33 WITH PROPORTIONAL BANK CONTROL:
$\delta_a = 0.333\ \phi - 2.59\ \delta_{AS}$
δ_{AS} = 1.53 IN.

Figure 11 RESULTS OF ANALOG COMPUTER INVESTIGATION OF PROPORTIONAL BANK CONTROL

Approved for Public Release

Contrails

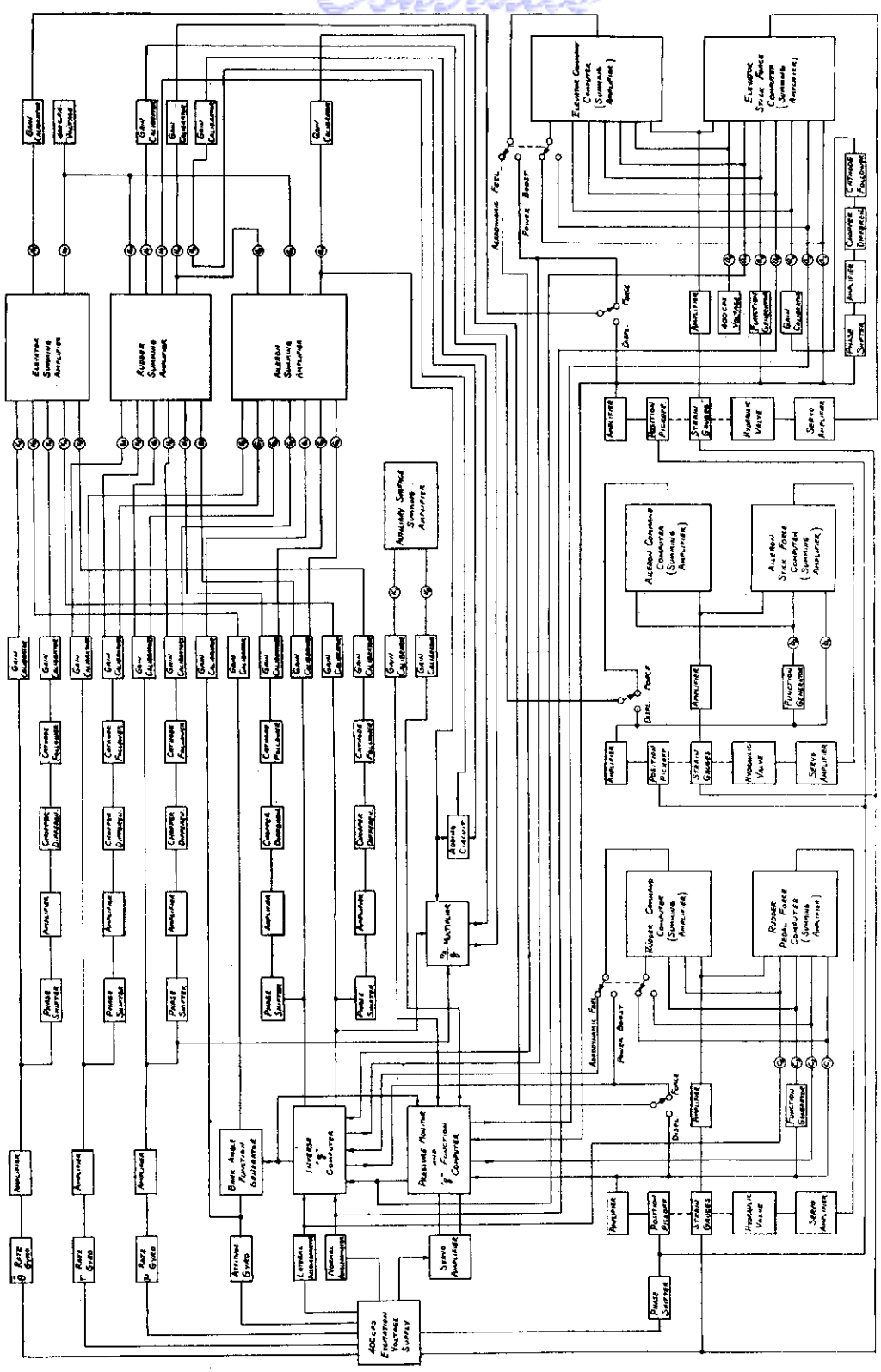

Figure 12 T-33 VARIABLE STABILITY SYSTEM, ELECTRICAL BLOCK DIAGRAM OF GAIN COMPUTER SECTION

Approved for Public Release

Contrails

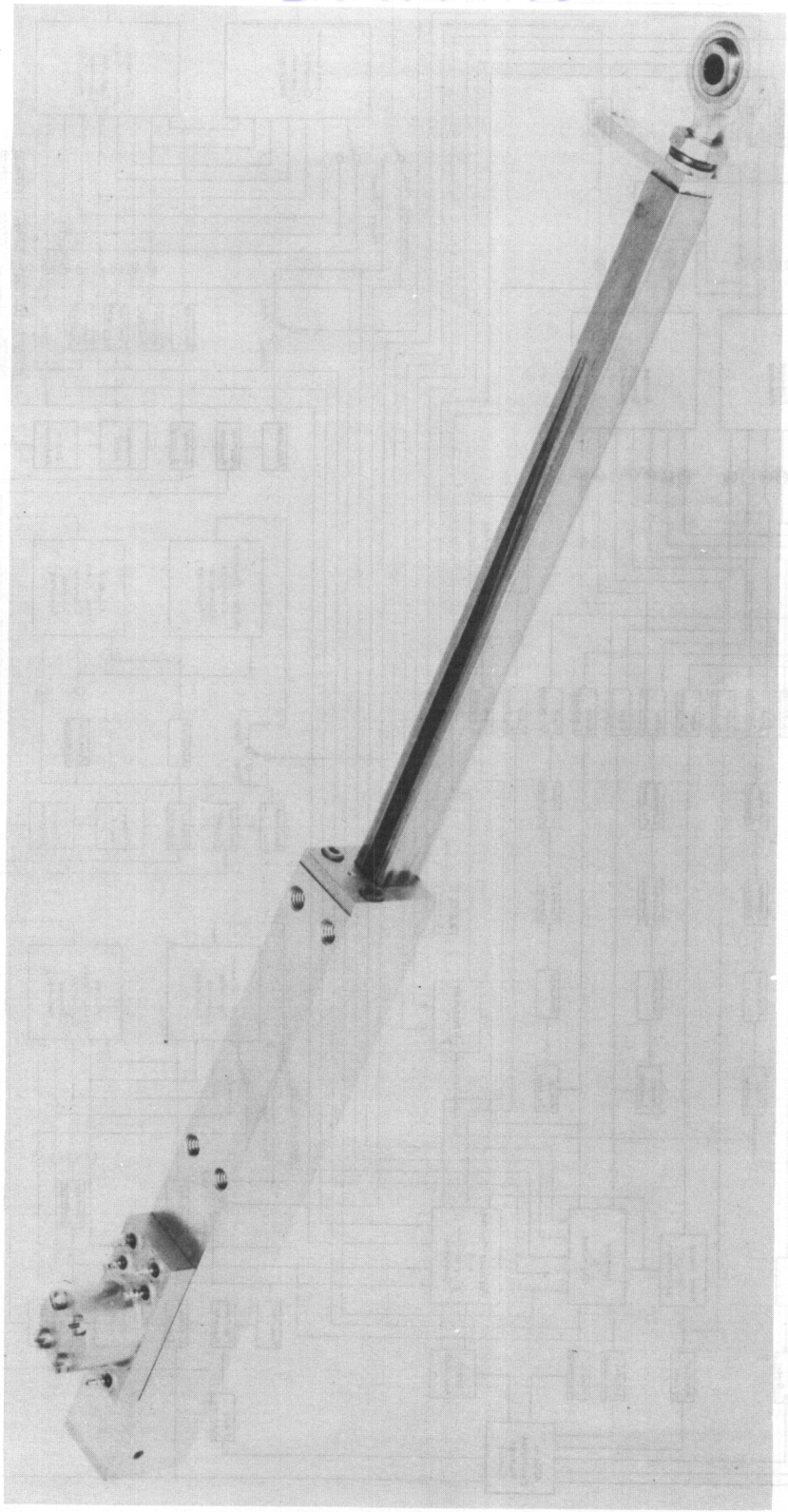

Figure 13 CAL RELUCTANCE LINEAR POSITION TRANSDUCER

Approved for Public Release

Contrails

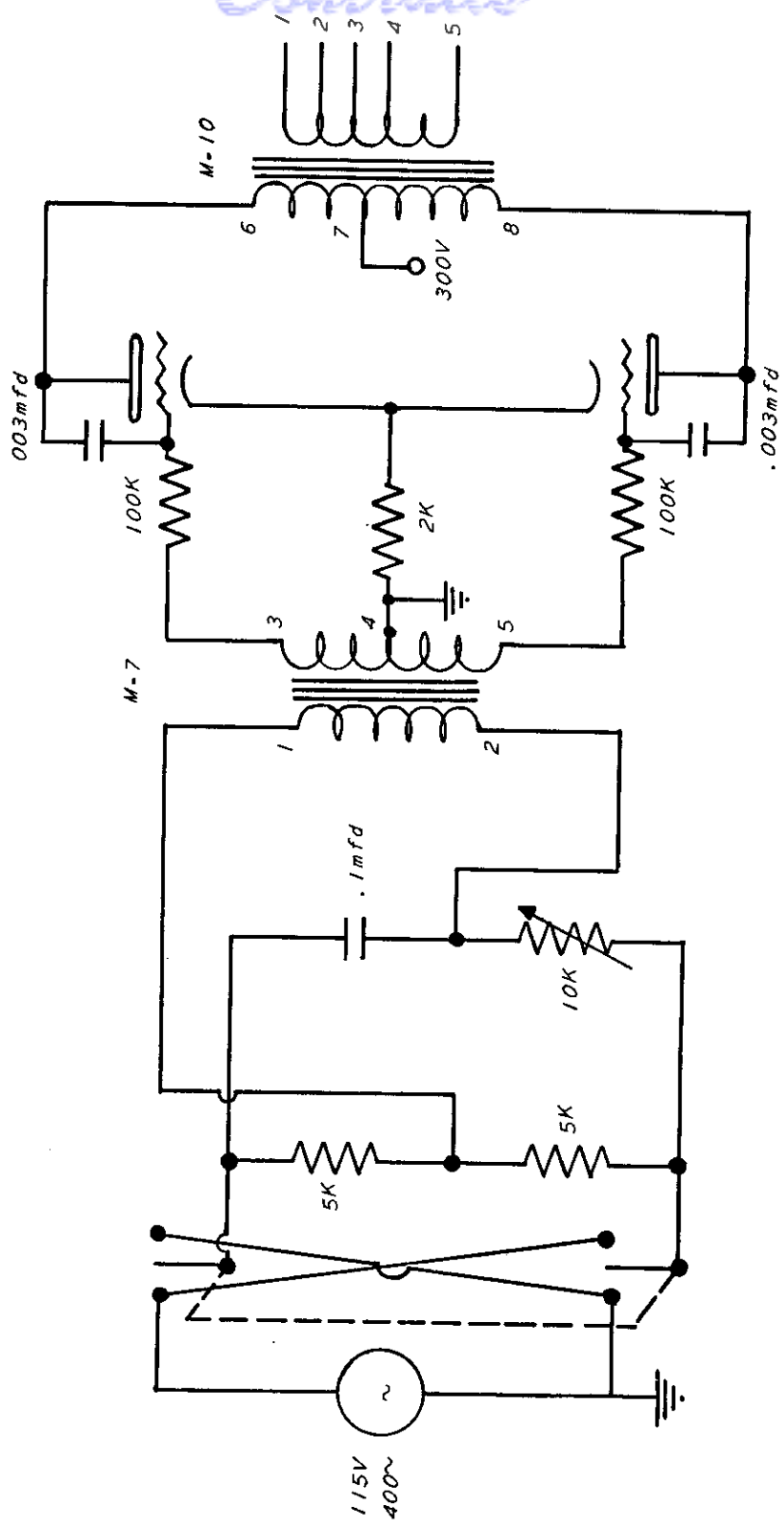

Figure 14 PHASE SHIFTER FOR SIGNAL CIRCUITS

Approved for Public Release

Contrails

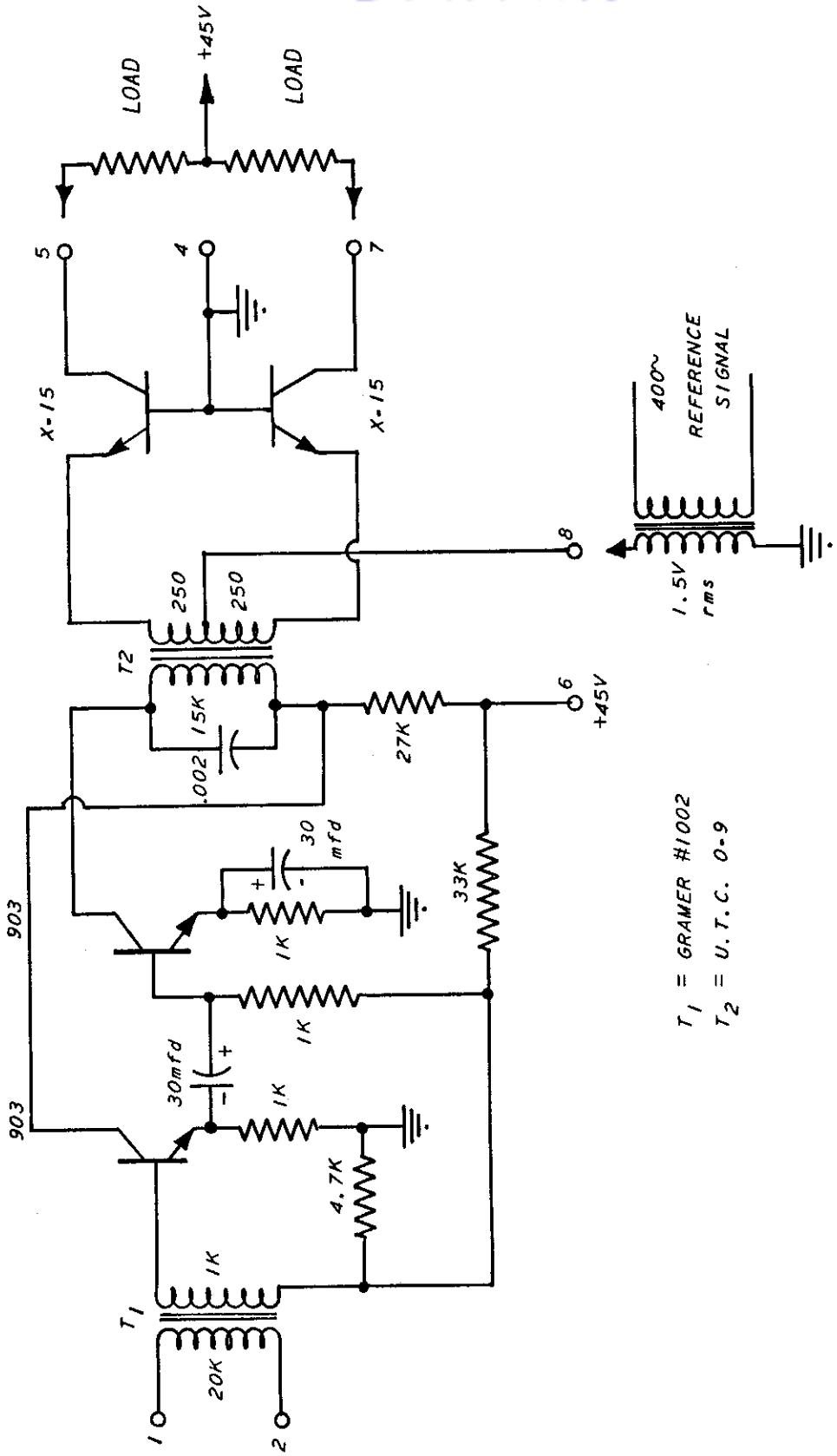

T_1 = GRAMER #1002
T_2 = U.T.C. 0-9

Figure 15 TRANSISTOR SERVO AMPLIFIER DIAGRAM

Approved for Public Release

Contrails

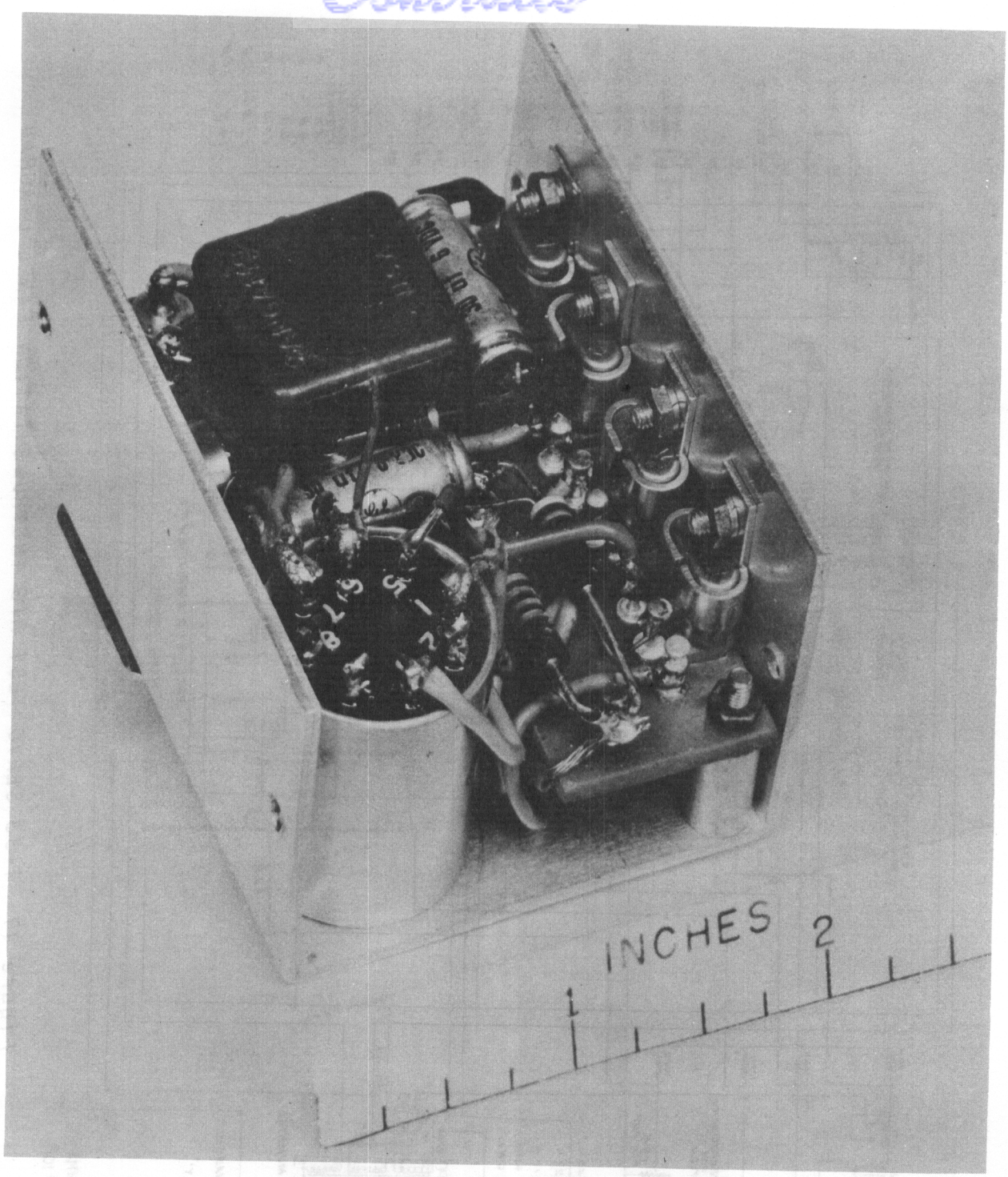

Figure 16 TRANSISTOR SERVO AMPLIFIER

Approved for Public Release

Contrails

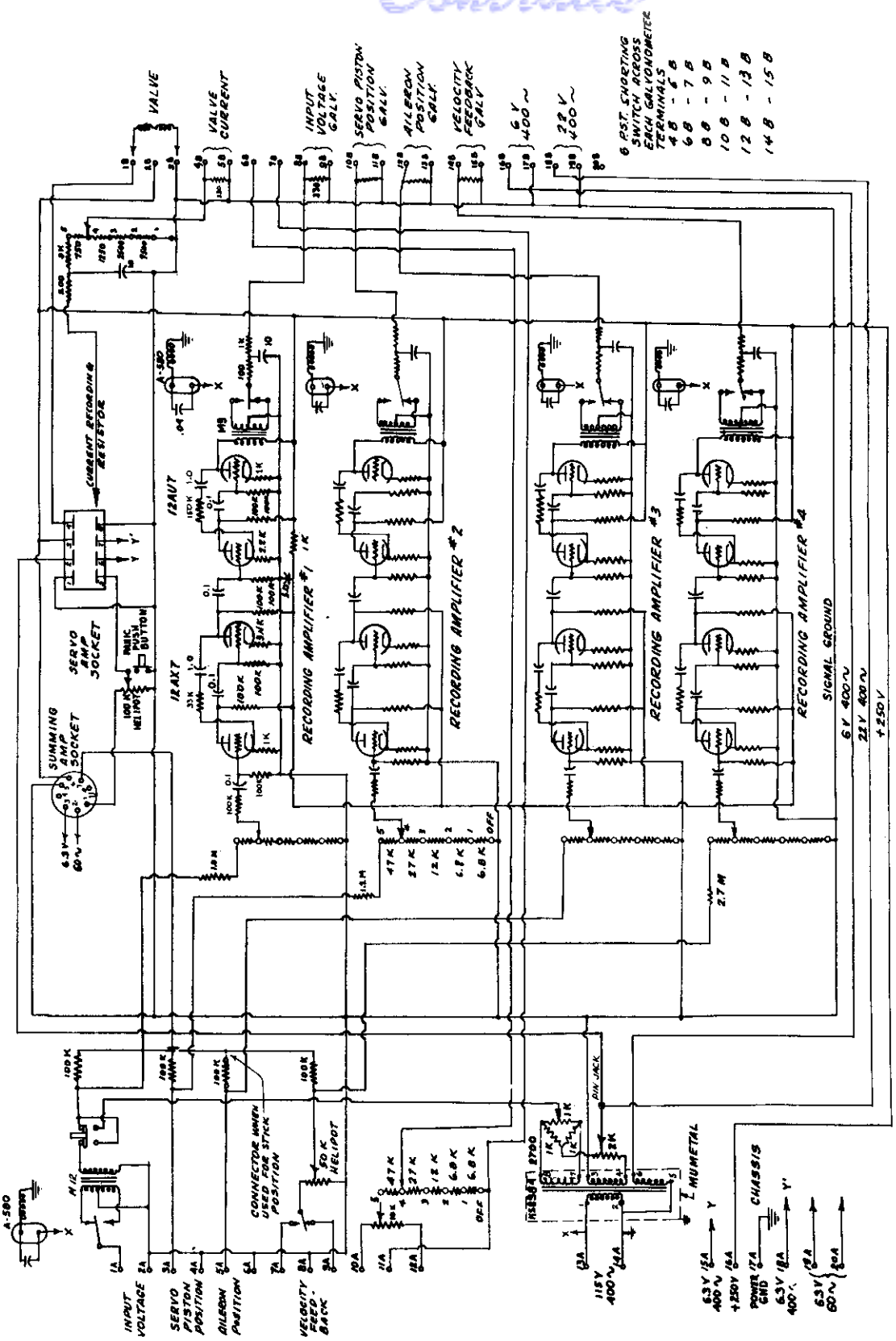

Figure 17 T-33 SERVO TEST RIG INSTRUMENTATION PANEL DIAGRAM

Approved for Public Release

Contrails

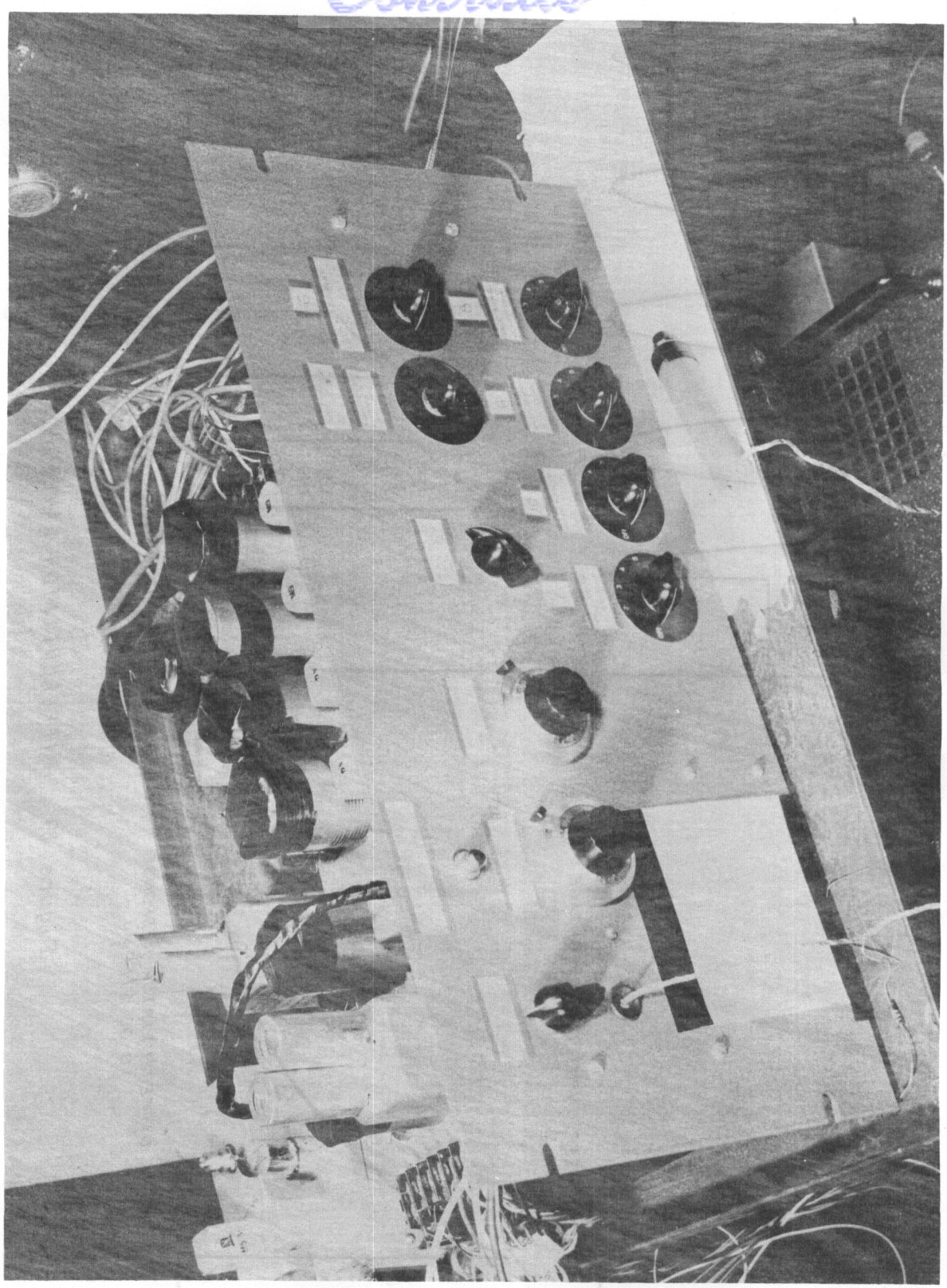

Figure 18 SERVO TEST RIG INSTRUMENTATION PANEL

Approved for Public Release

Contrails

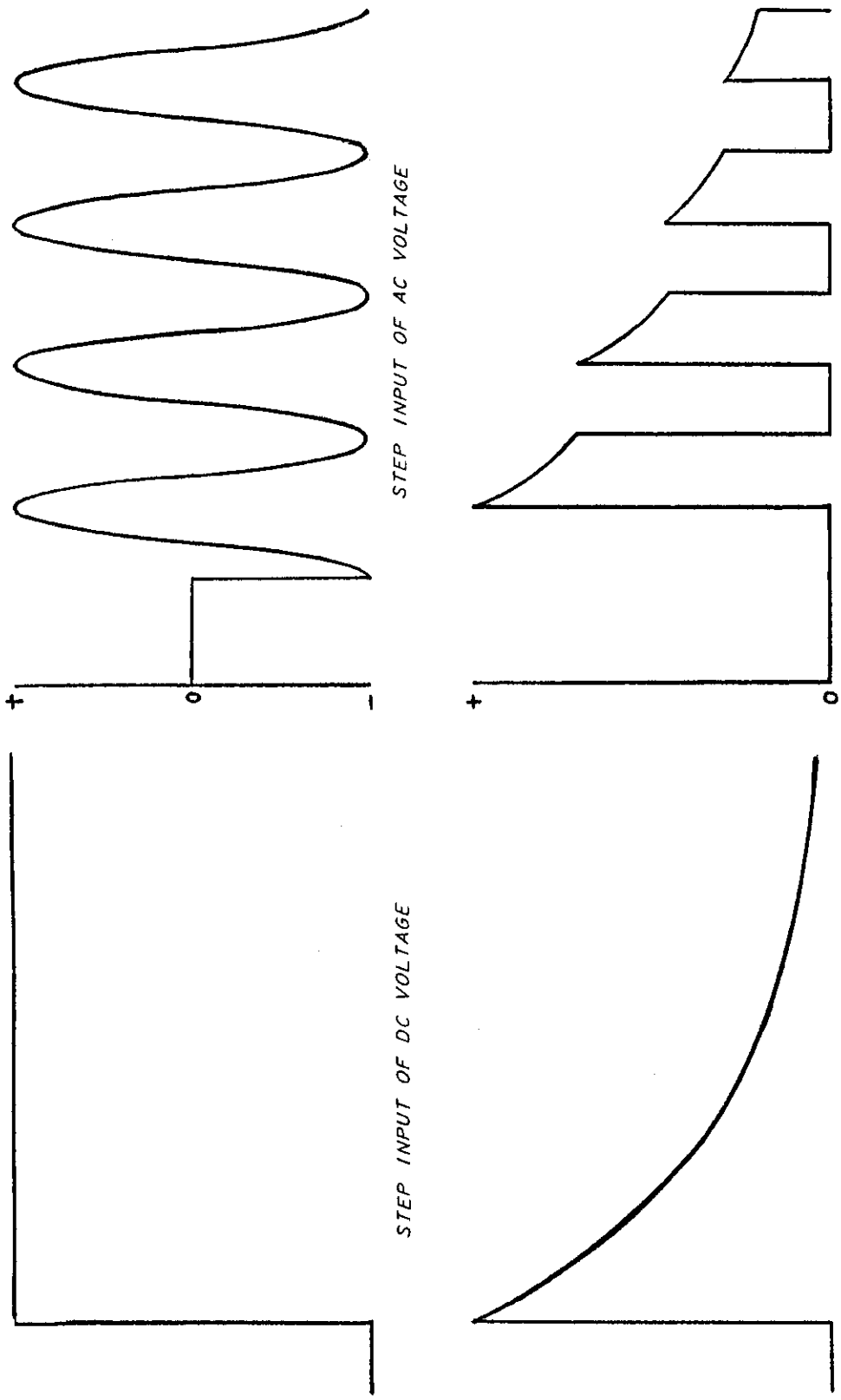

Figure 19 DIFFERENTIATOR WAVEFORMS

Approved for Public Release

Contrails

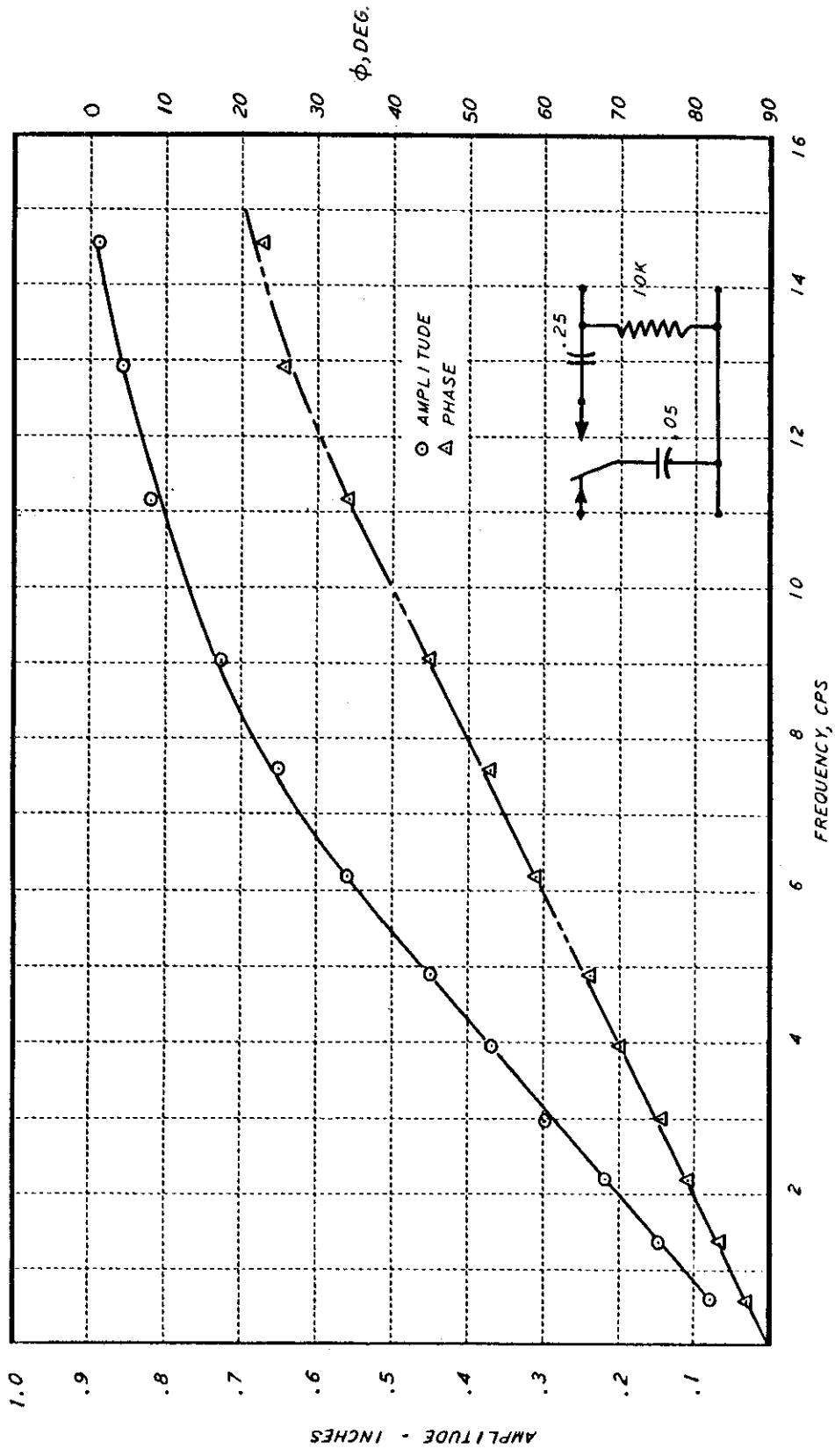

Figure 20 AMPLITUDE AND PHASE RESPONSE OF CHOPPER DIFFERENTIATOR

Approved for Public Release

Contrails

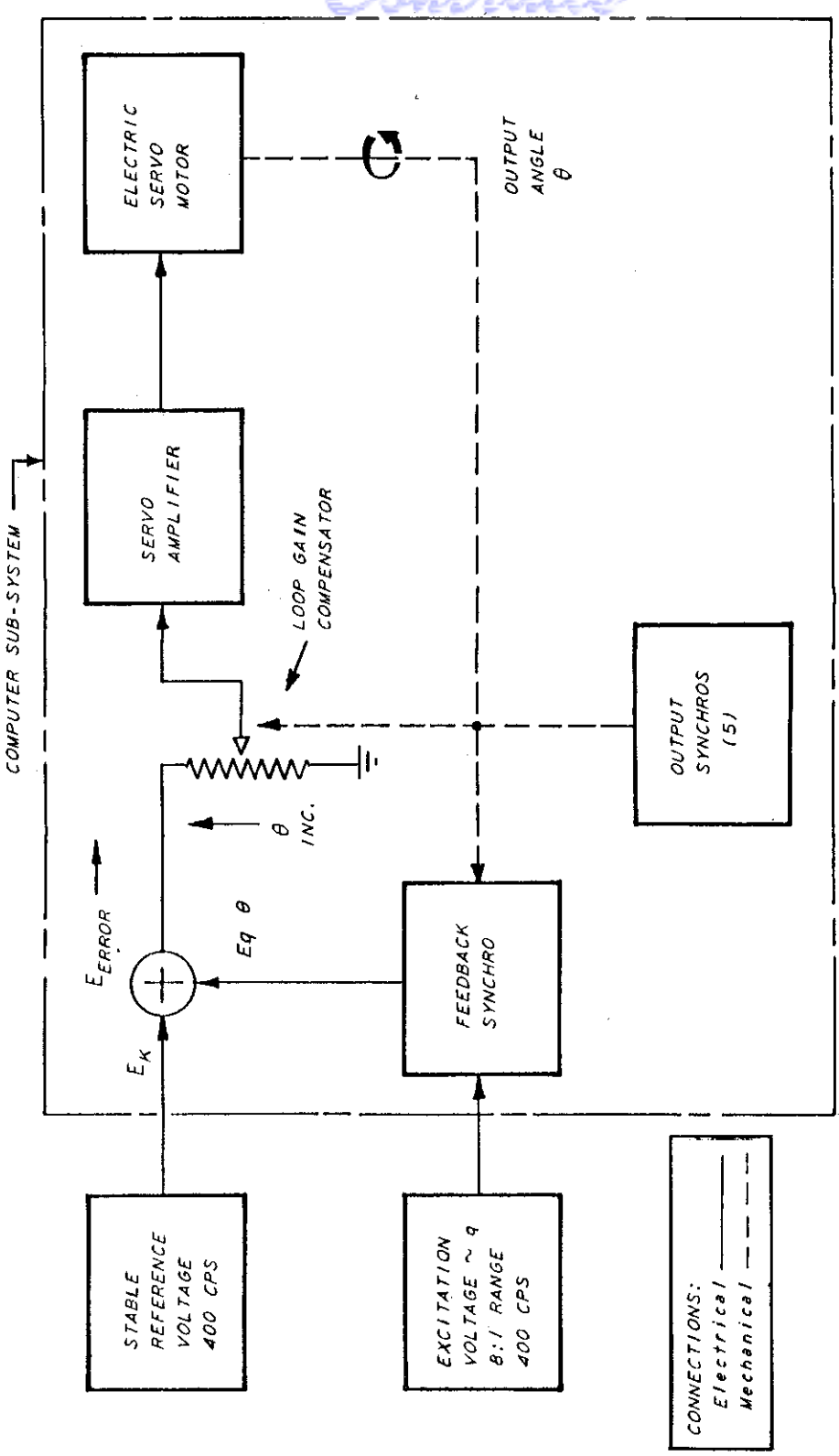

Figure 21 INVERSE q FUNCTION GENERATOR

Approved for Public Release

Contrails

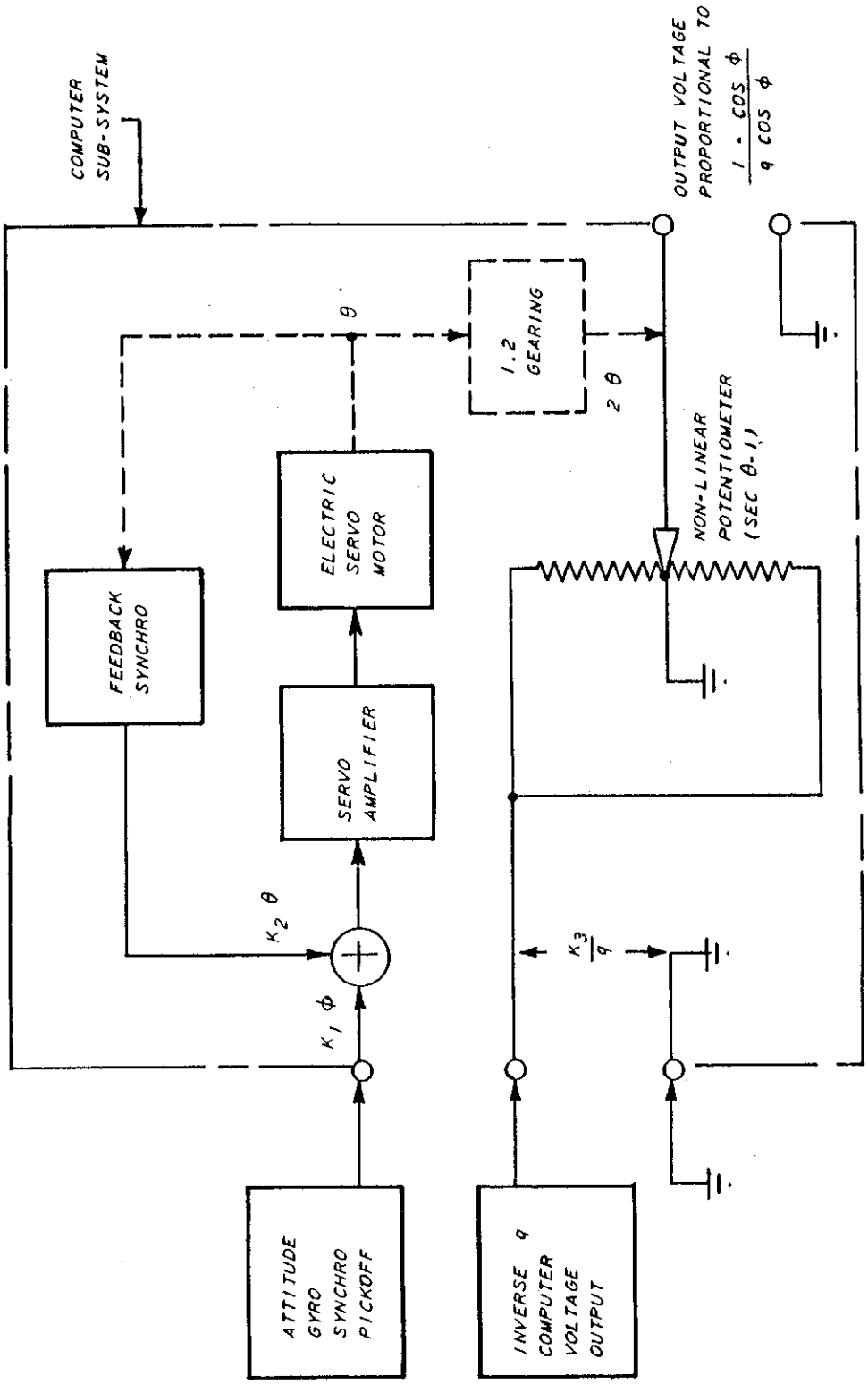

Figure 22 BANK ANGLE FUNCTION GENERATOR

Approved for Public Release

Contrails

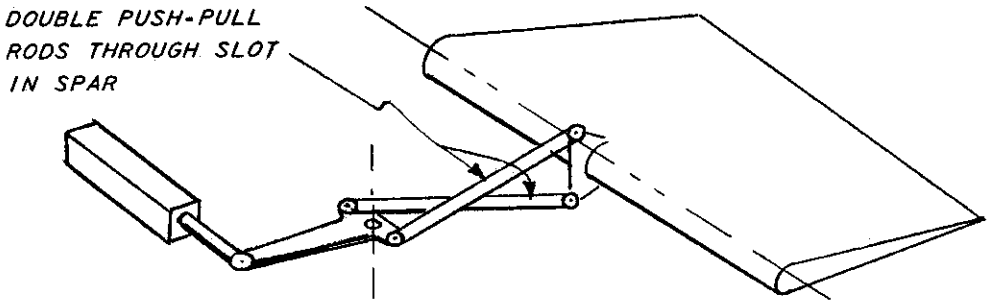

Fig. 23a ELEVATOR SERVO INSIDE STABILIZER

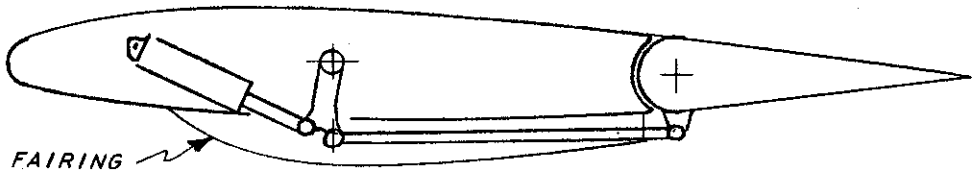

Fig. 23b SERVO CONNECTED EXTERNALLY TO ELEVATOR

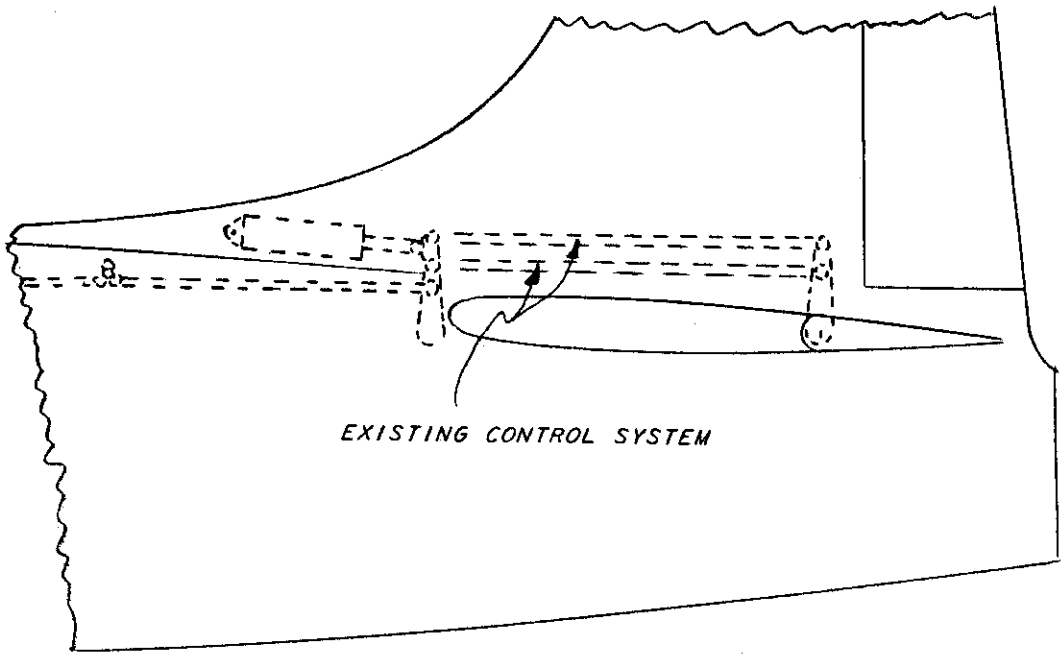

Fig. 23c ELEVATOR SERVO INSIDE FIN

Figure 23 PRELIMINARY SKETCHES OF ELEVATOR SERVO INSTALLATION

Approved for Public Release

Contrails

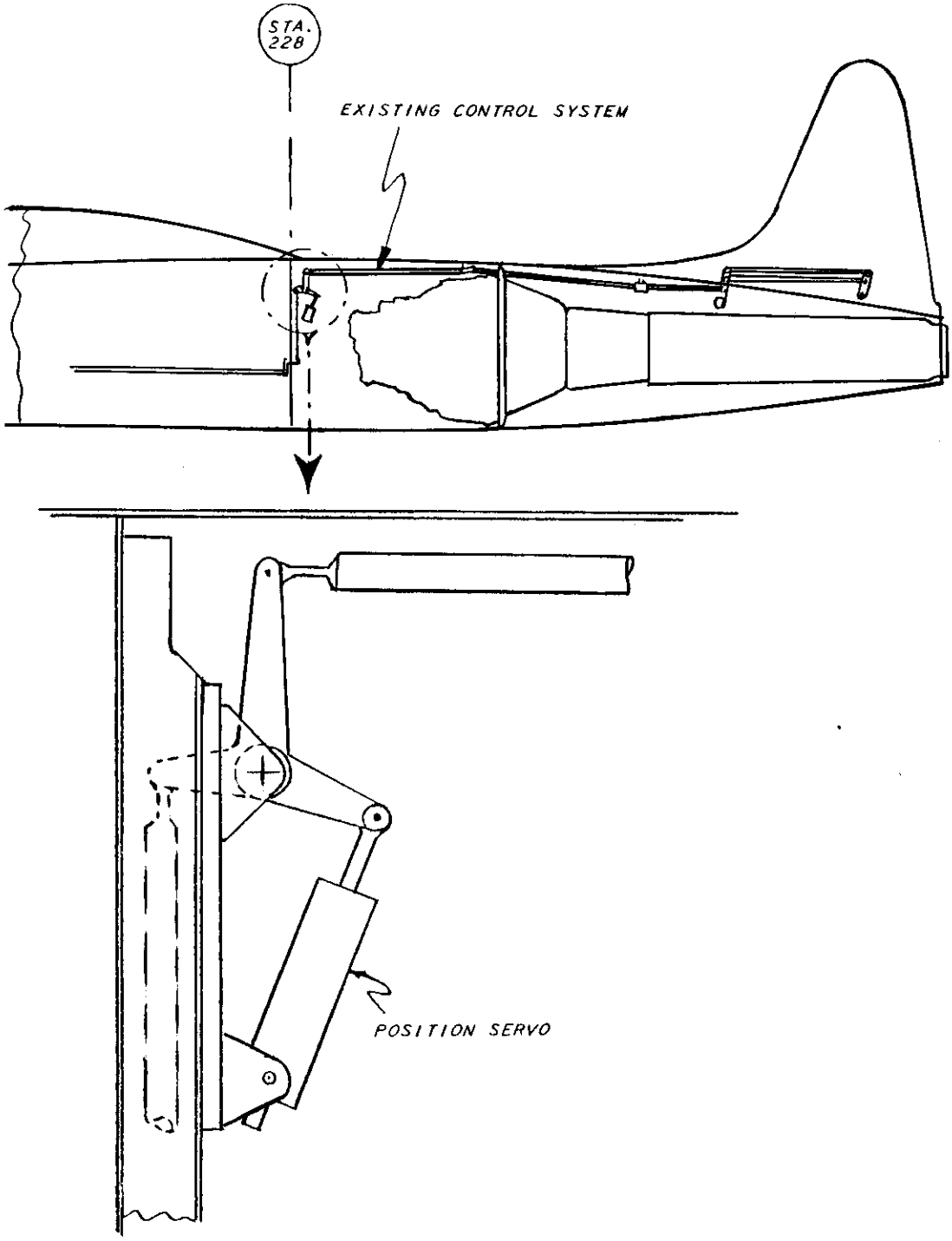

Figure 24 ELEVATOR SERVO IN ENGINE COMPARTMENT

Approved for Public Release

Contrails

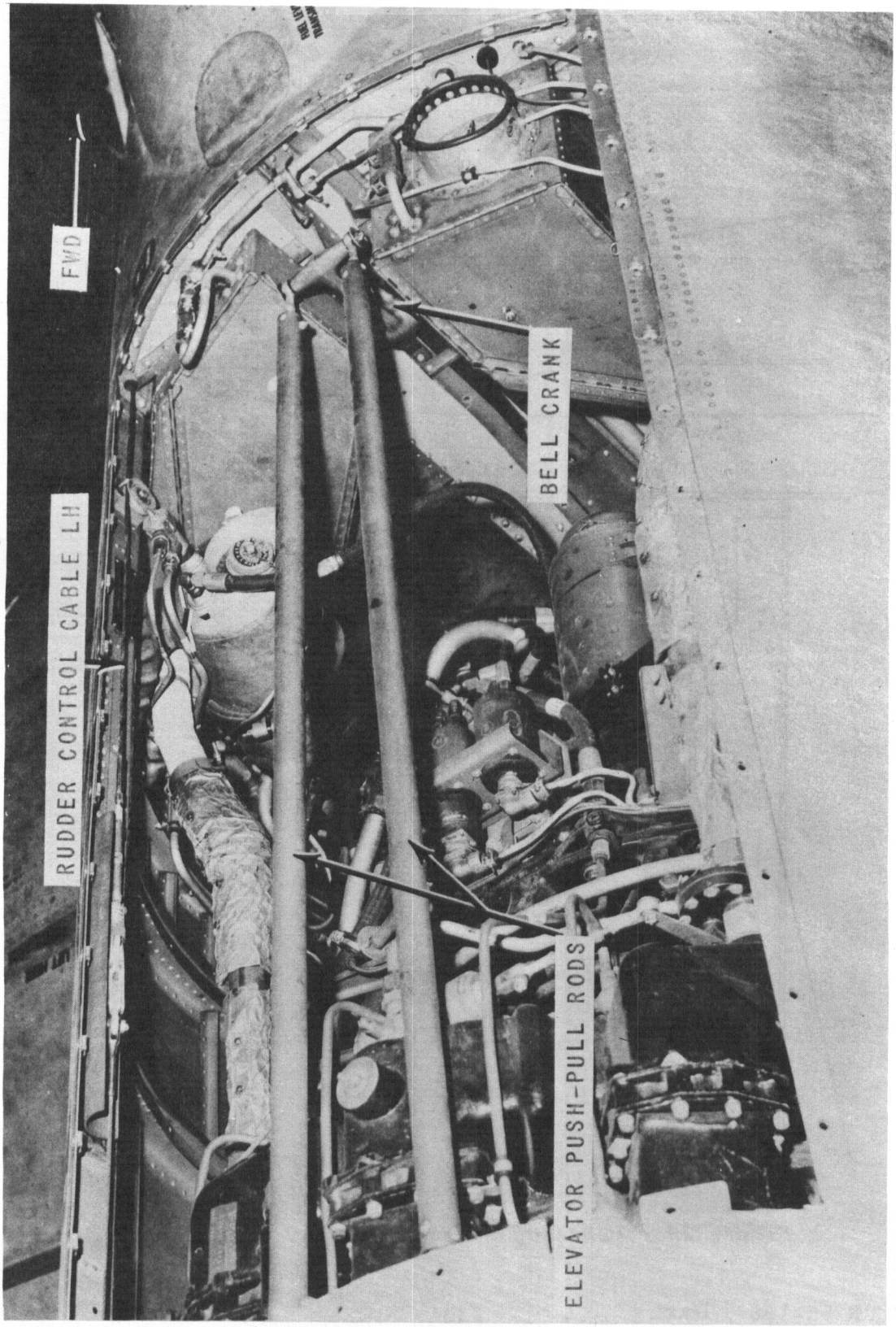

Figure 25 VIEW OF ENGINE COMPARTMENT SHOWING ELEVATOR AND RUDDER CONTROLS

Approved for Public Release

Contrails

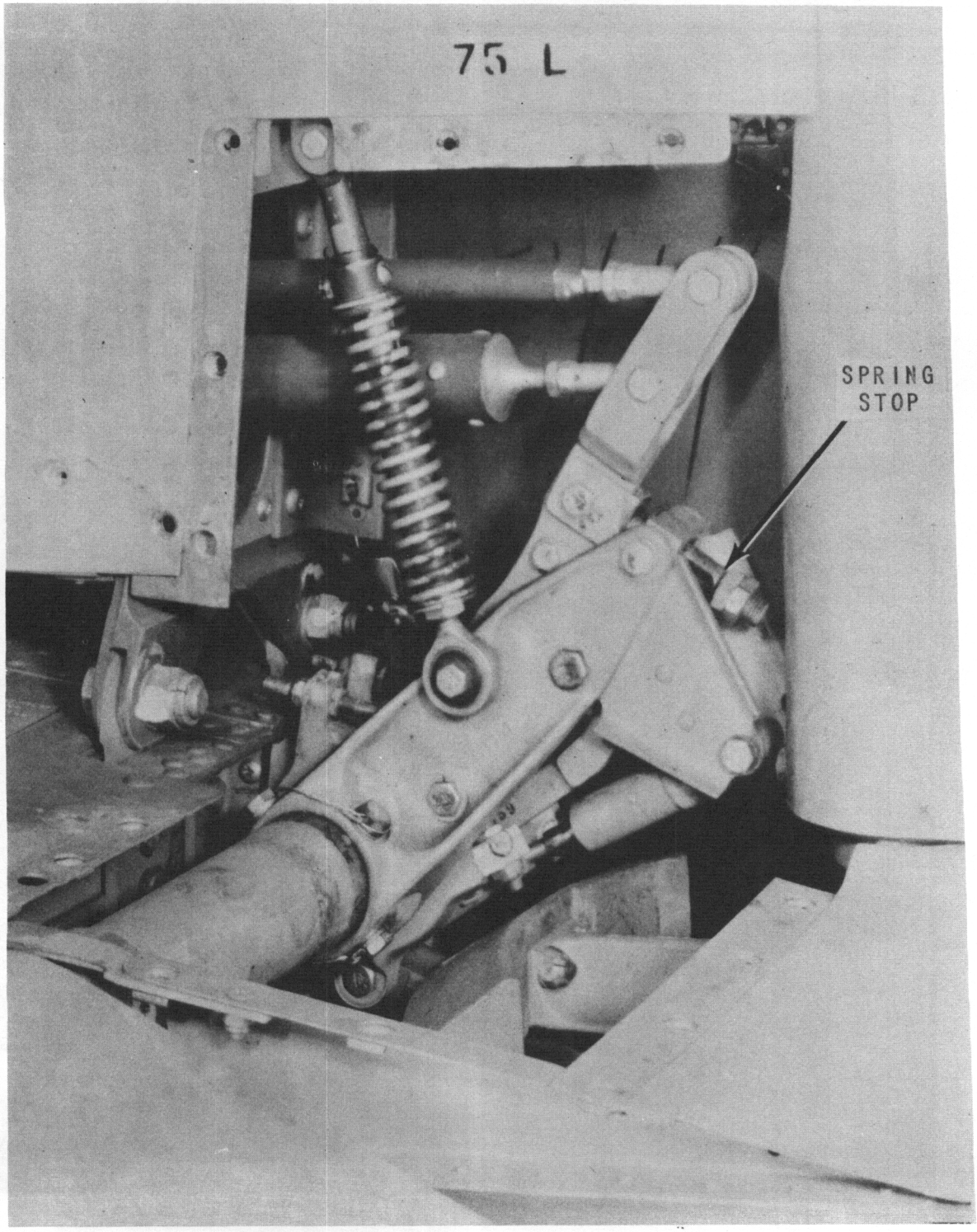

Figure 26 ELEVATOR SPRING TAB MECHANISM UNLOCKED T-33 AIRCRAFT

Approved for Public Release

Contrails

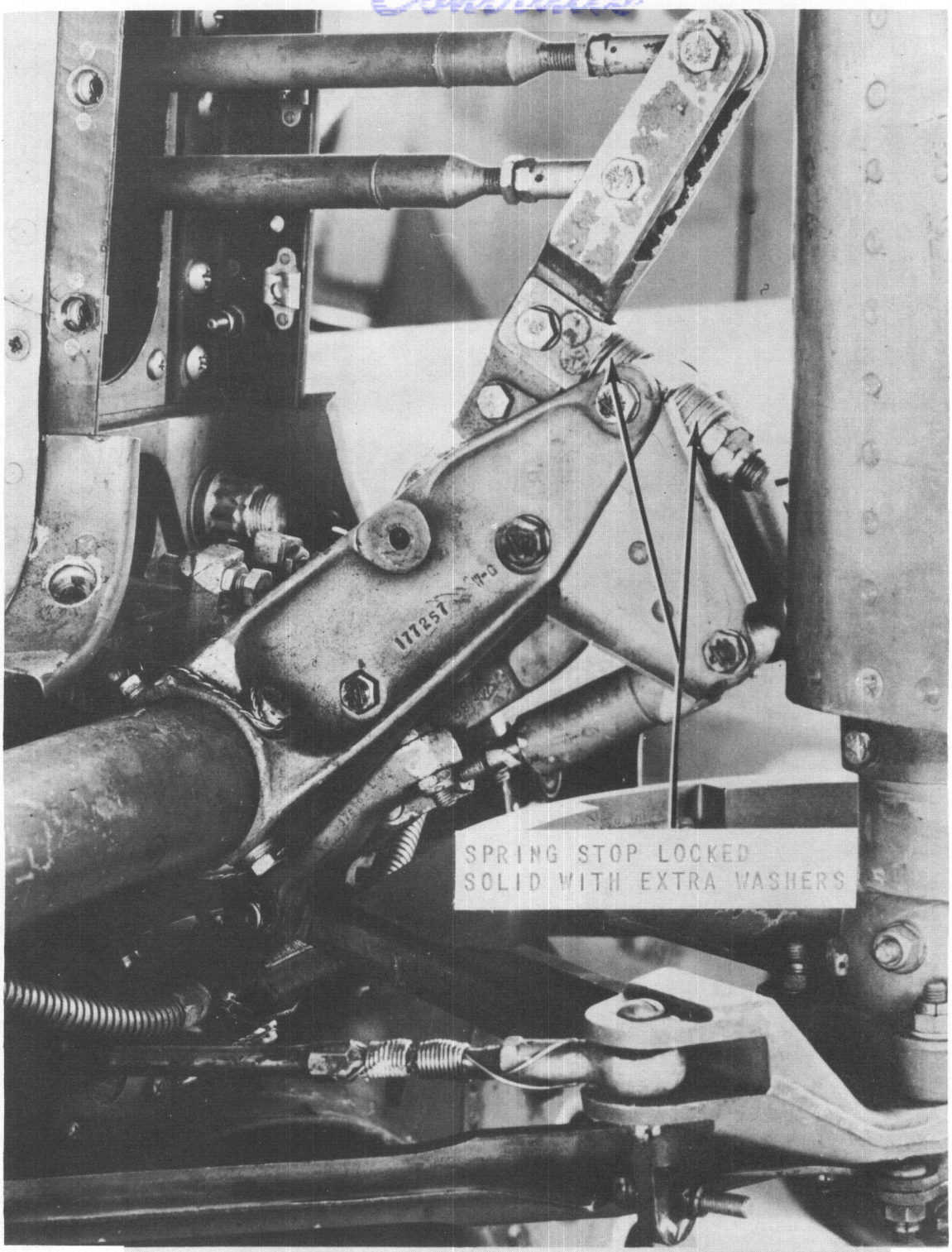

Figure 27 ELEVATOR SPRING TAB MECHANISM LOCKED
F-94 AIRCRAFT

Approved for Public Release

Contrails

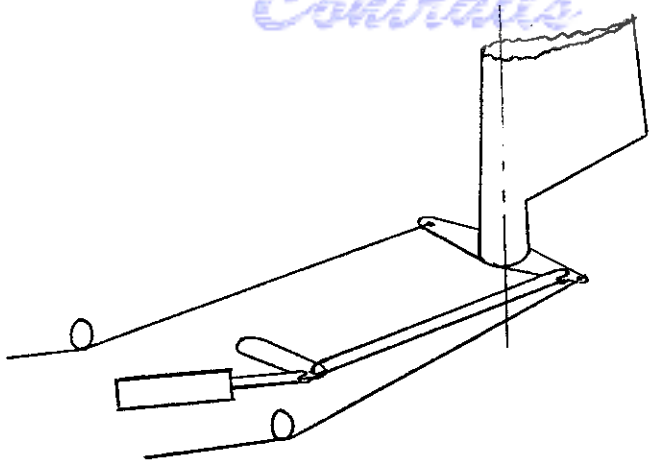

Fig. 28a

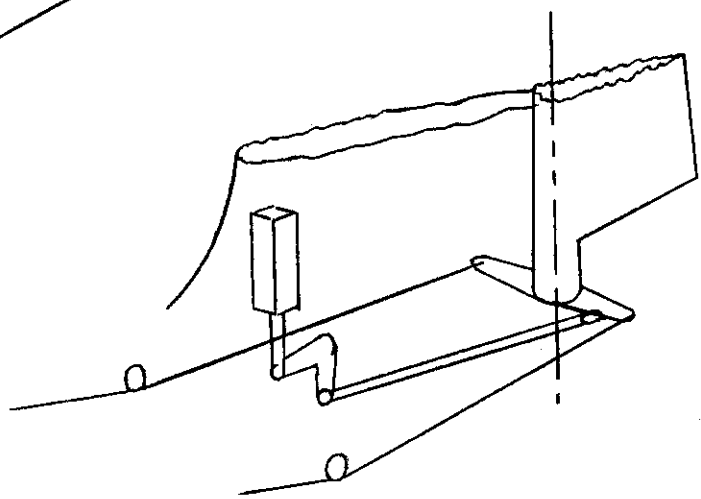

Fig. 28b

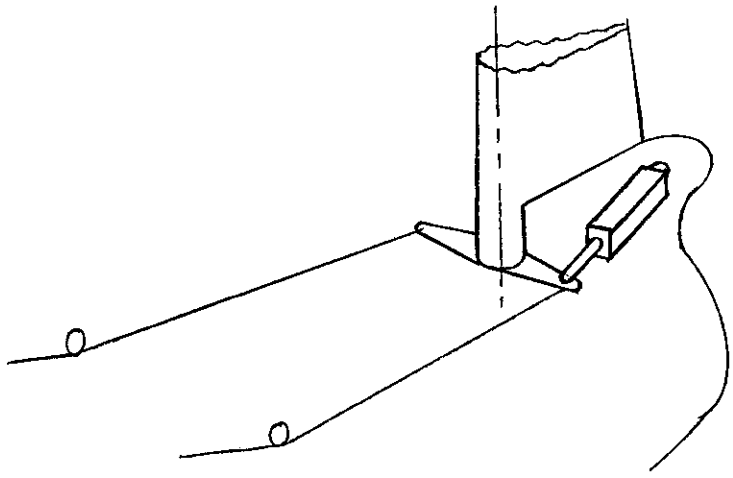

Fig. 28c

Figure 28 RUDDER SERVO INSTALLATION

Approved for Public Release

Contrails

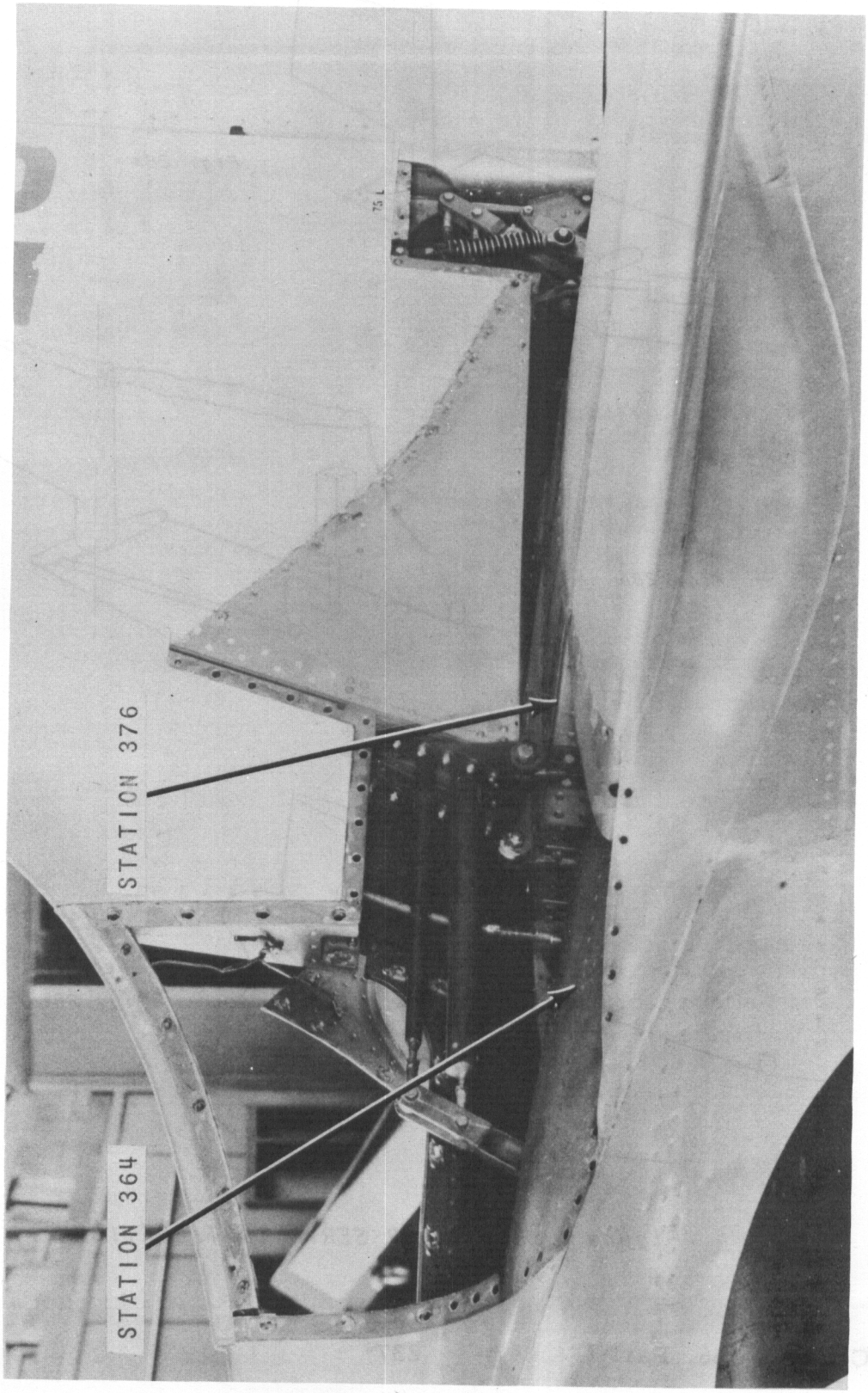

Figure 29 JUNCTION OF FUSELAGE, FIN, AND STABILIZER

Approved for Public Release

Contrails

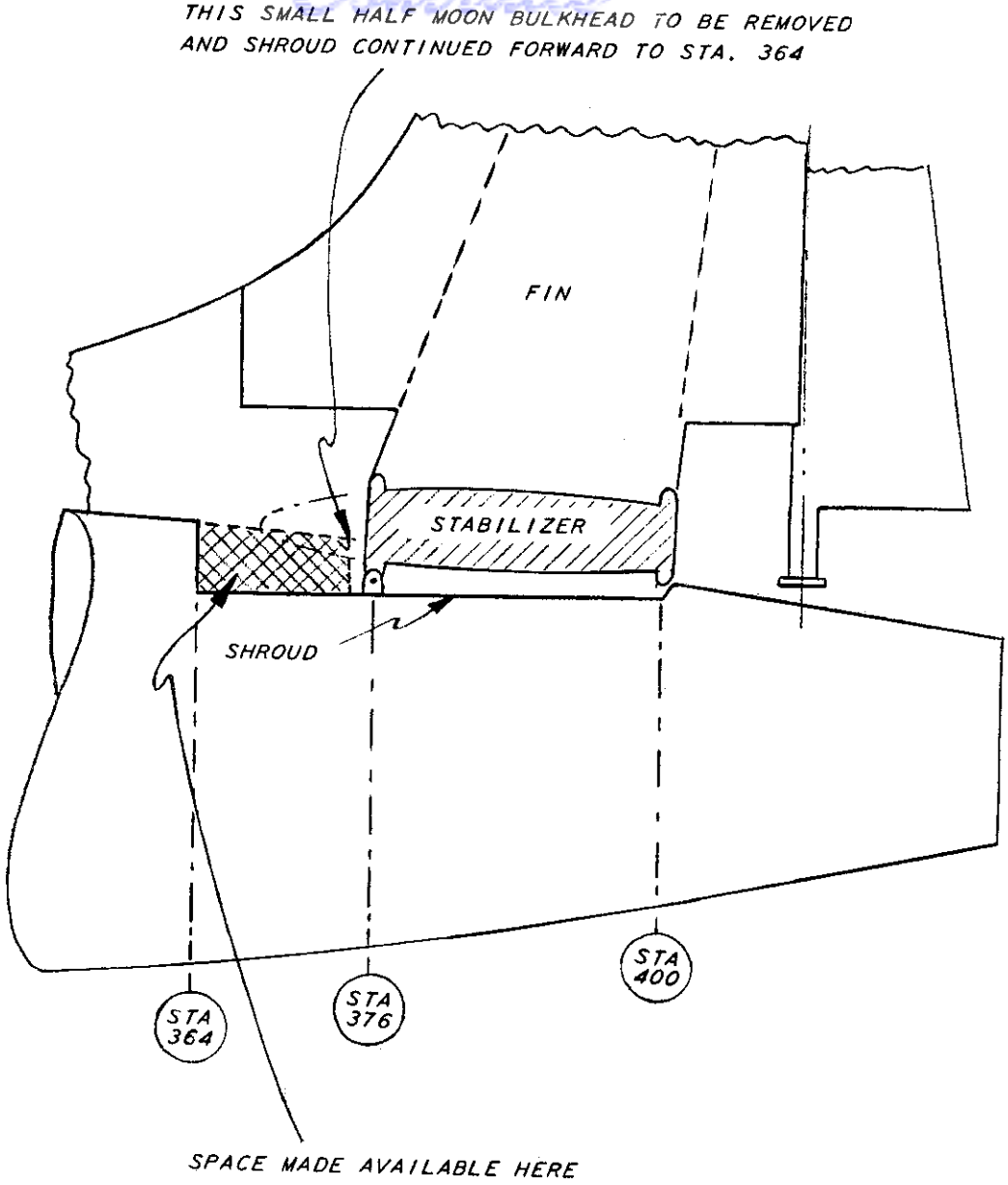

Figure 30 FUSELAGE MODIFICATION FORWARD OF STABILIZER

Approved for Public Release

Contrails

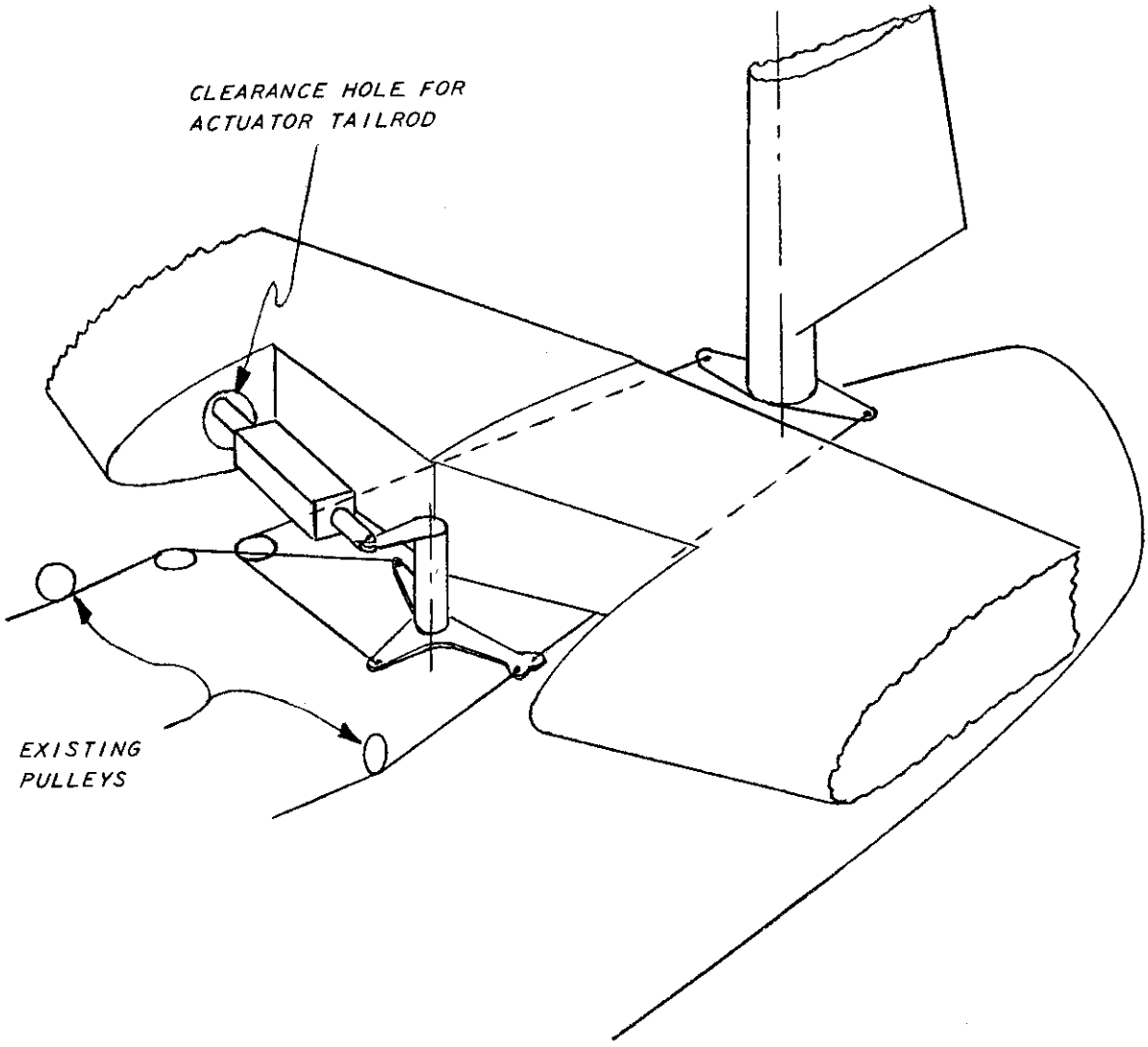

Figure 31 RUDDER SERVO INSTALLED IN MODIFIED FUSELAGE

Approved for Public Release

Contrails

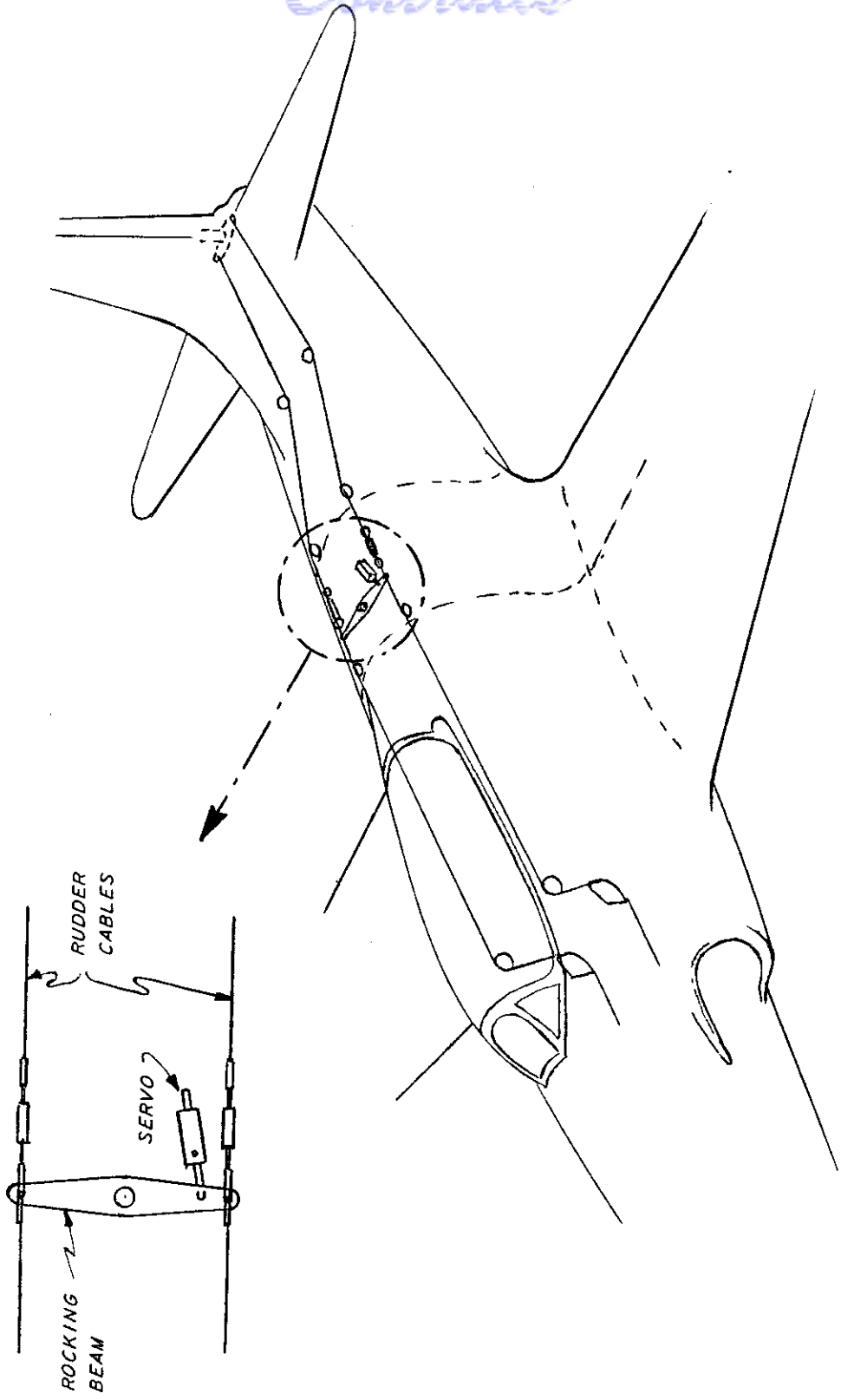

Figure 32 RUDDER SERVO INSTALLED IN ENGINE COMPARTMENT

Approved for Public Release

Contrails

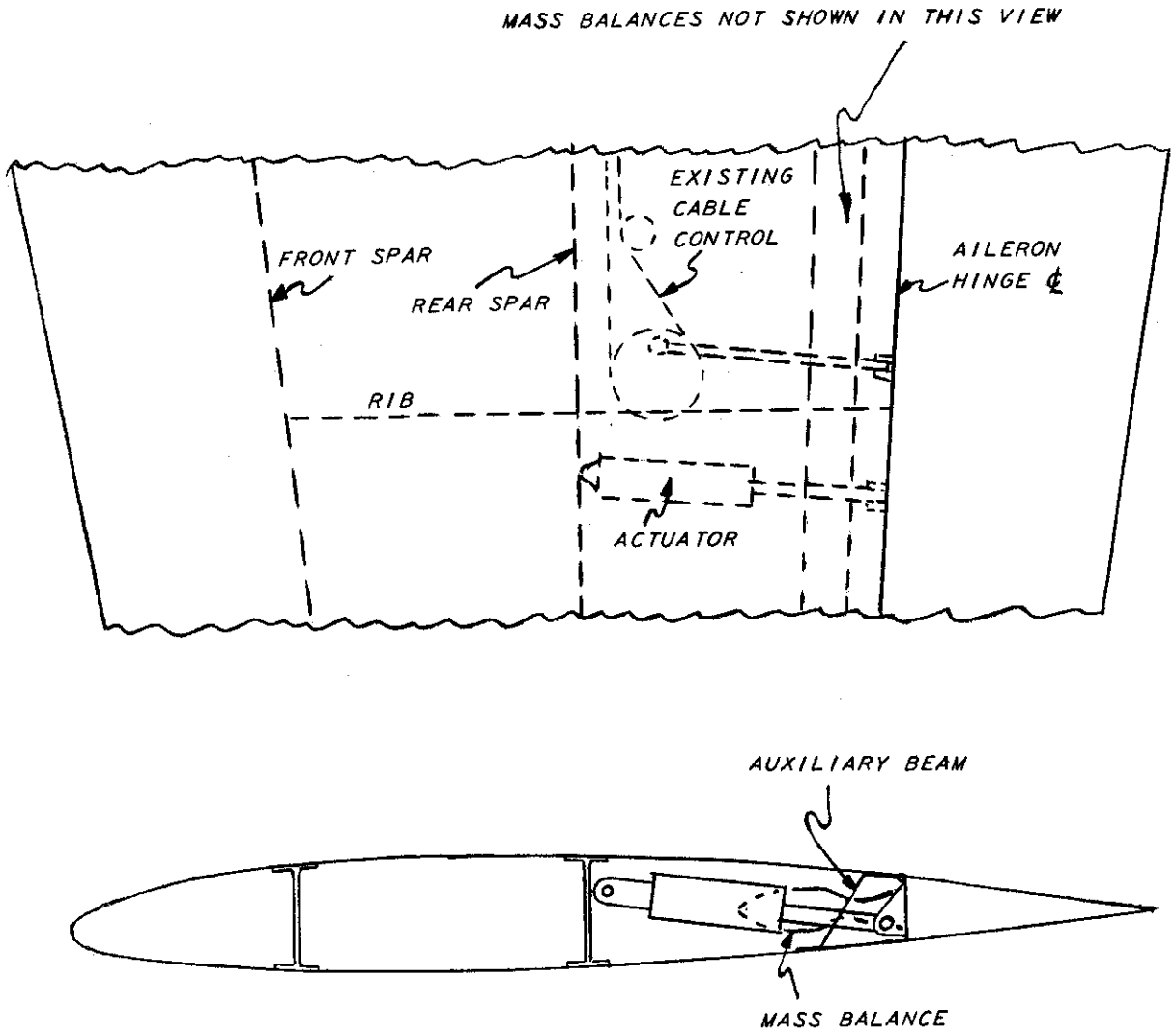

Figure 33 AILERON SERVO INSIDE WING

Approved for Public Release

Contrails

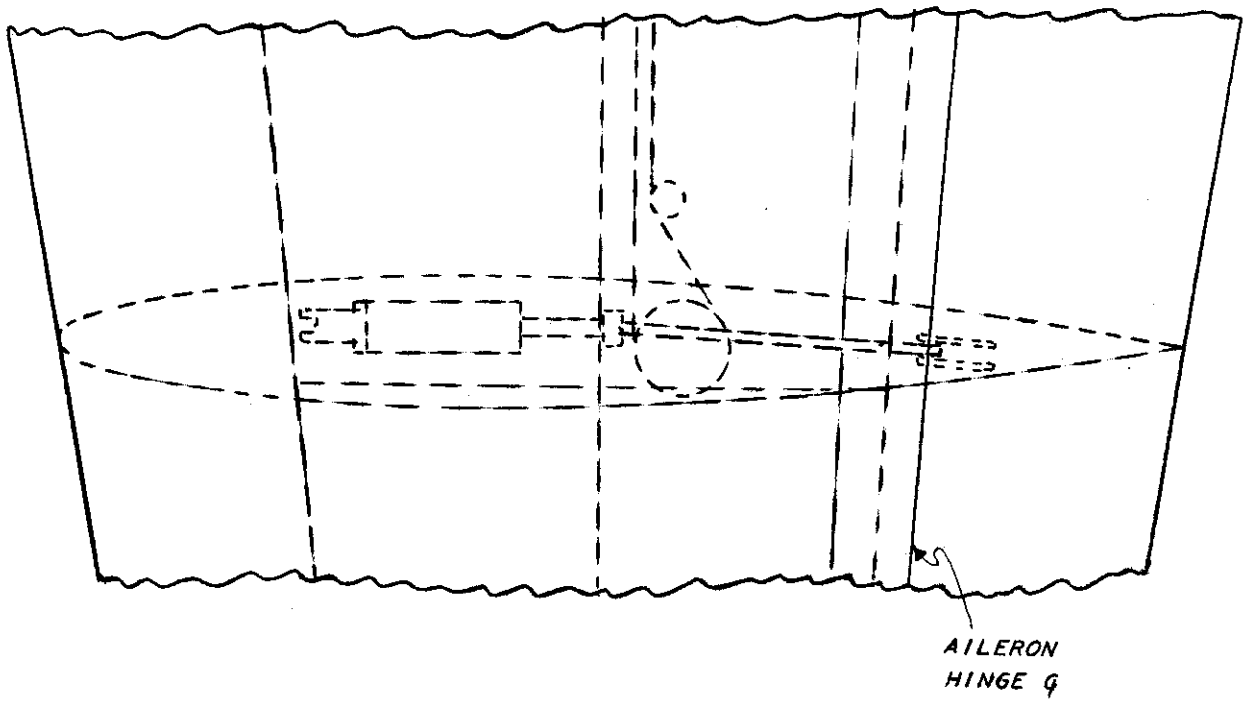

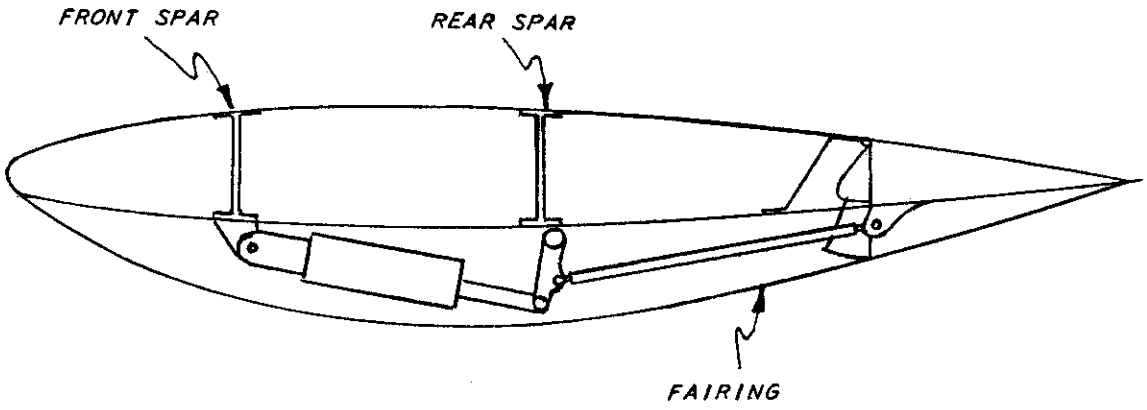

Figure 34 AILERON SERVO BELOW WING

Approved for Public Release

Contrails

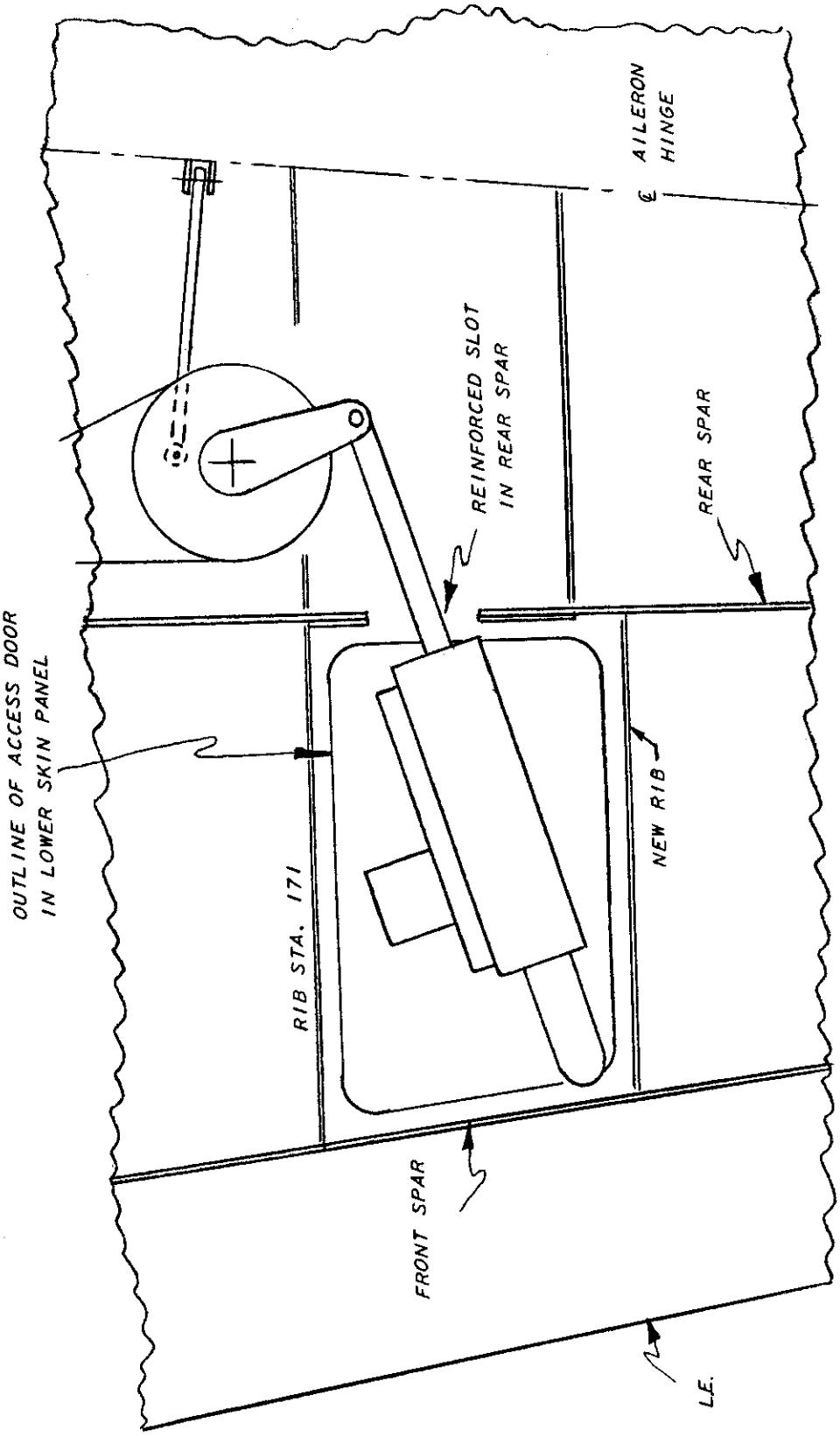

Figure 35 AILERON SERVO IN WING FUEL CELL

Approved for Public Release

Contrails

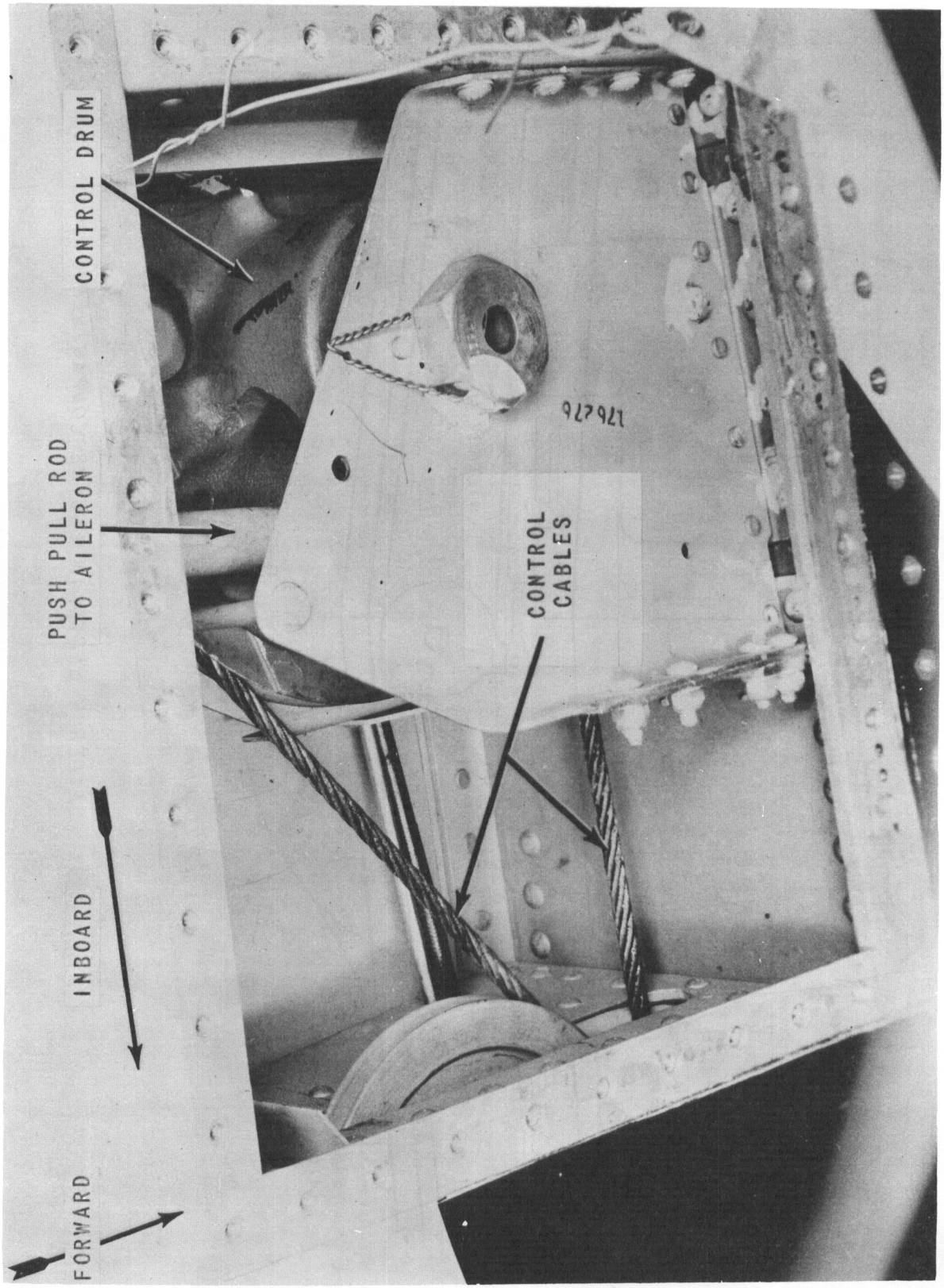

Figure 36 VIEW OF UNDERSIDE OF RIGHT HAND WING SHOWING AILERON CONTROL DRUM

Approved for Public Release

Contrails

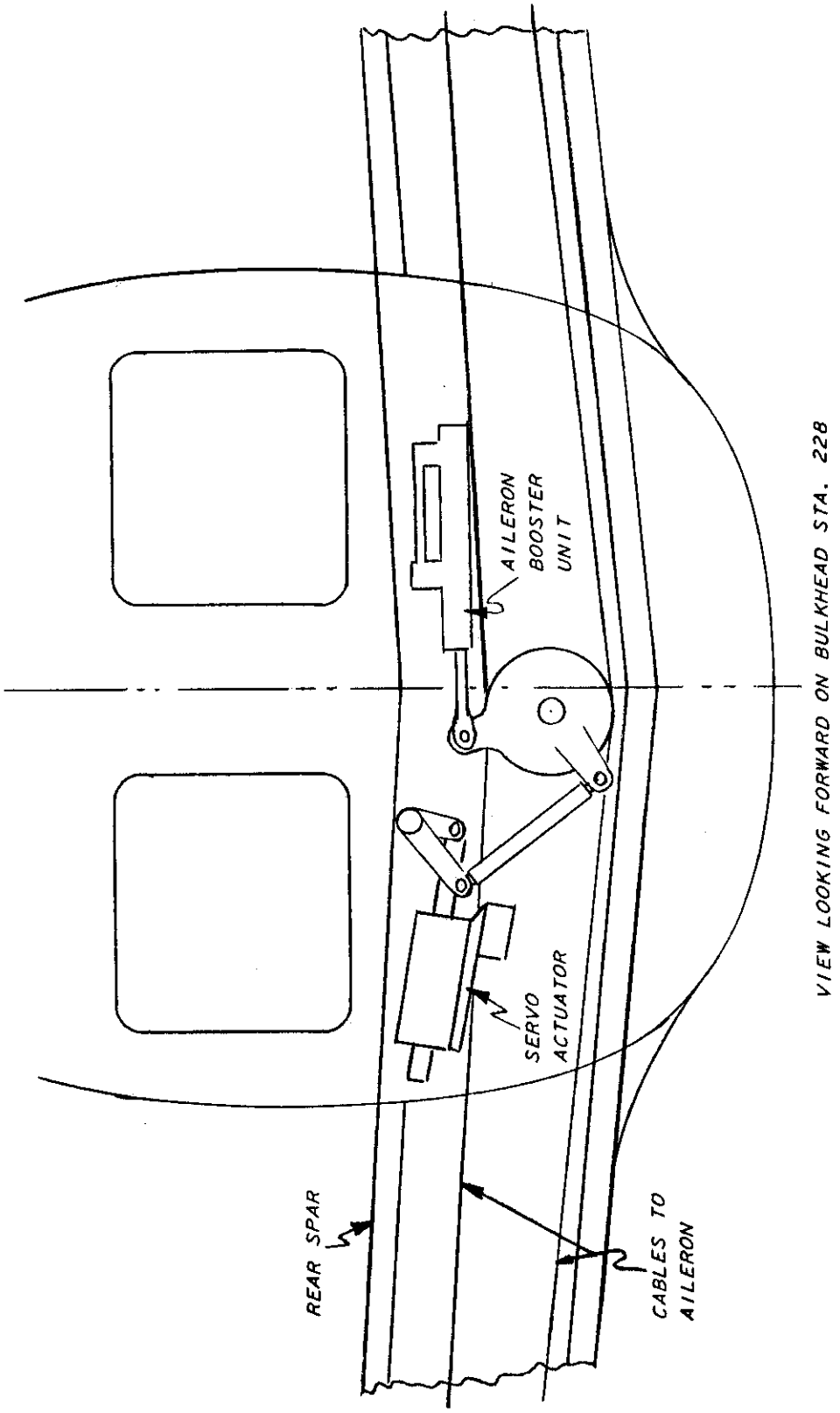

Figure 37 AILERON SERVO IN ENGINE COMPARTMENT

Approved for Public Release

Contrails

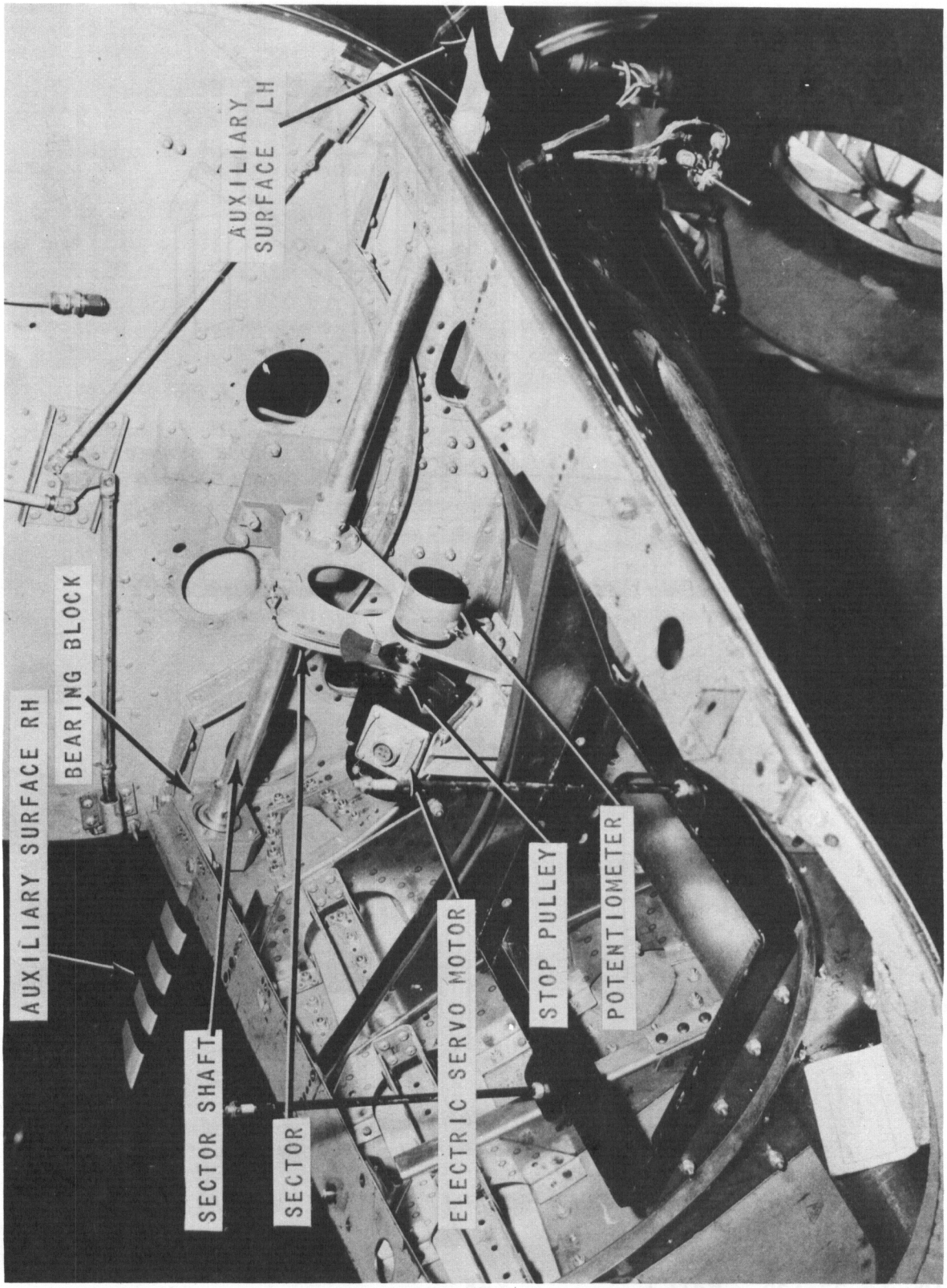

Figure 38 AUXILIARY SERVO INSTALLATION ON F-94 AIRCRAFT

Approved for Public Release

Contrails

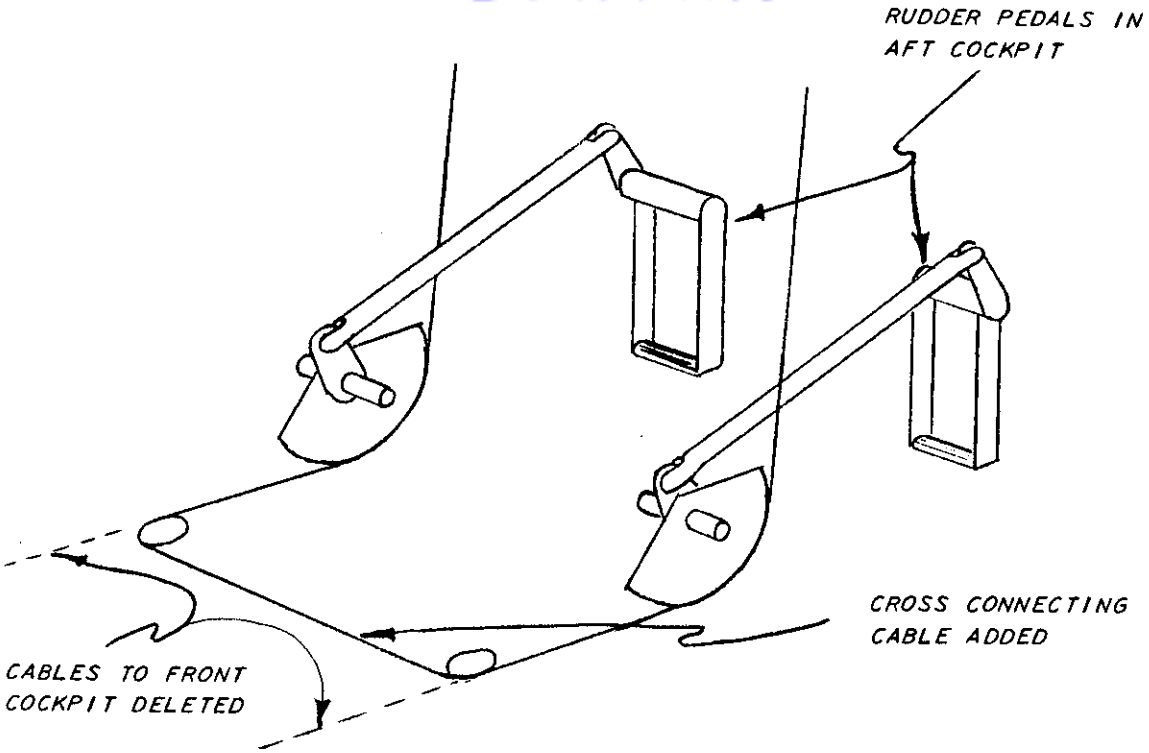

Fig. 39a REAR COCKPIT PEDALS, SHOWING CROSS CONNECTING CABLE

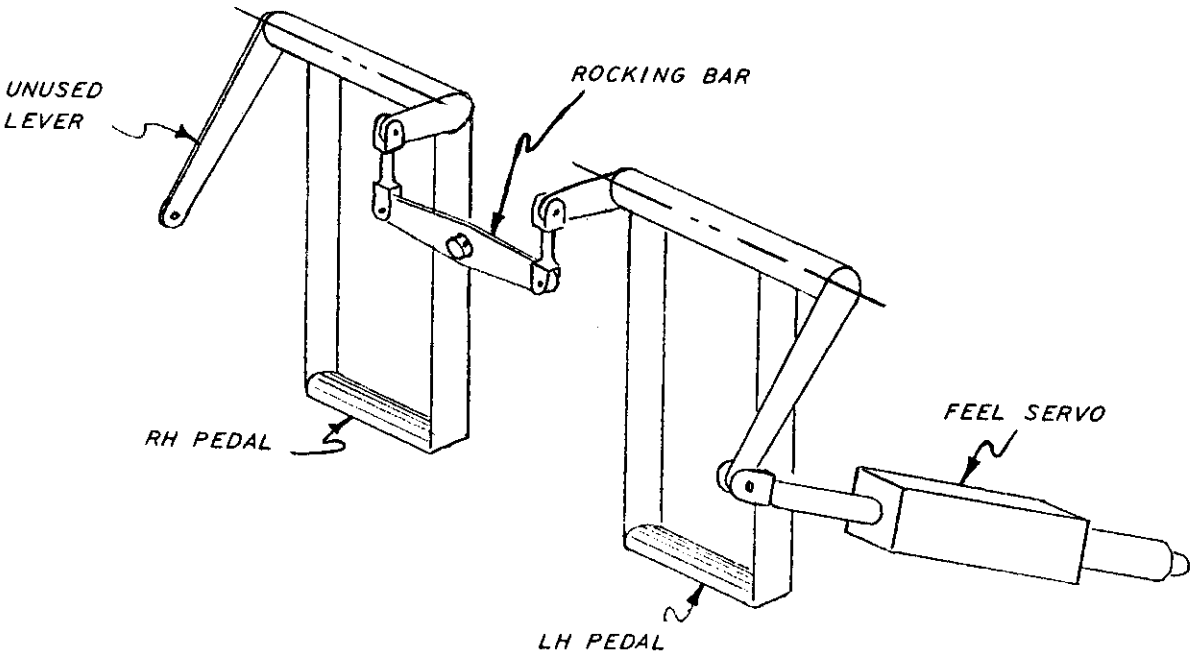

Fig. 39b FRONT COCKPIT RUDDER FEEL SERVO INSTALLATION

Figure 39 RUDDER COCKPIT CONTROL MODIFICATIONS

Approved for Public Release

Contrails

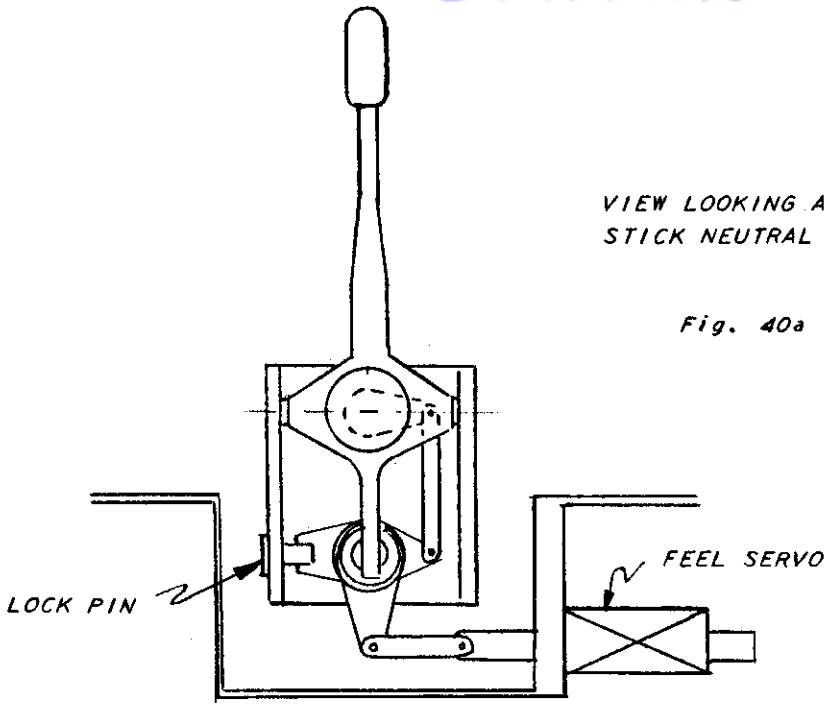

VIEW LOOKING AFT
STICK NEUTRAL

Fig. 40a

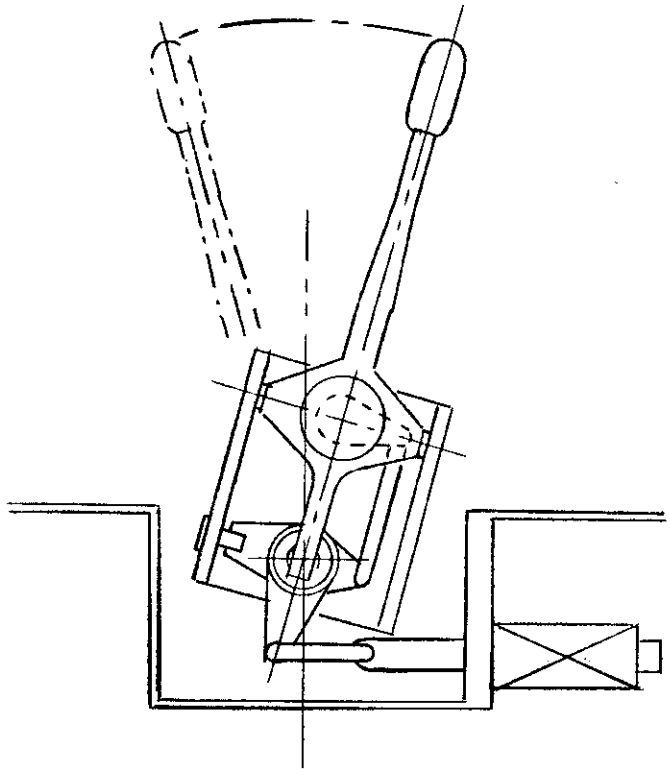

VIEW LOOKING AFT
FULL AILERON

Fig. 40b

Figure 40 AILERON FEEL SERVO - STICK CONTROL

Approved for Public Release

Contrails

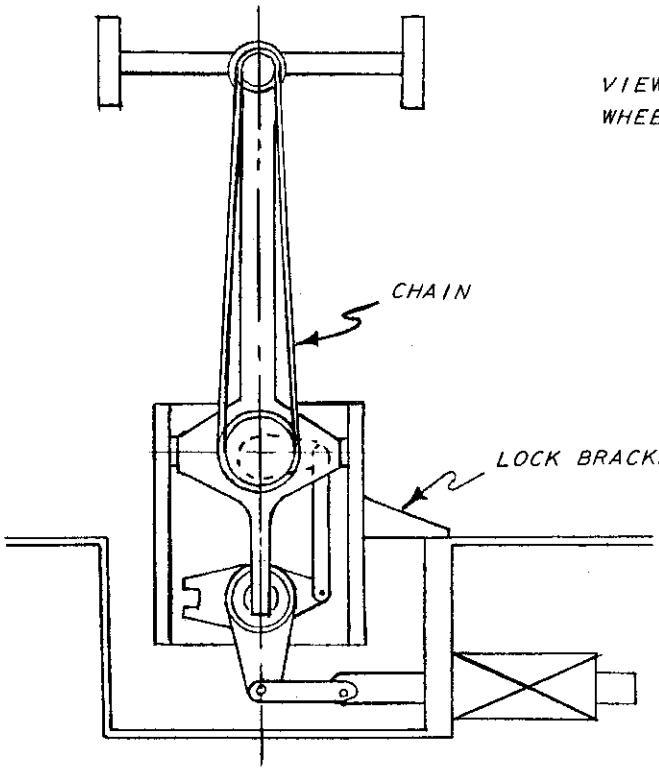

VIEW LOOKING AFT
WHEEL NEUTRAL

Fig. 41a

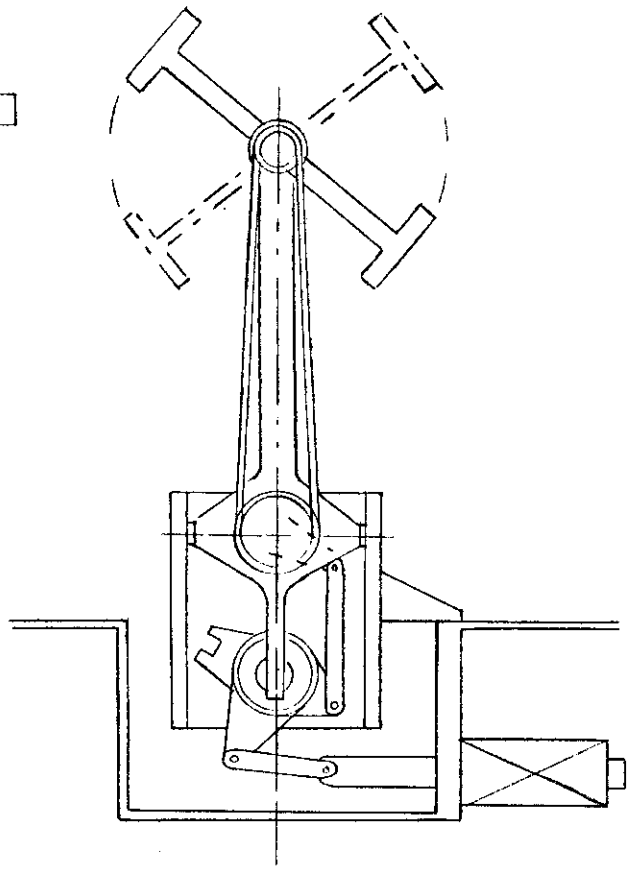

VIEW LOOKING AFT
FULL AILERON

Fig. 41b

Figure 41 AILERON FEEL SERVO - WHEEL CONTROL

Approved for Public Release

Contrails

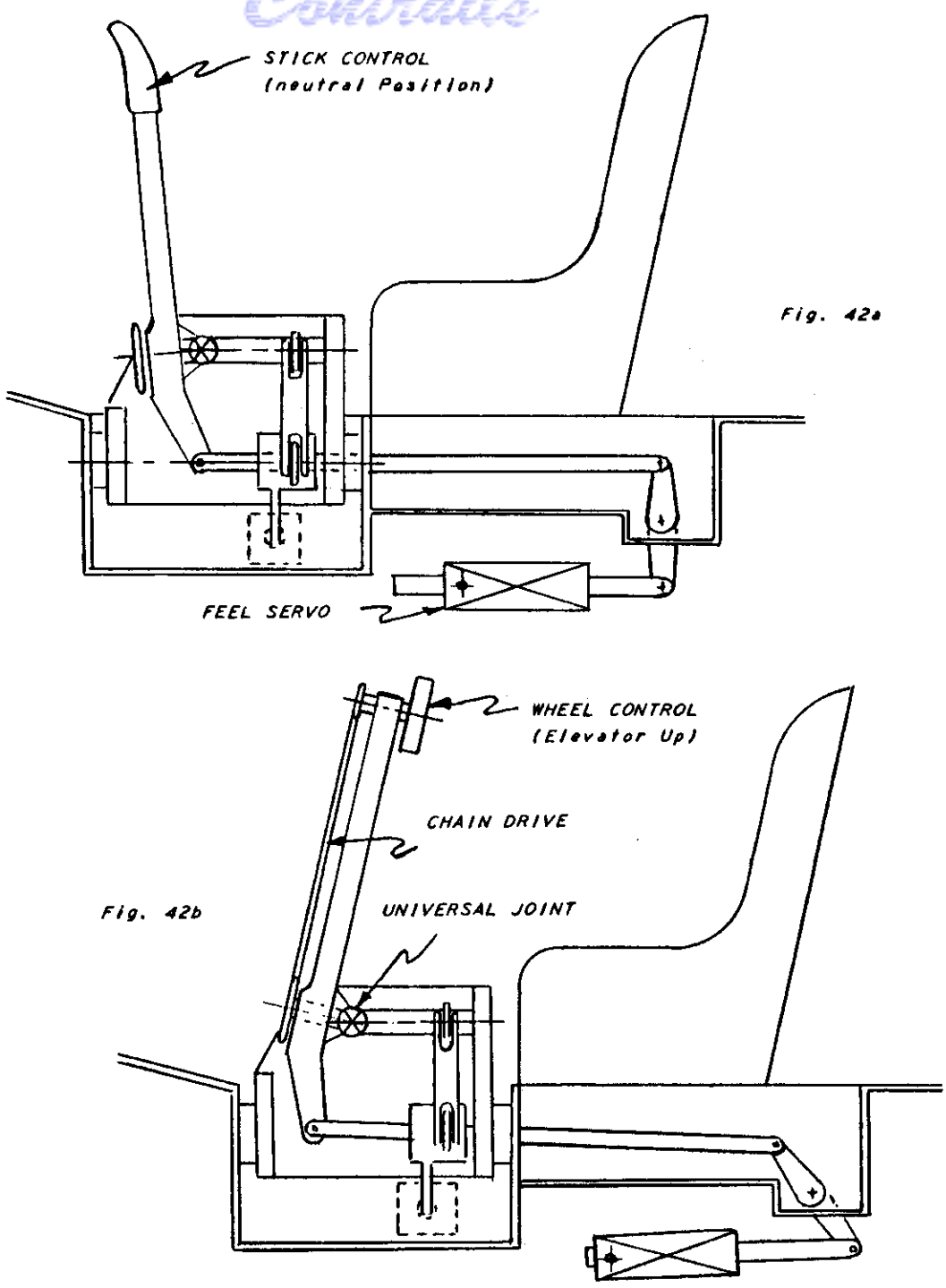

Figure 42 ELEVATOR FEEL SERVO

Approved for Public Release

Contrails

Figure 43 MOCK-UP OF WHEEL CONTROL IN FRONT COCKPIT

Approved for Public Release

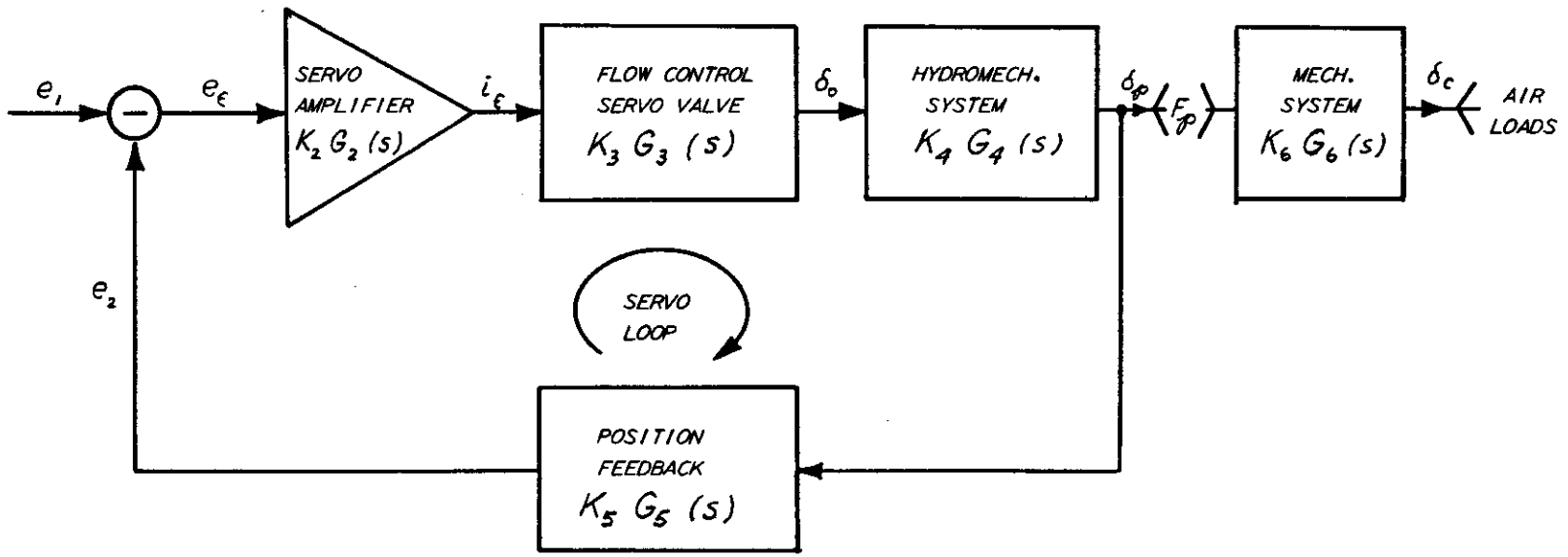

e_1 SERVO INPUT SIGNAL (VOLTS)

e_2 SERVO FEEDBACK SIGNAL (VOLTS)

$e_\epsilon = e_1 - e_2$ SERVO ERROR SIGNAL (VOLTS)

i_ϵ SERVOVALVE CONTROL CURRENT (MA)

δ_o EQUIVALENT FLUID DISPLACEMENT OUT OF SERVOVALVE (IN.)

δ_p SERVOPISTON POSITION (IN.)

δ_c CONTROL-SURFACE POSITION (IN.)

F_p SERVOPISTON FORCE (lb)

K STATIC TRANSFER FUNCTION

$G(s)$ DYNAMIC TRANSFER FUNCTION, IN TERMS OF THE LAPLACE VARIABLE, S

$K_V = K_1 K_3 K_4 K_5$ SERVOLOOP GAIN (VELOCITY GAIN), SEC^{-1}

Figure 44 POSITION SERVO BLOCK DIAGRAM

Approved for Public Release

Controls

DYNAMIC RESPONSE OF HINGE MOMENT COEFFICIENT PER UNIT SURFACE DEFLECTION $\left(\frac{C_h}{\delta_s}\right)$

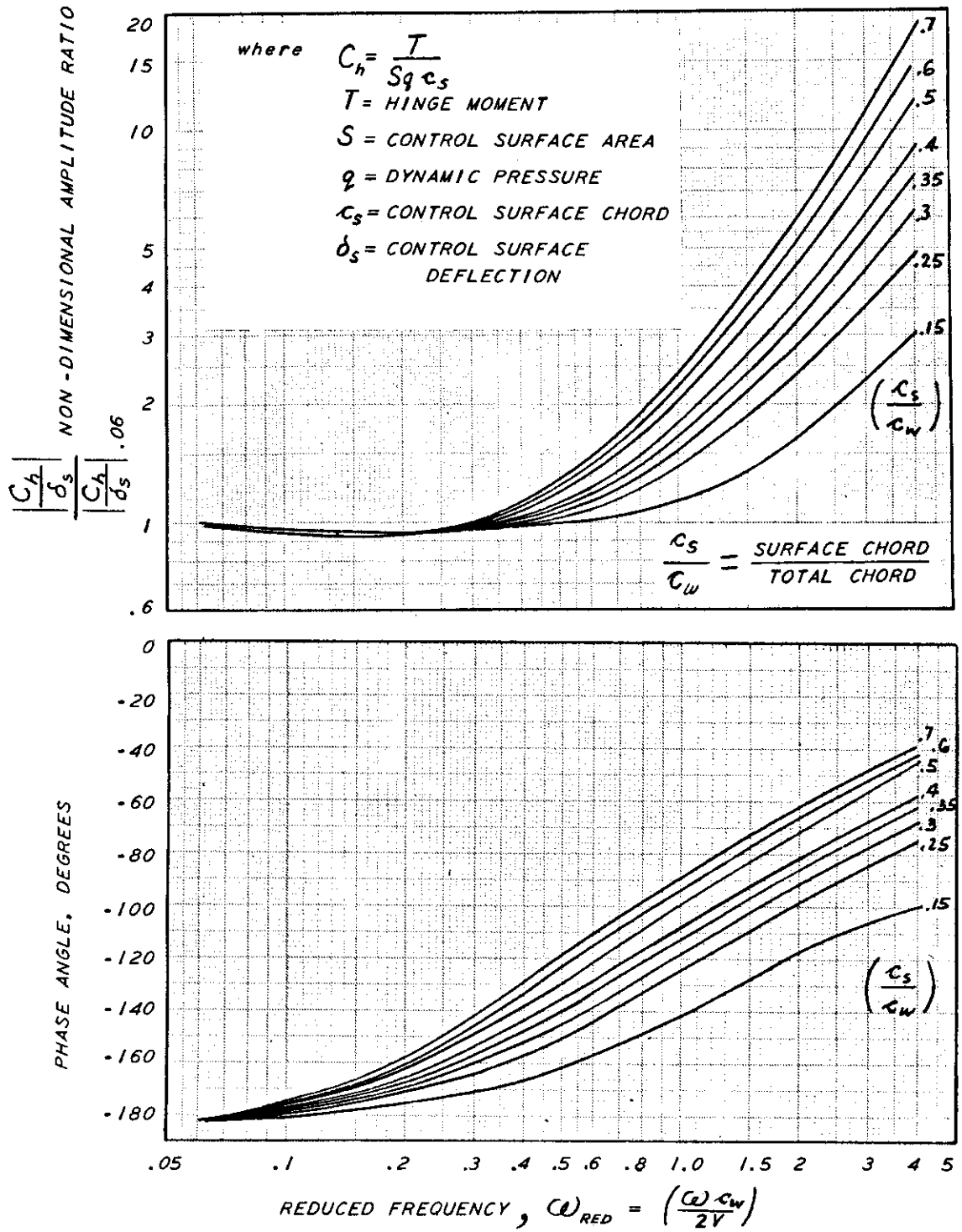

Figure 45 AERODYNAMIC LOADING OF CONTROL SURFACE

Approved for Public Release

Contrails

DYNAMIC RESPONSE OF TORQUE PER UNIT DEFLECTION $\left(\frac{F_s}{\delta_s}\right)$ FOR SIMPLE FIRST-ORDER TORSIONAL SYSTEM OF SPRING h_d AND DAMPER b_d

WHERE $\tau_1 = \frac{b_d}{h_d}$ SECONDS

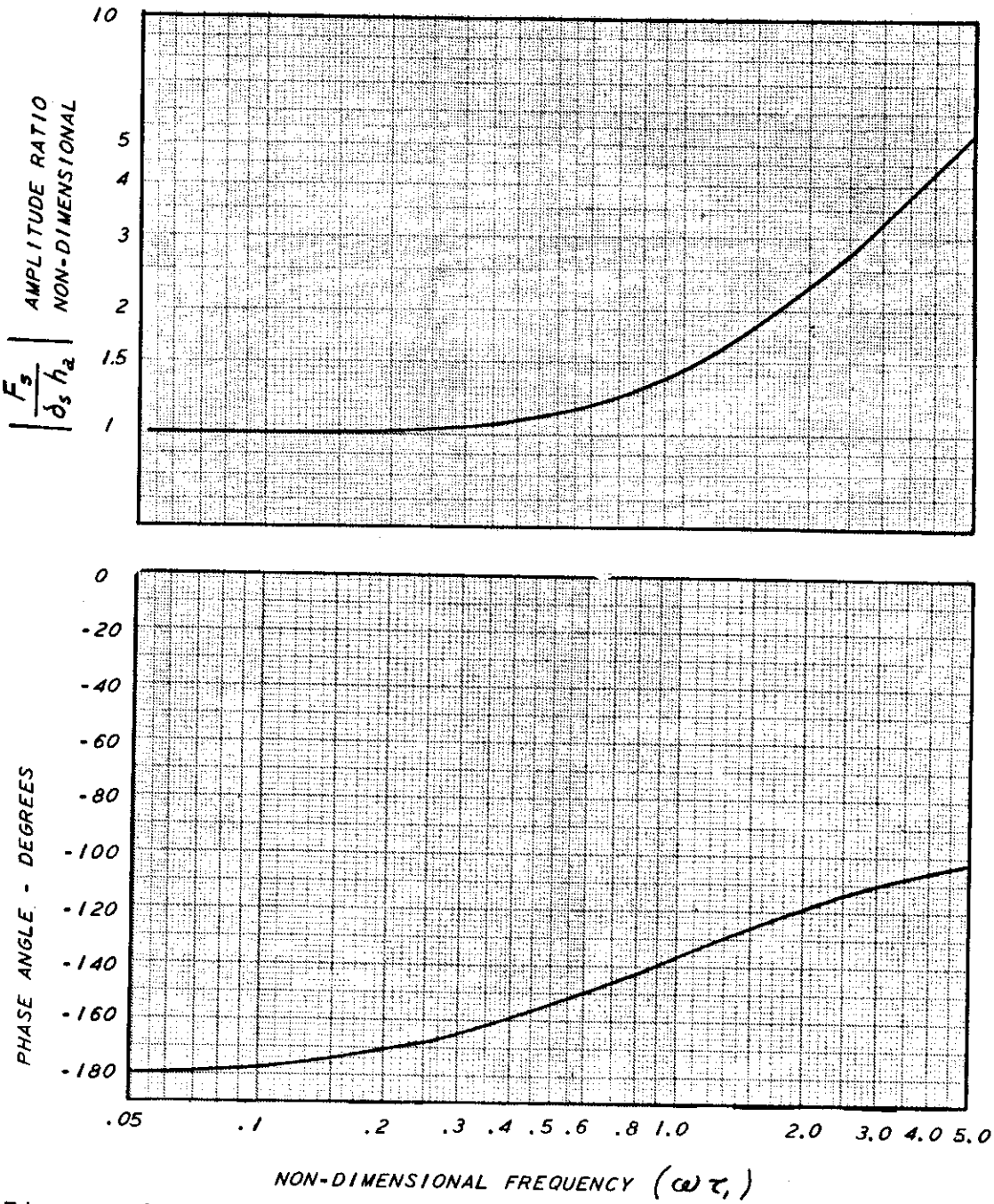

Figure 46 NON-DIMENSIONAL RESPONSE OF FIRST-ORDER SYSTEM

Approved for Public Release

Contrails

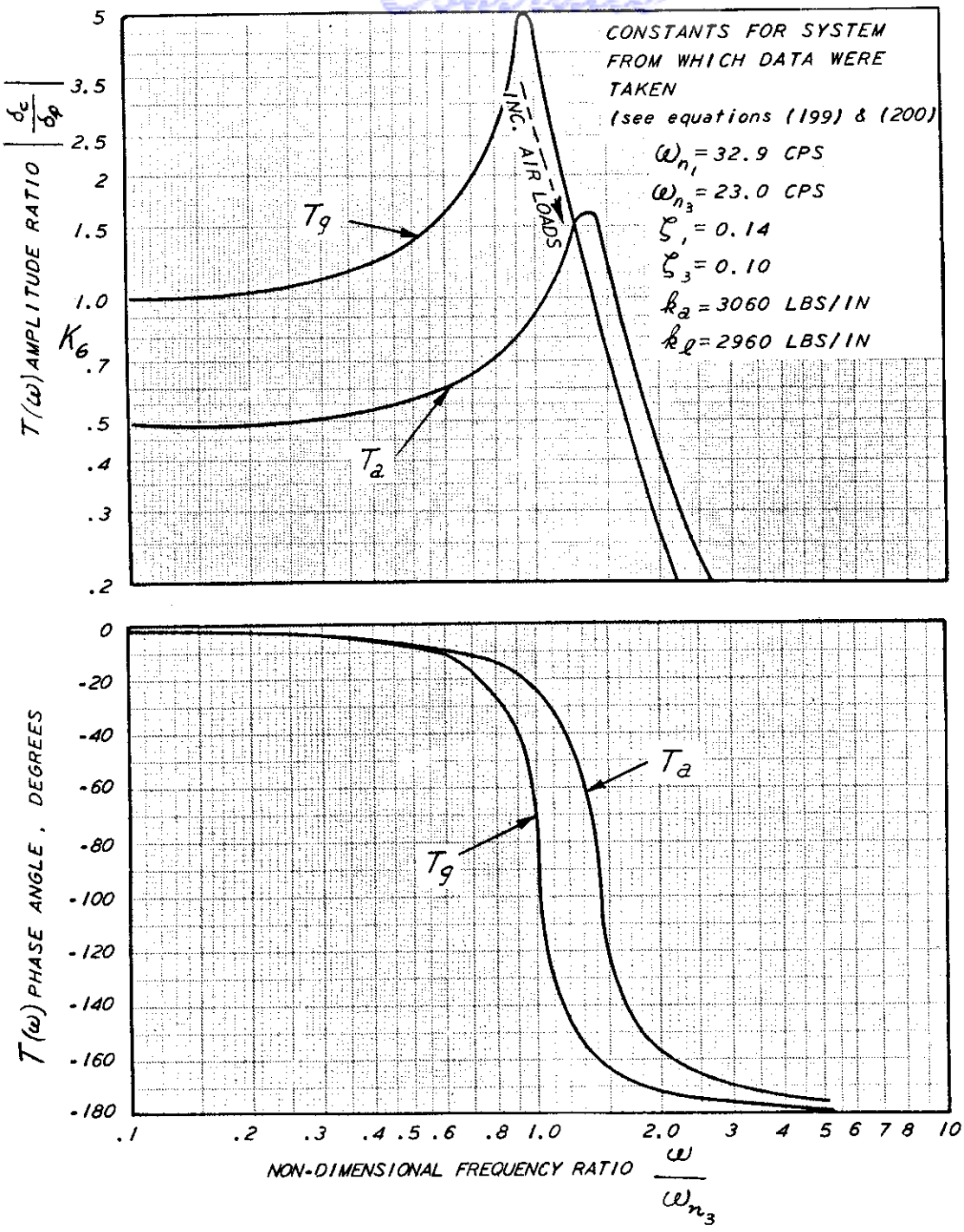

Figure 47 POSITION TRANSMISSION RATIO, FREQUENCY RESPONSE

TRANSMISSION RATIO, $T(\omega) = \left(\frac{\delta_c}{\delta_s}\right)(\omega)$

Approved for Public Release

Controls

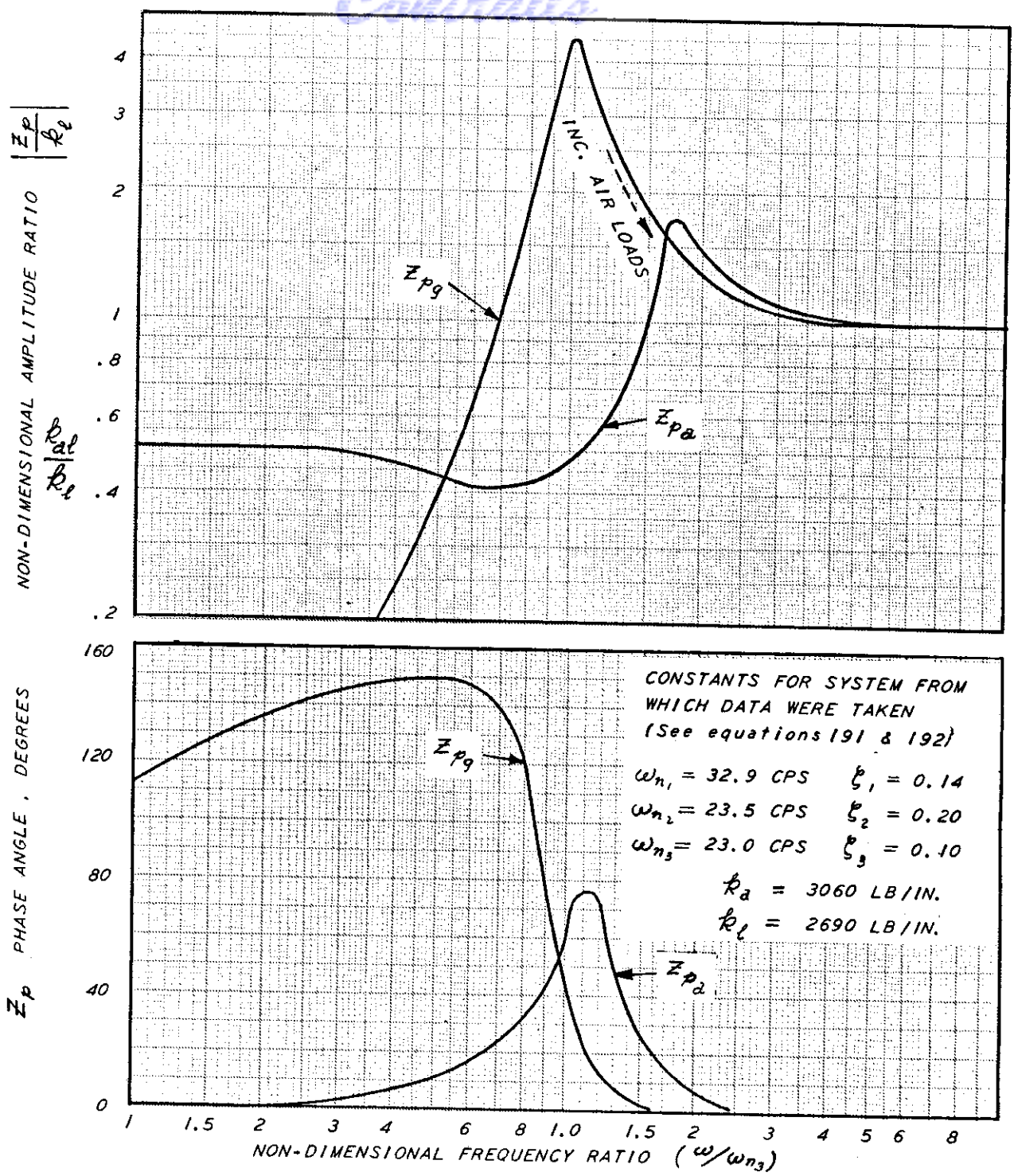

Figure 48 SERVO LOAD IMPEDANCE, FREQUENCY RESPONSE

SERVO LOAD IMPEDANCE, $Z_p = (F_p/\delta_p)$

Approved for Public Release

Controls

STATIC RESPONSE OF HYDRAULIC FLOW FROM SERVOVALVE AS A FUNCTION OF VALVE CONTROL CURRENT AND LOAD PRESSURE
(From "CONTRIBUTIONS TO HYDRAULIC CONTROL, PART 3, PRESSURE-FLOW RELATIONSHIPS FOR A 4-WAY VALVE" by J.F. Blackburn, ASME Paper 52-A-42 November 1952)

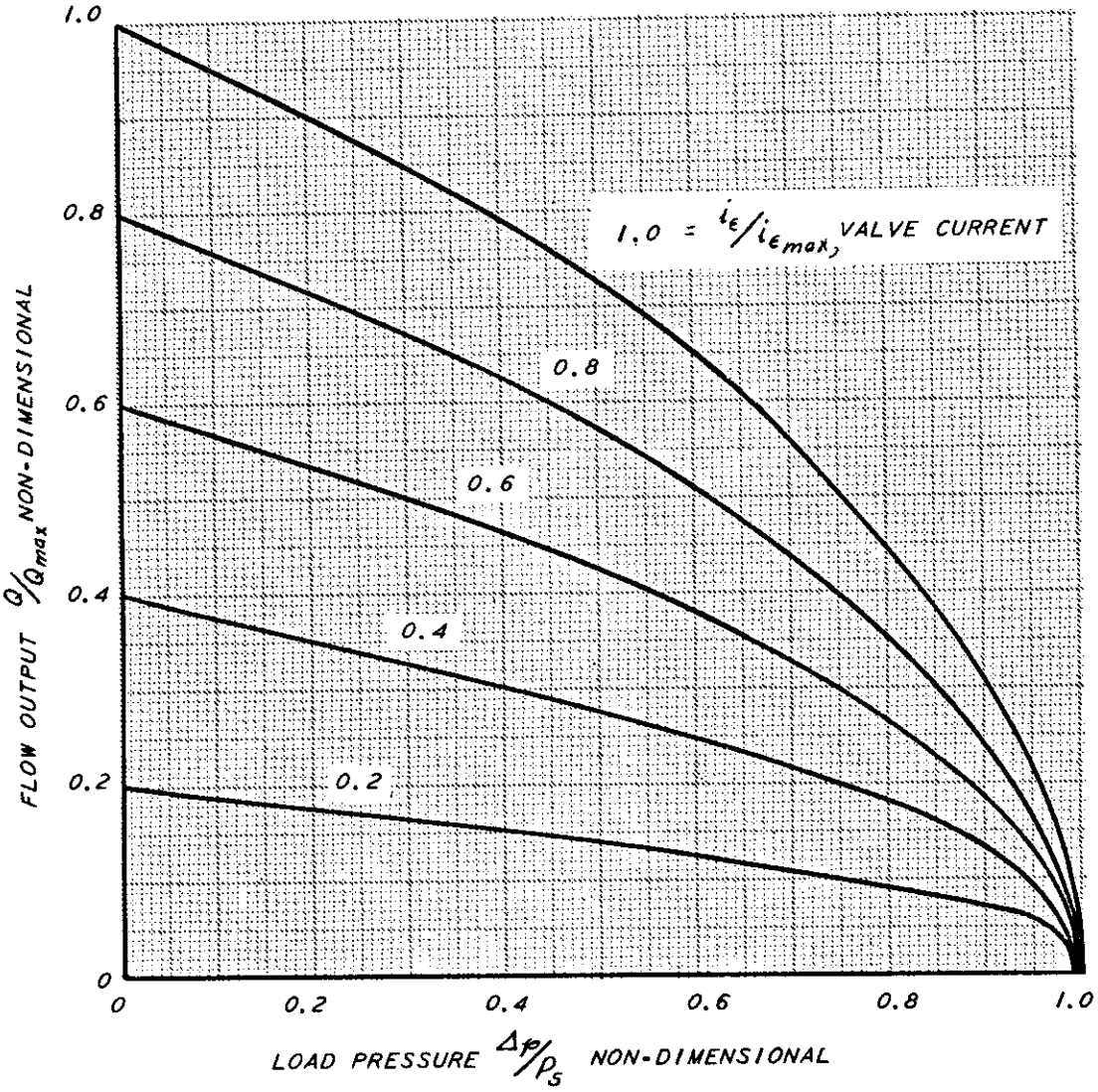

Figure 49 STATIC RESPONSE OF FOUR-WAY, FLOW-CONTROL SERVOVALVE WITH ZERO OVERLAP

Approved for Public Release

Contrails

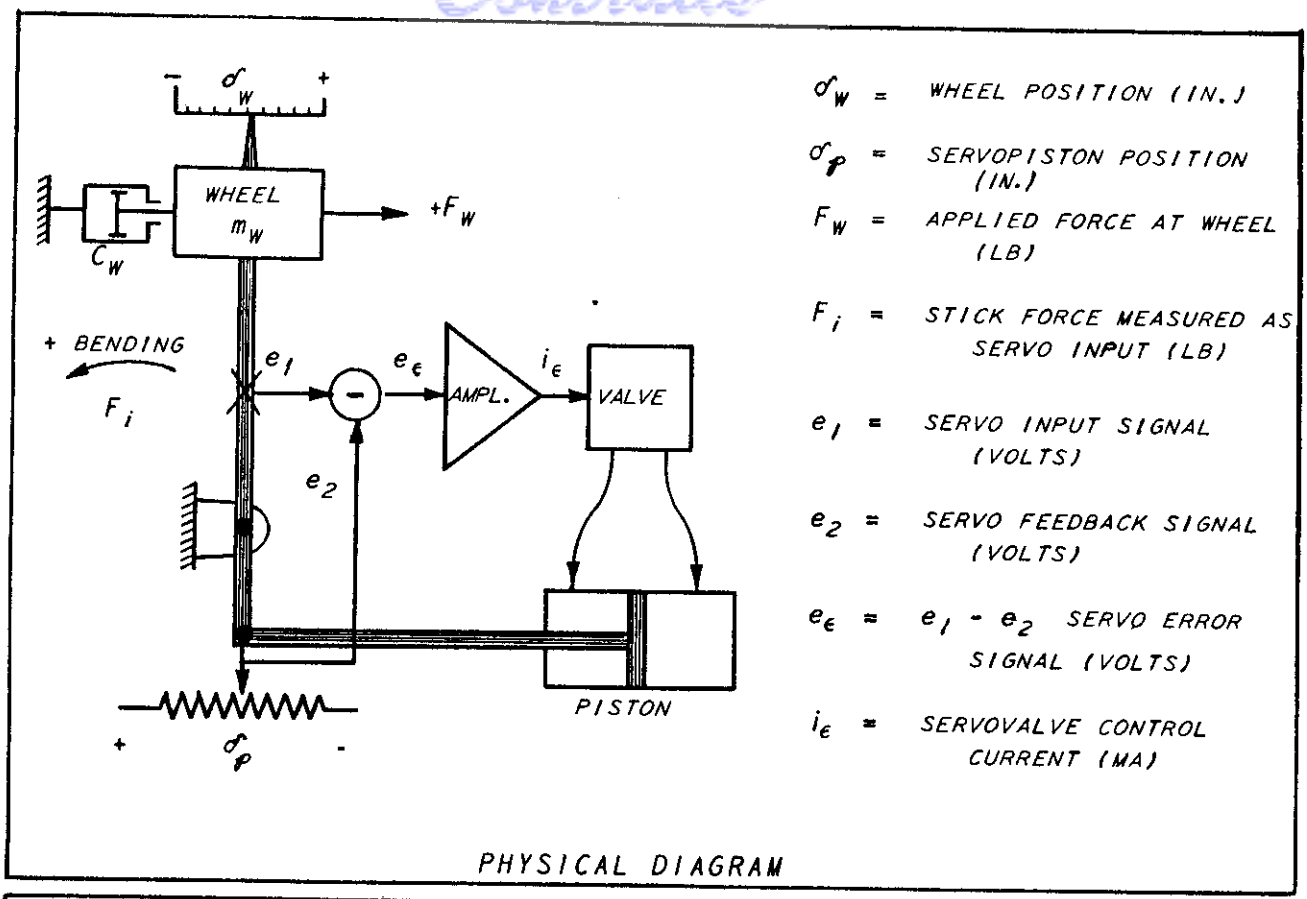

PHYSICAL DIAGRAM

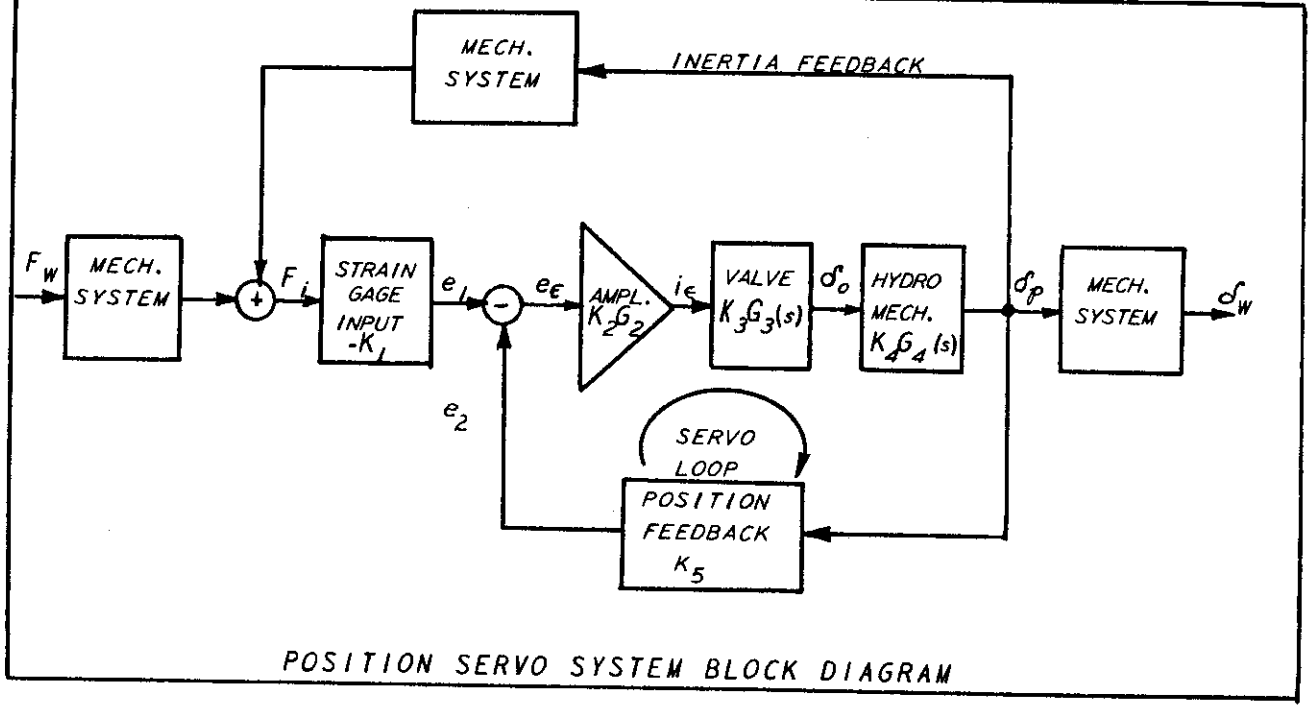

POSITION SERVO SYSTEM BLOCK DIAGRAM

Figure 50 FEEL SERVO WITH FLOW-CONTROL SERVOVALVE

Approved for Public Release

Contrails

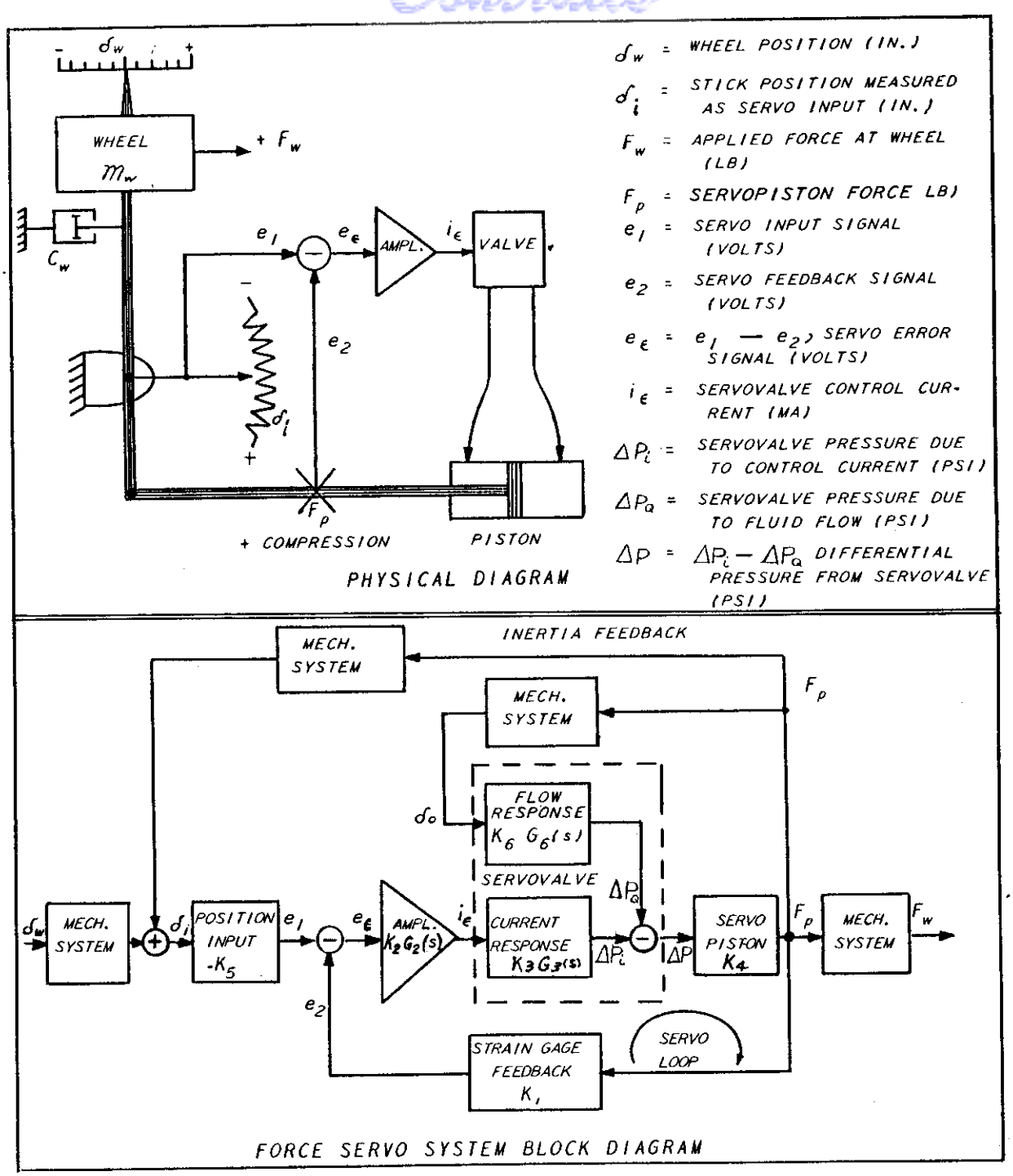

Figure 51 FEEL SERVO WITH PRESSURE-CONTROL SERVOVALVE

Approved for Public Release

Contrails

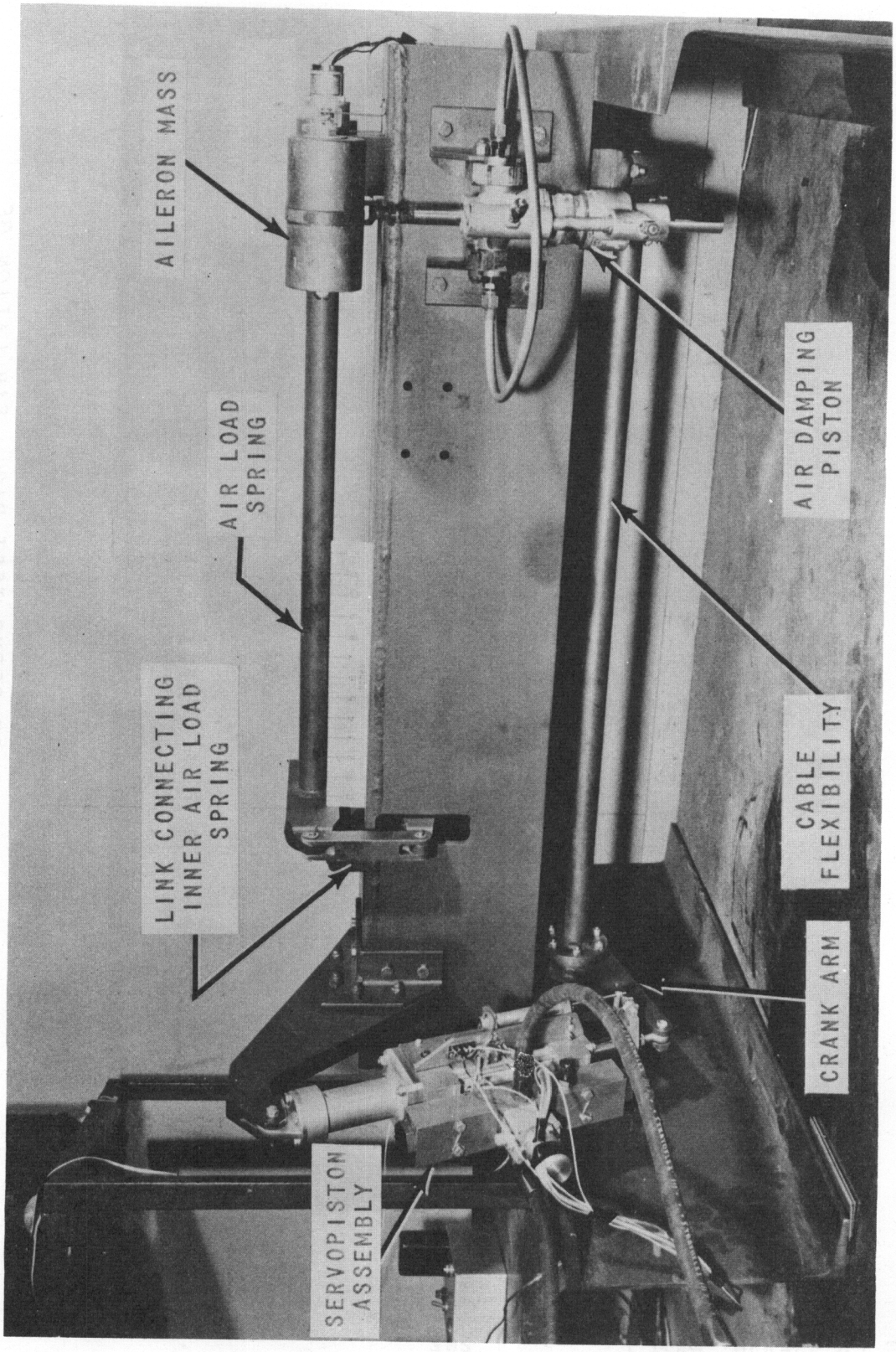

Figure 52 POSITION SERVO TEST RIG - SIMULATION OF FUSELAGE MOUNTED AILERON SERVO

Approved for Public Release

Contrails

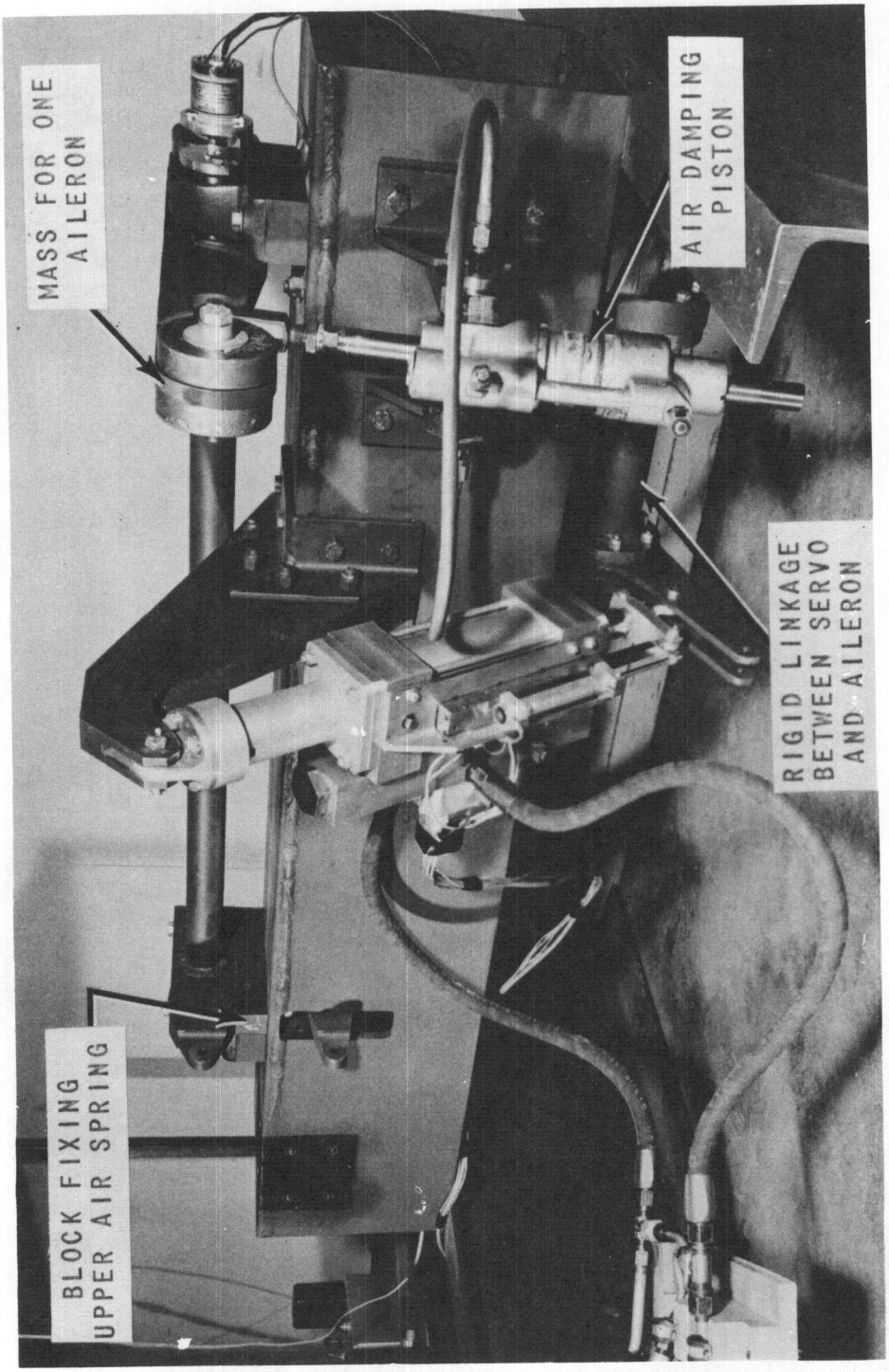

Figure 53. POSITION SERVO TEST RIG - SIMULATION OF WING MOUNTED AILERON SERVO

Approved for Public Release

Contrails

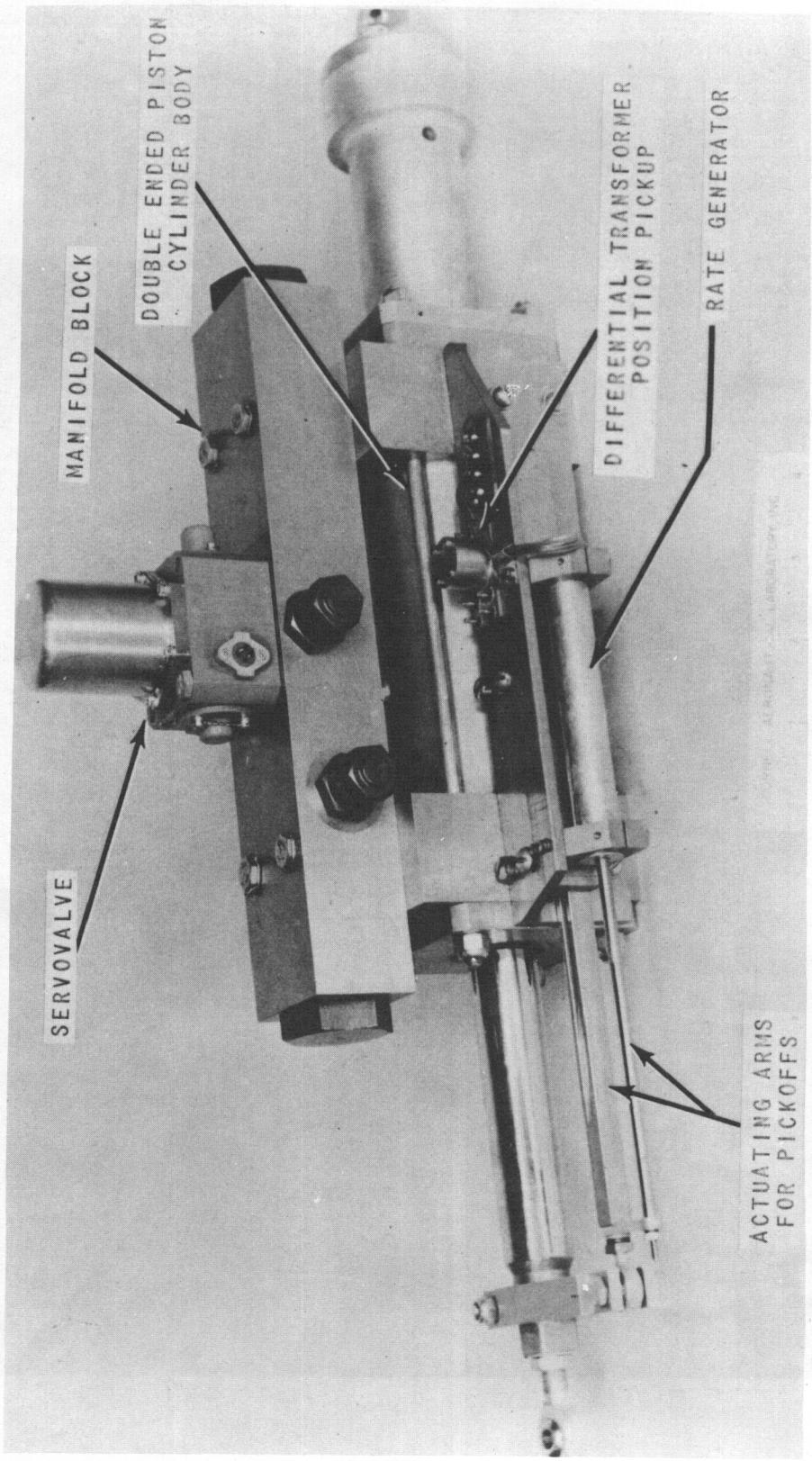

Figure 54 SERVOPISTON ASSEMBLY

Approved for Public Release

Contrails

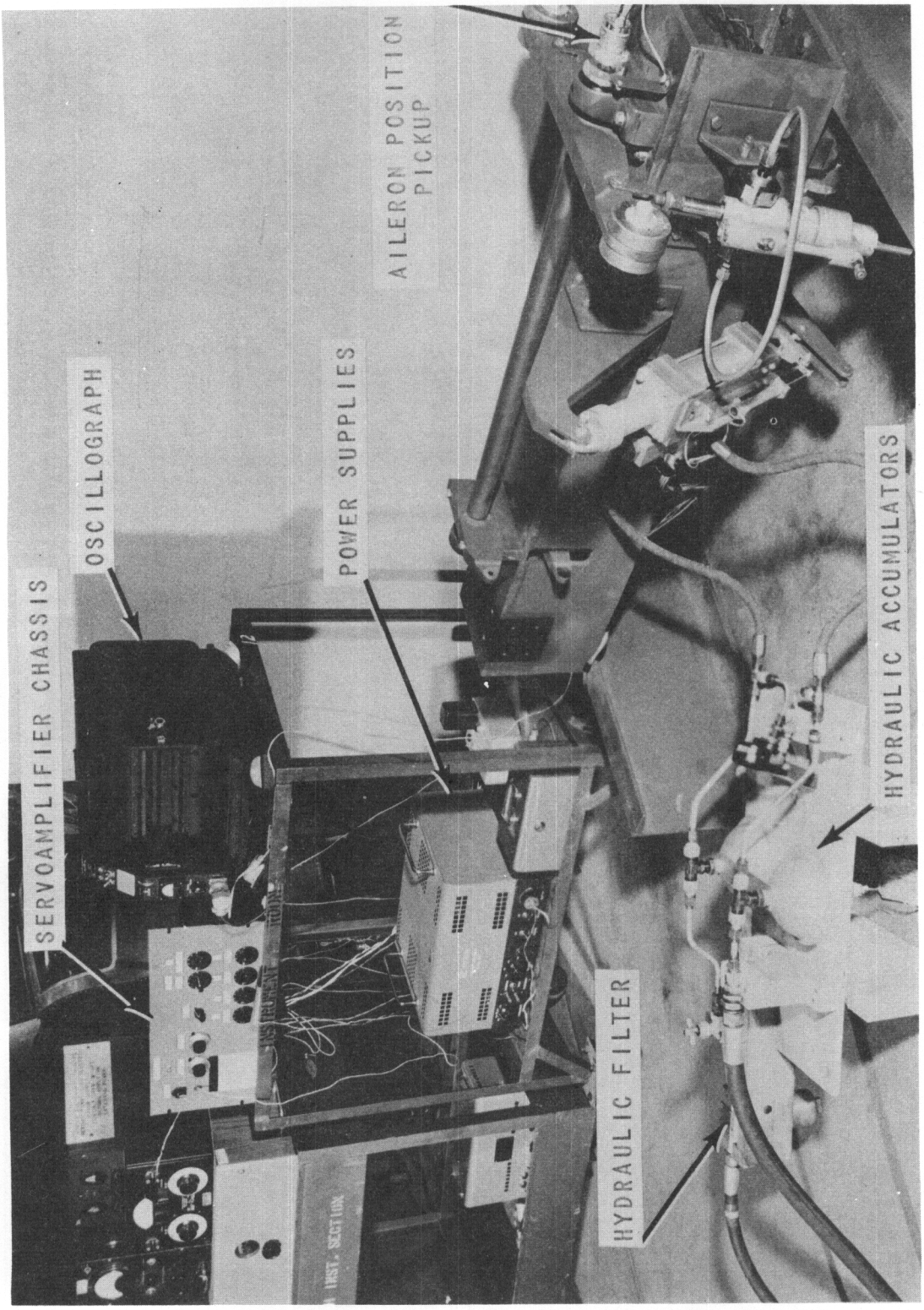

Figure 55 POSITION SERVO TEST AREA

Approved for Public Release

Contrails

SINUSOIDAL RESPONSES; FUSELAGE-MOUNTED SERVO,
HALF-SCALE LOADS, AIR OPERATION

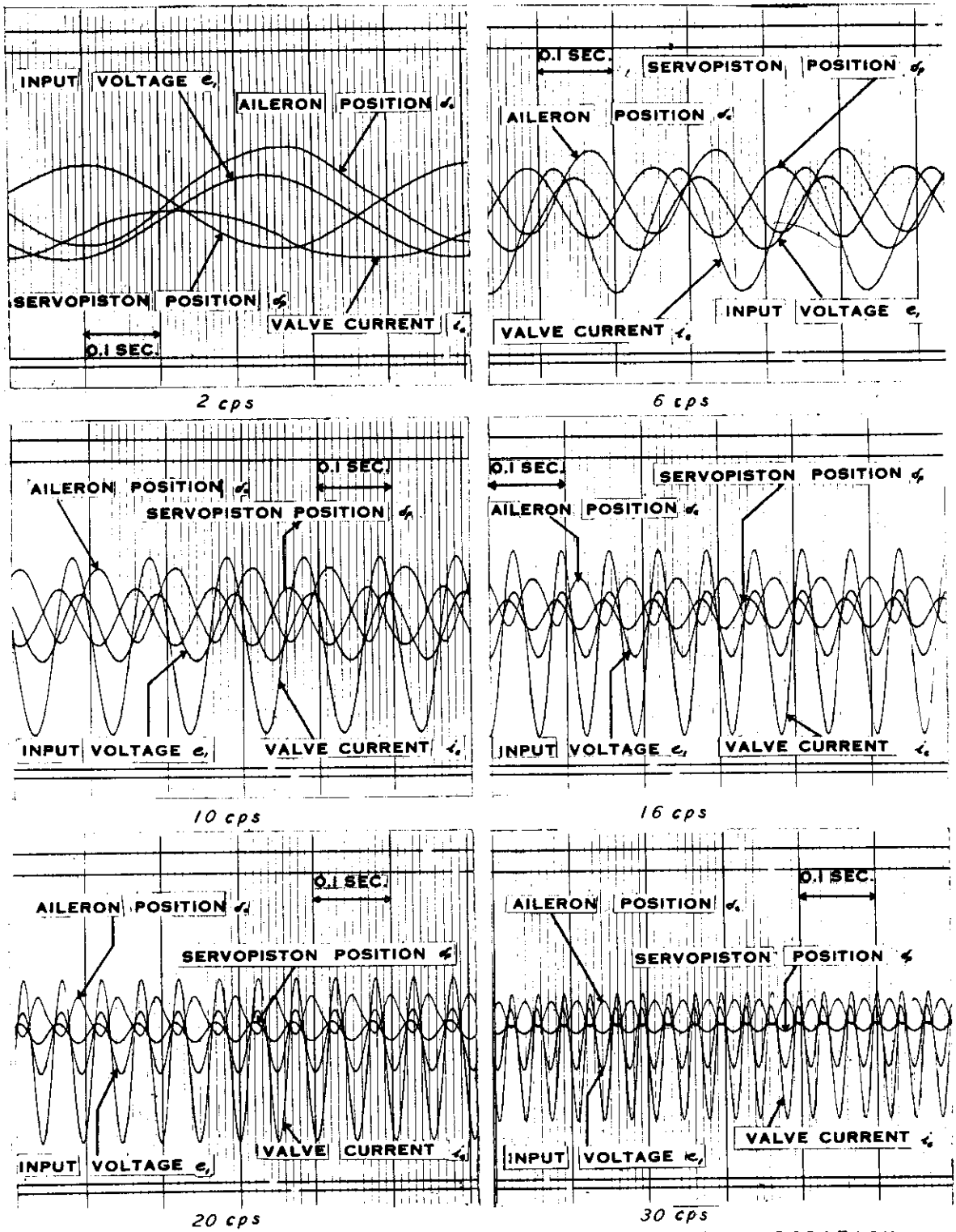

Figure 56 SINUSOIDAL OSCILLOGRAMS TAKEN ON POSITION SERVO TEST RIG

Approved for Public Release

Contrails

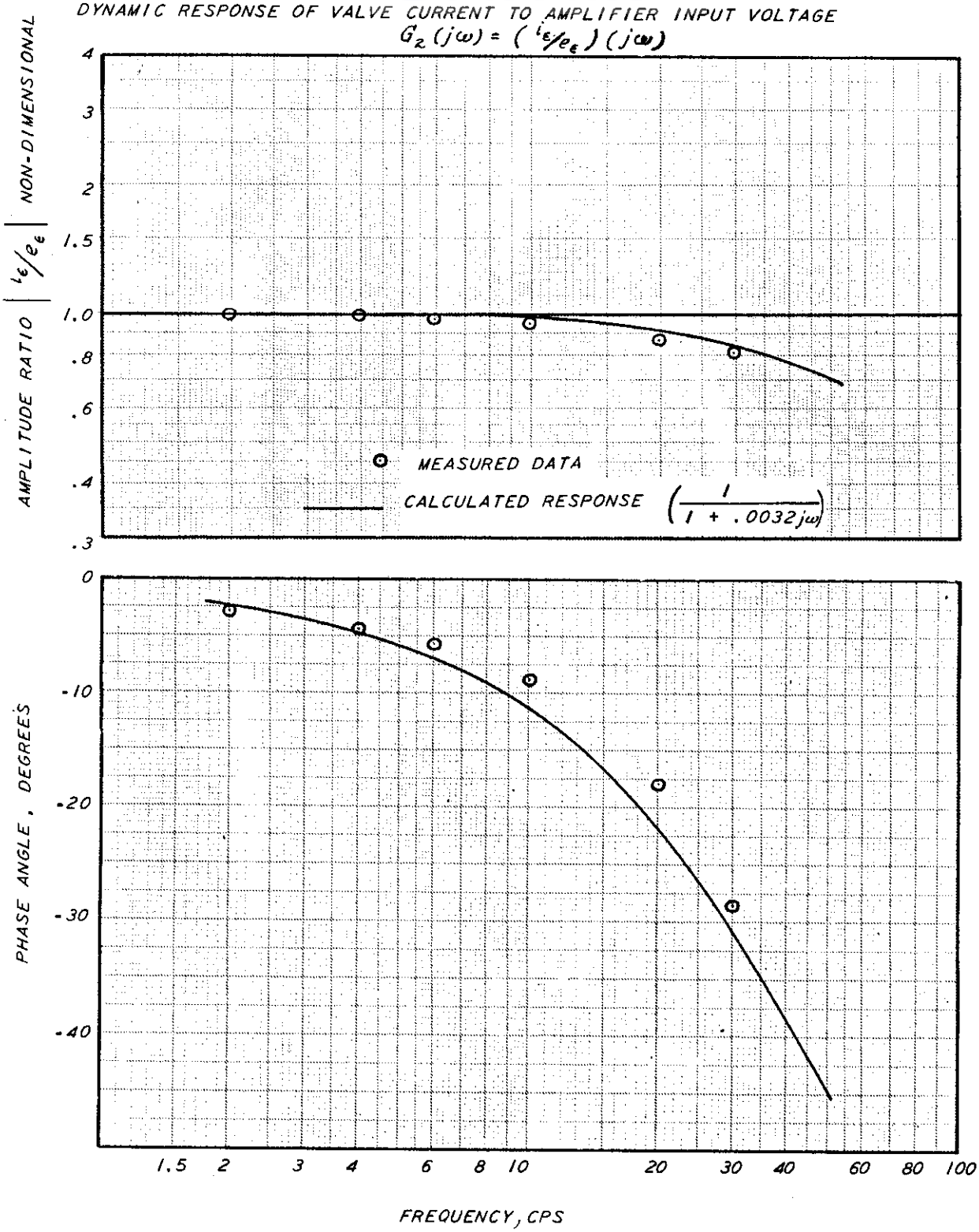

Figure 57 SERVOAMPLIFIER RESPONSE

Approved for Public Release

Contrails

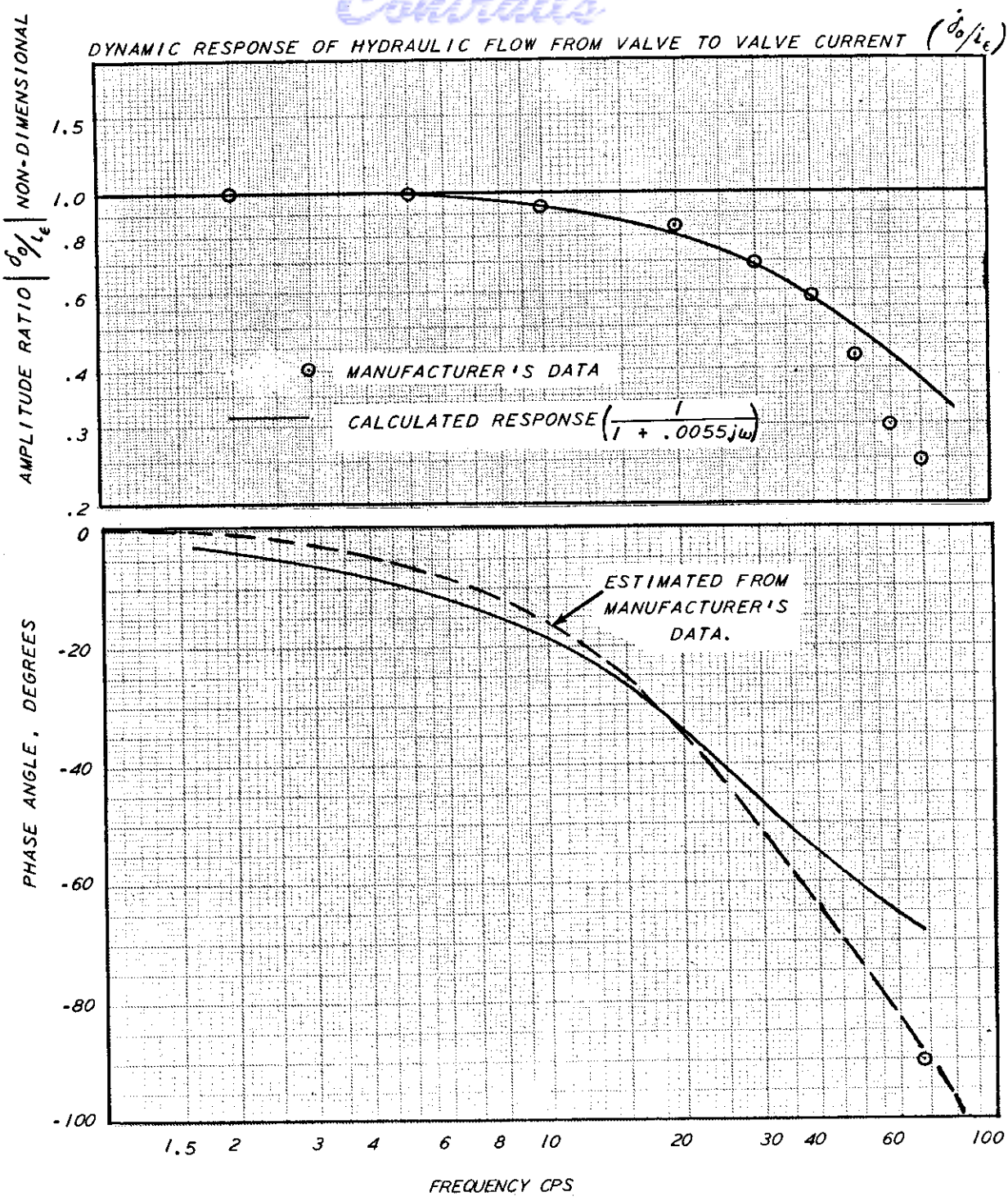

Figure 58 SERVOVALVE RESPONSE

Approved for Public Release

Contrails

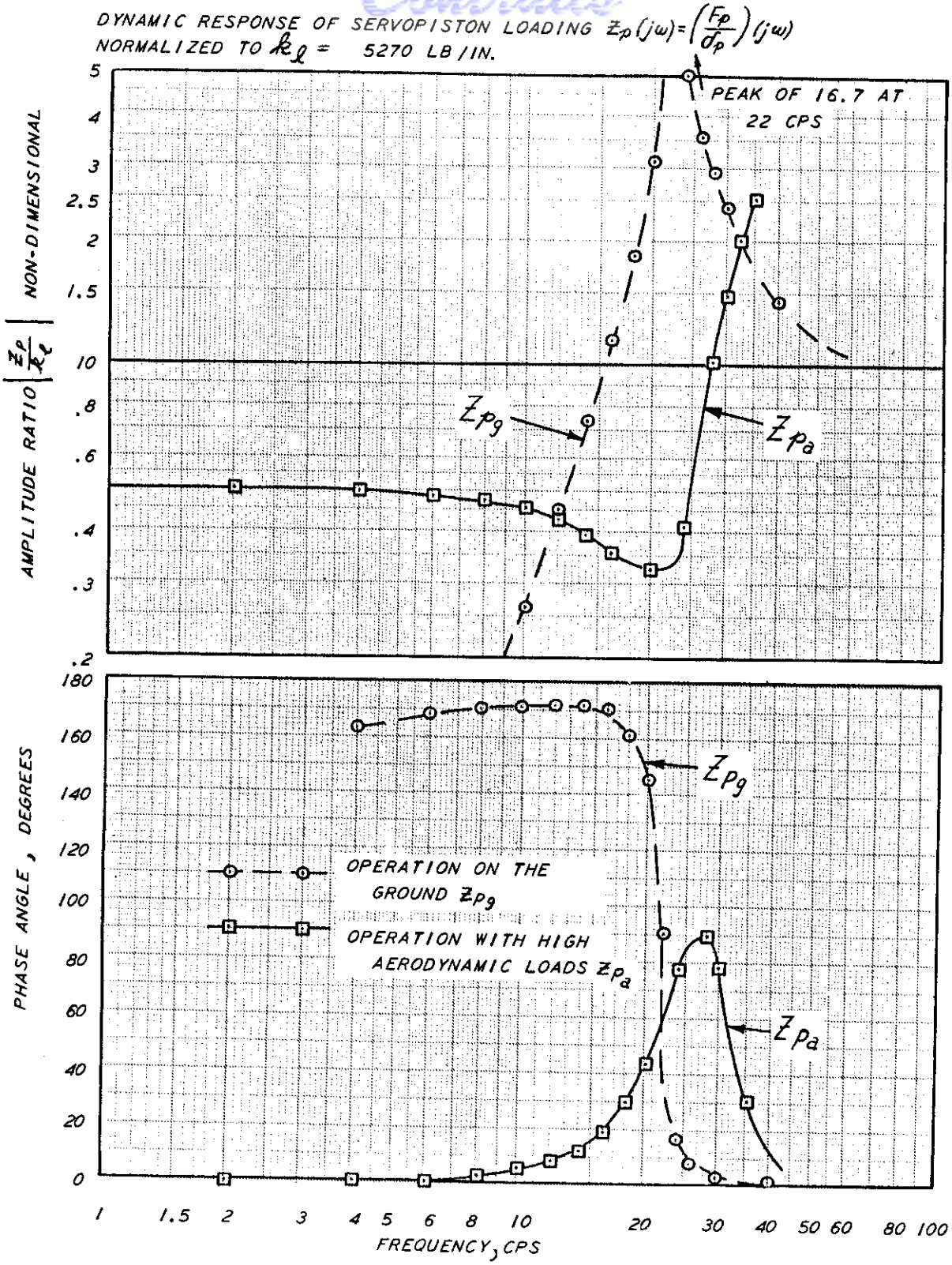

Figure 59 SERVO LOAD IMPEDANCE

Approved for Public Release

Contrails

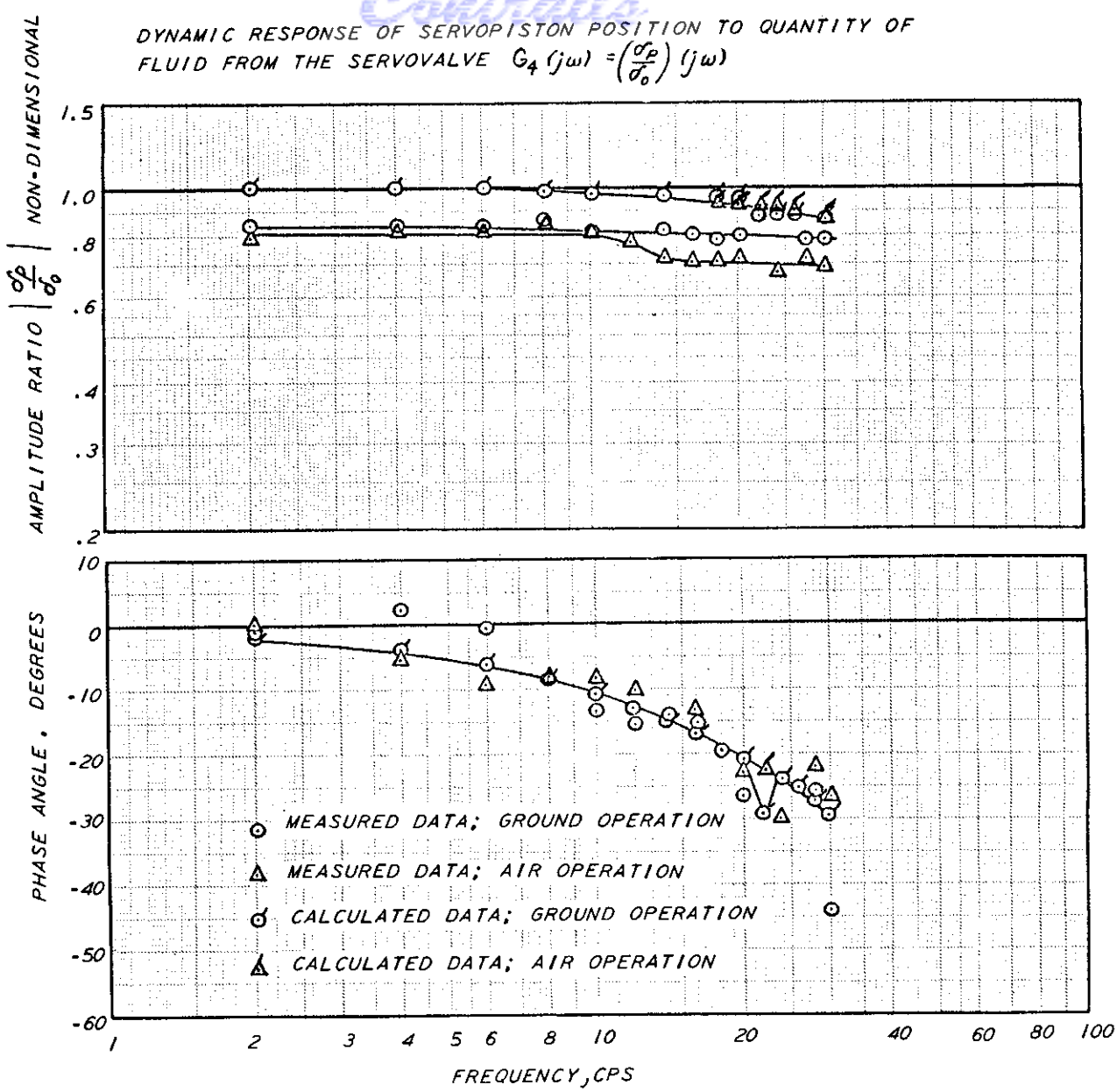

Figure 60 HYDROMECHANICAL SYSTEM RESPONSE

Approved for Public Release

Contrails

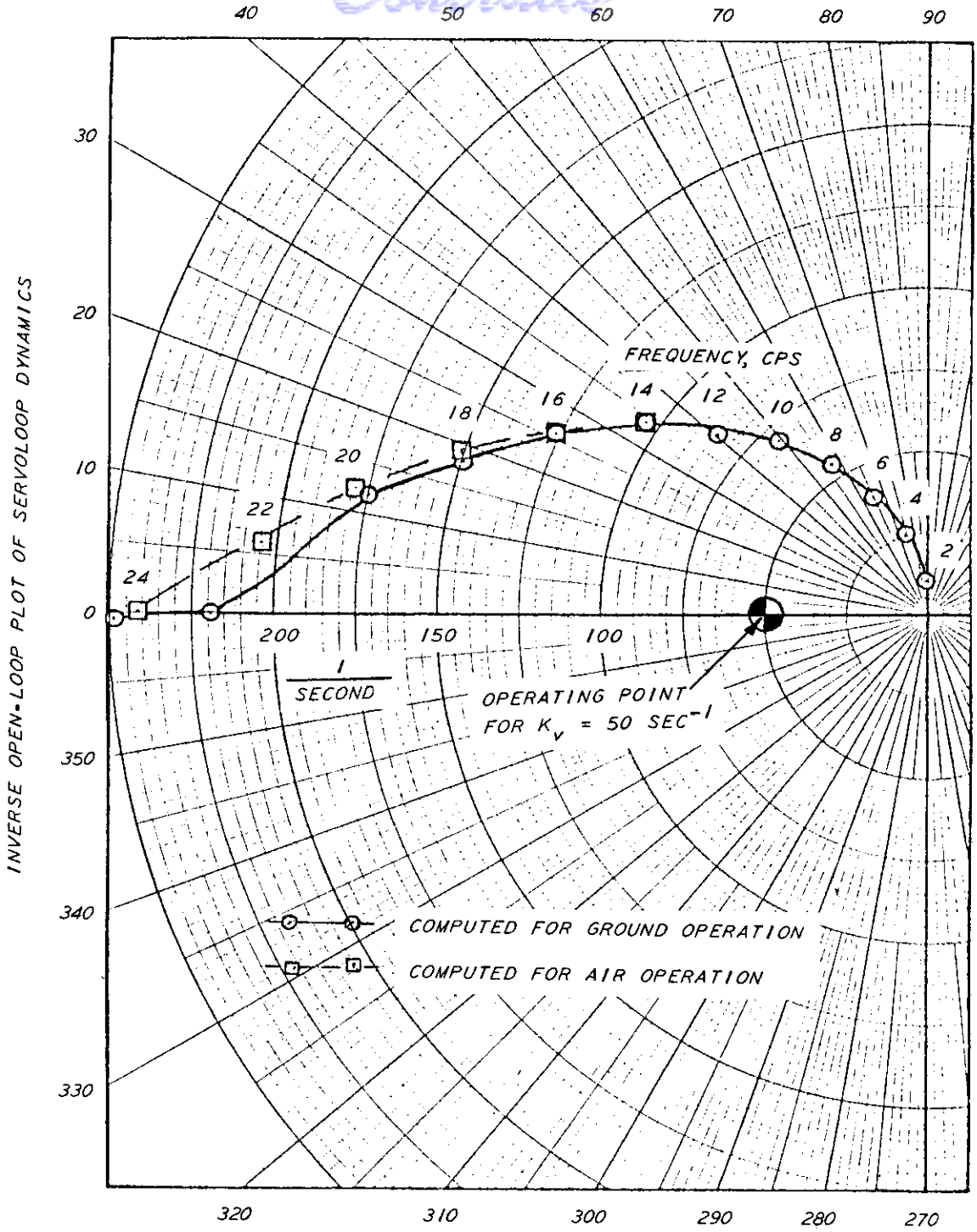

Figure 61 SERVOLOOP DYNAMICS

Approved for Public Release

Contrails

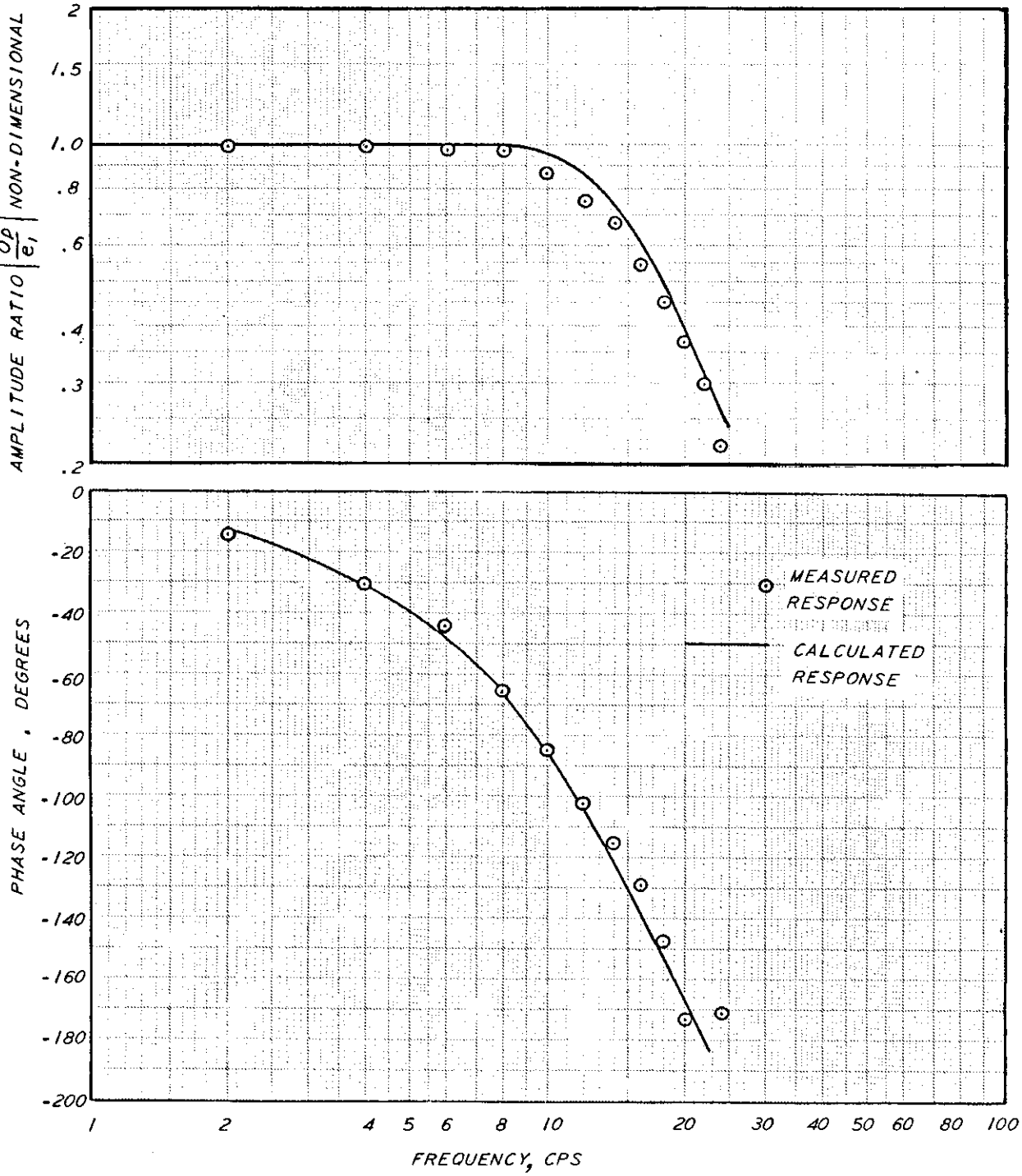

Figure 62 SERVOLOOP RESPONSE

Approved for Public Release

Contrails

DYNAMIC RESPONSE OF AILERON POSITION TO SERVOPISTON POSITION $T(j\omega) = \left(\frac{\sigma_c}{\sigma_p}\right)(j\omega)$

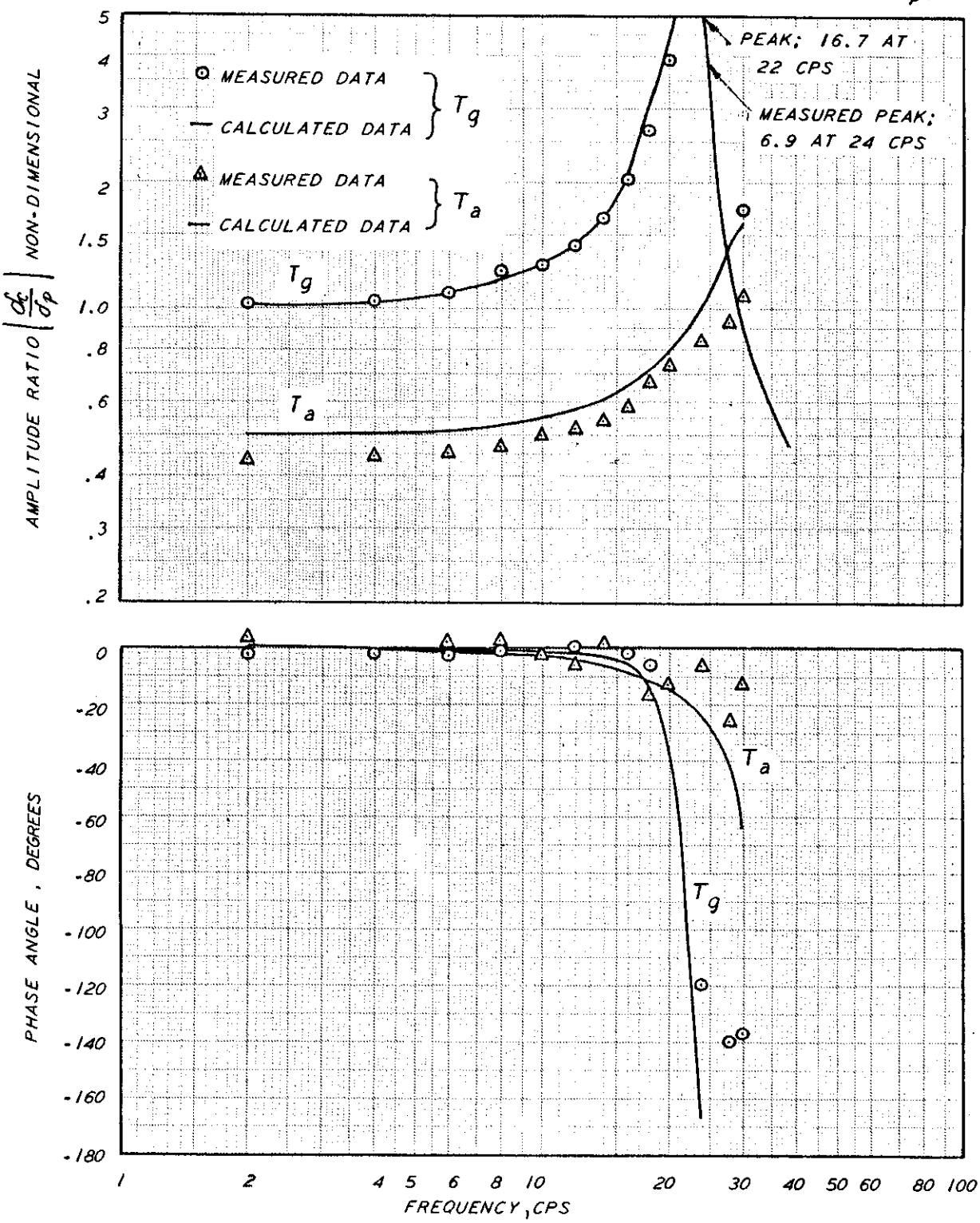

Figure 63 POSITION TRANSMISSION RATIO

Approved for Public Release

Contrails

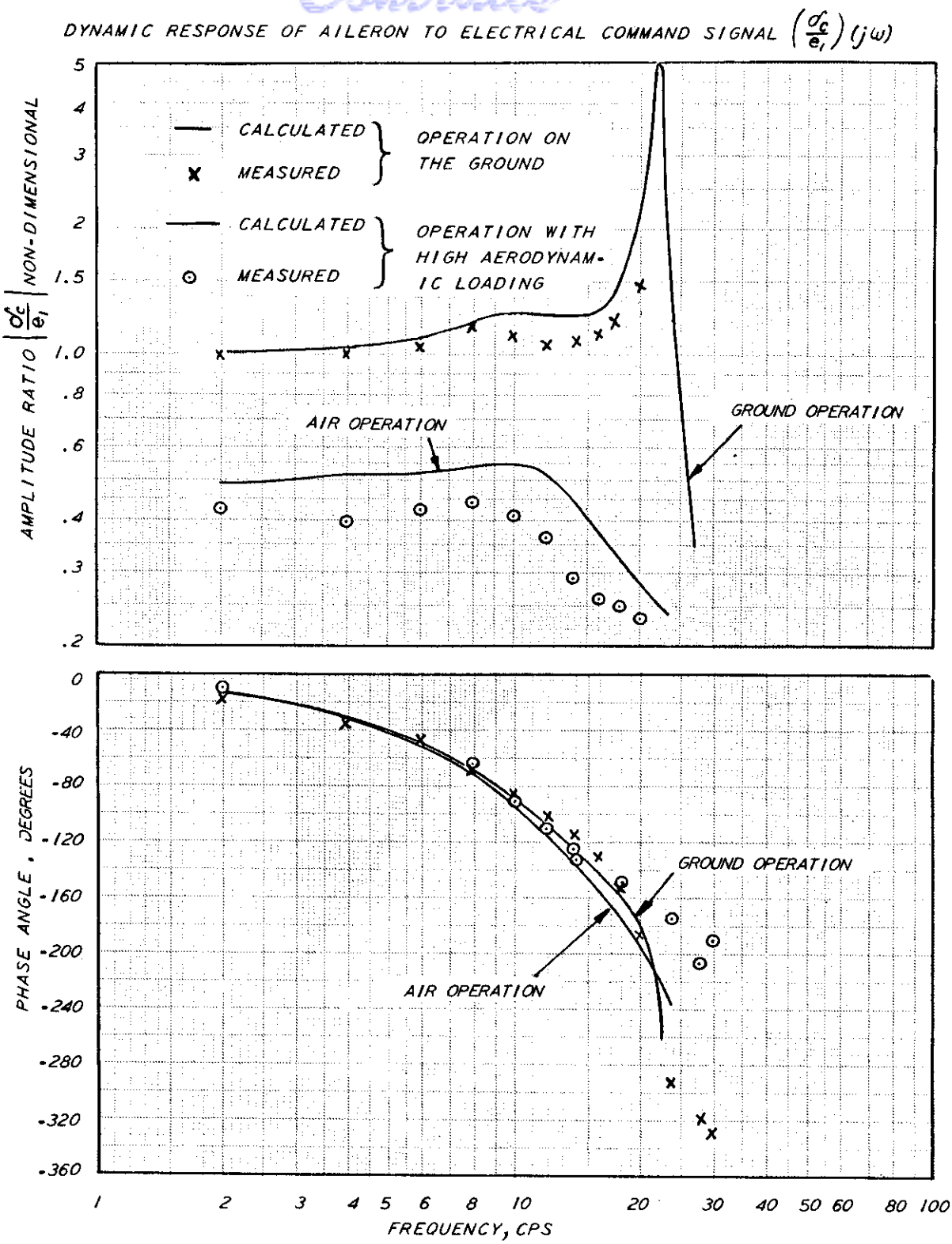

Figure 64 OVER-ALL FREQUENCY RESPONSE FOR TEST RIG SIMULATION OF FUSELAGE AILERON SERVO - HALF SCALE LOADS

Approved for Public Release

Contrails

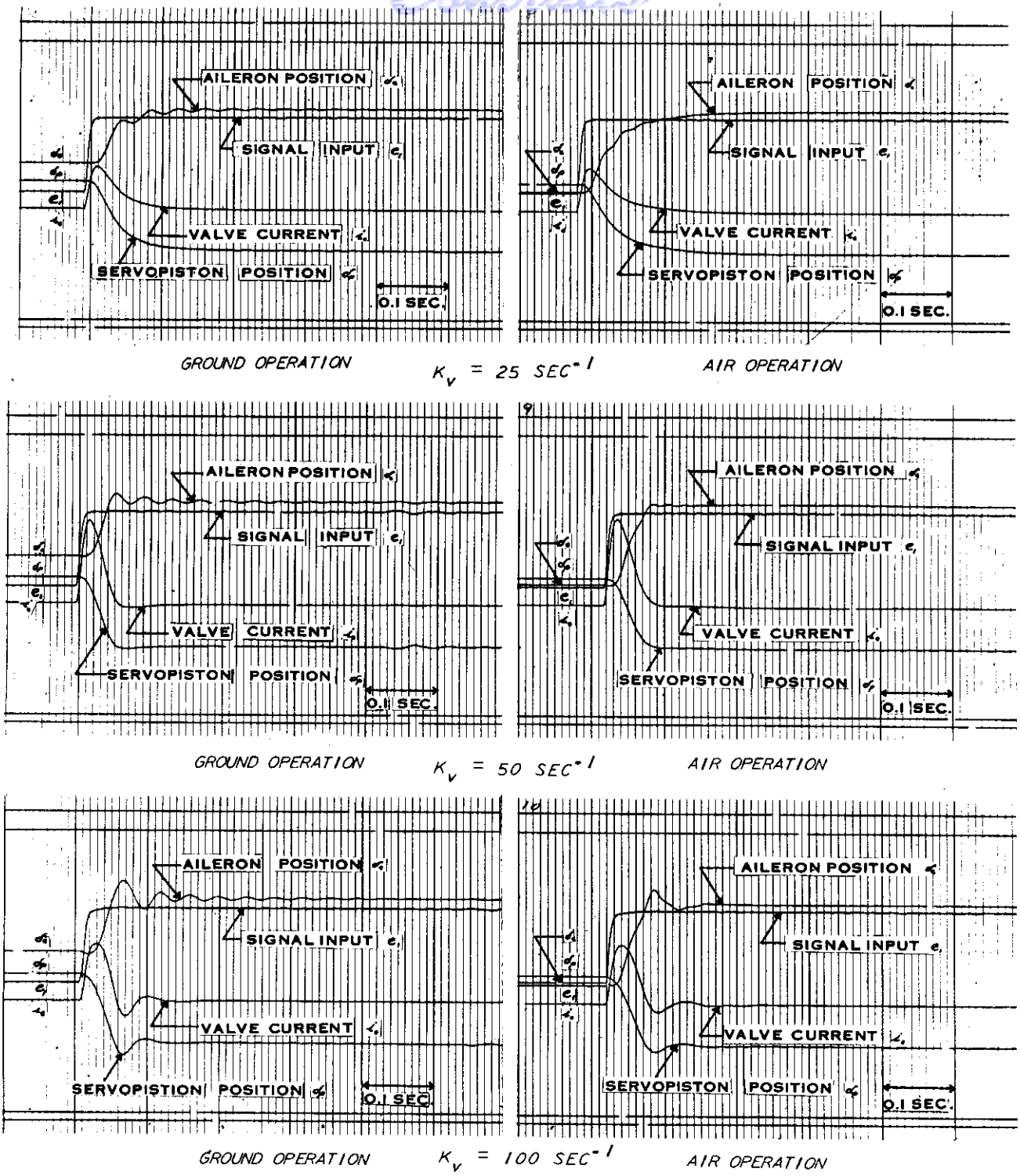

Figure 65 SERVOLOOP RESPONSE WITH INCREASING LOOP GAINS

Approved for Public Release

Contrails

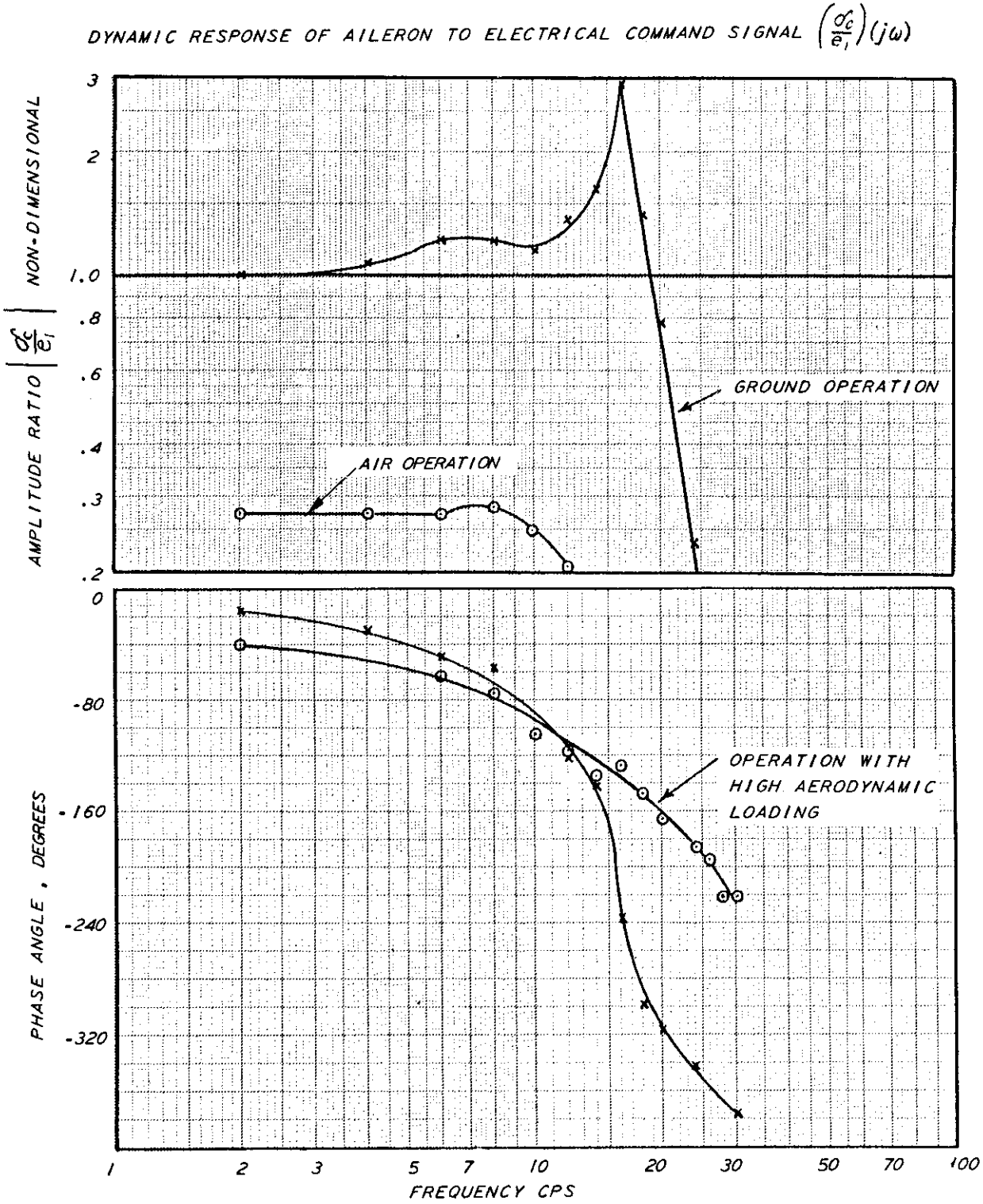

Figure 66 OVER-ALL FREQUENCY RESPONSE FOR TEST RIG SIMULATION OF FUSELAGE AILERON SERVO - FULL SCALE LOADS

Approved for Public Release

Contrails

DYNAMIC RESPONSE OF AILERON TO ELECTRICAL COMMAND SIGNAL FOR WING MOUNTED SERVO $\left(\frac{\sigma_c}{e_i}\right)(j\omega)$

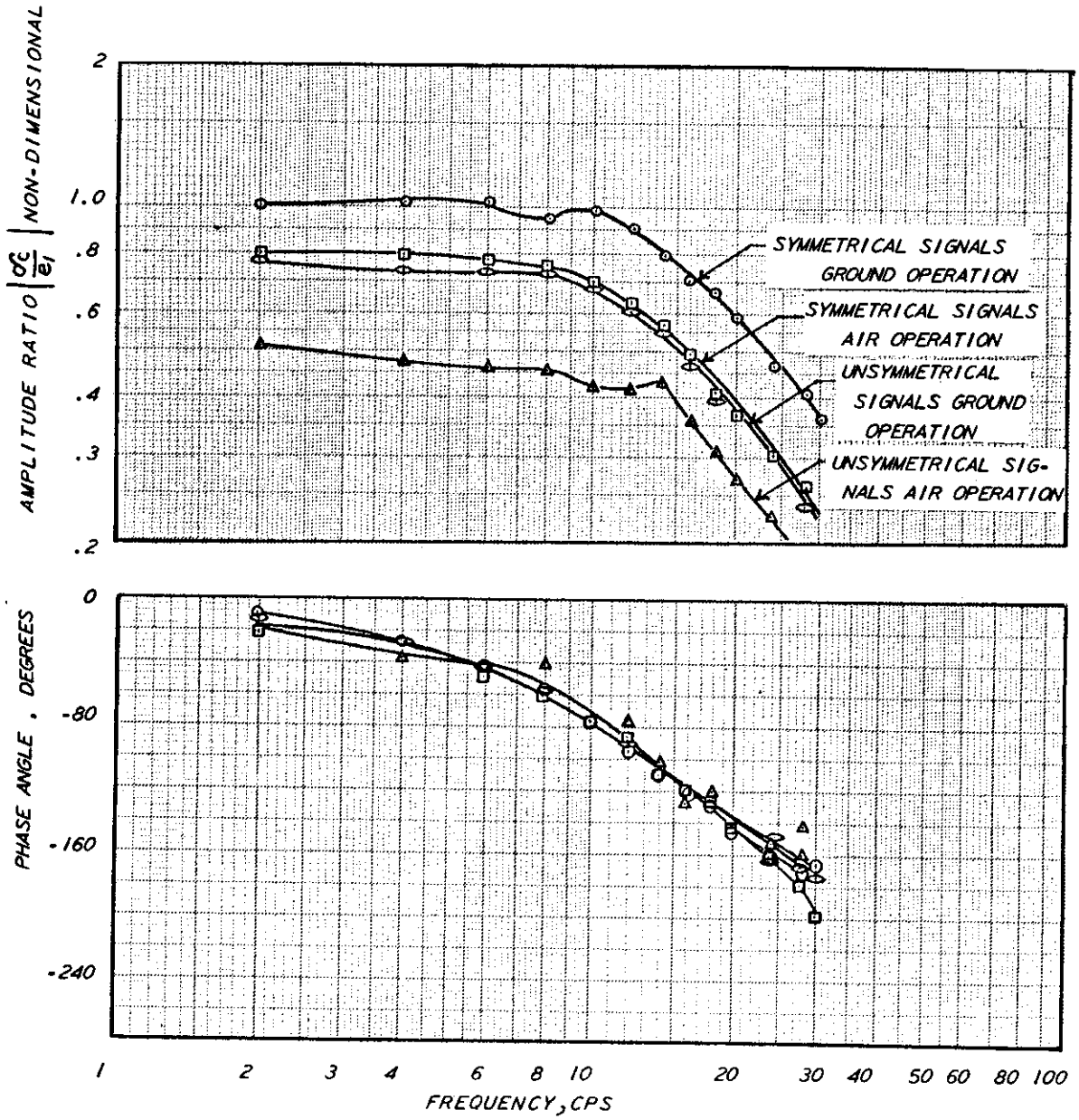

Figure 67 OVER-ALL FREQUENCY RESPONSE FOR TEST RIG SIMULATION OF WING MOUNTED AILERON SERVO

Approved for Public Release

Contrails

SERVOLOOP RESPONSE WITH K_v=100 SEC^{-1} WITH INCREASING AMOUNTS OF RATE FEEDBACK

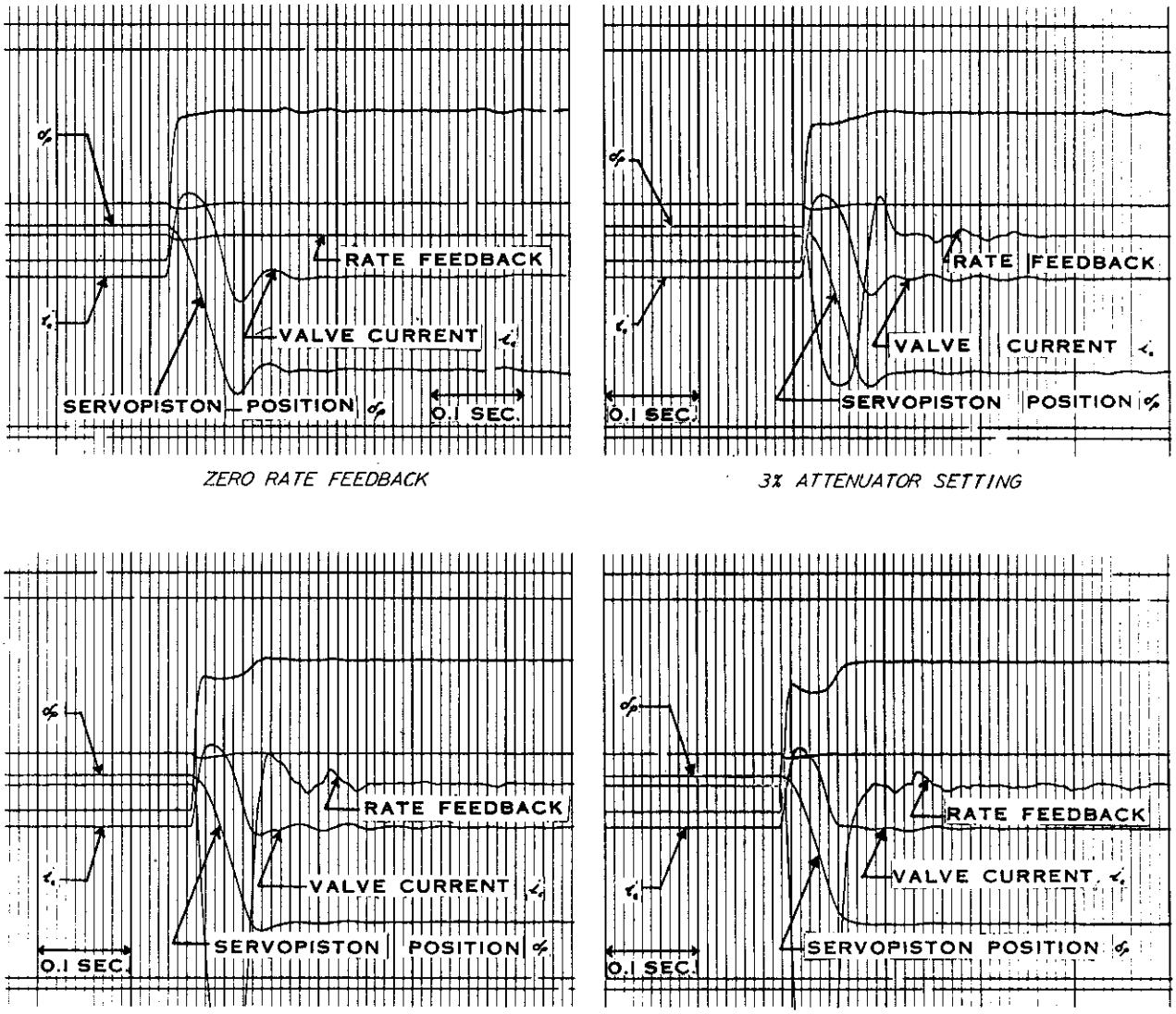

Figure 68 INCREASED DAMPING SERVOLOOP RESPONSE WITH RATE FEEDBACK

Approved for Public Release

Contrails

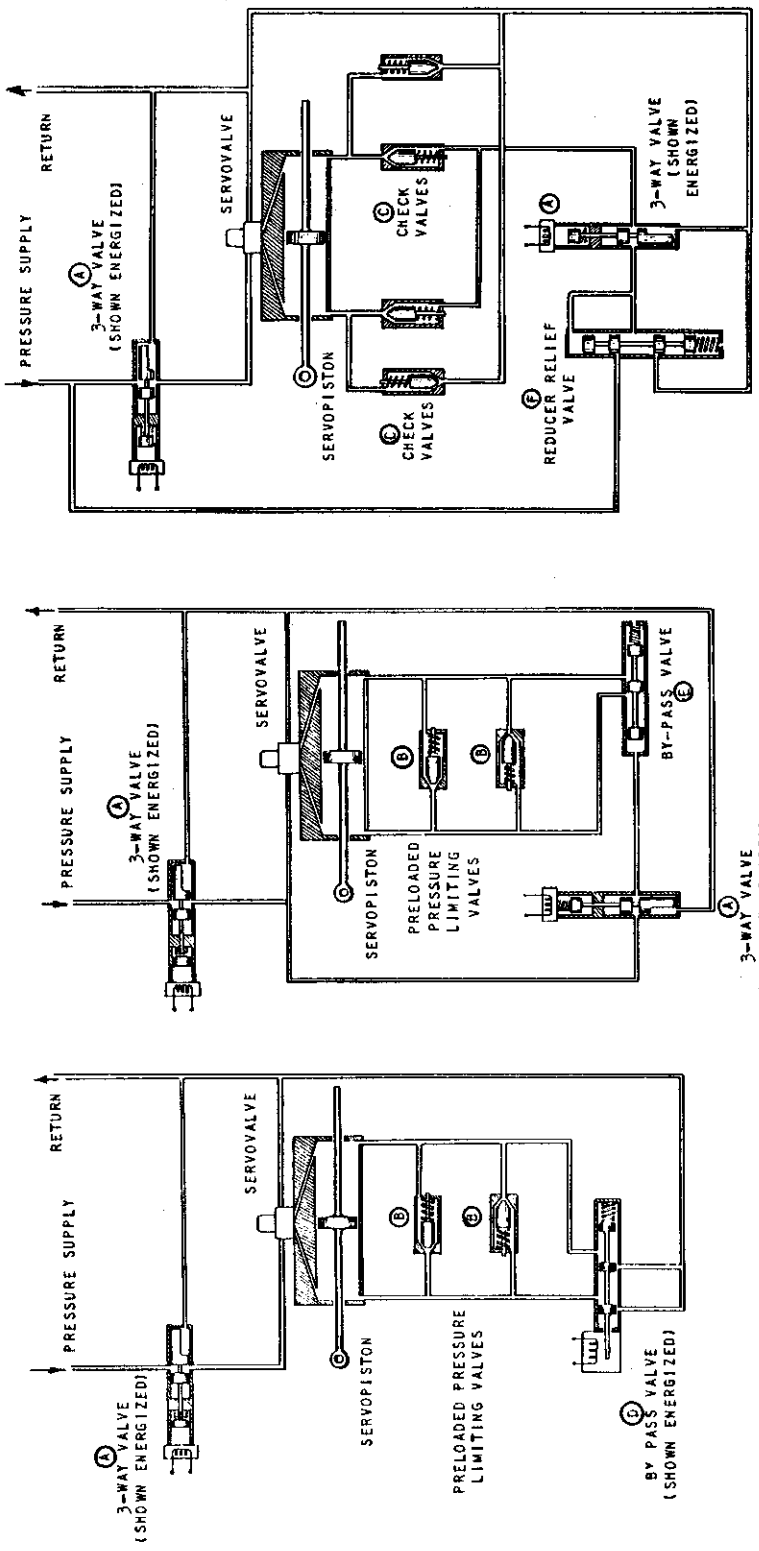

C-45 SYSTEM F-86 SYSTEM PROPOSED SYSTEM

VALVE	DESCRIPTION	NO. OF VALVES REQ'D FOR 3 SERVOS		
		C-45	F-86	PROPOSED
(A)	STANDARD SOLENOID 3 WAY VALVE	3	6	6
(B)	SPECIAL MODIFIED CHECK VALVE	6	6	0
(C)	STANDARD CHECK VALVE	0	0	12
(D)	SPECIAL 4 WAY VALVE	3	0	0
(E)	SPECIAL MODIFIED MOOG VALVE	0	3	0
(F)	STANDARD REDUCER RELIEF VALVE	0	0	1
TOTAL VALVES REQUIRED		12	15	19
TOTAL SPECIAL VALVES REQUIRED		9	9	0

Figure 69 COMPARISON OF SEVERAL AUXILIARY HYDRAULIC CONTROL CIRCUITS

Approved for Public Release

Contrails

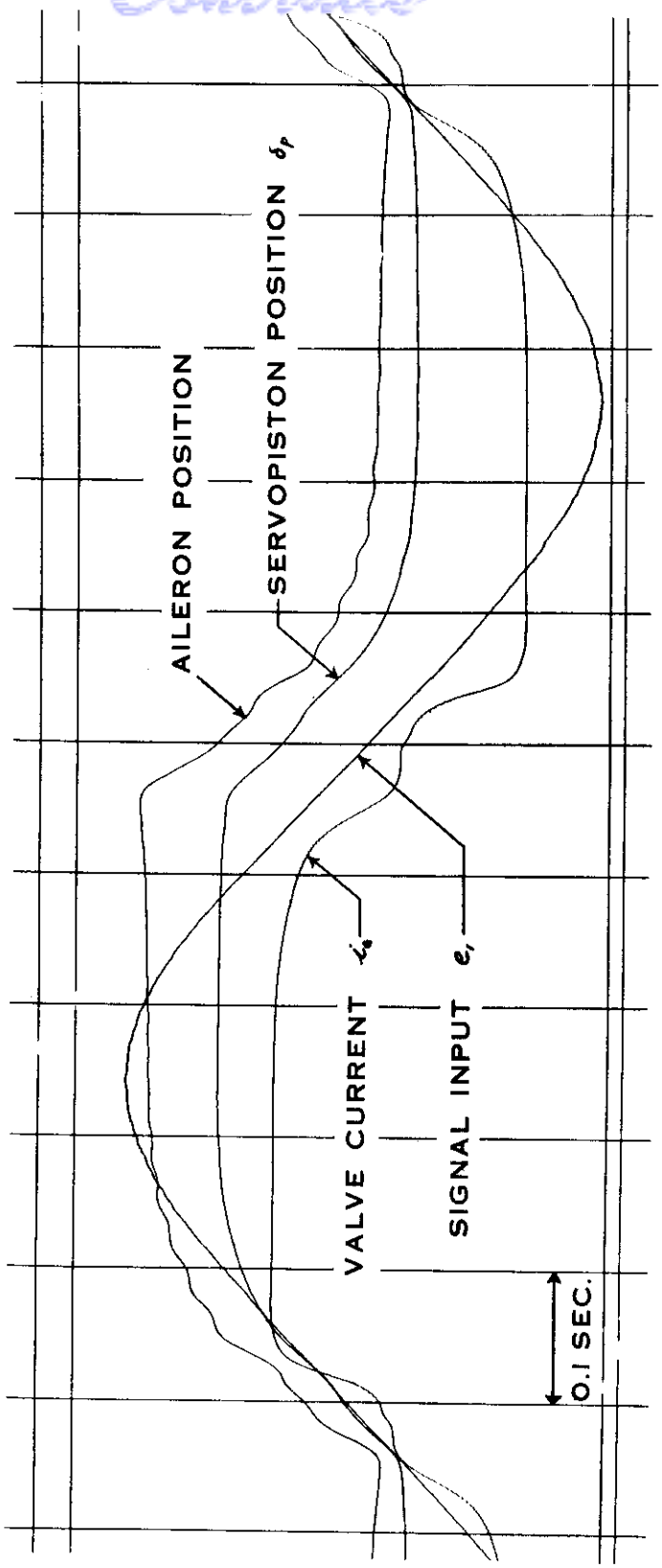

Figure 70 LIMITING ACTION OF PRESSURE RELIEF SYSTEM

Approved for Public Release

Contrails

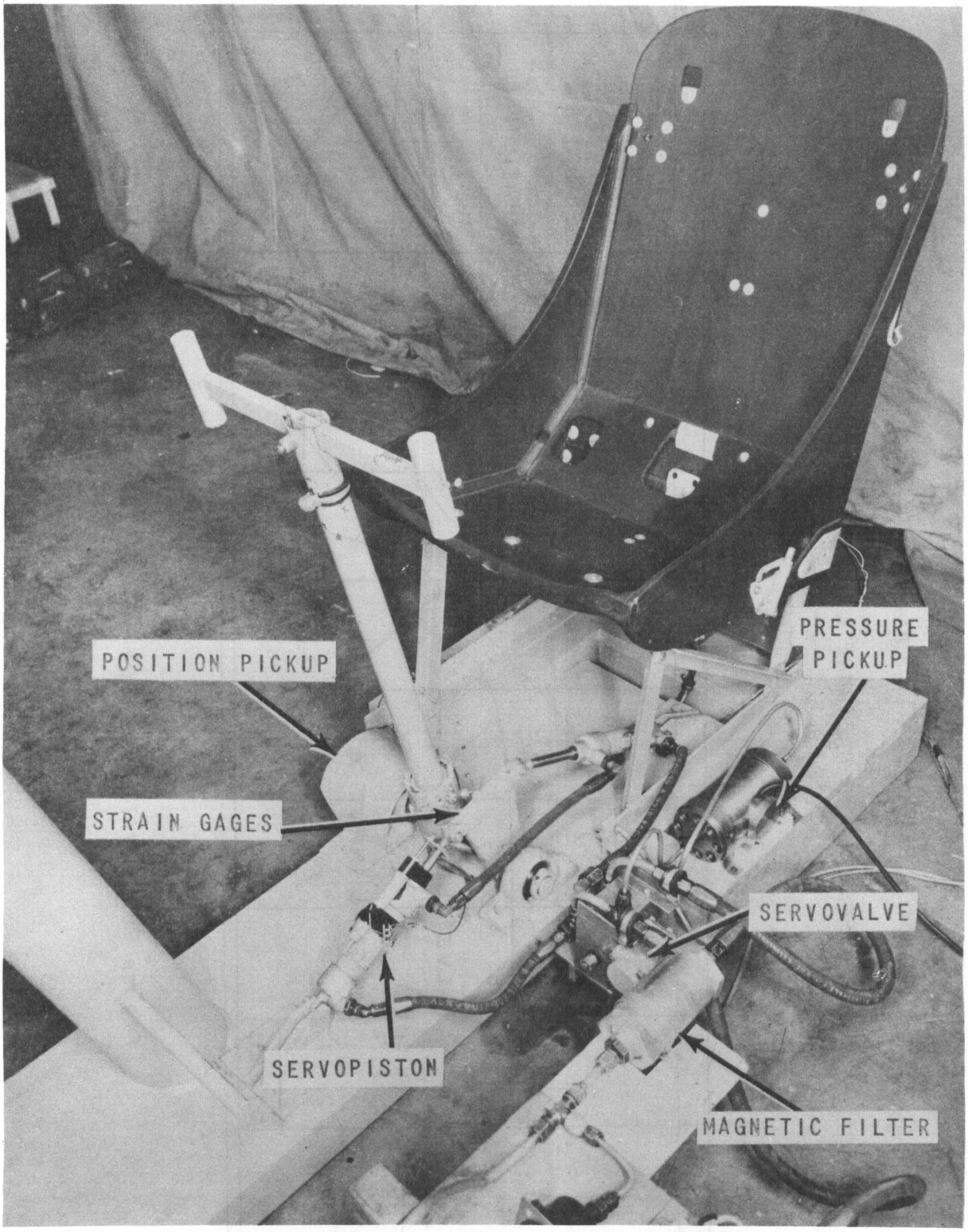

Figure 71 FEEL SERVO TEST RIG

Approved for Public Release

Contrails

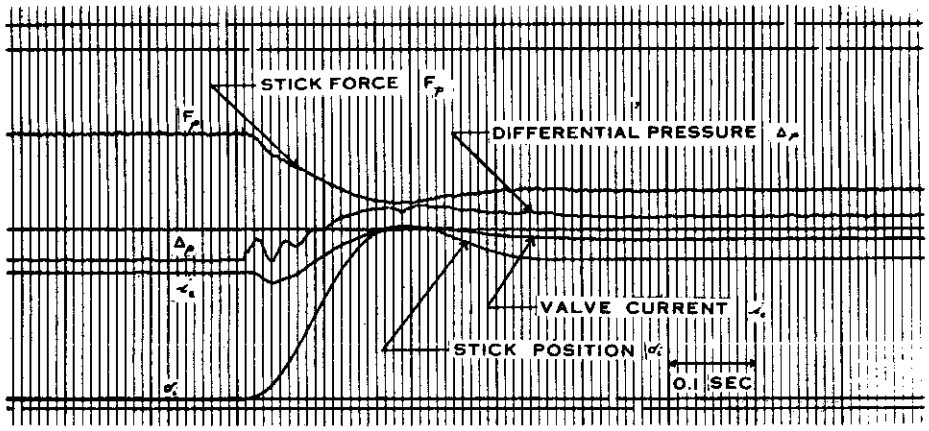

STIFFNESS AT WHEEL 10 lb/in.

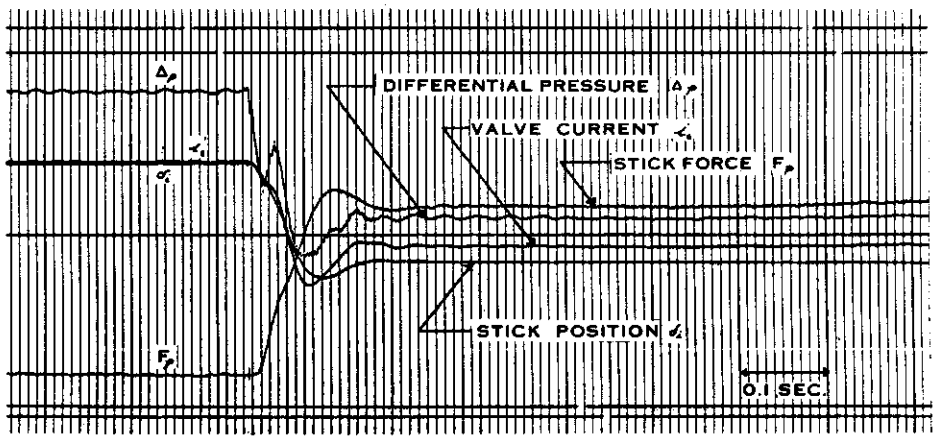

STIFFNESS AT WHEEL 44 lb/in.

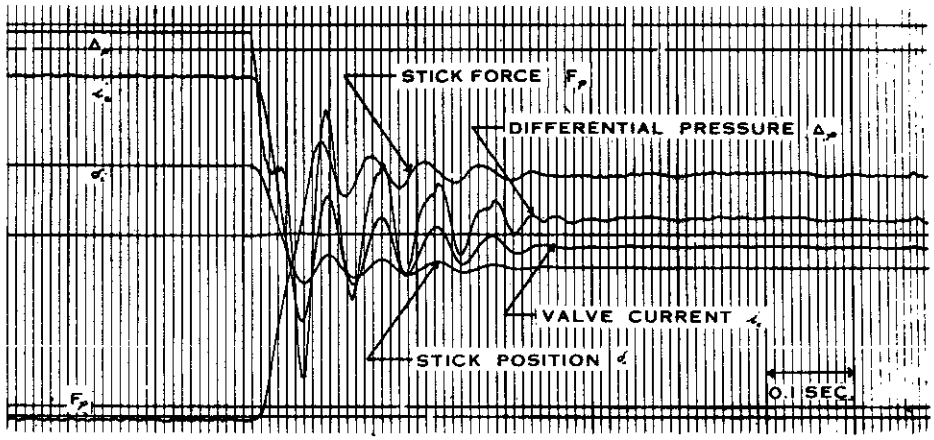

STIFFNESS AT WHEEL 63 lb/in.

Figure 72 STEP INPUTS OF STICK FORCE WITH VARIOUS STICK STIFFNESSES

Approved for Public Release

Contrails

DYNAMIC RESPONSE OF STICK POSITION (MEASURED AT BASE OF STICK) TO STICK FORCE WITH VARYING SYSTEM STIFFNESS PRODUCED BY CHANGING THE POSITION INPUT SIGNAL TO THE SERVO (SERVOLOOP GAIN CONSTANT)

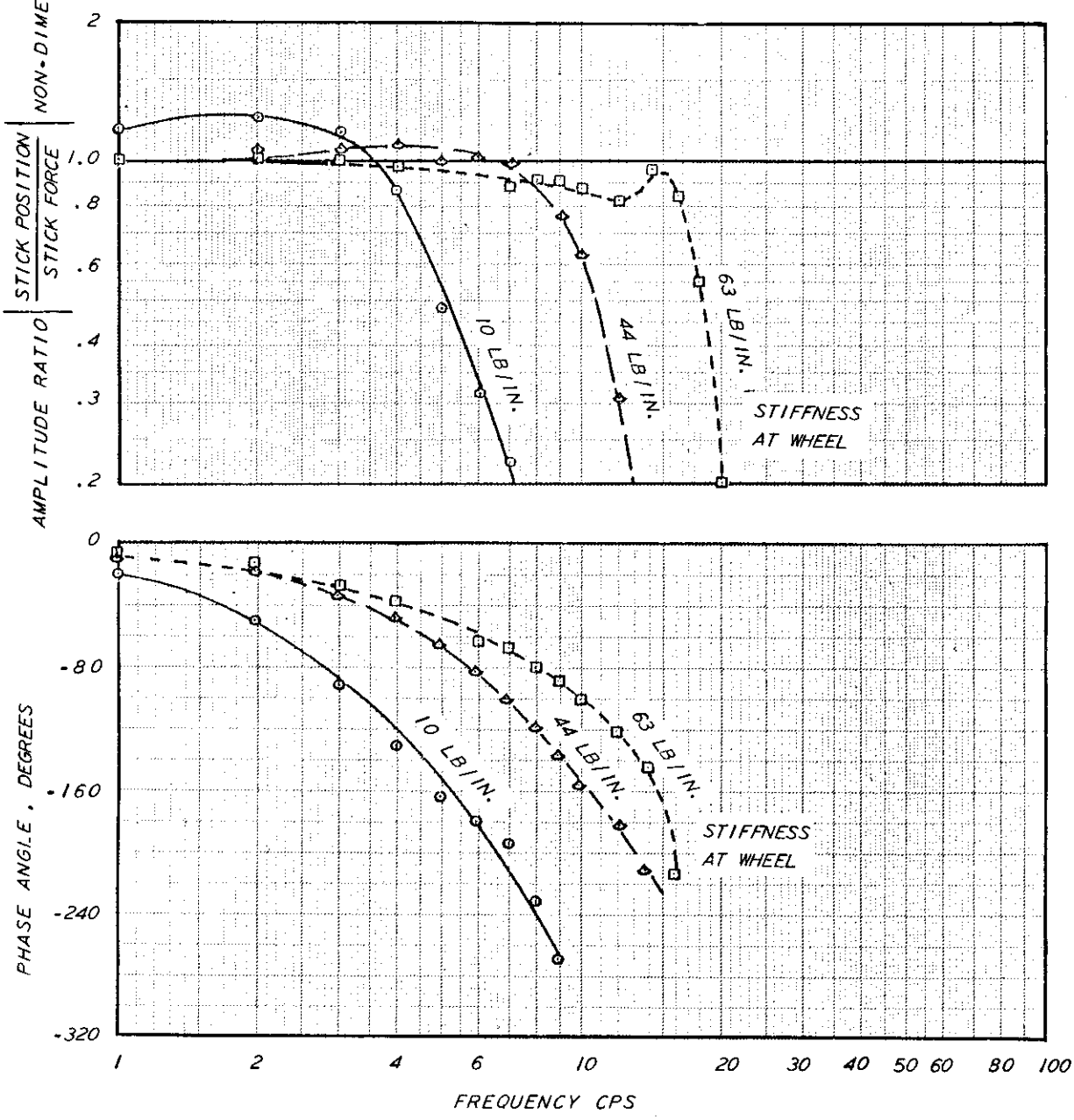

Figure 73 RESPONSE OF FEEL SYSTEM WITH VARIOUS STIFFNESSES

Approved for Public Release

Contrails

TABLE I

DEFINITIONS FOR COEFFICIENTS OF THE LONGITUDINAL EQUATIONS OF MOTION USED IN SECTION IV

$$D_v = \left(C_D - T_v + \frac{M}{2} C_{D_M}\right)\frac{1}{\tau} \quad \text{where} \quad T_v = \frac{\partial T/\partial V}{\rho V_o S}$$

$$D_\alpha = \left(C_{D_\alpha} - C_{L_o}\right)\frac{1}{2\tau}$$

$$D_\theta = \left(C_{L_o} + \eta T_c'\right)\frac{1}{2\tau}$$

$$L_v = \left(C_L + \eta T_v + \frac{M}{2} C_{L_M}\right)\frac{1}{\tau}$$

$$L_\alpha = \left(C_{L_\alpha} + C_D\right)\frac{1}{2\tau}$$

$$L_\delta = C_{L_{\delta_e}}\frac{1}{2\tau}$$

$$M_{\dot v} = C_{m_{DV}}\frac{2\mu_1}{i_y\tau} \quad \text{where} \quad C_{m_{DV}} = \frac{V_o}{\tau}\frac{\partial C_m}{\partial \dot V}$$

$$M_v = \left(C_{m_v} + 2C_{m_o} - 2\frac{Z_T}{C}T_v + MC_{m_M}\right)\frac{2\mu_1}{i_y\tau^2} \quad \text{where} \quad C_{m_v} = V_o\frac{\partial C_m}{\partial V}$$

$$M_\alpha = C_{m_\alpha}\frac{2\mu_1}{i_y\tau^2}$$

$$M_{\dot\alpha} = C_{m_{D\alpha}}\frac{2\mu_1}{i_y\tau} \quad \text{where} \quad C_{m_{D\alpha}} = \frac{1}{2\mu_1}\frac{\partial C_m}{\partial(\dot\alpha c/2V)}$$

$$M_{\dot\theta} = C_{m_{D\theta}}\frac{2\mu_1}{i_y\tau} \quad \text{where} \quad C_{m_{D\theta}} = \frac{1}{2\mu_1}\frac{\partial C_m}{\partial(\dot\theta c/2V)}$$

$$M_\delta = C_{m_{\delta_e}}\frac{2\mu_1}{i_y\tau^2}$$

$$\tau = \frac{m}{\rho V_o S}$$

$$\mu_1 = \frac{m}{\rho S c}$$

$$i_y = 4\frac{I_Y}{mc^2}$$

Approved for Public Release

Contrails

TABLE II

SUMMARY OF ANALOG COMPUTER RESULTS FOR SIMULATION OF CASE "A"

RECORD NO.	AIRCRAFT	CONDITION	CALCULATED		MEASURED FROM COMPUTER RECORD-n_z	
			DAMPING RATIO ζ	FREQUENCY f - CPS	DAMPING RATIO ζ	FREQUENCY f - CPS
1	"A"	TYPICAL SHORT PERIOD CHARACTERISTICS OF SUPERSONIC AIRCRAFT	0.229	1.628	0.24	1.52
2	NORMAL T-33	M= 0.65 h= 10,500 FT NO ARTIFICIAL STABILITY	0.605	0.424	0.61	0.42
3	T-33	M= 0.65 h=10,500 FT ARTIFICIAL STAB. - NO LAG	--	--	0.25	1.61
6	T-33	M= 0.65 h= 10,500 FT ARTIFICIAL STAB., 0.05 SEC LAG	--	--	0.23	1.59

Approved for Public Release

Contrails

TABLE III

SUMMARY OF ANALOG COMPUTER RESULTS
FOR SIMULATION OF CASE "B"

RECORD NO.	AIRCRAFT	CONDITION	CALCULATED		MEASURED FROM COMPUTER RECORD-n_z	
			DAMPING RATIO - ζ	FREQUENCY f - CPS	DAMPING RATIO - ζ	FREQUENCY f - CPS
1	"B"	TYPICAL SHORT PERIOD CHARACTERISTICS OF TRANSONIC AIRCRAFT	0.197	1.120	0.21	1.04
2	NORMAL T-33	M = 0.65 h = 10,500 FT NO ARTIFICIAL STABILITY	0.605	0.424	0.61	0.42
NONE	NORMAL T-33	M = 0.65 h = 18,500 FT NO ARTIFICIAL STABILITY	0.535	0.380	--	--
3	T-33	M = 0.65 h = 10,500 FT ARTIFICIAL STABILITY - NO LAG - L_α NOT MATCHED	--	--	0.23	1.02
4	T-33	M = 0.65 h = 18,500 FT ARTIFICIAL STABILITY - NO LAG - L_α MATCHED	--	--	0.24	1.04
5	T-33	M = 0.65 h = 18,500 FT ARTIFICIAL STABILITY 0.05 SEC FIRST-ORDER LAG	--	--	0.20	1.06
6	T-33	M = 0.65 h = 18,500 FT ARTIFICIAL STABILITY 0.0279 SEC FIRST-ORDER LAG	--	--	0.20	1.07
7	T-33	M = 0.65 h = 18,500 FT ARTIFICIAL STABILITY - SECOND-ORDER LAG - ζ = 0.70 f_n = 8.0 CPS	--	--	0.21	1.07
8	T-33	M = 0.65 h = 18,500 FT ARTIFICIAL STABILITY - FIRST-ORDER LAG - NO COMPENSATION	--	--	0.15	1.09
9	T-33	M = 0.65 h = 18,500 FT ARTIFICIAL STABILITY - SECOND-ORDER LAG - NO COMPENSATION	--	--	0.15	1.09

Approved for Public Release

Contrails

TABLE IV

DEFINITIONS OF COEFFICIENTS USED IN LATERAL EQUATIONS OF MOTION IN SECTION IV

$$Y_\beta = \frac{1}{mV_0}\frac{\partial Y}{\partial \beta} = \frac{C_{Y_\beta}}{2\tau} \qquad \tau = \frac{m}{\rho V_0 S} \qquad i_x = \frac{4I_x}{mb^2}$$

$$Y_r = \frac{1}{mV_0}\frac{\partial Y}{\partial r} = \frac{C_{Y_r}}{4\mu_z} \qquad \mu_z = \frac{m}{\rho S b} \qquad i_z = \frac{4I_z}{mb^2}$$

$$Y_p = \frac{1}{mV_0}\frac{\partial Y}{\partial p} = \frac{C_{Y_p}}{4\mu_z} \qquad i_{xz} = \frac{4I_{xz}}{mb^2}$$

$$Y_{\delta_r} = \frac{1}{mV_0}\frac{\partial Y}{\partial \delta_r} = \frac{C_{Y_{\delta_r}}}{2\tau}$$

$$k = \frac{1}{\left(1 - \frac{I_{xz}^2}{I_x I_z}\right)} = \frac{1}{\left(1 - \frac{i_{xz}^2}{i_x i_z}\right)}$$

$$Y_\phi = \frac{1}{mV_0} W\cos\gamma_0$$

$$Y_\psi = \frac{1}{mV_0} W\sin\gamma_0$$

$$L_\beta = \frac{k}{I_x}\left[\frac{\partial L}{\partial \beta} + \frac{I_{xz}}{I_z}\frac{\partial N}{\partial \beta}\right] = \frac{k}{i_x}\left[\frac{2\mu_2}{\tau^2}\right]\left[C_{L_\beta} + \frac{i_{xz}}{i_z}C_{n_\beta}\right]$$

$$L_r = \frac{k}{I_x}\left[\frac{\partial L}{\partial r} + \frac{I_{xz}}{I_z}\frac{\partial N}{\partial r}\right] = \frac{k}{i_x}\left[\frac{1}{\tau}\right]\left[C_{\ell_r} + \frac{i_{xz}}{i_z}C_{n_r}\right]$$

$$L_p = \frac{k}{I_x}\left[\frac{\partial L}{\partial p} + \frac{I_{xz}}{I_z}\frac{\partial N}{\partial p}\right] = \frac{k}{i_x}\left[\frac{1}{\tau}\right]\left[C_{\ell_p} + \frac{i_{xz}}{i_z}C_{n_p}\right]$$

$$L_{\delta_a} = \frac{k}{I_x}\left[\frac{\partial L}{\partial \delta_a} + \frac{I_{xz}}{I_z}\frac{\partial N}{\partial \delta_a}\right] = \frac{k}{i_x}\left[\frac{2\mu_2}{\tau^2}\right]\left[C_{\ell_{\delta_a}} + \frac{i_{xz}}{i_z}C_{n_{\delta_a}}\right]$$

$$L_{\delta_r} = \frac{k}{I_x}\left[\frac{\partial L}{\partial \delta_r} + \frac{I_{xz}}{I_z}\frac{\partial N}{\partial \delta_r}\right] = \frac{k}{i_x}\left[\frac{2\mu_2}{\tau^2}\right]\left[C_{\ell_{\delta_r}} + \frac{i_{xz}}{i_z}C_{n_{\delta_r}}\right]$$

Approved for Public Release

Contrails

TABLE IV (CONT'D)

DEFINITIONS OF COEFFICIENTS USED IN LATERAL EQUATIONS OF MOTION IN SECTION IV

$$N_\beta = \frac{k}{I_z}\left[\frac{\partial N}{\partial \beta} + \frac{I_{xz}}{I_x}\frac{\partial L}{\partial \beta}\right] = \frac{k}{i_z}\left[\frac{2\mu_2}{\tau^2}\right]\left[C_{n_\beta} + \frac{i_{xz}}{i_x}C_{\ell_\beta}\right]$$

$$N_r = \frac{k}{I_z}\left[\frac{\partial N}{\partial r} + \frac{I_{xz}}{I_x}\frac{\partial L}{\partial r}\right] = \frac{k}{i_z}\left[\frac{1}{\tau}\right]\left[C_{n_r} + \frac{i_{xz}}{i_x}C_{\ell_r}\right]$$

$$N_p = \frac{k}{I_z}\left[\frac{\partial N}{\partial p} + \frac{I_{xz}}{I_x}\frac{\partial L}{\partial p}\right] = \frac{k}{i_z}\left[\frac{1}{\tau}\right]\left[C_{n_p} + \frac{i_{xz}}{i_x}C_{\ell_p}\right]$$

$$N_{\delta_a} = \frac{k}{I_z}\left[\frac{\partial N}{\partial \delta_a} + \frac{I_{xz}}{I_x}\frac{\partial L}{\partial \delta_a}\right] = \frac{k}{i_z}\left[\frac{2\mu_2}{\tau^2}\right]\left[C_{n_{\delta_a}} + \frac{i_{xz}}{i_x}C_{\ell_{\delta_a}}\right]$$

$$N_{\delta_r} = \frac{k}{I_z}\left[\frac{\partial N}{\partial \delta_r} + \frac{I_{xz}}{I_x}\frac{\partial L}{\partial \delta_r}\right] = \frac{k}{i_z}\left[\frac{2\mu_2}{\tau^2}\right]\left[C_{n_{\delta_r}} + \frac{i_{xz}}{i_x}C_{\ell_{\delta_r}}\right]$$

Approved for Public Release

Contrails

TABLE V

DEFINITION OF COEFFICIENTS IN TRANSFORMED ROLLING MOMENT AND YAWING MOMENT EQUATIONS (97) AND (98)

$$L'_\beta = L_\beta + L_r Y_\beta$$

$$L'_\phi = L_r Y_\phi$$

$$L'_{\delta_r} = L_{\delta_r} + L_r Y_{\delta_r}$$

$$N'_{\dot\beta} = -(N_r + Y_\beta)$$

$$N'_\beta = N_\beta + N_r Y_\beta$$

$$N'_p = N_p - Y_\phi$$

$$N'_{\delta_r} = N_{\delta_r} + N_r Y_{\delta_r}$$

$$N'_\phi = N_r Y_\phi$$

Approved for Public Release

Contrails

TABLE VI

AERODYNAMIC, GRAVITY, AND INERTIA COEFFICIENTS FOR T-33 FLYING AT $M = 0.70$ AT 10,000 FEET.

V_o = 753 FPS	C_{Y_β} = -.625	Y_β = -.250		
b = 37.5 FT	C_{Y_r} = .34			
W = 12,500 FT	C_{Y_p} = -.025			
S = 235 FT^2	C_{L_o} = .1070	Y_ϕ = .0428		
i_x = .0659	$C_{Y_{\delta_r}}$ = .199	Y_{δ_r} = .0796		
i_z = .209	C_{ℓ_β} = -.050	L_β = -25.4	L'_β = -25.6	
i_{xz} = -.0050	C_{ℓ_r} = .070	L_r = .896		
τ = 1.250 SEC	C_{ℓ_p} = -.527	L_p = -6.41		
μ_z = 25.1	$C_{\ell_{\delta_a}}$ = -.130	L_{δ_a} = -63.5		
q = 497 psf	$C_{\ell_{\delta_r}}$ = .021	L_{δ_r} = 11.21	L'_{δ_r} = 11.28	
	C_{n_β} = .084	N_β = 13.51	N'_β = 13.66	
	C_{n_r} = -.160	N_r = -.631		
	C_{n_p} = .005	N_p = .1734	N'_p = .1306	
	$C_{n_{\delta_a}}$ = -.0075	N_{δ_a} = .365		
	$C_{n_{\delta_r}}$ = -.085	N_{δ_r} = 13.35	N'_{δ_r} = 13.40	
			L'_ϕ = .0383	
			N_ϕ = -.0270	
			$N'_{\dot{\beta}}$ = -.881	

Approved for Public Release

Contrails

TABLE VII

SUMMARY OF PROPOSED DESIGN DATA FOR T-33 AUXILIARY SURFACE

AREA:	0.827 FT^2 (SUM OF BOTH SIDES)
SPAN:	1.104 FT (13 1/4 IN.) (ONE SIDE)
CHORD:	0.375 FT (4 1/2 IN.)
ASPECT RATIO:	APPROXIMATELY 3.0 (ONE SIDE)
PLANFORM SHAPE:	RECTANGULAR

HINGE AT: 1/4 CHORD OF 1-1/8 IN. AFT OF LEADING EDGE.

LOCATION OF HINGE ON AIRPLANE: APPROXIMATELY AT FUSELAGE STA. 44

ESTIMATED LIFT CURVE SLOPE: (INCLUDING END-PLATE EFFECT) 4.50 RAD^{-1}

PITCHING MOMENT EFFECTIVENESS: $\partial C_m / \partial \delta$ = .00057 DEG^{-1}

WHERE C_m = AIRPLANE PITCHING MOMENT COEFFICIENT

δ = AUXILIARY SURFACE DEFLECTION

MAXIMUM DEFLECTION: ±15°

MAXIMUM ESTIMATED HINGE MOMENT: 1000 INCH-LB
(SUM OF BOTH SIDES, M = .80. ALTITUDE = 5,000 FT, AIRPLANE ANGLE OF ATTACK = 2°, AUXILIARY SURFACE DEFLECTION 15°, LIFT CURVE SLOPE OF AUXILIARY SURFACE = 4.50 RAD^{-1}, CENTER OF PRESSURE AT 1/2 CHORD.)

MAXIMUM ESTIMATE NORMAL LOAD: 450 LB
(ONE SIDE, FOR THE SAME CONDITIONS AS THE HINGE MOMENT.)

Approved for Public Release

Contrails

TABLE VIII

SUMMARY OF PHUGOID PERIODS ATTAINABLE AT VARIOUS T-33 FLIGHT TEST CONDITIONS

T-33 FLIGHT CONDITION	ARTIFICIAL STABILITY FOR SHORT PERIOD SIMULATION	AUXILIARY SURFACE SERVO GAIN $\partial\delta_e/\partial(\Delta q/q)$	ASSUMED PHUGOID DAMPING RATIO	PHUGOID PERIOD (SEC)	TIME TO REACH e TIMES INITIAL AMPLITUDE (SEC)
1. ALTITUDE = 0, M = .70	$\Delta C_{m_\alpha} = 3.40$	+ 300 DEG	.1	-	11.0
		0	.1	112	
	$\Delta C_{m_{D\theta}} = 0$	- 300 DEG	.1	48	
2. ALTITUDE = 35,500 FT, M = .50	$\Delta C_{m_\alpha} = -1.00$	+ 300 DEG	.1	-	21.6
		0	.1	69	
	$\Delta C_{m_{D\theta}} = 0$	- 300 DEG	.1	45	
3. ALTITUDE = 20,000 FT, M = .566	$\Delta C_{m_\alpha} = 0$	+ 300 DEG	.06	-	4.3
		0	.06	95	
	$\Delta C_{m_{D\theta}} = 0$	- 300 DEG	.06	23	

$$\Delta C_{m_\alpha} = C_{m_{\delta_e}} \left(\frac{\partial \delta_e}{\partial \alpha} \right)$$

$$\Delta C_{m_{D\theta}} = \frac{1}{\tau} C_{m_{\delta_e}} \left(\frac{\partial \delta_e}{\partial \dot{\theta}} \right)$$

Approved for Public Release

Contrails

TABLE IX

SUMMARY OF PHUGOID DAMPING RATIOS ATTAINABLE AT VARIOUS T-33 FLIGHT TEST CONDITIONS

T-33 FLIGHT CONDITION	ARTIFICIAL STABILITY	AUXILIARY SURFACE SERVO GAIN $\partial\delta_p/\partial\dot{q}$	AVAILABLE CHANGE OF PHUGOID DAMPING RATIO $\Delta\zeta$
1. ALTITUDE = 0 M = .70	$\Delta C_{m_\alpha} = -3.40$ $\Delta C_{m_{D\theta}} = C_{m_v} = 0$	+10 Deg/psf/sec -10	-2.90 +2.90
2. ALTITUDE = 35,000 FT M = .50	$\Delta C_{m_\alpha} = 1.00$ $\Delta C_{m_{D\theta}} = C_{m_v} = 0$	+10 -10	-.17 +.17
3. ALTITUDE = 20,000 FT M = .566	$\Delta C_{m_\alpha} = 0$ $\Delta C_{m_{D\theta}} = C_{m_v} = 0$	+10 -10	-3.84 +3.84

$$\Delta C_{m_\alpha} = C_{m_{\delta_e}} \frac{\partial \delta_e}{\partial \alpha}$$

$$\Delta C_{m_{D\theta}} = \frac{1}{\tau} C_{m_{\delta_e}} \frac{\partial \delta_e}{\partial \dot{\theta}}$$

Approved for Public Release

Contrails

TABLE X

RANGE OF GAINS REQUIRED FOR SIMULATION OF AIRPLANE MOTION

	RANGE OF GAIN VALUES
$\partial\delta_p/\partial\left(\frac{\Delta q}{q}\right)$	± 300 DEG
$\partial\delta_p/\partial\dot{q}$	± 10 DEG.SEC/PSF
$\partial\delta_e/\partial\alpha$	+ 5.0 TO -1.0
$\partial\delta_e/\partial\dot{\alpha}$	+ .50 SEC TO -.40 SEC
$\partial\delta_e/\partial\dot{\theta}$	+ 1.0 SEC TO -.30 SEC
$\partial\delta_e/\partial\ddot{\theta}$	± .10 SEC^2
$\partial\delta_r/\partial r$	+ 3.5 SEC TO -.46 SEC
$\partial\delta_a/\partial r$	-.80 SEC TO +.19 SEC
$\partial\delta_r/\partial p$	+.65 SEC TO -.80 SEC
$\partial\delta_a/\partial p$	+2.5 SEC TO -.22 SEC
$\partial\delta_r/\partial\beta$	-10 TO +9
$\partial\delta_a/\partial\beta$	+10 TO -6
$\partial\delta_r/\partial\dot{r}$	±.302 SEC^2
$\partial\delta_a/\partial\dot{r}$	±.076 SEC^2
$\partial\delta_r/\partial\dot{p}$	±.149 SEC^2
$\partial\delta_a/\partial\dot{p}$	±.064 SEC^2
$\partial\delta_r/\partial\dot{\beta}$	-3.5 SEC TO +.41 SEC
$\partial\delta_a/\partial\dot{\beta}$	+.45 SEC TO -.27 SEC
NOTE: $\partial\left(\frac{\Delta n_z}{q}\right)/\partial(\Delta\alpha)$	.00217 FT^2/LB.DEG
$\frac{\partial\left(\frac{\Delta n_y}{q}\right)}{\partial(\Delta\beta)}$	-.000206 FT^2/LB-DEG

Approved for Public Release

Contrails

TABLE XI

EXTREME VALUES OF STABILITY DERIVATIVES OBTAINED FROM DATA FOR FOUR FIGHTER AIRCRAFT

		MAXIMUM	MINIMUM
$C_{n_{r_1}}$		-.950	-.01
$C_{\ell_{r_1}}$		+.55	-.025
$C_{n_{p_1}}$		-.265	+.15
$C_{\ell_{p_1}}$		-.60	0
$C_{n_{\beta_1}}$		+.69	+.017
$C_{\ell_{\beta_1}}$		-.258	+.003
A		+.925	+.925
B	EMPTY TIP TANKS ON THE T-33	-1.24	+.795
C	FULL INTERNAL FUEL SUPPLY	+2.48	+2.48
D		-.475	+.314

Approved for Public Release

TABLE XII

EXTREME GAINS REQUIRED FOR SIMULATION OF CONTROL SYSTEMS

GAIN RATIO	RANGES OF VALUES
$\partial F_{ES}/\partial \delta_{ES}$	250 TO .8 LB/IN.
$\partial F_{ES}/\partial (q\delta_{ES})$	.500 TO .004 FT^2/IN.
$\partial F_{ES}/\partial \dot{\delta}_{ES}$	6 TO .05 $\frac{LB\text{-}SEC}{IN.}$
$\partial F_{ES}/\partial \dot{n}_z$	25 TO 0.5 LB/g
a_6 , TRIMMING FORCE (NO SPEED FEEL)	50 LB. PUSH TO 90LB. PULL
a_7 , TRIMMING FORCE (WITH SPEED FEEL)	.188 FT^2 PUSH TO .438 FT^2 PULL
K_θ , ELEVATOR TRIMMING	-15 TO +5 DEG
$\partial \delta_e/\partial \delta_{ES}$	20 TO .2 DEG/IN.
$\partial \delta_e/\partial (a_1 \delta_{ES})$	-2.5 TO -.008 DEG/LB
$\partial \delta_e/\partial (a_2 \delta_{ES})$	-500 TO -4.0 DEG/FT^2
$\partial \delta_e/\partial \left(\frac{1-\cos\phi}{q\cos\phi}\right)$	-400 TO -60 DEG-PSF
AILERON TRIMMING	+20 TO -20 DEG
$\partial F_{AS}/\partial \delta_{AS}$	250 TO .5 LB/IN.
$\partial \delta_a/\partial \delta_{AS}$	40 TO .57 DEG/IN.
$\partial \delta_a/\partial (b_1 \delta_{AS})$	11.4 TO .023 DEG/LB

GAIN RATIO	RANGES OF VALUES
$\partial \delta_a/\partial \delta_{r_c}$	-1.2 TO +.4 DEG/DEG
$\partial \delta_a/\partial \phi$	2 TO 0 DEG/DEG
RUDDER TRIMMING	+15 TO -15 DEG
$\partial F_{RP}/\partial \delta_{RP}$	300 TO 1.5 LB/IN.
$\partial F_{RP}/\partial (q\delta_{RP})$	.60 TO .0075 FT^2/IN.
$\partial F_{RP}/\partial n_y$	400 TO 10 LB/g
$\partial \delta_r/\partial \delta_{RP}$	60 TO 1.0 DEG/IN
$\partial \delta_r/\partial (c_1 \delta_{RP})$	4.67 TO .023 DEG/LB
$\partial \delta_r/\partial (c_2 \delta_{RP})$	933 TO 11.7 DEG/FT^2
$\partial \delta_r/\partial \delta_{a_c}$	+1.5 TO -1.5 DEG/DEG
$\frac{\partial \delta_r/\partial \left(\frac{n_z}{q}\ \delta_{a_c}\right)}{\partial \delta_r/\partial \delta_{a_c}}$	0 TO -576 PSF/g
$\partial \delta_r/\partial \left(\frac{n_z}{q}\ p\right)$	0 TO 28.8 PSF-SEC/g

Approved for Public Release

Contrails

TABLE XIII

MAXIMUM EXPECTED VALUES OF AIRPLANE RESPONSE VARIABLES

THIS TABLE IS BASED ON MAXIMUM VALUES OF AIRPLANE MOTION REPORTED IN REFERENCE 4 OR ANTICIPATED FOR SEVERAL PRESENT-DAY OPERATIONAL AND NEAR-OPERATIONAL JET FIGHTERS. IN SOME CASES (ROLL RATE AND ACCELERATION FOR EXAMPLE), THE T-33 CAN NOT SIMULATE THE MAXIMUM VALUES, AND SO REASONABLE ESTIMATES OF THE T-33 CAPABILITIES ARE GIVEN IN THESE CASES.

ANGULAR ACCELERATIONS	
$\ddot{\theta}$	2.5 RAD/SEC^2
$\dot{p}$	10.0 RAD/SEC^2
$\dot{r}$	1.2 RAD/SEC^2
ANGULAR VELOCITIES	
$\dot{\theta}$	0.7 RAD/SEC
p	5.0 RAD/SEC
r	0.5 RAD/SEC
ANGLES OF ATTACK AND SIDESLIP	
$\dot{\alpha}$	.6 RAD/SEC
α	+10 TO -8 DEG
$\dot{\beta}$	.5 RAD/SEC
β	15 DEGREES
LOAD FACTORS	
n_z	+7.3 TO -3.0
n_y	1.0
DYNAMIC PRESSURE	
q	80 TO 800 PSF
Δq	144 PSF
$\Delta q/q$	0.20
$\dot{q}$	10 PSF/SEC

Approved for Public Release

Contrails

TABLE XIV

MAXIMUM VALUES OF CONTROL SYSTEM VARIABLES

F_{ES}	=	200 LB
δ_{ES}	=	5 IN. FWD. TO 9 IN. AFT
$\dot{\delta}_{ES}$	=	25 IN/SEC
δ_e	=	+16° TO -20°
F_{AS}	=	100 LB
δ_{AS}	=	±7 IN.
δ_a	=	±20° FOR EACH AILERON
F_{RP}	=	300 LB
δ_{RP}	=	±4 IN.
δ_r	=	±30°

Approved for Public Release

Approved for Public Release

TABLE XV

POSITION SERVO DESIGN VALUES FOR T-33 AND F-86 SYSTEMS

1	2	3	4	5	6	7	8	9	10	11	12	13	14	15	16	17
CONTROL SURFACE	LIMIT HINGE MOMENT	DEFLECTIONS AT MAX. AIR LOAD	MOMENT OF INERTIA	MAXIMUM WORKING PRESSURE	(AT)	$\dot{\delta}_{max}$	Q_{max}	δ_{max} (NO LOAD)	$\frac{\delta_{max}}{4(Ar)B\eta}$	M_s/δ_s		Z_p/k_s		CONTROL SURFACE MAX. TRAVEL	ACTUAL SERVO PISTON STROKE	ACTUAL SERVO PISTON AREA
	IN-LB	DEG	LB-IN^2	LB/IN^2	IN^3	RAD/SEC	IN^3/SEC	RAD	(IN-LB)$^{-1}$	SPRING (IN-LB) RAD	INERTIA SLUG-IN^2	SPRING NO DIMENSIONS	PERIOD SEC.	DEG	INCHES	IN^2
T-33 AILERON (ONE)	7200	4.8	* 1522	700	10.3	1.2	12.4	0.70	δ 1.06 x 10^{-7}	8.6 x 10^4	47.3	0.91 x 10^{-2}	6.46 x 10^{-4}	⊙ 80	⊙ 3.5	⊙ 4.11
T-33 ELEVATOR	2625	3.66	++ 826	700	3.75	1.2	4.5	0.63	δ 2.64 x 10^{-7}	4.1 x 10^4	26.7	1.08 x 10^{-2}	7.50 x 10^{-4}	36	3.0	.752
T-33 RUDDER	2480	3.26	oo 594	700	3.54	1.2	4.3	1.05	δ 4.35 x 10^{-7}	4.7 x 10^4	18.4	2.04 x 10^{-2}	8.15 x 10^{-4}	60	3.0	1.166
F-86 RUDDER	1870	1.0	1316	2000	0.94	12.0	11.3	0.70	δ 13.9 x 10^{-7}	10.7 x 10^4	41.0	14.9 x 10^{-2}	21.8 x 10^{-4}	50	1.8	.45

δ FOR F-86
B = 0.2 x 10^6, AND η = .67

δ FOR T-33
B = 0.2 x 10^6, AND η = .80

* ONE AILERON PLUS ½ CONTROL STICK

++ ELEVATOR PLUS STICK

oo RUDDER PLUS ONE SET PEDALS

⊙ VALUES FOR SINGLE SERVO ACTUATOR DRIVING TWO AILERONS. CONTROL SURFACE TRAVEL IS LEFT PLUS RIGHT AILERON MOTION.

TABLE XVI

DESIGN VALUES FOR PRESSURE- CONTROL TYPE FEEL SERVOS

1	2	3	4	5	6	7	8	9	10	11	12	13	14
PILOT'S CONTROL	MAXIMUM FORCE	MAXIMUM TRAVEL	MAXIMUM RATE	MAXIMUM SPRING	MINIMUM SPRING	R	$\frac{F}{\Delta P}=(AR)$	A	A	$(AR$	F_{max}	Q_{max}	PISTON STROKE
	LB.	IN.	IN/SEC	LB/IN	LB/IN	NO DIM.	IN^2	IN^2	IN^2	IN^2	LB	IN^3/SEC	IN
	*		□				⊙*	*	ACTUAL	ACTUAL	ACTUAL	ACTUAL	ACTUAL
ELEVATOR STICK GRIP **	200	11.0	21.0	294	8	.287	.200	.695	.752	.216	216	4.5	3.0
ELEVATOR WHEEL GRIP +○	200	12.4	23.6	294	8	.252	.200	.795	.752	.190	190	4.5	3.0
AILERON STICK GRIP △	100	15.4				.131	.100	.763	.752	.099	99	1.7	2.0
AILERON WHEEL RIM ○-○	100	13.6	16			.147	.100	.680	.752	.111	111	1.65	2.0
RUDDER PEDALS	300	8.32	19			.360	.300	.833	.835	.300	300	5.7	3.0

NOMINAL VALUES MARKED *

NOMINAL VALUES MARKED *

⊙ FOR ΔP = 1000 PSI

○-○ AT WHEEL RIM OF 6.5 IN. RADIUS

+○ TRAVEL AND FORCE AT 24.0 IN RADIUS

** TRAVEL AND FORCE AT 21.2 IN. RADIUS

△ TRAVEL AND FORCE AT 25.7 IN. RADIUS

□ FOR 1.2 RAD/SEC CONTROL SURFACE RATE

Approved for Public Release

Approved for Public Release

TABLE XVII

TABLE OF POSITION SERVO TEST RIG PARAMETERS

CONFIGURATION	r	k_ℓ	m_c	k_a	c_a	ω_{n_1}	ζ_1	ω_{n_2}	ζ_2	ω_{n_3}	ζ_3
	SERVO-PISTON RADIUS	CABLE STIFF-NESS	AILERON INERTIA	AIR LOAD STIFF-NESS	AIR LOAD DAMPING	$\sqrt{\frac{k_\ell + k_a}{m_c}}$	$\frac{1}{2}\frac{c_a}{\sqrt{(k_\ell + k_a)m_c}}$	$\sqrt{\frac{k_a}{m_c}}$	$\frac{1}{2}\frac{c_a}{\sqrt{k_a m_c}}$	$\sqrt{\frac{k_\ell}{m_c}}$	$\frac{1}{2}\frac{c_a}{\sqrt{k_\ell m_c}}$
	IN.	IN-LB/DEG	LB-IN.^{2}	IN-LB/DEG	$\frac{\text{IN-LB}}{\text{DEG/SEC}}$	CPS		CPS		CPS	
FUSELAGE SERVO HALF-SCALE LOADS	3.75	1295	1500	1340	4*	31.4	0.15*	22.3	0.21*	22.1	0.03
FUSELAGE SERVO FULL-SCALE LOADS	7.5	1295	3000	3150	8.1*	29.0	0.17*	24.2	0.20*	15.6	0.04
WING SERVO SYMMETRICAL LOADS	3.75	31,000	1500	1340	4*	110.0	0.04*	22.3	0.21*	108.0	0.005
WING SERVO UNSYMMETRICAL LOADS	3.75	31,000	1500	3150	4*						

* These values of damping achieved only when the frequency-amplitude product at the aileron is 50 in-cps.

Contrails

APPENDIX

T-33 DATA OBTAINED AT LOCKHEED AIRCRAFT CORPORATION ON AUGUST 4-5, 1954

A-1 Table of Dimensional Data for the T-33A Airplane

A-2 Weight and Balance Data for the T-33A Airplane.

A-3 Moment of Inertia Summary for Model L245 (T-33B) Airplane

A-4 Miscellaneous Comparative Data

A-5 Lift Curve, Drag Polar and Elevator Floating Angle of the T-33A Airplane

A-6 Static Longitudinal Stability Data for the T-33A Airplane

A-7 Damping in Pitch Derivatives for the T-33A Airplane

A-8 Elevator Effectiveness for Large Deflections

A-9 Linear Elevator Effectiveness and Hinge Moment Data for the T-33 Airplane

A-10 Sideslip Derivatives for T-33 Airplane (Tip Tanks Off)

A-11 Sideslip Derivatives for T-33 Airplane (Tip Tanks On)

A-12 Rolling Derivatives for T-33 Airplane (Tip Tanks On and Off)

A-13 Yawing Derivatives for T-33 Airplane (Tip Tanks On and Off)

A-14 Lateral Control Effectiveness for T-33A Airplane

A-15 Lateral Control Effectiveness and Hinge Moment Data for the T-33A Airplane

A-16 T-33A Tabulated Stability Derivatives Used for IBM Calculations of Responses

A-17 Calculated T-33A Response Data, Tip Tanks Off, Short Period Motion

A-18 Calculated T-33A Response Data, Tip Tanks Off, Dutch Roll Motion

A-19 Three View Drawing of T-33 Airplane

NOTE: UNLESS OTHERWISE SPECIFIED, ALL DATA ARE FOR FLAPS UP AND TIP TANKS OFF.

Approved for Public Release

Contrails

A-I TABLE OF DIMENSIONAL DATA FOR THE T-33A AIRPLANE

BASIC DATA

A. WING

AREA, S		234.8 SQ FT
SPAN, b		37.54 FT
MAC, $\bar{c}$		80.6 IN. = 6.72 FT
ASPECT RATIO, A		6.00
TAPER RATIO		.355
SWEEPBACK (L.E.)		9.31°
SWEEPBACK ($\bar{c}$ .25)		5.0°
STRAIGHT ELEMENT, 52% OF CHORD	FUS. STA.	227.2
DIHEDRAL (WING REF. PLANE)		3.83°
INCIDENCE (ROOT)		1.0°
GEOMETRIC TWIST (ROOT STA. TO W.S. 222)		-1.5°
AIRFOIL SECTION	NACA	65_1-213
CHORDS		
ROOT (W.S.-0)		110.0 IN.
TIP (W.S. 216)		41.89 IN.
LOCATION OF 25% $\bar{c}$ FUS. STA.		205.45

B. AILERON (EACH SIDE)

AREA, S_a	8.75 SQ FT
MEAN CHORD, $\bar{c}_a$	1.17 FT
DEFLECTION LIMITS, δ_a	±20°
TAB AREA, S_{at}	.399 SQ FT
TAB MEAN CHORD, c_{at}	3.86 IN.
TAB DEFLECTION LIMITS	±20°

C. WING FLAPS (EACH SIDE)

TYPE	SPLIT
AREA, S_f	15.32 SQ FT
MEAN CHORD, c_f	1.8 FT
MAXIMUM DEFLECTION	45°

D. HORIZONTAL TAIL

AREA, S_t		43.5 SQ FT
SPAN, b_t		15.58 FT
MEAN CHORD, $\bar{c}_t$		3.12
ASPECT RATIO, A_t		5.58
TAPER RATIO		.319
AIRFOIL SECTION	NACA	65_2-010

Approved for Public Release

Contrails

CHORDS	
ROOT	4.33 FT
TIP (EQUIV.)	1.38 FT
$\bar{Y}/\frac{b}{2}$ (SPANWISE MAC LOCATION)	.412
STRAIGHT ELEMENT, 75% OF CHORD	
$\bar{V}_1[(S_t/S)\ (\ell_t/\bar{c})]$	.438
ℓ_t (.25 $\bar{c}$ to .25 $\bar{c}_t$)	15.9 FT
$\ell_t/\bar{c}$	2.37

E. ELEVATOR (SAME FOR T-33A AND F-94A AND B)

AREA (BOTH SIDES)	8.70 SQ. FT
MEAN CHORD $\bar{c}_e$	.708 FT.
DEFLECTION LIMITS (AF TRAINING LIMITS)	-20° TO +16°

F. VERTICAL TAIL

AREA, S_v		22.5 SQ. FT
SPAN, b_v		6.42 FT
ASPECT RATIO, A_v		1.83
MEAN CHORD, $\bar{c}_v$		3.89 FT
TAPER RATIO		.309
AIRFOIL SECTION	NACA	65_2-010
CHORDS		
ROOT		5.42 FT
TIP (EQUIV.)		1.79 FT
ℓ_t (.25 $\bar{c}$ TO .25 $\bar{c}_t$)		16.08
$\bar{V}_1[(S_t/S)(\ell_t/b)]$		.041
ℓ_t/b		.428

$\bar{z}/b = .1112 - .00748\alpha$ (T-33A FOR ANY α)

G. RUDDER

AREA, S_r	5.3 SQ. FT
MEAN CHORD $\bar{c}_r$	1.09 FT
DEFLECTION LIMITS, σ_r	±30°

H. DIVE FLAPS (EACH SIDE)

AREA, S_{df}	2.95 SQ. FT.
MEAN CHORD, $\bar{c}_{df}$	2.22 FT.
MAXIMUM DEFLECTION, σ_{df}	45°

Approved for Public Release

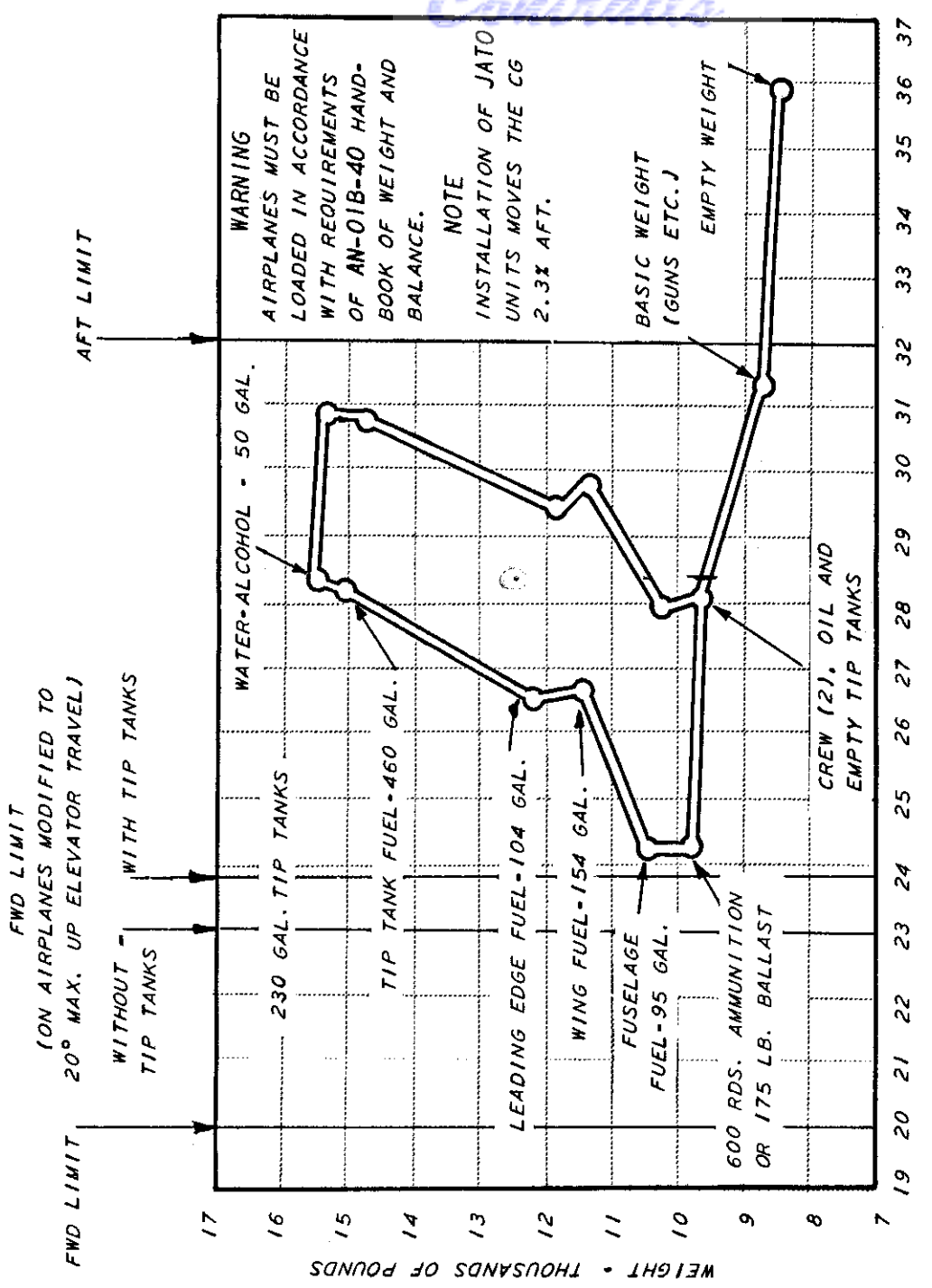

A-2 WEIGHT AND BALANCE DATA FOR T-33A AIRPLANE
(TAKEN FROM FLIGHT HANDBOOK)

Approved for Public Release

Contrails

A-3 MOMENT OF INERTIA SUMMARY FOR MODEL L245 (T-33B) AIRPLANE *

SLUG-FT^2

CONDITION (GEAR UP)	$I_{X_{cg}}$ ROLL	$I_{Y_{cg}}$ PITCH	$I_{Z_{cg}}$ YAW	ΣWXZ_{cg}	$\bar{X}$	$\bar{Z}$	WEIGHT LBS.
NON-EXPEND. USEFUL LOAD-NO FUEL	7,735	20,072	26,292	527	236.2	100.6	9,919
1/3 WING	7,747	20,235	26,633	499	236.7	101.5	11,194
2/3 WING	8,264	20,274	27,166	485	237.2	101.1	11,519
FULL INTERNAL	8,932	20,299	27,833	479	237.5	100.8	11,870
FULL INT. AND EMPTY TIP TANKS	13,480	20,522	32,589	476	237.8	100.6	12,267
FULL INT. AND FULL TIP TANKS	47,687	21,761	67,967	470	238.3	99.8	15,257

CG LOCATION

L.E. = 211.9 M.A.C.

* BASED ON THE NAVIGATIONAL VERSION WITH STANDARD EQUIPMENT (NO TEST INSTRUMENTATION) AS ADJUSTED FROM ACTUAL WEIGHT AT PLANT B-9, DECEMBER 9, 1953. THIS AIRPLANE CONTAINS 258 POUNDS OF FIXED NOSE BALLAST (X = 27): UP TO 467 POUNDS MORE (AVERAGE ARM X = 59.5) MAY BE USED TO SHIFT THE CG FORWARD OF 33% M.A.C. INERTIA FIGURES DO NOT INCLUDE THE 467 POUNDS FLIGHT TEST BALLAST. FUTURE MODIFICATIONS MAY INCLUDE RUDDER EXTENSION, RELOCATED DRAG CHUTE, NOSE STEERING, VARIABLE RATIO BOOST, JET SILENCER, AND REVERSE THRUST. EACH ONE POUND INCREASE IN THE TAIL AREA WILL REQUIRE APPROXIMATELY ONE POUND INCREASE IN FIXED NOSE BALLAST.

Approved for Public Release

THE T-33 HAS THE SAME WING AS THE F-80. IT ALSO HAS THE SAME EMPENNAGE AND THE SAME CONTROL SYSTEM. THE FUSELAGE HAS BEEN LENGTHENED 14 INCHES AFT OF THE WING AND 30 INCHES FORWARD OF THE WING. THE 14 INCHES ADDED AFT OF THE WING MAINTAINS THE SAME LONGITUDINAL STABILITY AS THAT OF THE F-80.

THE F-94A ALSO HAS THE SAME WING AND SAME VERTICAL TAIL AS THE F-80. IT HAS THE SAME HORIZONTAL TAIL OUTSIDE OF THE FUSELAGE BUT THE TAIL SPAN IS GREATER BECAUSE THE FUSELAGE IS WIDER AT THE REAR. THE F-94A ALSO HAS THE SAME CONTROL SYSTEM AS THE F-80.

THE VARIATION OF ZERO LIFT PITCHING MOMENT COEFFICIENT WITH MACH NUMBER FOR THE T-33 CAN BE JUDGED FROM THE OLD NACA AMES LABORATORY TEST OF THE F-80. THE CURVE CAN BE SHIFTED TO MATCH THE LOW MACH NUMBER VALUE FOR THE T-33.

THE T-33B IS ALMOST 300 LBS. HEAVIER THAN THE T-33A.

Approved for Public Release

Contrails

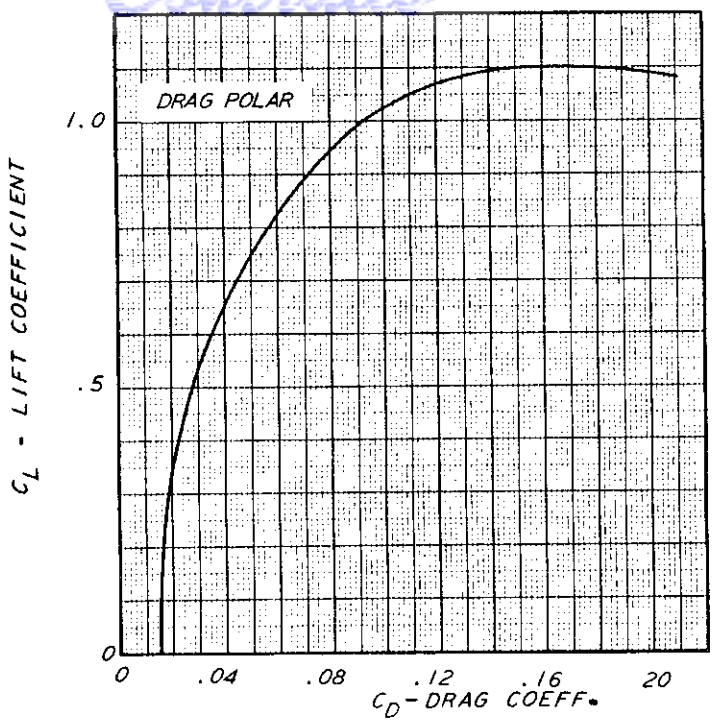

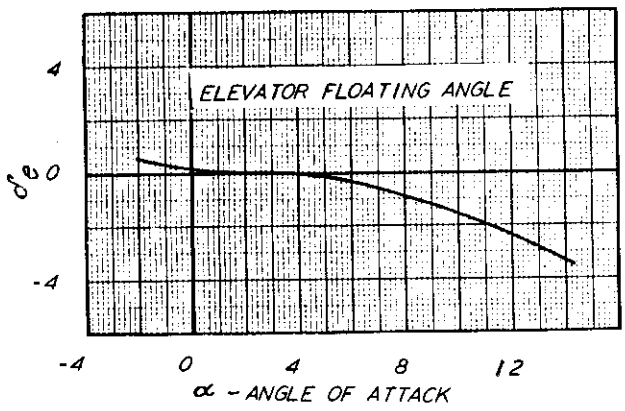

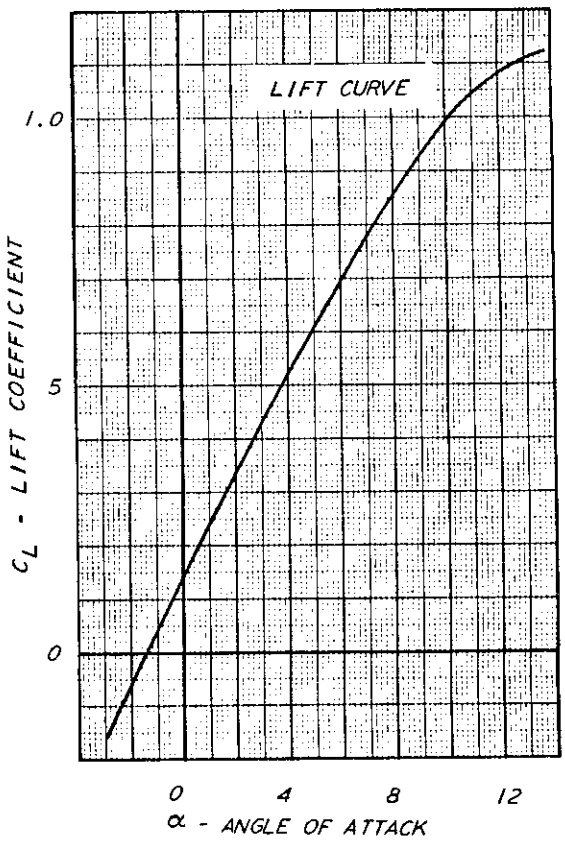

A-5 LIFT CURVE, DRAG POLAR AND ELEVATOR FLOATING ANGLE OF THE T-33A AIRPLANE

FROM: LAL REPORT 127. EFFECT OF FUSELAGE AND CAB MODIFICATIONS ON PITCH DATA - FLAPS UP

Approved for Public Release

Contrails

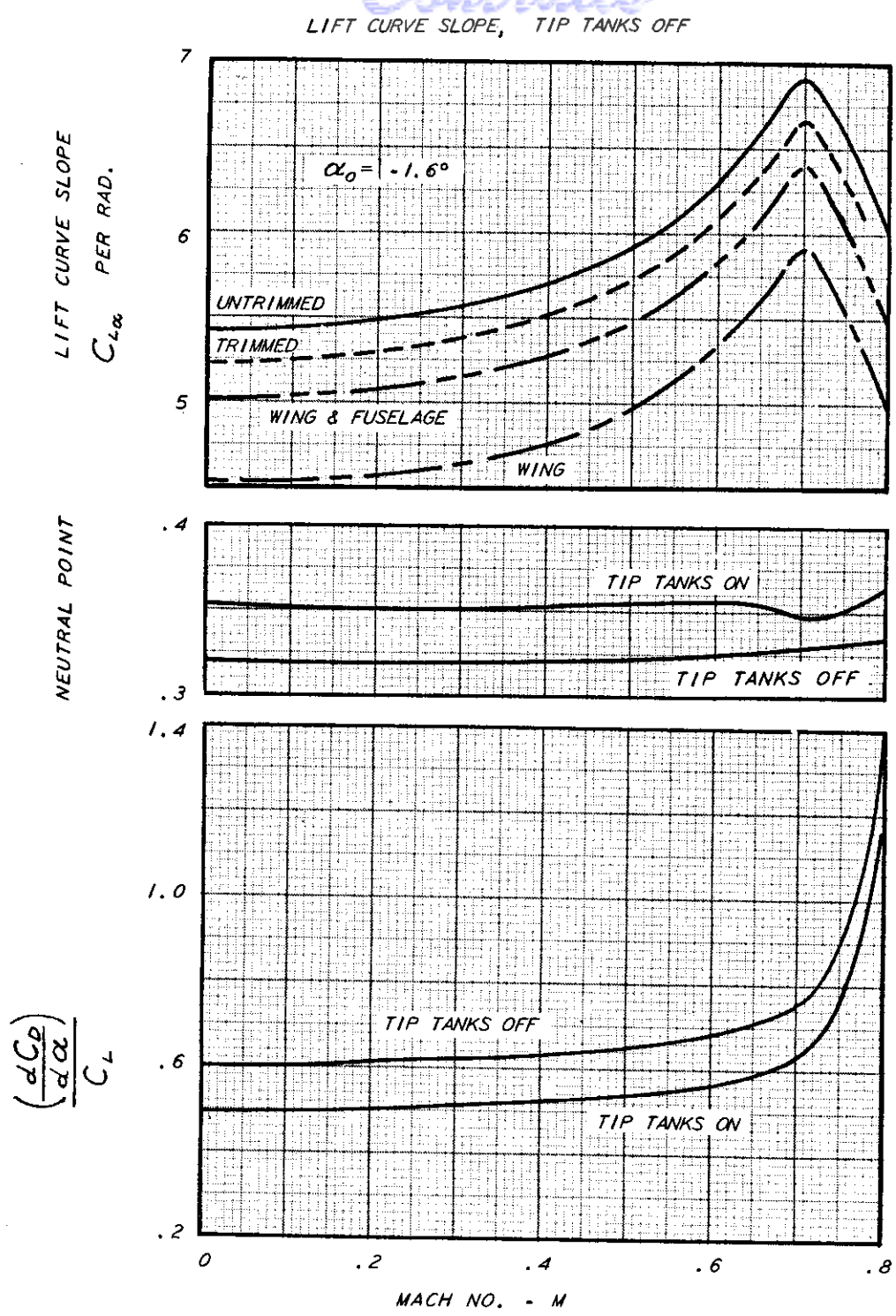

A-6 STATIC LONGITUDINAL STABILITY DATA FOR THE T-33A AIRPLANE

Approved for Public Release

Contrails

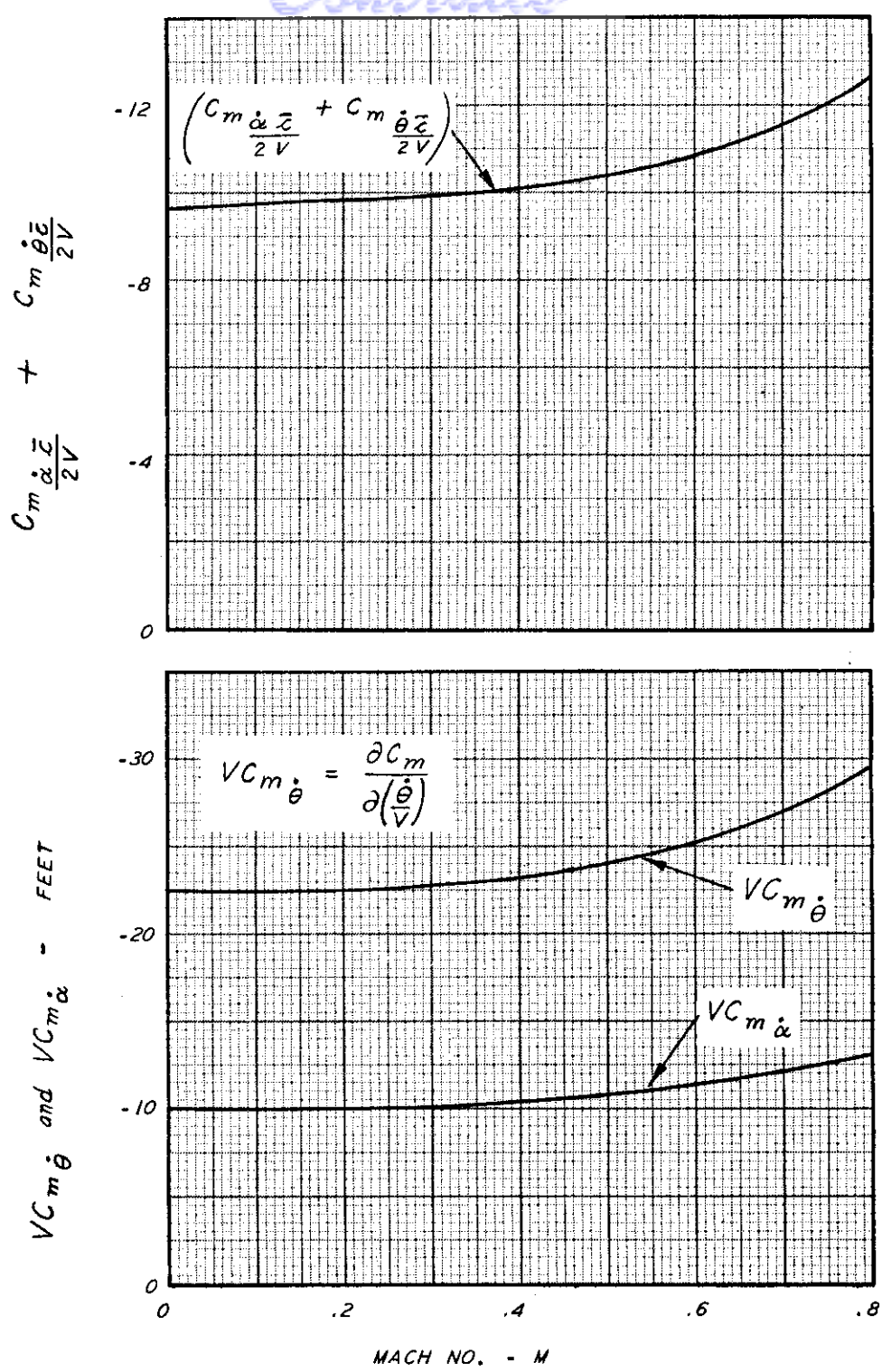

A-7 DAMPING IN PITCH DERIVATIVES FOR THE T-33A AIRPLANE
$[\bar{c}/_2 = 3.36]$

Approved for Public Release

Contrails

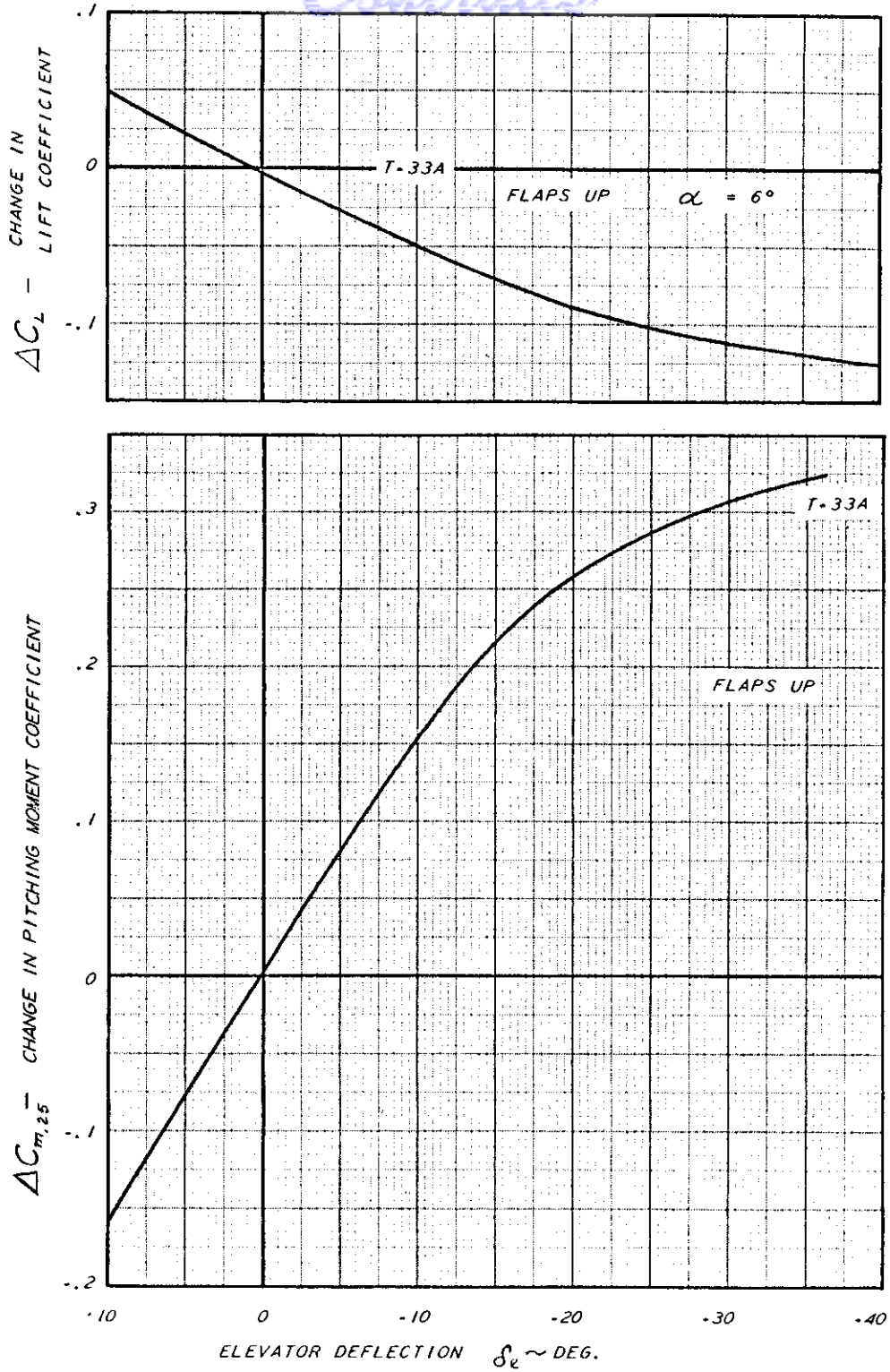

A-8 ELEVATOR EFFECTIVENESS FOR LARGE DEFLECTIONS

Approved for Public Release

Contrails

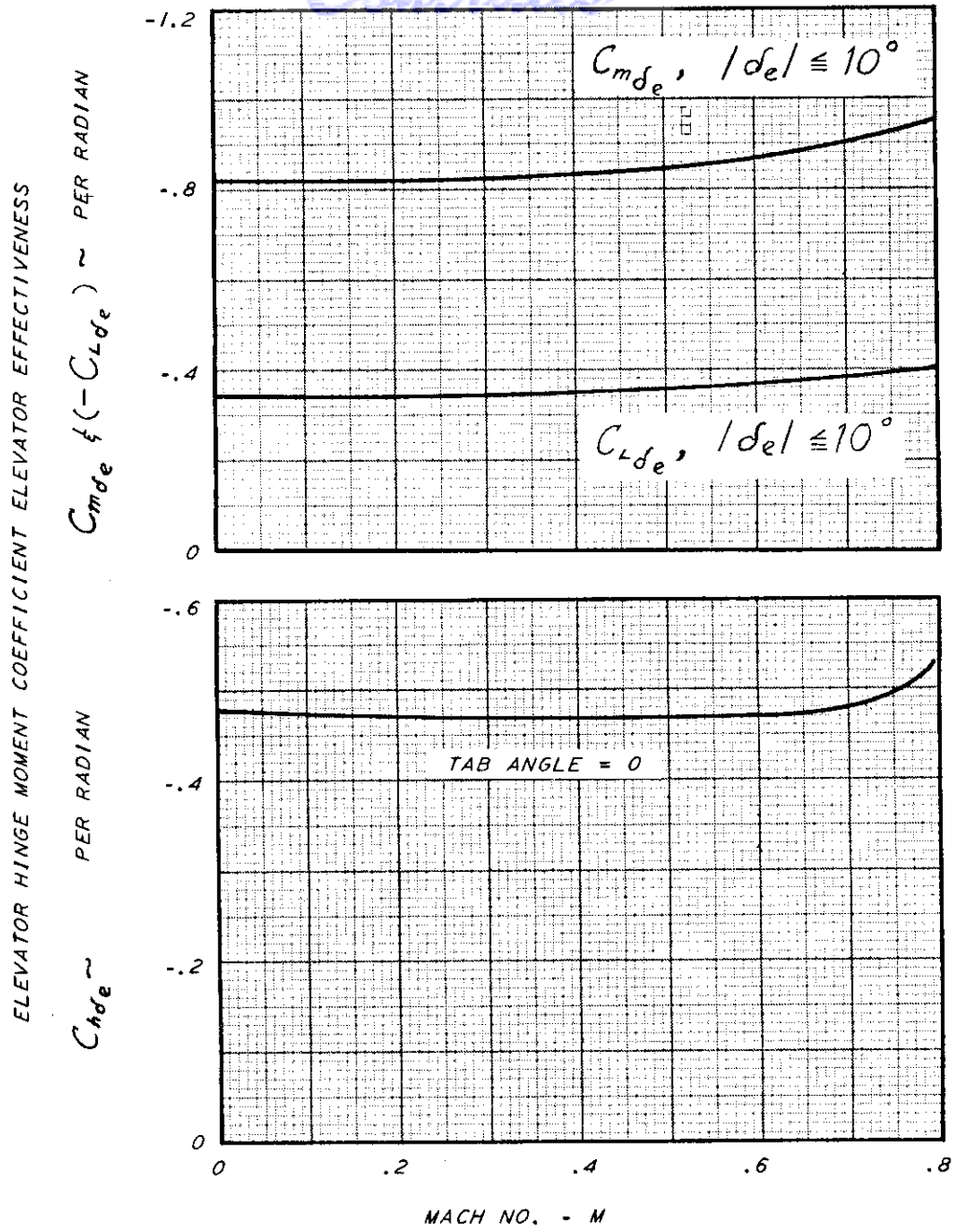

A-9 LINEAR ELEVATOR EFFECTIVENESS AND HINGE MOMENT DATA FOR THE T-33A AIRPLANE

Approved for Public Release

Contrails

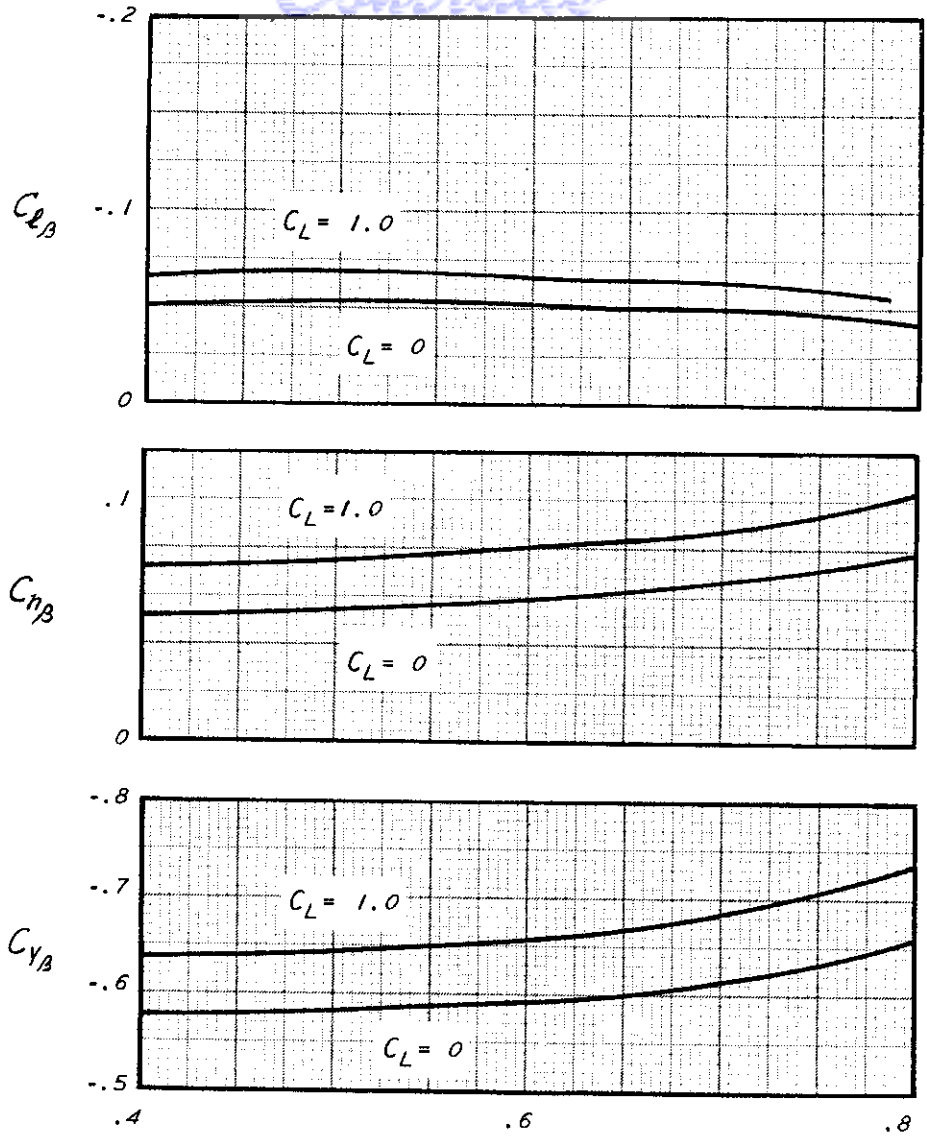

A-10 SIDESLIP DERIVATIVES FOR T-33 AIRPLANE
(TIP TANKS OFF)

Approved for Public Release

Contrails

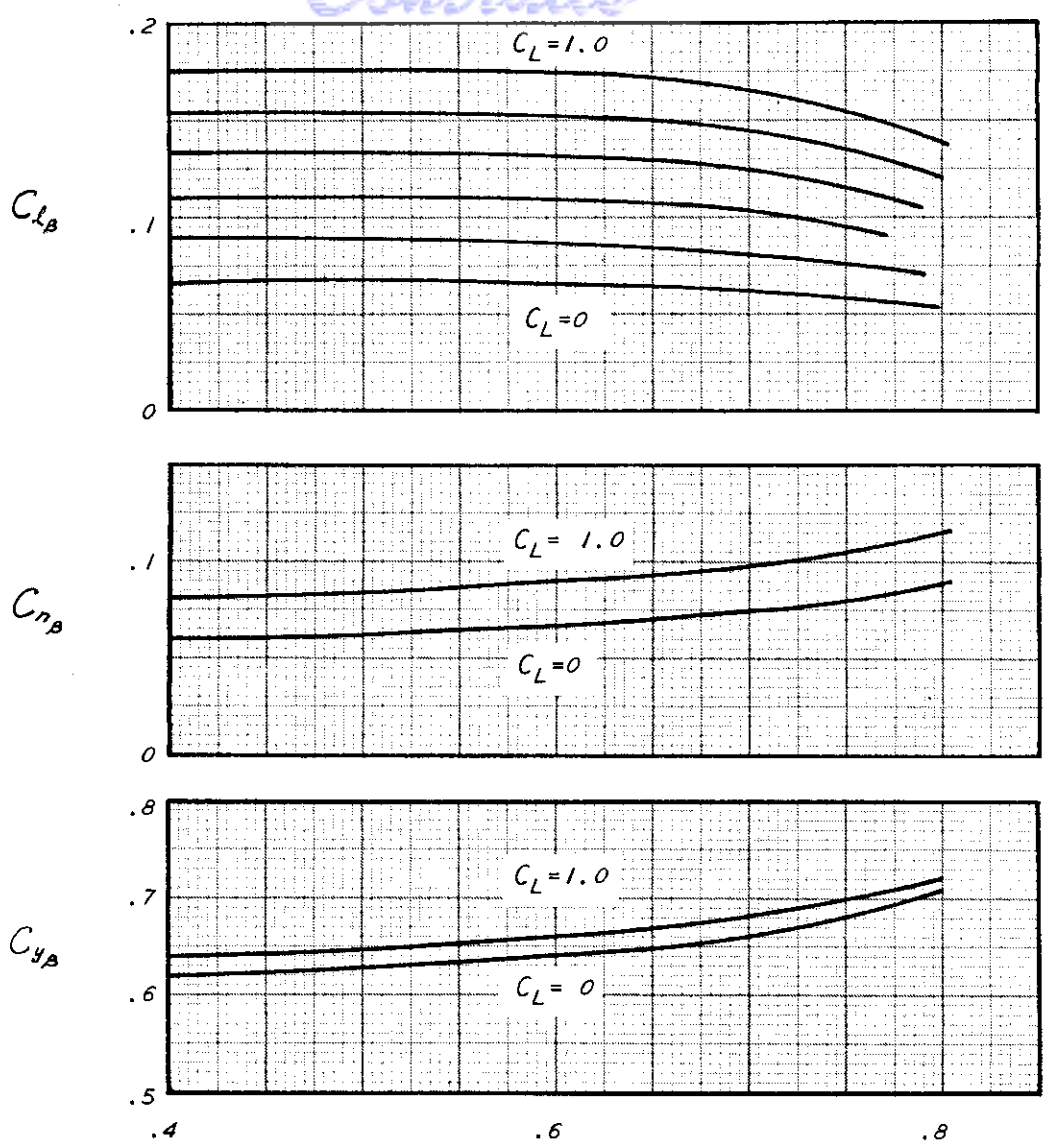

A-11 SIDESLIP DERIVATIVES FOR T-33 AIRPLANE (TIP TANKS ON)

Approved for Public Release

Contrails

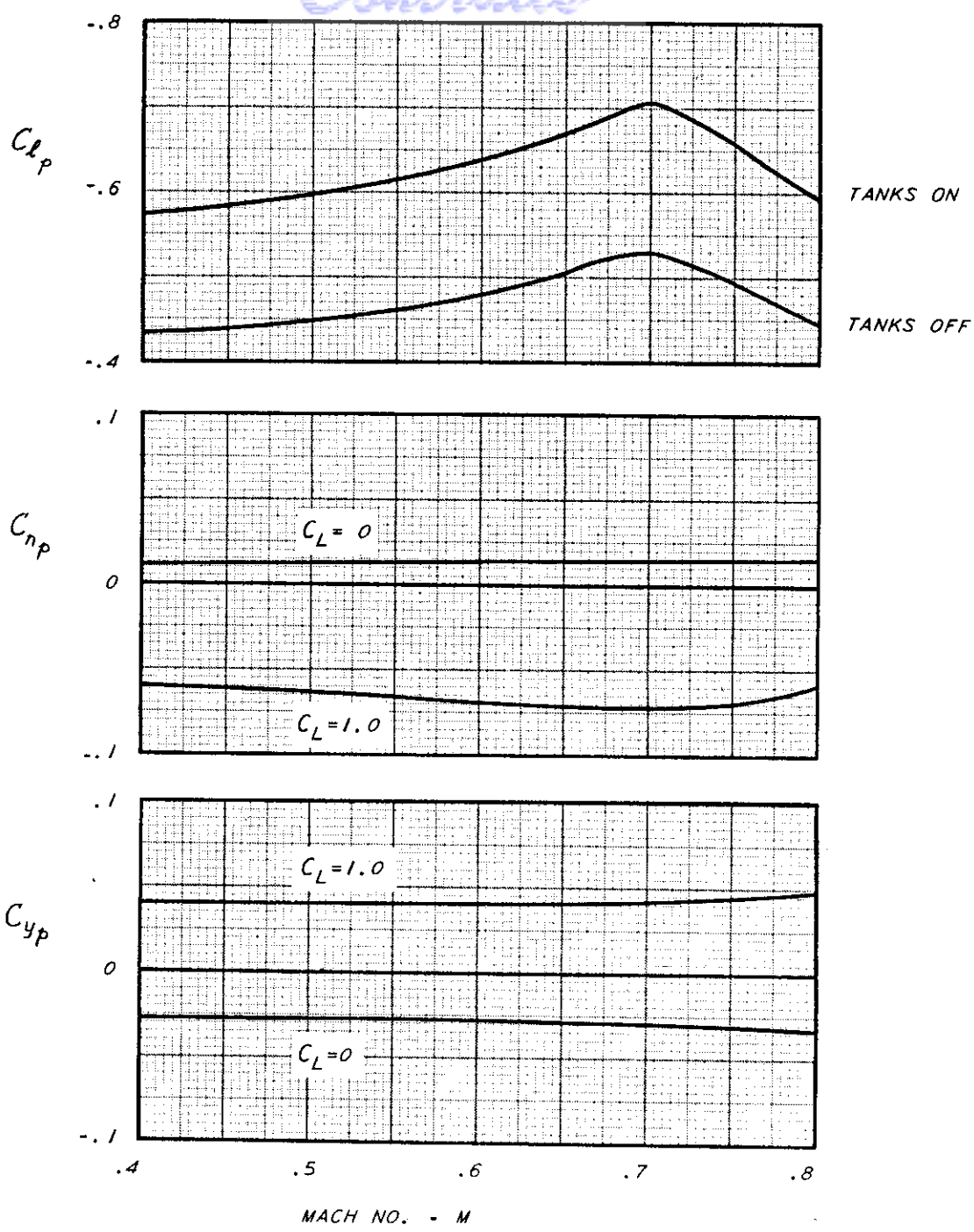

A-12 ROLLING DERIVATIVES FOR T-33 AIRPLANE (TIP TANKS ON AND OFF)

Approved for Public Release

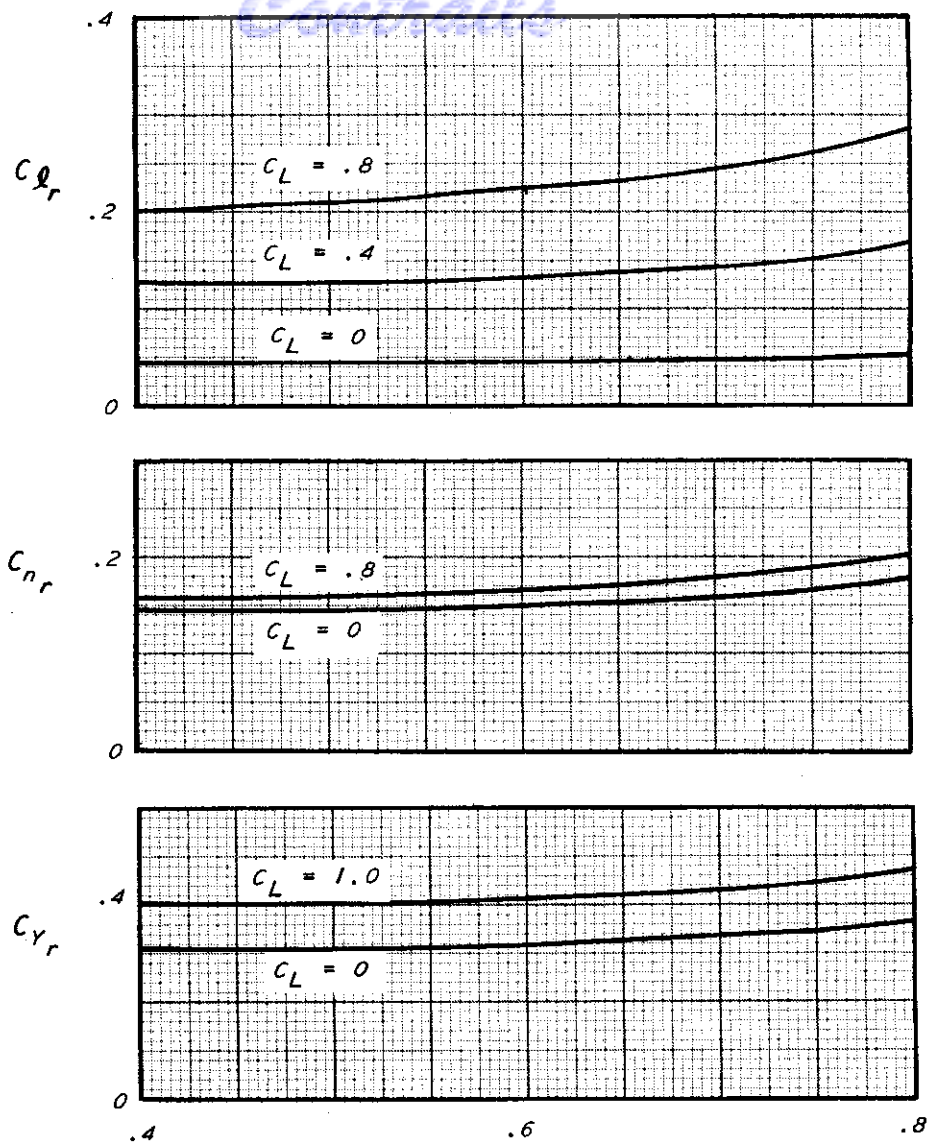

A-13 YAWING DERIVATIVES FOR T-33 AIRPLANE
(TIP TANKS ON AND OFF)

Approved for Public Release

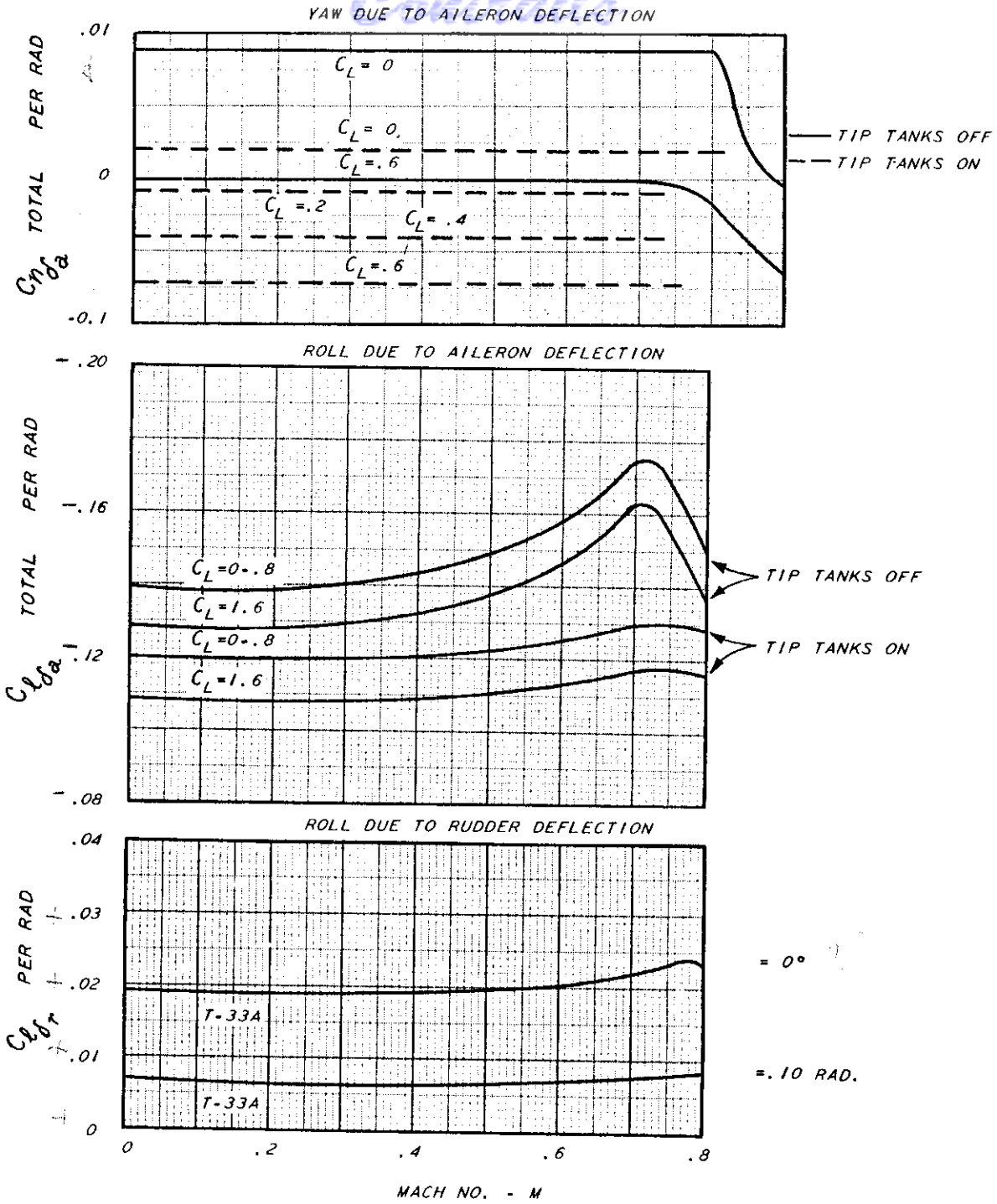

A-14 LATERAL CONTROL EFFECTIVENESS FOR T-33A AIRPLANE

NOTE: +1° AILERON = PORT AILERON T.E. DOWN ½°, STARBOARD AILERON UP ½°

Approved for Public Release

Contrails

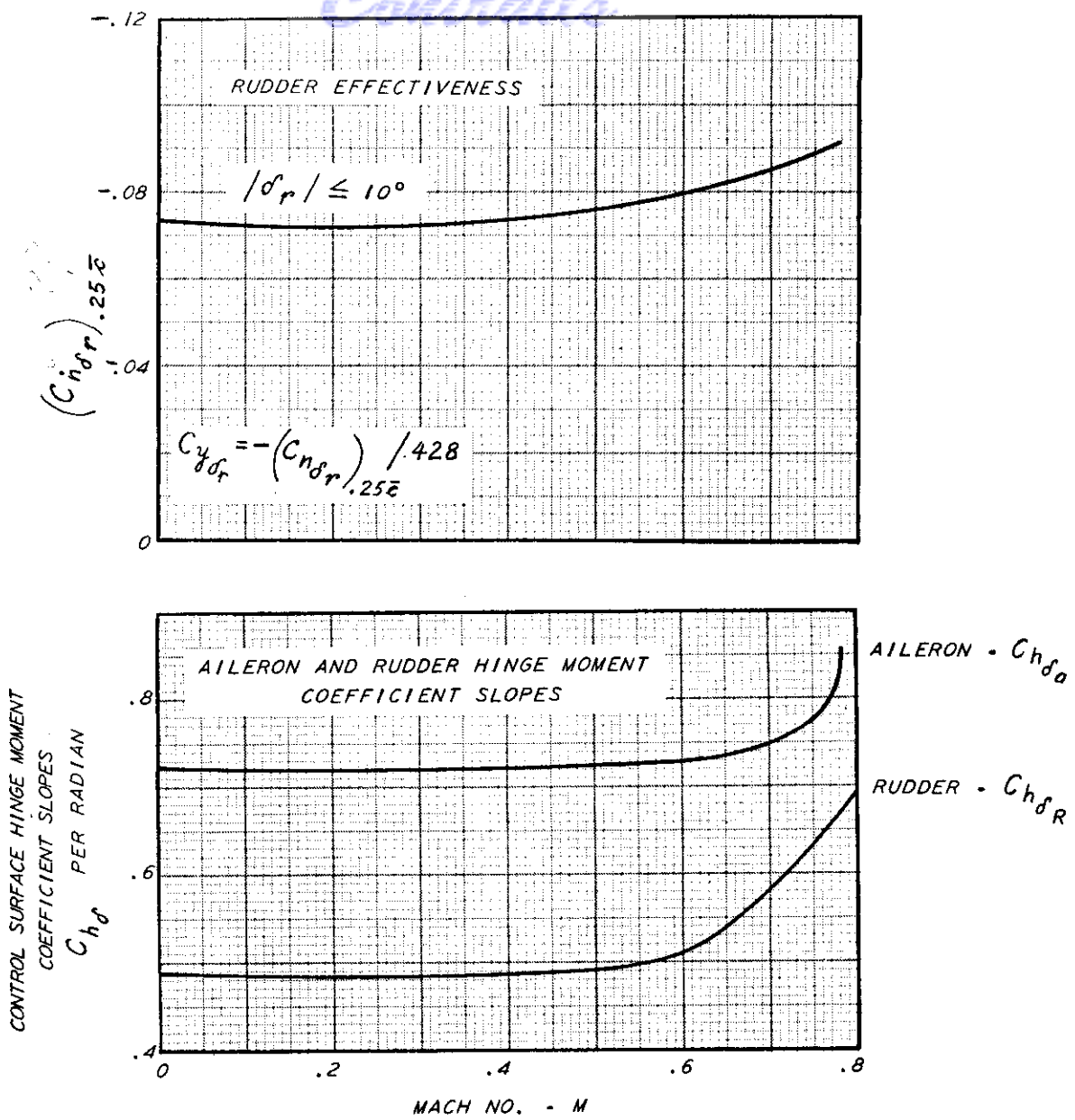

A-15 LATERAL CONTROL EFFECTIVENESS AND HINGE MOMENT DATA FOR THE T-33A AIRPLANE

Approved for Public Release

Contrails

A-16 T-33A STABILITY DERIVATIVES USED FOR IBM CALCULATIONS OF RESPONSES

NOTE: THIS DATA WAS TAKEN FOR A TIP TANKS OFF CONDITION

	ALTITUDE	MACH NO	V FT/SEC	C_L	C_{L_α} 1/RAD	C_{L_M}	C_D	C_{D_α} 1/RAD	C_{D_M}	C_{m_α} 1/RAD	C_{m_M}	$C_{m_{D\alpha}}$ 1/RAD	$C_{m_{D\theta}}$ 1/RAD
1	0	.3	335	.400	5.375	.13	.021	.248	.00601	-.198	-.00415	-.0147	-.033
2		.5	558	.144	5.73	.09	.0125	.0937	.00148	-.218	-.00527	-.0155	-.0345
3		.7	780	.0735	6.66	0.	.0130	.0551	.0160	-.310	-.00467	-.0176	-.0389
4	15,000	.3	316	.711	5.375	.25	.044	.441	.0205	-.198	-.00733	-.00923	-.0207
5		.5	528	.255	5.73	.13	.015	.166	.00406	-.218	-.0095	-.00978	-.0217
6		.7	739	.131	6.66	0.	.014	.0984	.0227	-.310	-.00828	-.0110	-.0244
7		.75	792	.1135	6.30	-.33	.015	.102	.0481	-.314	+.00208	-.0113	-.0255
8	35,000	.5	486	.613	5.73	.32	.035	.399	.0293	-.218	-.0228	-.00481	-.0107
9		.7	680	.313	6.66	0.	.0196	.235	.0530	-.310	-.0199	-.00543	-.0120
10		.75	729	.273	6.30	-.56	.022	.245	.083	-.314	+.00481	-.00567	-.0125

			μ_1	C_{Y_β} 1/RAD	C_{n_β} 1/RAD	C_{l_β} 1/RAD	C_{Y_p} 1/RAD	C_{n_p} 1/RAD	C_{l_p} 1/RAD	C_{Y_r} 1/RAD	C_{n_r} 1/RAD	C_{l_r} 1/RAD	C_{m_T}
1	0	.3	103.6	-.600	.075	-.060	0.	-.020	-.420	.360	-.150	.125	.00156
2		.6	103.6	-.590	.071	-.055	-.017	0.	-.445	.327	-.150	.075	.00093
3		.7	103.6	-.617	.084	-.050	-.025	.080	-.630	.344	-.162	.062	.00097
4	15,000	.3	164.2	-.620	.083	-.063	.040	-.065	-.420	.380	-.151	.185	.00328
5		.5	164.2	-.603	.074	-.056	-.010	-.010	-.445	.340	-.150	.095	.00112
6		.7	164.2	-.622	.086	-.051	-.035	-.042	-.530	.350	-.161	.080	.00104
7		.75	164.2	-.650	.089	-.048	-.025	-.005	-.490	.360	-.170	.088	.00112
8	35,000	.5	334.	-.620	.086	-.063	.015	-.033	-.445	.385	-.152	.175	.00260
9		.7	334.	-.630	.090	-.055	-.040	-.040	-.530	.350	-.165	.135	.00144
10		.75	334.	-.658	.096	-.060	-.012	-.010	-.490	.380	-.172	.120	.00164

i_y = 4.81 $\quad$ T_v = 0
i_x = .0659 $\quad$ z_t = .25 FT
i_z = .209 $\quad$ z_t/c = .0372
cg at .283 $\bar{c}$ $\quad$ η = 0
W = 12,500 LBS.

	ALTITUDE	M	τ	μ_2	i_{xz}
1	0	.3	2.08	18.5	-.00334
2		.5	1.26	18.5	.00394
3		.7	.891	18.5	.00693
4	15,000	.3	3.49	29.4	-.01170
5		.5	2.09	29.4	.00107
6		.7	1.49	29.4	.00459
7		.75	1.39	29.4	.00406
8	35,000	.5	4.62	59.8	-.00792
9		.7	3.30	59.8	.000648
10		.75	3.08	59.8	.00581

Approved for Public Release

Contrails

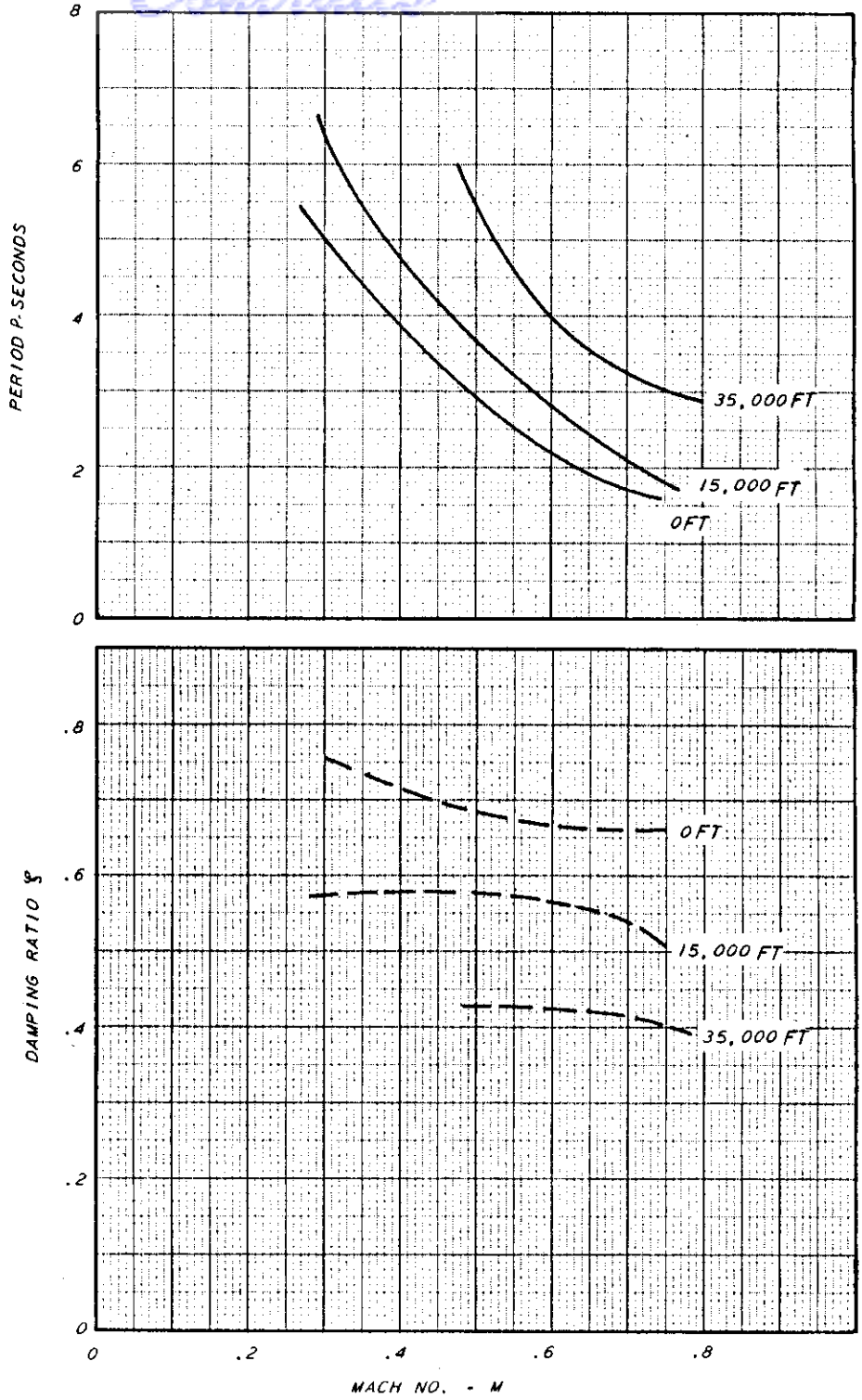

A-17 CALCULATED T-33A RESPONSE DATA, TIP TANKS OFF, SHORT PERIOD MOTION

Approved for Public Release

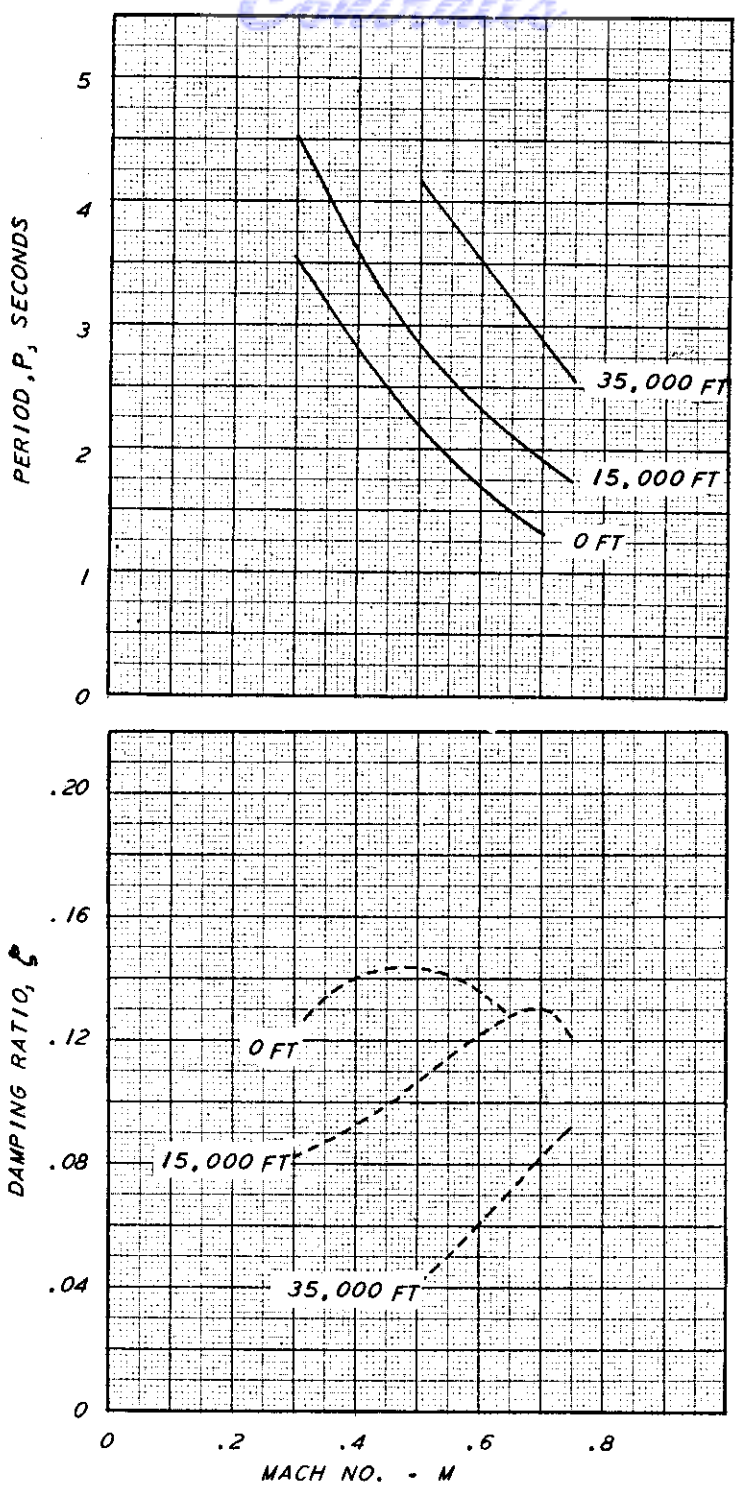

A-18 CALCULATED T-33A RESPONSE DATA, TIP TANKS OFF, DUTCH ROLL MOTION

Approved for Public Release

Contrails

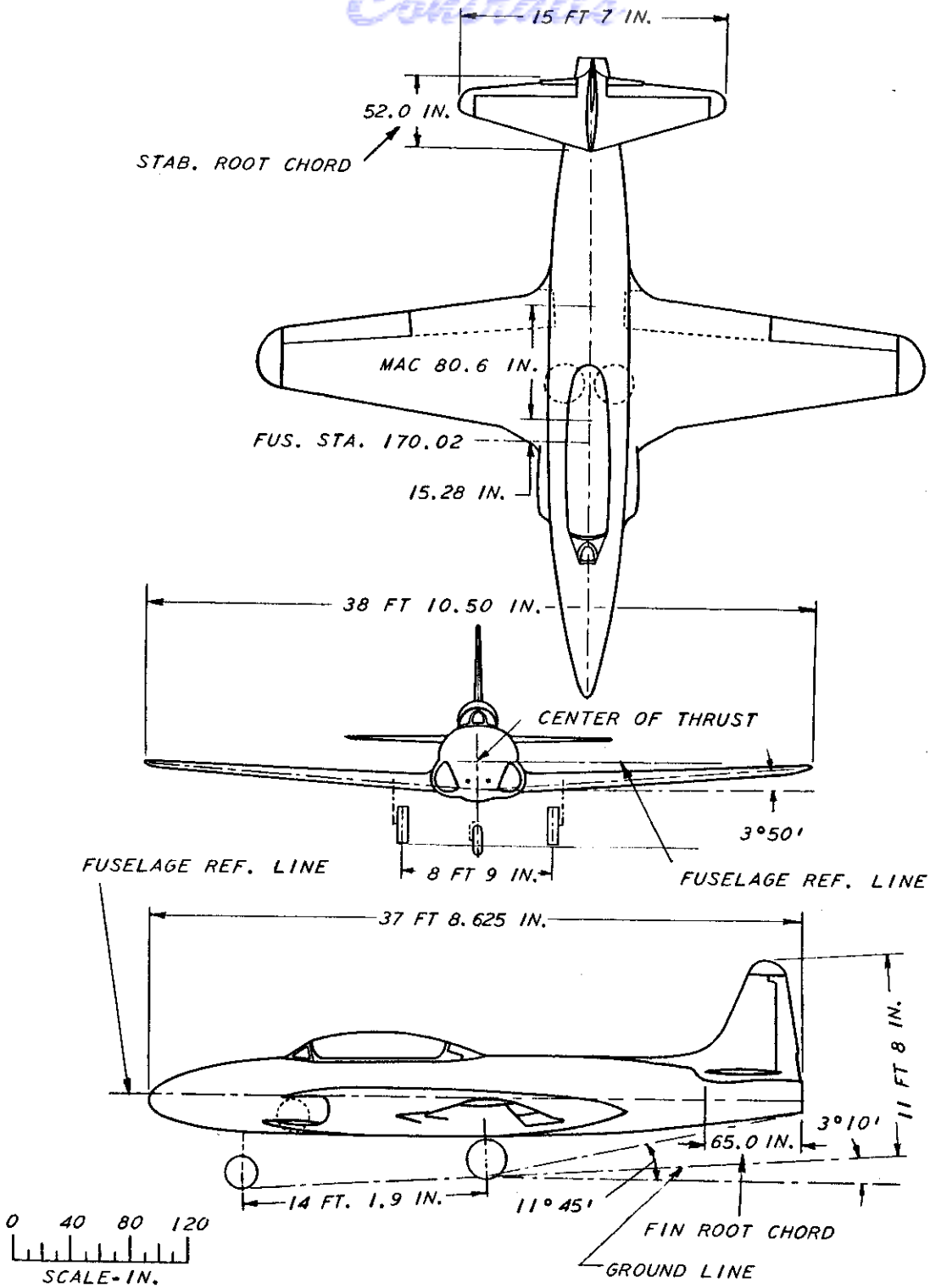

A-19 THREE VIEW DRAWING OF T-33 AIRPLANE

Approved for Public Release